SLOPE STABILITY INVESTIGATIONS OF ROAD CUT SLOPES: NH-58, RISHIKESH TO DEVPRAYAG

Ph.D. THESIS

by

TARIQ SIDDIQUE

DEPARTMENT OF EARTH SCIENCES
INDIAN INSTITUTE OF TECHNOLOGY ROORKEE
ROORKEE – 247 667 (INDIA)
JANUARY, 2019

SLOPE STABILITY INVESTIGATIONS OF ROAD CUT SLOPES: NH-58, RISHIKESH TO DEVPRAYAG

A THESIS

Submitted in partial fulfilment of the
Requirements for the award of the degree

of

DOCTOR OF PHILOSOPHY

in

EARTH SCIENCES

by

TARIQ SIDDIQUE

DEPARTMENT OF EARTH SCIENCES
INDIAN INSTITUTE OF TECHNOLOGY ROORKEE
ROORKEE – 247 667 (INDIA)
JANUARY, 2019

INDIAN INSTITUTE OF TECHNOLOGY ROORKEE
ROORKEE

CANDIDATE'S DECLARATION

I hereby certify that the work which is being presented in the thesis entitled **"SLOPE STABILITY INVESTIGATIONS OF ROAD CUT SLOPES: NH-58, RISHIKESH TO DEVPRAYAG"** in partial fulfilment of the requirements for the award of the Degree of Doctor of Philosophy and submitted in the Department of Earth Sciences of the Indian Institute of Technology Roorkee, Roorkee is an authentic record of my own work carried out during a period from July, 2014 to January, 2019 under the supervision of Dr. S.P. Pradhan, Assistant Professor, Department of Earth Sciences, Indian Institute of Technology Roorkee, Roorkee and Dr. M.E.A. Mondal, Department of Geology, Aligarh Muslim University, Aligarh.

The matter presented in the thesis has not been submitted by me for the award of any other degree of this or any other Institute.

(TARIQ SIDDIQUE)

This is to certify that the above statement made by the candidate is correct to the best of our knowledge.

(S.P. Pradhan)
Supervisor

(M.E.A. Mondal)
Supervisor

The Ph.D. Viva-Voce Examination of Tariq Siddique, Research Scholar, has been held on 22nd July, 2019.

Chairperson, SRC **External Examiner**

This is to certify that the student has made all the corrections in the thesis.

(S.P. Pradhan)
Supervisor

(M.E.A. Mondal)
Supervisor

Head of the Department

Date: 22nd July, 2019

Abstract: The Himalayan orogenic belt is well known for its active neotectonism, frequent seismicity, and multifarious geological and geotechnical environment. This mountain belt is also characterized by multiple phases of deformation and metamorphism that formed rugged topography with extensively elevated mountains and deep ravines. Substantial exogenic and endogenic factors are contributing towards widespread slope destabilization. From a couple of decades, the acceleration in rising demands for urbanization and constrain for mega civil engineering projects in the eco-sensitive terrains like the Himalayas are prime factors that are deteriorating the geoenvironmental fragility of the region. The acceleration in such pessimistic factors had amplified rampant landslides in the region. The swift progression and intervention of anthropogenic factors are being questioned since long but effective endeavor is rarely being undertaken to reduce them. Consequently, every year numerous death tolls and massive loss infrastructure are being proclaimed from distinct sectors of the region particularly along transportation corridors. Rampant slope failures are deliberately endangering the plight of the Himalayan ecosystem. Due to the lack of railways and airways network, roadways have exceptional significance in hassle-free transportation and communication in the Himalayan terrain. Transportation corridors within perilous and precarious Himalayan region experience incessant landslides, particularly along the sections that are manifested by geological discontinuities. Due to enormous deformation and contraction, the rock mass at certain sections along the highway is extensively fractured and sheared. One such route is national highway-58 which connects Indo-Gangetic plains to mountainous region leading to Badrinath in India. NH-58 has remarkable importance due to the extensive inflow of tourists from different parts of the world and pilgrimage activities. Chronic and recurrent landslides cause frequent blockage along the highway. During a traverse along NH-58, extensively high sub-vertical to vertical cut sections can be witnessed with rare preventive measures. Moreover, civilizations along seasonal valleys, debris dumps along hairpin bends are some common adverse practices along the highway. Demarcation of landslide-prone sections, quantification of the probability of slope failures and correspondingly implementation of restitutive and remedial measures are some major pre-requisite to attaining safe and economically functional design along the highway.

The present investigation encompasses the geotechnical appraisal along the strategic tactical transportation route. The investigation incorporates diverse issues pertaining to a variety of landslides along NH-58 from Rishikesh to Devprayag, Uttrakhand. Road cut slope stability appraisal is being conducted in prolonged stages including preliminary literature survey, demarcation of hazard-prone zones along the highway, extensive field survey to obtain data pertaining to slope stability, laboratory experiments to assess geomechanical properties.

The results were synthesized by integrating field and laboratory data. During the preliminary stage of the project, hazard-prone sections were demarcated. By considering complex terrain conditions, vulnerable road cut slopes were identified and targeted for much detailed inspection was conducted via distinct proxies. The failure pattern was assessed during the initial field surveys and different approaches were selected to deal with rock and debris failures.

In rock slopes, Rock mass classification technique viz. Rock Mass Rating (RMR), Slope Mass Rating (SMR), Continuous Slope Mass Rating (CSMR), Geological Strength Index (GSI) were applied to assess the stability levels of twenty vulnerable road cut slopes. Furthermore, the kinematic analysis technique was also carried out to identify the potential for different modes of structurally controlled failures. Moreover, much advanced and computer-aided numerical modeling technique was also performed by using plain strain simulator 'Phase 2D'. Shear strength reduction technique was conducted by finite element modeling. The non-linear Generalized Hoek-Brown (GHB) criterion was adopted. Critical SRF (equivalent to factor of safety) and shear strain contours were determined for each cut slope. According to FoS values, the cut slopes have been categorized into three classes. For FoS less than 1 as unstable, for 1 to 1.3 as marginally stable and for FoS greater than 1.3 as stable. As per the outcomes, five slopes (S6, S7, S18, S19, and S20) are unstable; four slopes (S2, S9, S13, and S17) are marginally stable while S1, S3, S4, S5, S8, S10, S11, S12, S14, S15 and S16 are stable. The above categorization is based on overall FoS which considers the mass failure only. However, there are certain slopes in the investigated section that are having reasonably fair FoS but having varying potential for occasional block failures. Such failures can be evaluated by kinematic analysis and accordingly remedies may be undertaken. Furthermore, the linear Mohr-Coulomb (MC) criterion was also adopted for comparative analysis. The critical obtained by employing GHB and MC was compared. For lower FoS, both GHB and MC are giving similar outcomes but for higher FoS values, MC underestimates the increase of stability and disparities among outcomes. As Himalayan rock mass comprises of jointed rock mass, the non-linear GHB criterion is much applicable as compared to linear MC criterion.

In debris slopes, circular and talus failures were evidenced during initial field surveys and keeping such aspects in mind numerical models were prepared by incorporating bedrock. Geological and geotechnical data pertaining to slope stability was collected during extensive field inspection and representative samples of debris were collected. Geomechanical properties were determined by rigorous laboratory experiments as per the standard procedures. The deterministic assessment of eight vulnerable road cut debris slopes is being conducted by using

different limit equilibrium methods and finite element modeling. In all debris slopes, MC criterion was adopted while for debris slopes having shallow underlying bedrock GHB (for rock) and MC (for debris) criteria were applied simultaneously. FoS and shear strain contours were determined for each slope to assess determine the overall stability grade and pattern of failure. Similar to rock slopes, the categorization was being done on the basis of critical SRF values that determine the overall stability of slopes. From eight investigated road cut debris slopes, six slopes (L1, L3, L4, L5, L6, and L7) are unstable; slope L8 is marginally stable whereas slope L2 is stable. Furthermore, multi-parameter sensitivity analysis was also conducted in the limit equilibrium technique to evaluate the influence of geomechanical parameters instability of slopes. According to the outcomes obtained by various methods, an attempt has been made to suggest general guidelines for prevention and stabilization of critical slopes along the highway and it has been also recommended to conduct similar geotechnical investigations in hazard-prone Himalayan and similar terrains.

Acknowledgement

First and foremost, I would like to express my sincere gratitude to my supervisor Dr. S.P. Pradhan for his continuous support, patience, motivation, and guidance throughout my research. I could not have imagined a better mentor for my Ph.D. other than him. He inspired my curiosity in slope stability appraisal along strategic transportation route in the Himalayas of great socio-economic importance. Besides my supervisor, my sincere thanks goes to my co-supervisor Dr. M.E.A. Mondal for his critical reviews and suggestions that helped me a lot to improve the quality of the work presented in the thesis. I would also like to thank Dr. V. Vishal and Dr. T.N. Singh who gave me access to the laboratory facilities and simulation work. Their insightful comments and encouragement always incented me to widen my research from various perspectives. I am also thankful to all the authors to whom I consulted during my work and anonymous reviewers and editors of the journals viz. Natural Hazards, Environmental Earth Sciences, Current Science and Journal of Rock Mechanics and Geotechnical Engineering for insightful reviews and publishing my Research articles. Their critical reviews and comments helped me a lot to improve the quality of work presented in the thesis.

My special thanks goes to committee members, Dr. M. Israil, Dr. A. Chamoli and Dr. S. Chikarmane for their valuable support and advice throughout. My work would not have been possible without the financial support provided by the Ministry of Human Resource Development during full-time research fellow period. I would also like to pay my sincere gratitude to the Head of Department of Earth Sciences for their cooperation. I am also thankful to the technical and non-technical staff of Department of Earth Sciences, Indian Institute of Technology Roorkee for the immense assistance and time to time guidance for the official work.

I am eternally thankful to my fellow lab mates Mr. Aditya Kumar Anand, Mr. Nani Das, Mr. Amulya Ratna Roul, Mr. Soumya Darshan Panda and Sumit Kumar for the stimulating discussions, for the sleepless nights we were working together before deadlines and for the immense support they have provided to me during the field and laboratory investigations.

Last but not the least I would like to thanks my beloved parents, sisters, brother and fiancée for their unconditional support, continual motivation, and cooperation during my research. The efforts made by them are uncountable. I am also thankful to my friends Mr. Mujeeb Hasan, Mr. Mohd Rehan and Mr. Arshan Khan who always managed to create an elated environment during my stay at the Institute.

Contents

List of Figures

List of Tables

Chapter 1
Introduction

1.1. Background: Landslide is a part of active denudation and upliftment cycle of the Earth. The landslide may be defined as a downward and outward motion of geomaterials primarily under the influence of gravity by sliding, falling, flowing and rolling action or any combination of these (Varnes, 1954 and 1978; Cruden, 1991; Cruden and Varnes, 1996). They often used to occur much frequently in mountainous regions characterized by enormously hills with high relief and deep ravines such as the Himalayas, Alps, Andes, Rockies, and the Appalachians. All landslides do not occur in isolation rather they are triggered by certain other hazards and often associated with some other hazard like seismicity, rainfall, cloudburst, tsunami, hailstorms, and volcanic activity. Landslides are caused by complex and dynamic coupling among several factors related to geology, geomorphology, seismicity, meteorology etc (Reddy, 2014). These factors can be categorized as controlling and triggering factors. Certain geometrical parameters like slope angle, aspect and altitude; geological conditions; drainage characteristics; geomechanical parameters of slope forming material are some common and widespread controlling factors while precipitation, cloudburst, seismic shaking and anthropogenic factors are some common triggering factors (Zihin et al. 2012; Barbano et al. 2014; Pappalardo et al. 2014; Devkota et al. 2015; Kavzoglu et al. 2015; Aghdam et al. 2017; Fan et al. 2017; Shang et al. 2017; Pourghasemi et al. 2018; Amanzio et al. 2019). In hilly terrains, debris slides are often associated with internal erosion caused by water (Balaji et al. 2010). Apart from irrepressible ongoing natural factors, the exponential and unprecedented growth of urban settlements in eco-sensitive Himalayan terrain is endangering and deteriorating environment and ecosystem of the Himalayas to a great extent. India is a global hotspot for fatal landslides across the globe. In a global spatio-temporal analysis of non-seismic fatal landslides from January 2004 to December 2016 total number of 55,997 casualties caused by 4,862 landslides (Froude and Petley, 2018). According to the analysis, among these global landslide events, 75% occurred in Asia with a substantial number of events in the Himalayan region. As per the dataset, the construction and mining related landslides in India were 28% and 12% of the global scenario respectively. These percentages are highest across all nations of the world. It may be due to the fact that in India, building and construction regulations do not consider geoenvironmental constraints properly and many often lack of sound technical experts also aggravates the issue (Kumar and Pushplata, 2015). It is also noteworthy that, 3,971 fatalities were caused by 245 landslides in India (Parkash, 2011). The Indian subcontinent is one of the global hotspots for landslides

events. By the rapid expansion and intervention of anthropogenic factors, the condition is approaching detrimental. According to the Geological Survey of India, in India, 15% (~0.49 million Km^2) land area is affected by landslides. The majority of this area is covered by Himalayan region along with a notable area of Western and Eastern Ghats. Landslides pose massive changes in morphology of landscapes and deteriorate natural and artificial structures of the Earth and cause huge social-economic loss (Kavzoglu et al. 2014; Crepaldi et al. 2015). In the Himalayan region, the enormous number of casualties and fatalities along with a massive loss of infrastructure and economy is being reported every year.

1.2. Motivation for research: Slope stability assessment is an utmost and fundamental component of geotechnical engineering practices. To tackle with large scale landslides in the Himalayan region, proper attention is to be given by the scientific community and public organizations. Due to lack of airfields and sparse railway network in the region, the roadways are the best efficient means of transportation and communication. These routes are often aligned by excavating natural hillslopes thereby a large number of hairpin bends along with vertical to sub-vertical cut slopes are quite common. Chronic and recurrent landslides cause frequent blockage along the highway and often block the natural course of the river which led to sediment bulking (Sundriyal et al. 2015; Scaringi et al. 2018). The vulnerability assessment along these routes should be of prime concern for the government and the authorities associated with road and transportation sectors. To ensure the sustainable socio-economical development of the region, the continual threat due to landslides should be reduced by restoring and reinforcing the stability of road cut slopes. The national highway-58 (NH-58), connecting Delhi to Badrinath has remarkable importance due to the massive influx of tourists and pilgrims. A variety of slope failures ranging from small occasional block failures to massive mass failure of rock or debris have been reported the section of NH-58. Many researchers have studied the instability related issues along the route (Uniyal, 2004; Sati et al, 2011; Sarkar et al. 2015; Sajwan and Sushil, 2016; Vishal et al. 2017; Veerappan et al. 2017; Sarkar et al. 2018). They have carried out geotechnical investigation by using various techniques like rock mass classification, kinematic analysis, numerical modeling, hazard zonation, remote sensing, and GIS tool. Majority of them have also quantified the potential landslide hazard and have also suggested the best efficient remedies. The suggested remedial measures should be implemented by proper consideration of geotechnical complexities, available resources, and significance of the route. Despite rigorous geotechnical evaluation of the health of cut slopes, there are a large number of sections along NH-58 particularly the section from Rishikesh to Devprayag to be

evaluated. Stability appraisal has to be conducted on road cut rock and debris slopes along the section. The state of existing cut slopes, road, building, and bridges has been tremendously affected due to the rapid expansion of the road without any proper consideration of geological and geotechnical complexities of the region.

1.3. Objectives of the research: The main objective of research involves geotechnical investigations of cut slopes along critical and strategic transportation corridor NH-58 and sub-objectives are as follows:

a) Delineation of landslide-prone road cut slopes along NH-58.
b) Determination of causes, mechanism, and type of slope failures.
c) Rock and slope mass characterization of identified critical slopes.
d) Slope stability analysis by limit equilibrium method and finite element method.
e) Comparison of Generalized Hoek Brown (GHB) and Mohr-Coulomb (MC) criteria for stability analysis within the jointed rock mass.
f) Optimization of the slope geometry to enhance the stability of slopes.

1.4. Study area: Uttarakhand state is also known as Uttaranchal, was formed on November 9th, 2000 as the 29th state of India by separating the northern part of Uttar Pradesh. It covers an area about 53,483 sq. km and encompasses very rare animal and plant species which are well acknowledged for pharmaceutical purposes. Uttarakhand is often said Devbhumi "Land of Lords". Char Dhams "Four Abodes" are Hindu pilgrimage centers viz. Badrinath, Dwarka, Puri, and Rameshwaram. The other famous pilgrimage centers like Yamunotri, Gangotri, Kedarnath, and Badrinath are known as 'Chota Char Dham'. The capital of Uttarakhand is Dehradun in Dun valley. This state is broadly categorized into two parts: Garhwal region (Dehradun, Haridwar, Uttarkashi, Tehri Garhwal, Pauri Garhwal, Rudraprayag, and Chamoli) and Kumaon region (Pithoragarh, Bhageshwar, Almora, Nainital, Udham Singh Nagar, and Champawat). The state is well known for rich natural resources, dense forests and extensively high mountain peaks are covered by massive glaciers. Uttarakhand is the largest producer of hydropower generation. Several major rivers (Tons, Yamuna, Bhagirathi, Bhilangana, Alaknanda, Ganga, Mandakini, Ramganga, Gori, Kali, Dhauli, Pinder, Parbar, Madmaheshwar etc.) are lifeline and backbone for the socio-economic development of the residents and for the nation as well. Uttarakhand is also known as Urja Pradesh "Energy State" as it hosts more than 180 large and small hydroelectric projects (HEP) that are expected to generate more than 21,200 MW electricity out of which 12, 235 MW comes just from 95 HEP on Alaknanda and

Bhagirathi (Valdiya, 2014). Broadly, the state has two distinct topographic conditions, hills and relatively plain region. Hilly portions of the state experience intense cold winters with snowfall in upper parts for a long duration. The beauty of the Himalayan mountains, pilgrimage centers, swift flowing rivers, snowfall at higher regimes, mild summers, and extensive glacier caps empowers tourism activities around the year. The average annual rainfall increases up to 1229 m and it starts in late April and continues up to September with some high peaks during June and July. At certain places in the region, temperature in summers may even reach up to 40° C with a lot of humidity and in winters may be less than 5° C. As per National Institute of Disaster Management (NIDM) the highest and lowest recorded temperatures are 40° to 50° C and -5° to -7° C respectively. Highly variable meteorological phenomena and tremendously dynamic weather circumstances occur in response to its unique geomorphological conditions and geographical location. Beautiful landscapes, unique ecosystem and holy shrines attract tourists and pilgrims across the globe. In the present study, critical slopes along NH-58 from Rishikesh to Devprayag have been demarcated and detailed stability assessment is being conducted.

1.4.1. Disaster profile in Uttarakhand: Uttarakhand is very much prone to severe earthquakes, large and small scale landslides, cloudburst and flash floods. In addition, the state is also prone to forest fires, hailstorm, drought, avalanches, lightning etc. Such disasters had caused immense loss to life, property, and health. Due to the rapid pace for urbanization and development, such incidents have been aggravated in recent past due to much interference of humans. Distinct governmental sectors and authorities are continuously trying to control and minimize the impacts posed due to such disasters. Although such endeavors had gained significant success, sometimes natural processes are unpredictable and very difficult to cope with. However, incessant evaluation and accordingly immediate implementation of remedial measures can reduce hazardous impacts to a great extent. Seismicity in India is well concentrated in the seismo-tectonically active Himalayan region. According to the Bureau of Indian Standards (BIS, 2002), most part of Uttarakhand is highly vulnerable and Rishikesh to Devprayag region lies under zone IV. According to the National Institute of Disaster Management (NIDM), the entire state can be divided into zones V and IV. The state has experienced many large and small earthquakes with their epicenters located within the Himalayan region. The state has witnessed two major earthquakes in recent past i.e. Uttarkashi earthquake in 1991 and Chamoli earthquake 1999, caused 768 and 106 fatalities respectively. Snow avalanches are the sudden downslope slide of a huge mass of snow that is predominantly

controlled by weather, slope, atmospheric temperature, vegetation, snow packs etc. Upper regions of the state are covered by extensive glaciers which are under continuous threat to be triggered due to avalanches. Cloudburst refers to extreme precipitation for a short period of time and often associated with hails and thunderstorms. Many cloudburst events cause flash floods. Consequently, provoke instability to the slopes and led to large scale landslides. Landslides are very frequent during and just after the monsoon. The state is severely affected by landslides due to various natural and anthropogenic factors. Alternate Hydro Energy Centre of Indian Institute of Technology Roorkee (IITR) prepared landslide susceptibility map of Uttarakhand. In hilly regions, roadways are the primary means of transportation. Frequent blockage due to landslides affects the socio-economic activities of the region. Prevailing climatic conditions, ongoing tectonic activities, rugged geomorphological configuration, extensive human intervention etc. are prime factors controlling landslides in the region. According to Sarkar et al. (2006) debris slides, debris flows, rock slides, and rock falls are common types of landslides that occur along Rishikesh-Badrinath highway in Uttarakhand. Sati et al. (2011) illustrated the role of major influencing factors of landslides along this highway. In recent years, significant attempts have been made for regional assessment via remote sensing and GIS platform along the strategic route NH-58 in Uttarakhand state. National Remote Sensing Centre (NRSC, 2001) generated 14 thematic maps and prepared Landslide Hazard Zonation (LHZ) map of 10 Kms on eider side of transportation corridor from Rishikesh to Badrinath. Furthermore, Ramesh et al. (2017) integrated remote sensing and GIS tool and prepared LHZ map using frequency ratio and analytical hierarchy models.

1.4.2. Geological framework of the study area: The Himalayan orogen is a young mountain chain which is formed by the typical continent-continent collision of Indian and Eurasian plates (Dewey and Bird, 1970; Dewey and Burke, 1973; LeFort, 1975; Valdiya, 1995). This huge mountain range is arc-shaped which is convexing southwards with syntaxial bands at western and eastern flanks (Wadia, 1953; Valdiya, 1980). It displays a perfect southward-convex arcuate bulge (Heim and Gansser, 1939) with a radius of 1500 km and center at 90°E and 40°N. Irrespective to international boundaries, Yin (2006) defined the geographical distribution of the Himalayan ranges. According to Yin (2006) ranges lie between eastern syntaxis represented by Namcha Barwa and western syntaxis represented by Nanga Parbat peaks. The northern boundary is marked by eastward-flowing Yalu Tsangpo River and westward flowing Indus River. The southern margin is represented by Main Frontal Thrust (MFT) which marks a boundary between high ranges of Himalaya and lower depressions of Indo-Gangetic plains.

Extensive Himalayan ranges control the climate and its change in Indian and nearby continents to a great extent. LeFort (1975) defined structural boundaries of the Himalayan orogen as Indus-Tsangpo suture zone in North, Chaman fault in the west, Sagaing fault in East, MFT in the southern margin. Many faults of the Himalayan orogen are very active and led to neotectonism, dislocation, deformation of Pleistocene and Holocene landforms (Valdiya, 1992, 2002). Many researchers have conducted geological mapping in different parts of the Himalayas. Most of the studies conducted broadly that classify these mountains into different longitudinal sections trending roughly NW-SE. However, some deviations from this general trend can be noticed in discrete parts. One of the earliest and successful attempts have been made by Heim and Gansser (1939) for the broad classification of distinct regional geological units in the Himalayan orogen. They are divided into four E-W trending geographic belts that correspond to different geological domains:

a) Sub-Himalaya (Siwaliks) comprises of Cenozoic rocks.
b) Lower Himalaya or Lesser Himalaya (Himachal) comprises of non-fossiliferous low-grade metamorphic rocks.
c) Higher Himalaya or Great Himalaya (Himadri) is predominantly composed of a crystalline complex consisting of granites and gneisses.
d) Tethys Himalaya is marine and fossiliferous.

Later, Gansser (1964) classified Himalaya into four litho-tectonic units as:

Indus Tsangpo Suture Zone (ITSZ)
Tethys Himalaya
South Tibetan Detachment (STD)
Greater or Higher Himalaya
Main Central Thrust (MCT)
Lesser Himalaya
Main Boundary Thrust (MBT)
Outer Lesser Himalayas or Siwaliks
Himalayan Frontal Thrust (HFT)

Outer Himalayas or Siwaliks: The outer Himalayas or Siwalik ranges comprise of clastic freshwater molassic sediments of Middle Miocene to Middle Pleistocene in age, accumulated in a long narrow foredeep formed at the South of rising Himalaya (Tripathi, 1986). This sequence is bounded by Himalayan Frontal Thrust (HFT) in the south and Main Boundary Thrust in the north.

Lesser Himalaya: The lesser Himalayan sequence comprises of highly folded Proterozoic sedimentary rocks and few outcrops of older crystalline rocks (Valdiya, 1980; Bhattacharya,

2008). Structurally it is bounded by Main Boundary Thrust in the south and Main Central Thrust (MCT) in the north.

Greater or Higher Himalaya: The Greater or Higher Himalaya comprises of metamorphic rocks and granites of Proterozoic to Cambrian age with some leucogranites of Miocene age in upper parts (Sorkhabi, 2010). Structurally it is bounded by Main Central Thrust (MCT) in the south and South Tibetan Detachment (STD) in the north.

Tethys Himalaya: Tethys Himalaya comprises of thick pile of sedimentary rocks of Cambrian to lower Eocene sediments. The sediments are predominantly fossiliferous within synclinorium type basin (Bagati, 1990). Tethys Himalaya is structurally confined between South Tibetan Detachment (STD) in the south and Indus Tsangpo Suture Zone (ITSZ) in the north.

In the Garhwal region, the lesser Himalayan sequence can be categorized into two broad units i.e. outer and inner Lesser Himalaya (Valdiya, 1980). The geological formations within the lesser Himalayan sequence are exposed in six different synclines namely Krol, Pachmunda, Nigalidhar, Mussorie, Garhwal and Nainital synclines extending over 300 Kms (Jiang et al. 2003). The study area lies in a part of Garhwal syncline. Garhwal syncline is a regional non-cylindrical fold trending NW-SE and this polyharmonic synform that incorporates a number of synclines and anticlines like Lansdowne syncline, Hyunil anticline and Amri syncline (Dubey, 2014). The Regional stratigraphy study area that lies in outer Lesser Himalaya has been illustrated in table 1.1.

Table1.1: Regional stratigraphy of outer Lesser Himalayas of Garhwal region (after Valdiya, 1980; Srivastava and Mitra, 1994; Yin, 2006)

	Gumalikhet Formation
Almora Group	Champawat Granodiorite
	Saryu Formation
	Almora Thrust
Ramgarh Group	Debguru Porphyroid
	Nathuakhan Formation
	Ramgarh thrust
Sirmur Group	Subhatu Formation
	Singtali Formation
	Tal Formation
Mussoorie Group	Krol Formation
	Blaini Formation
	Nagthat Formation
Jaunsar Group	Chandpur Formation
	Mandali Formation
	Krol Thrust
Damtha Group	Rautgara Formation
	Chakrata Formation

As per the Survey of India toposheets, the study area lies in toposheet number 53J/8 and 53J/12 i.e. in the Lesser Himalayas which predominantly comprises of meta-sedimentary sequence (Heim and Gansser, 1939; LeFort, 1975; Schelling and Arita, 1991) along with some volcanics, meta-volcanics and Gneiss (Frank et al. 1995; Upreti, 1999). The Lesser Himalayan sequence experienced multiple phases of contraction and structurally bounded by Main Boundary Thrust (MBT) in the south and by Main Central Thrust (MCT) in the north (Valdiya, 1983; Célérier et al. 2009). Furthermore, many researchers proposed that the geological formations of the lesser Himalayan sequence can be categorized into two major subdivisions i.e. Garhwal and Kumaon lesser Himalaya (Auden, 1935; Heim and Gansser, 1939; Valdiya, 1980). The study area lies under the outer Garhwal Himalayas. It comprises Damtha, Tejam, Jaunsar, Mussoorie, Sirmur, Ramgarh and Almora group of rocks. The investigated slopes lie along national highway-58 in the north-western flank of Garhwal syncline of the outer Lesser Himalaya i.e. running parallel to the holy river the Ganga (figure 1.1).

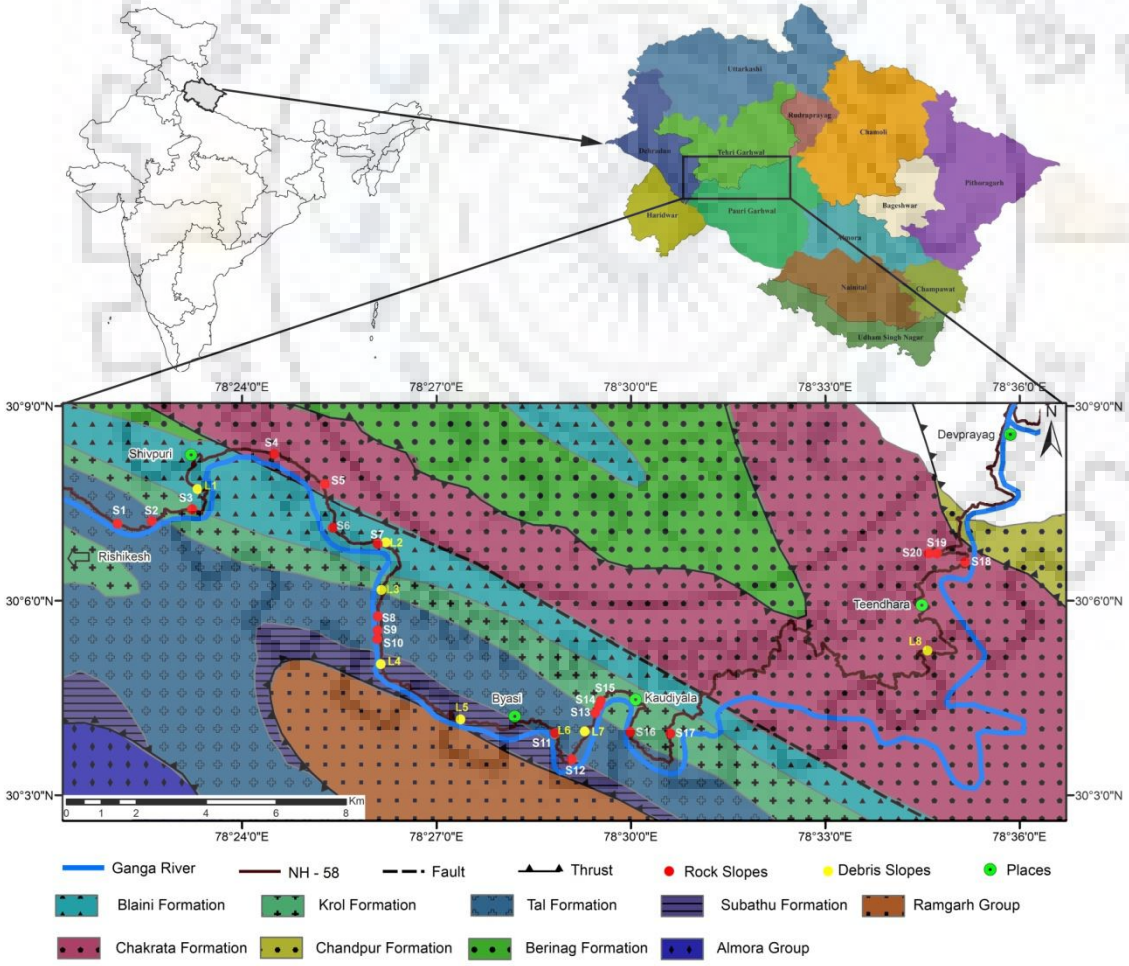

Figure 1.1: Investigated road cut slopes on geological map of the study area (modified after Valdiya, 1980)

A variety of meta-sedimentary rock formations were encountered in the stretch (shale, siltstone and conglomerates of Blaini Formation; limestone of Infra-Krol Formation, calcareous rocks including limestones and dolomites of Krol Formation; argillaceous, arenaceous, siliceous and calcareous rocks of Tal Formation; quartzite of Nagthat Formation and sandstone of Chakrata Formation) of Proterozoic to Cambrian in age (Valdiya 1980, Srivastava and Mitra, 1994; Jiang et al. 2003; Tiwari et al. 2013). According to Kumar and Dhaundiyal (1979), the rocks in the study area had experienced noteworthy crustal stresses that resulted in fan folding due to which central portion of Garhwal synform represents a doubly plunging anticline with local synclines and anticlines in the crest. Among regional thrust faults of Himalayas, MBT is the most proximal. Being the plane of underthrusting of Indian plate under the extensive Himalayas, MBT is geodynamically active (Valdiya, 1983). Apart from MBT, there exist few major faults in the Garhwal synform itself. These are Pulinda, Bedasini, Fatehpur, Bonga, Singtali, Duwadhar and Maidan (Kumar and Dhaundiyal, 1979 and 1980; Valdiya, 1980; Sati et al. 2011). Among these, Duwadhar and Singtali faults dissect cut slopes at distinct locations along NH-58. However, the care must be taken as Singtali thrust fault is also named as Garhwal and Binj thrust in the literature. Singtali thrust often cross-cut the road section several times due to which slopes near Shivpuri and Kaudiyala are very much fragile. Such adverse structural setting is largely responsible for aggravation of slope instability in the region. Furthermore, ongoing tectonism and seismic vulnerability are some crucial geophysical components that should be understood properly to explore the concealed behavior of the rock mass. Such incessant adverse phenomenon is responsible for extensive degradation in the quality of rock mass. The entire Himalayan region is inherently fragile while the greater Himalayas had experienced much frequent seismic events as compared to the Lesser Himalayas. But, it should be noted that in context of the seismic event of higher magnitude, the extensively deformed and fragile lesser Himalayan terrain remained calm and quiet since a long time in the aspect of higher magnitude earthquake. The stress regime within the lesser Himalayan sequence is aggravating in a cumulative and progressive manner. It is due to enormous horizontal stresses due to sub-surface Delhi-Haridwar, Faizabad, Monghr-Saharsa ridges that are underlying extensions of Delhi-Aravalli, Vindhyan and Satpura rocks respectively (Valdiya, 1992). Such giant stress is capable enough to trigger enormous seismic activities in the near future which would be capable enough to prompt a large number of landslides in the region. Furthermore, Valdiya (2002) considered the major events throughout the evolution of the Himalayas and suggested that spasmodic rise of marginal Lesser Himalayan sequence and extensive contraction within Siwaliks range at 1.6 million years ago caused rampant landslides. Sati et al.

(1998) studied the relationship of regional tectonic setting with large scale landslides and suggested that WNW-ESE trending slopes are most fascinating. It is due to the fact that extensively high horizontal stress is perpendicular to the regional trend of the Himalayas. Consequently, the slopes which are parallel to this trend would form widespread shattered and sheared zone. Mithal (1988) also studied litho-tectonic landslides of Garhwal-Kumaon region and suggested that rapidly rising dynamic forces are primarily due to a large number of developmental activities due to excavation for the purpose of alignment of roads and large hydroelectric projects.

1.5. Research Methodology: The research methodologies adopted to address the noted objectives are as follows:

a) Detailed review of relevant literature.
b) Demarcation of landslide-prone zone and slopes during the initial reconnaissance field survey.
c) Detailed geological and geotechnical field investigation.
d) Determination geotechnical parameters of slope forming material in the laboratory.
e) Slope stability analyses by rock mass characterization and numerical simulation.
f) Optimization of slope geometry for stability enhancement of the slopes.

During a traverse along NH-58 from Rishikesh to Devprayag, 28 vulnerable slopes (20 rock and 8 debris slopes) were identified for the study. A different approach has been used to evaluate the stability of rock and debris slopes as follows:

a) Rock slopes

Rock mass classification (RMR, SMR, CSMR, and GSI)

Kinematic analysis

Optimization of slope geometry

b) Numerical simulation by FEM

Debris slopes

Numerical simulation by LEM and FEM

In rock slopes, rock mass classification is being done by employing various rock mass classification systems. The rating based RMR_{1989} system is being employed to seek an overview of existing stability grades. To rate the various parameters in the RMR system, required field and laboratory data were generated and analyzed as per the standards. The

unconfined compressive strength (UCS) test was conducted as per the guidelines of the International Society of Rock Mechanics (ISRM, 1978). The test was conducted in a Universal testing machine by extracting cylindrical core samples of NX-size from chunks of rock. For weaker rocks like slate and phyllite, point load index test was conducted to determine the compressive strength. The test was conducted as per the standard procedure suggested by BIS (1998). As drill cores were not available, the rock quality designation (RQD) was estimated volumetric joint count method suggested by Palmstrom (1974 and 1982). Discontinuity spacing; discontinuity conditions like persistence, aperture, roughness, infilling and weathering; groundwater conditions and orientation of discontinuities were determined as per Bureau of Indian Standards (BIS, 1987). All the parameters were rated as per the values and conditions at the particular site and RMR_{basic} and adjusted RMR values were determined. Furthermore, RMR_{basic} values were used in SMR which much exhaustive classification system and widely used for slopes. The most prominent type of structurally controlled failure was identified by kinematic analysis and SMR for vulnerable discontinuity or set of discontinuity was calculated by quantifying the adjustment factors in SMR (Romana, 1985; 1991; 1993; 1995; 2001). In addition to SMR, the CSMR was also calculated by employing continuous functions. GSI values were determined in light of the chart proposed by Hoek et al. (1995) and quantification of GSI chart was done by Sonmez and Ulusay (1999 and 2002). Furthermore, discrete spatial representation of stability classes obtained by different rock mass classification systems was prepared by using Geographical Information System (GIS). In conjunction with conventional approaches, much advanced and sophisticated analysis is being conducted by the numerical simulation tool. The shear strength reduction technique was employed to determine the factor of safety in finite element modeling by plain strain Phase 2D simulator. Furthermore, shear strain contours were obtained to determine the stress concentration and failure pattern in road cut rock slopes. As the rock mass in the investigated section is highly jointed with multiple sets of discontinuities, so the non-linear criterion is being adopted for in the study. Generalized Hoek-Brown (GHB) and Barton-Bandis (B-B) failure criteria were adopted for rock mass and joints respectively. The Hoek and Brown parameters were determined according to the standard procedure suggested by Hoek et al. (2002). The various inputs for B-B model were determined as per the methods suggested by Barton (1972; 1972); Barton and Choubey (1977). The detailed description of the measurement and calculation of each parameter has been illustrated in chapter 3 ‘Field and Laboratory investigations’. Furthermore, thin section microscopy was also carried explore the lithological, mineralogical and textural constraints in the rocks. For

jointed rock mass, the applicability of linear Mohr-Coulomb (MC) criterion is assessed by a comparative study among GHB and MC failure criterion.

In debris slopes, the conventional limit equilibrium approach was applied for deterministic and multi-parameter sensitivity analyses. The linear MC criterion was adopted during modeling. However, certain slopes are having bedrock below debris cover. In such slopes, GHB criterion was adopted for the bedrock portion. The geological and geomechanical properties of bedrock and overlying debris were determined by conducting a rigorous field survey and laboratory experiments. The grain size distribution was determined by sieve analysis was conducted by following the procedure suggested by American Society of Testing Materials (ASTM, 1998) and the stiffness characteristics of soil were identified by performing Atterberg limit test according to the method suggested by ASTM (2005). Furthermore, the outcomes from the sieve and Atterberg tests were used to characterize soil according to the Unified soil classification system. Furthermore, shear strength parameters i.e. cohesion and angle of friction were determined by performing direct shear testing according to the Bureau of standards (BIS, 1986). For the slopes having bedrock, certain geomechanical properties were determined during the field survey. The GSI values were estimated by chart-based approach suggested by Marinos et al. (2005). The disturbance factor (D) was determined by visual inspection during the survey. For the estimation of D values, the guidelines by Hoek et al. (2002) were followed. The Schmidt hammer rebound values were taken during field survey to determine the unconfined compressive strength of the bedrock. The density of samples collected from bedrock was determined in the laboratory and unit weight was calculated. The microscopic studies were also undertaken to identify the mineralogical content and their alteration products. By using all these geomechanical inputs the model was generated in the LE software SLIDE and FoS was determined by Ordinary/Fellenius, Bishop's, Janbu's simplified, Janbu's corrected, Spencer and GLE/Morgenstern-Price method. Furthermore, the same models have been imported into plain-strain finite element simulator Phase 2D. The critical SRF (equivalent to FoS) is compared with FoS obtained by various LE methods. Furthermore, a multi-parameter sensitivity analysis was also conducted to identify the contribution of various input parameters towards FoS. The outcomes obtained by applying different proxies helped in exploring the existing stability of road cut slopes along NH-58 from Rishikesh to Devprayag. Considering all the investigated factors and issues certain preventive, restorative and stabilization measures are suggested to overcome the occurrence of slope failures in the future.

Chapter 2

Literature review

2.1. Slope stability: Slope stability assessment of natural and engineered slopes is one of the major challenging tasks in rock and soil engineering. Slope instability problems have been faced throughout the history of humans. Increasing demands of urbanization and socio-economic development have increased the demand for engineered slopes. Stability assessment of natural and engineered slopes is a foremost process for the development of transportation facilities such as roads, railways, canals, and airfields. According to Pantelidis (2009) potential for failure of a rock cutting is a function of its condition and the impact of triggering factors for failure and triggering mechanisms for failure involve triggering factors like infiltration of water and earthquake and by development or pre-existence of any unfavorable conditions for slope stability like blocked drainage paths, small distance from the epicentre. Landslides involve a variety of phenomena like commencement and propagation of fractures and cracks; generation and development of failure surface; movement of slope forming material by the coupled effect of block movement, rotation, fragmentation (Tang et al. 2017). Landslide may be defined as the downward and outward movement of slope-forming material primarily under the influence of gravity by varieties of motions like sliding, falling, flowing or by any combination of these (Varnes, 1954, 1978; 1984; Cruden, 1991; Cruden and Varnes, 1996; Highland and Bobrowsky, 2008; Hungr et al. 2014). The stability of slopes is governed by certain natural factors such as geological characteristics and hydro-meteorological controls. Furthermore, rapidly rising anthropogenic factors hampers stability of slopes to a greater extent (Shroder and Bishop, 1998; Leroueil, 2001; Pradhan et al. 2015; Vishal et al. 2015; Siddique et al. 2016; Umrao et al. 2017). The quantitative evaluation of the health of slopes requires a rational understanding of geological, geomorphological and geotechnical attributes. Furthermore, sound understanding related to tectonics, hydrology, meteorology is necessary for effective judgment. Recognition of type of slope and the most prominent movement laid the pavement for further investigation. Accordingly, different chart and table based conventional methods and computer-aided advanced simulation methods are to be selected.

2.2. Himalayan slope stability: The Himalayan orogeny had formed by collision of Indian and Tibetan lithospheric plates after the complete subduction of the Tethys Ocean due to which the region is characterized under high tectonics stress (Wadia, 1953; Gansser, 1964; Dewey and Bird, 1970; Dewey and Burke, 1973; LeFort, 1975; Yin, 2006). The mountain chains within the

Himalayas are well known for active neotectonism, extremely rugged topography having enormously high hills and unfathomable ravines. Due to continuous ongoing northward drifting of Indian plate, the rocks are extensively fractured, sheared, folded, faulted, thrusted (Malik and Mohanty, 2007; Jain et al. 2012; Jain et al. 2016), as a consequence inherent slope instability is being imparted to the slopes. Adverse geomorphological, geological and geomechanical constraints in the Himalayan region have prompted many large scale slope failure in the region. As Himalayan rock slopes are manifested by sets of discontinuities, they are inherently very poor and the unscientific planning during excavations of cut slopes further exposes new rock surfaces which become avenues for additional slope failures (Singh et al. 2008). Certain natural hazards like frequent floods, seismicity, cloudburst, landslides, lightning, forest fires etc. are very common in the Himalayan region. Several such hazards are interlinked with each other and their impact is often being aggravated by site-specific parameters. The occurrence of any such event is hazardous and the impacts are escalated to manifolds when one event triggers another which occurs on the usual basis in the Uttarakhand state. The coupled occurrence of such hazardous events often led to catastrophic impacts. Such incidence had taken place in recent past in the Kedarnath valley of Uttarakhand. During this tragedy, the area witnessed exceptionally heavy rainfall and cloudburst occurred during 16^{th} and 17^{th} June 2013. Such extreme event occurred as a response to the fusion of westerlies with the Indian monsoonal cloud system (Nair and Singh, 2014). Nature's furry was most profound and extreme, the whole state experienced massive flash flooding and consequently, landslides were triggered at certain sections and certain old slides were activated (Dobhal et al. 2013; Dubey et al. 2013). As per the report of National Institute of Disaster Management (NIDM), the death toll was 4000 and approximately a similar number of people presumed to be missing. It has been reported that more than 9 million people were affected and certain regions of the state being cut off for several days and experienced the scarcity of many essential commodities. Bhageshwar, Chamoli, Pithoragarh, and Rudraprayag were the worst affected districts of the state. Furthermore, Map the Neighbourhood in Uttarakhand (MANU) report has been prepared by Ahmad et al. (2015). The damage within Bhagirathi-Ganga-Nayar valley has been quantified and it has been reported that 1034 landslides were either initiated or re-activated during the Kedarnath disaster. The temporal control over landslides is directly linked with heavy rainfall during monsoon. In recent times, ample research has been conducted to highlight the impact of rainfall on landslides (Gabet et al. 2004; Dahal et al. 2009; Kanungo and Sharma, 2014, Nirupama, 2015). Gerrad (1994) evaluated the impact of geological constraints and human control over Himalayan landslides. The swift expansion of roadway network, hydroelectric and

tunnel projects had disturbed the equilibrium conditions of slopes in the region (Haigh and Rawat, 2011; Umrao et al. 2017; Ahmad et al. 2013; Singh et al. 2014; Kundu et al. 2016; Sarkar et al. 2016; Dudeja et al. 2017; Kundu et al. 2017; Siddique et al. 2017; Singh et al. 2017). Frequent landslides in the Himalayan region are affecting the socio-economic augmentation and ecosystem of the region. Large scale destabilization of slopes often led to massive debris flow in the valleys. Such processes degrade the quality of flowing water and also increase the problem of siltation in downstream reservoirs. Landslide phenomenon also causes severe injuries and economic loss and often triggers fatalities (Chakraborty et al. 2011; Nirupama, 2015; Satendra et al. 2015; Pal et al. 2016). As per the historical records compiled by Parkash (2011), the death toll in western and north-western Himalayan region from the year 1800 to 2011 was 2000 while during same duration 1500 lives were claimed in the eastern and north-eastern region of India. To cope up with such an enormous loss of life and property, extensive research is to be conducted. To attain disaster resilience design, the holistic and multidisciplinary approach needs to be adopted. Landslide susceptible zones must be determined and their vulnerability should be evaluated by careful evaluation and scientific monitoring. Due to extremely complex terrain conditions, certain domains are so inevitable that sometimes remedial measures are extremely costly and ineffective too (Ghosh et al. 2014).

2.3. Landslides along Himalayan roads: In mountainous terrains like the Himalayas, railway and airway networks are rare and sparse. So, roads are the effective means for transportation and communication. Moreover, roadway networks are treated as the arteries in the promotion of tourism, pilgrimage and socio-economic activities of the region. Landslide scars along the road cut slopes in the Himalayan region are very common particularly in those areas having adverse geological and geotechnical conditions of the slope. The sections dissected by major discontinuities are very much prone to slope failures. Majority of roads in the Himalayan region are being often aligned by excavating natural hill slopes. The vibrations induced during blasting often generate additional fractures and discontinuities. In parts of Kumaun Lesser Himalayas, the frequency of naturally occurring and excavation induced chronic landslides is 0.72 per km^2 (Valdiya and Bartarya, 1989). They also evaluated that landslides 20.3% landslides occurred along roads and most of them are fault concentrated. Large numbers of challenges are witnessed to attain landslide resilience design along crucial highways. Although, fractional and controlled blasting for such sensitive and precarious terrains have been suggested by Mondal et al. (2016). But, inadequately performed excavations along with poor and faulty geotechnical consideration during excavation for road construction and widening projects

hampered the stability of slopes (Sati et al. 2011). Due to unplanned and deprived implementation during the expansion of the existing road, the national highway-58 had manifested frequent slope failures at distinct sections (Sati et al. 2011; Siddique et al. 2015). The enormous numbers of road cut slopes that are dissected by multiple sets of adversely oriented joints that initiate varying sized potential falling and sliding blocks. To mitigate the impact of landslides, routine and enhanced landslide hazard assessment is to be performed for a much better understanding of landslide behavior which can be achieved by continual observations of some typical landslides for a long period of time. During reconnaissance and preparedness stages of the project, critical examination of landslide inventory should be performed to determine the root cause or the pattern of landslides. Furthermore, Landslide vulnerable zones must be identified and their evaluation ought to be done by means of various geotechnical methods and subsequently, cost-effective remedial measures must be suggested and implemented.

2.4. Rock mass classification: Most empirical and numerical approaches to design in rock mechanics incorporate rock mass classification to calculate input parameters stress-based failure criteria (Milne, 2007). Rock mass classification system is considered one of the most reliable tools in rock engineering practices. Rock mass classification schemes aim to quantify the most significant parameters that affect the stability of rock mass. Such systems are considered to be much reliable in the initial stages of the engineering project where much detailed information is not available. During the feasibility and preliminary stages of the project when limited data are available, a comprehensive understanding of rock mass behavior can be judged by employing various rock mass classification schemes. Such classification techniques are widely employed in rock engineering practices that facilitate quantitative evaluation of rock mass properties and serve as ease in communication among constructors, designers, explorers, engineers and to predict rock mass behavior and to generate safe and economically viable design. Rock mass classification provides a common basis to communicate, to identify rock mass within one of the groups having well-defined characteristics and also to provide basic input data for engineering design. Rock mass are classified for different purposes: (i) To identify most significant factors controlling the behavior of rock mass; (ii) To identify quality grade in terms of stability; (iii) To formulate quantitative engineering design; (iv) To recommend support for tunnels, mines, slopes, foundation etc. Rock mass classifications were developed to create some order out of chaos in site investigation procedures and provide desperately needed design aids (Bieniawski, 1989). Rock mass classification systems never

intend to the ultimate solution to engineering design problems, but they are convenient means to derive an approximate solution to the end. According to Dev and Sharma (2011), such classification systems provide the desperately needed design approaches and they are not intended to replace analytical studies, field observations, and measurements. Two widely used terminologies rock mass characterization and rock mass classification looks like same and have some relevance but they have certain practical differences. Palmstrom (1995) defined rock mass characterization as the designation of rock mass quality based on numbers and descriptive terms of certain features in the rock mass while rock mass classification combines certain features of rock into classes or groups. According to Potvin et al. (2012), rock mass characterization should be generic in nature, capturing the basic input parameters that can be used in classification systems and empirical design methods. Bieniawski (1989) defined rock mass classification as the arrangement of objects into groups on the basis of their relationships. There are large numbers of rock mass classification systems that are available in the literature but none of them covers all possible parameters and situations. To minimize such drawbacks of rock mass classification approach depth rock engineering sense is required to judge most effective system for the specific purpose. Bieniawski (1989 & 1990) have given major pitfalls of rock mass classification systems: using rock mass as the ultimate empirical cookbook i.e. ignoring analytical and observational design methods; using only one classification systems; classification without enough input data; using rock mass classifications without full realization of their conservative nature and their limits arising from database on which they are developed. The primary objective of the rock mass classification system is to quantify different engineering properties related to the stability of rock mass based on past experience. Stille and Palmstrom (2003) have given main requirements for true classification system capable of solving rock engineering problems:

1. Reliability of classes to assess given rock engineering problem must be estimated.
2. Classes must be exhaustive and mutually exclusive.
3. Principles of division governing assignment into classes must be added on suitable indicators and must include the possibility of being updated during construction using gained experience.
4. Rules must be so flexible that additional indicators can be incorporated.
5. Uncertainties or the quality of the indicators must be established so that the probability of misclassification can be estimated.
6. A useful system should be practical and robust so that it can give an economic and safe design.

As different rock mass classification systems emphasize different parameters, it is often recommended that at least two methods should be used simultaneously for good engineering judgment of the rock mass. Bieniawski (1989) suggested that various parameters have different significance and only when they are combined they can give satisfactory results to describe rock mass quality. It is necessary to adopt an existing classification system to the actual condition and problem and to calibrate existing rock mass classification systems against the experience gained from a specific project (Stille and Palmstrom, 2003). Rock mass classification systems have been widely used with great benefit in Austria, South Africa, USA, Europe and India due to the following reasons: (Singh and Goel, 1999)

1. It provides better communication among geologists, designers, contractors, and engineers.
2. Engineer's observations, experience, and judgment are correlated and consolidated more effectively by a quantitative classification system.
3. Engineers prefer numbers in place of descriptions. Hence, a quantitative classification system has considerable application in an overall assessment of the rock quality.
4. Classification approach helps in the organization of knowledge.

A large number of classification schemes has been developed by different researchers for specific and general geotechnical purposes as well (table 2.1). The earliest accessible rock mass classification system was proposed by Agricola (1556) in his famous book De Re Metallica. He classified the ore bodies and surrounding host rocks as crumbling, hard, harder and hardest and also given a short description of each category. The generalized approach given by Agricola has the least practical significance with available modern day technology and classification systems.

Table 2.1: Summary of the existing rock mass classification schemes (modified after Pantelidis, 2009; 2010; Siddique et al. 2017)

Name of the System (Abbreviations)	Authors and Year of Development	Application
–	Ritter (1879)	Tunnels
Rock Load	Terzaghi (1946)	Tunnels
Stand-up time	Lauffer (1958)	Tunnels
Rock Quality Designation (RQD)	Deere (1963)	General
New Austrian Tunneling Method (NATM)	Rabcewicz (1964)	Tunnels
Rock Classification for Rock Mechanics Purposes	Patching and Coates (1968)	General
Rock Structure Rating (RSR)	Wickham et al. (1972)	Small Tunnels
Rock mass rating (RMR)	Bieniawski (1973)	Tunnels
Rock Tunneling Quality Index (Q)	Barton et al. (1974)	Tunnels
Size-strength classification	Franklin et al. (1975)	Tunnels
Mining Rock mass rating (MRMR)	Laubscher (1977)	Mines
Geodurability Classification	Olivier (1979)	Tunnels
Rock Mass Strength (RMS)	Selby (1980)	Cuttings
Unified Rock Classification System (URCS)	Williamson (1980)	General
Excavability Index (N)	Kristen (1982)	Excavation
Modified Basic RMR (MBR)	Kendorski et al. (1983)	Mines
Simplified Rock mass rating (R)	Brook and Dharmaratne (1985)	Mines
Slope mass rating (SMR)	Romana (1985)	Cuttings
CMRS Geomechanics Classification	Venkateshwarlu (1986)	Mines
Slope Rock mass rating (SRMR)	Robertson (1988)	Cuttings
Mining Rock mass rating (MRMR)	Haines and Terbrugge (1991)	Mines
Modified Slope mass rating	Anbalagan et al. (1992)	Cuttings
Ramamurthy and Arora Classification	Ramamurthy and Arora(1993)	General
Coal Mine Roof Rating (CMRR)	Molinda and Mark (1994)	Mines
Index of Rock Mass Basic Quality (BQ)	NSCGPRC (1994)	Cuttings
Natural Slope Methodology (NSM)	Shuk (1994)	Mines
Chinese Slope mass rating (CSMR)	Chen (1995)	Cuttings
Rock Mass Number (N)	Goel et al. (1995)	Tunnels
Geological Strength Index (GSI)	Hoek et al. (1995)	General
Rock Mass Index (RMi)	Palmstrom (1995)	General
Modified Rock mass rating (M-RMR)	Ünal (1996)	Mines
Rock Slope Deterioration Assessment (RDA)	Nicholson and Hencher (1997)	Cuttings
Slope Stability Probability Classification (SSPC)	Hack (1998)	Cuttings
In-situ Rock mass rating (IRMR)	Laubscher and Jakubec (2000)	General
Dam Mass Rating (DMR)	Romana (2003)	Dams
Modified Rock Mass Classification	Şen and Sadagah (2003)	General
Volcanic Rock Face Safety Rating (VRFSR)	Singh and Connolly (2003)	Cuttings
Rock Mass Excavability (RME)	Bieniawski et al. (2006)	Tunneling
Slope Failure Index (SFi)	Jeong et al. (2007)	Cuttings
Continuous Slope mass rating	Tomás et al. (2007)	Cuttings
Rock Mass Fabric Indices (F)	Tzamos and Sofianos (2007)	Tunnels
Korean Slope mass rating (KSMR)	Song et al. (2008)	Cuttings
Modified Slope mass rating (M-SMR)	Rahim et al. (2009)	Cuttings
Hazard Index (HI)	Pantelidis (2010)	Cuttings
Slope Stability Rating (SSR)	Taheri And Tani (2010).	Cuttings
Fuzzy Slope mass rating (FSMR)	Daftaribesheli et al. (2011)	Cuttings
Graphical Slope mass rating (GSMR)	Tomás et al. (2012)	Cuttings
New Slope mass rating (NSMR)	Singh et al. (2013)	Cuttings
Rock Mass Quality Rating (RMQR)	Aydan et al. (2014)	General
Slope Quality Rating (SQR)	Fereidooni et al. (2015)	Cuttings
Slope Quality Index (SQI)	Pinheiro et al. (2015)	Cuttings
Continuous Rock mass rating	Rad et al. (2015)	General

* ISRM: International Society of Rock Mechanics; CMRS: Central Mining Research station; NSCGPRC: National Standards Compilation Group of the People's Republic of China

Brief summaries of classification systems quoted in table 2.1 have been highlighted here. Ritter (1879) designed an empirical approach for support required during tunneling. Foundation to modern classification was laid by Terzaghi (1946) by estimating rock loads carried by steel sets and developed a descriptive classification scheme for the design of tunnel support. He categorized rocks into different classes as intact, stratified, moderately jointed, blocky and seamy, swelling and squeezing rock and given a brief description of each category. Lauffer (1958) estimated stand up time for an unsupported span in tunnels. Later significant modification has been made by Pacher et al. (1974). Core recovery obtained from boreholes provides valuable information regarding the nature of rock mass in respect to the degree of fracturing or fracture frequency. But, many often core recovery was not efficient to describe the quality of rock mass. Deere et al. (1963) proposed Rock Quality Designation Index (RQD) as a quantitative basis to estimate core recovery by incorporating only those core samples having a length equal or more than 10 cm. RQD was originally developed for predicting tunneling conditions and support requirements but later the applications of RQD were extended to slope engineering and correlation with in-situ rock mechanical properties and ultimately became as a basic element in several classification systems. Deere and Deere (1988) illustrated background related to the development of RQD and briefly discussed the usage of RQD in various classification systems like RMR and Q system. They also discussed the questions raised over the applications of RQD. To determine RQD, International society of rock mechanics (ISRM) recommended core size of NX-size diameter with double tube core barrel using a diamond bit. Palmstrom (2005) illustrated limitations of RQD and have shown differences arises in RQD value by changing drilling directions. The orientation of joint relative to the observation surface or direction of drilling influence RQD value drastically i.e. joints parallel to drilling direction will give least RQD value and perpendicular will give poor value. To overcome this limitation, Hudson and Priest (1983) recommended drill three boreholes in different directions to get the actual 3-Dimensional view of the joints present in the rock mass. As conducting drilling in every project is expensive and practically cannot be performed in each site, there are some indirect methods for estimation of RQD. Singh and Goel (1999) briefly illustrated some indirect methods (seismic, volumetric joint count weighted joint density) to determine RQD. Furthermore, by the experience gained from Austrian Alpine Tunneling, Rabcewicz (1964) developed New Austrian Tunneling Method (NATM). This system monitors rock mass deformation to determine the required support system. Later, many multi-parameter schemes were developed by coupling various parameters. Rock Structure Rating (RSR) by Wickham et al. (1972) described the quality of rock mass quantitatively. RSR classification is based on

three parameters viz. geology, geometry or orientation of discontinuities and groundwater conditions. Bieniawski (1973) introduced Rock mass rating (RMR) classification system or geomechanics classification system. Initially, Bieniawski considered eight parameters (rock strength, rock quality designation, discontinuity spacing, separation of joints, continuity of joints, groundwater conditions, weathering, conditions of joints, strike and dip orientation of tunnels). Over years, this system has been successfully refined and after examining more case histories and due to a better understanding of the importance of different parameters and detailed elaboration can be consulted from Bieniawski (1974; 1975; 1976; 1989; 1990). The major revisions in RMR have been compiled by Milne et al. (1998). RMR system has been widely applied by many researchers as a systematic tool to describe rock mass quality primarily for tunneling purposes. It is based on six fundamental controlling factors: unconfined compressive strength (UCS) of intact rock samples, rock quality designation (RQD%), spacing of discontinuities, conditions of discontinuities, groundwater condition and relative orientation of discontinuities. A rating of each parameter is summed on the basis of their values and conditions. Rock Quality Index (Q-system) was developed at Norwegian Geotechnical Institute (NGI) by Barton et al. (1974) for underground excavations. Since 1974 two revisions in support chart have been made by Grimstand and Barton (1993) on the basis of 1050 examples from Norwegian underground excavations and Grimstand et al. (2002) updated the system on the basis of more than 900 examples from underground excavations from Norway, Switzerland, and India. Q-values varies on a logarithmic scale from 0.001 to 1000 calculated on the basis of several parameters i.e. RQD%, joint set number, joint roughness, joint alteration, water conditions and stress reduction factor. Support categories are suggested on the basis of equivalent dimension and Q-value by chart proposed by Barton et al. (1974) which was further updated by Grimstand and Barton (1993). Furthermore, Franklin et al. (1975) given a two-parameter based classification named as size-strength classification for rock masses. They considered block size and uniaxial compressive strength and given graphical divisions of rock quality classes. Laubscher (1977) developed Mining Rock mass rating (MRMR) as an extended version of Bieniawski's RMR system by considering some adjustment factors in addition to RMR_{basic}. Olivier (1979) considered unconfined compressive strength and free swelling potential to develop engineering geological rock durability classification named as Geodurability classification. Selby (1980) developed Rock Mass Strength (RMS) classification system to explain the relationship between rock mass strength and long term stable slope angles of natural rock outcrops. RMS system considered the strength of intact rock, state of rock weathering, joint spacing, aperture of joints, orientation of joints with respect to slope, joint

continuity and outflow of groundwater. Williamson (1980) proposed Unified Rock Classification System (URCS) by considering weathering, strength, discontinuity, and density of rock materials. Kristen (1982) proposed an Excavability Index (N) for excavation natural materials. He considered mass strength number, RQD, number of joint sets, joint roughness and relative ground structure number to calculate the excavability index. Kendorski et al. (1983) modified Bieniawski's RMR classification to develop Modified Basic RMR (MBR) for mining purposes by including an adjustment for blasting damage and induced stresses. They also included adjustment rating for distance to cave line, block size and orientation factor in adjusted MBR to suggest permanent support permanent drift support. According to Brook and Dharmaratne (1985) joint spacing were mysteriously obtained in MRMR system and suggested that RQD values are not required and developed a modified system as Simplified Rock mass rating (R) in which key parameters involved are: intact rock strength, joint spacing, joint type including continuity, surface, separation and gauge properties of joints and groundwater conditions. Later, Romana (1985) developed Slope mass rating (SMR) as a sequel of Bieniawski's RMR method which was almost impossible to apply on slopes due to lack of quantitative description of adjustment for discontinuity orientation factor in RMR. Detailed quantitative consideration of correction factors for relative orientation of discontinuities with respect to slope makes it more reliable and exhaustive to be used in stability evaluation of slopes. SMR technique is most widely employed a method for stability assessment of slopes and has gained a lot of attention of practitioners in recent years. In subsequent years it has been modified by much experience and case studies. Venkateshwarlu (1986) modified Bieniawski's geomechanics classification for estimating roof conditions and support in Indian coal mines and developed Central Mining Research Station Geomechanics Classification (CMRS Geomechanics Classification). This system includes the following parameters: layer thickness, structural features, weatherability using swelling strain and slake durability methods, strength of rock, groundwater flow. On the basis of which design guidelines for roof support in Indian Coal mines having roof span of 4.2 to 4.5 m have been suggested. Robertson (1988) suggested that groundwater parameter should not be included in RMR method because the effect of moisture is well accounted in rock strength parameter. He developed Slope Rock mass rating by increasing rating of strength of intact rock material by 15. Haines and Terbrugge (1991) used MRMR method for evaluating the stability of rock masses and proposed design charts for rock slopes using slope height, slope angle and MRMR values. Geomechanics classification SMR system proposed by Romana (1985) have only accounted for the planar and toppling mode of failures in rock slopes. A special case of structurally controlled failure i.e. wedge

failure was incorporated into the existing SMR method by Anbalagan et al. (1992) and proposed Modified Slope mass rating (MSMR). In MSMR they included correction factors for the orientation parameter for wedge mode of failure also. Ramamurthy and Arora (1993) proposed a classification on the basis of compressive strength of intact rock and modulus values in the unconfined state in a jointed rock mass. Molinda and Mark (1994) developed the Coal Mine Roof Rating (CMRR) system with the premise that the structural competence of mine rock is determined mainly by discontinuities that weaken the rock fabric. CMRR enables different aspects of mine planning including longwall pillar design roof support selection, extended cut evaluation etc. Rock Mass Basic Quality (BQ) index was proposed by National Standards Compilation Group of the People's Republic of China (NSCGPRC, 1994). This index encompasses five components to evaluate the quality of rock mass viz. compressive strength of rock mass, groundwater, weak structural planes and in-situ stress rate to classify rock mass into five different grades. Shuk (1994) developed Natural Slope Methodology (NSM) as a direct tool to assess geotechnical probabilistic slope stability with least cost and time. NSM is obtained by using two basic geometrical parameters i.e. by measuring hydrological and vertical lengths of natural slopes which can be easily obtained by topographic maps with an appropriate scale using sequential cumulative contour interval method. Chen (1995) modified Romana's SMR method and proposed a sequel of SMR as Chinese Slope mass rating (CSMR) by incorporating slope height and discontinuity factor. Rock Mass Number (N) proposed by Goel et al. (1995) is modified from Barton's Q system. Due to uncertainties and problems in obtaining a correct rating of Barton's strength reduction factor (SRF) parameter they have not considered SRF in N system. Furthermore, Hoek et al. (1995) introduced the Geological Strength Index (GSI) to estimate the reduction in rock mass strength for different geological conditions. The strength of a jointed rock mass depends upon properties of intact rock pieces and the freedom of these pieces to slide and rotate under different stress conditions which are controlled by their geometrical shapes (Hoek and Brown, 1980). According to Hoek et al. (1995) in jointed rock mass strength characteristics are governed by size and shape of blocks and on surface conditions of joints. But the quality of rock mass is best described as an integration of evaluation of both intact rock and rock mass. GSI system is chart based classification system. It is being estimated by visual interpretation of blockiness and surface conditions of discontinuities in the rock mass. With experience and more case studies, the GSI system was refined and modified several times. Furthermore, Palmstrom (1995) developed the Rock Mass Index (RMi) which involves compressive strength of intact rock, block volume, roughness, alteration and size of joint. RMi is widely used for tunnel support, TBM progress

evaluation. Later, Unal (1996) proposed Modified Rock mass rating (M-RMR) system by incorporating some new parameters in Bieniawski's RMR system for better characterization of rock mass condition by including weak, stratified, anisotropic and clay-bearing rock mass. Nicholson and Hencher (1997) proposed Rock Slope Deterioration Assessment (RDA) for assessing the susceptibility of rock cut slopes. RDA includes scoring of the rock mass is done using intact rock strength, material weathering grade, spacing and aperture of discontinuities. Obtained score is converted into rock slope susceptibility class by numerical adjustments related to engineering factors (rate and method of excavation, slope geometry, slope treatment measures, drainage), stress factors (dynamic stress due to blasting, unbalanced static stress due to excavation and surcharge loading), environmental factors (climatic influences such as moisture, temperature which are directly related to weathering). Hack (1998) developed Slope Stability Probability Classification (SSPC) by the three-step approach and probabilistic assessment of independently different failure mechanisms of slopes. Laubscher (1977) introduced Mining Rock mass rating (MRMR) by developing a CSIR geomechanics classification system by incorporating in and adjusted ratings along with some parameters related to complex mining situations. Laubscher's Mining Rock mass rating (MRMR) has been modified several times and the most recent modification was made to MRMR by Laubsher and Jakubec (2000) and named as In-situ Rock mass rating (IRMR) by incorporating rock block strength. Due to difficulty in the effective use of RMR for dam foundation purposes Romana (2003) proposed a sequel of RMR as Dam Mass Rating (DMR). According to Romana (2003) water pressure as pore pressure varies along dam foundation and also dam operates at changing water level, lack of guidelines of the adjustment factor for joint orientation are some major problems with RMR system which makes it less effective to be used in dam foundation assessment. To overcome such difficulties in the RMR system Romana introduced DMR system which quantifies adjustment factor for joint orientation. Sen and Sadagah (2003) developed Modified Rock mass rating (M-RMR) by replacing classical lump rating system by continuous grading system to remove the ambiguity of an inexperienced engineer in allocating grades based on the quantitative assessment by field and laboratory tests. This approach reduced the subjectivity of the RMR system by introducing continuous charts. Furthermore, Singh and Connolly (2003) developed Volcanic Rock Face Safety Rating (VRFSR) an empirical classification method for determining safety during excavation within volcanic rocks. It includes material strength, discontinuity spacing, rock condition, groundwater condition, the relationship between slope angle dip and its direction, height of rock face, excavation method and adjustment for overhang. On the basis of detailed evaluation of 700 road cut slopes, Jeong

et al. (2007) proposed a new geomechanical classification for slopes as Slope Failure Index (SFi). SFi evaluates the failure of cut slopes sequentially: classification of ground condition with behavioral characteristics, evaluation of internal failure factors, determination of SFi indices and failure assessment. Tomas et al. (2007) developed a Continuous slope mass rating (CSMR) by incorporating arc tangent and asymptotical continuous functions for orientation adjustment factors to reduce subjective interpretation. This method also reduced the doubts for the score to be assigned to the values near to the border of discrete classification. Tzamos and Sofianos (2007) grouped RMR, Q, GSI, and RMi classification systems and generated a Rock Mass Fabric Indices (F) for building proper design, characterization of the rock mass and better translation between among different geotechnical systems. Song et al. (2008) substituted GSI values in place of RMR parameters accept rock strength and groundwater condition in calculating SMR value and developed Korean Slope mass rating (KSMR). They also compared results of KSMR and SMR, which showed minor differences and suggested that KSMR results are close to the real stability of the slopes because the slope height is not considered in SMR. They also included optimal adjustment value for slope height using a genetic algorithm to calculate adjusted KSMR and to obtain final hazard class. Pantelidis (2010) quantified failure hazard of rock cuttings in the form of tables to develop Hazard Index (HI) method. Pantelidis gave failure hazard for seven different types of failures in rock cuttings which examine hazard for each type separately. Daftaribesheli et al. (2011) suggested that Romana's SMR classification is based on classic set theory and characterization of the rock mass is very complex. According to the classic set theory, the results may be ambiguous. So they developed a fuzzy set theory to SMR method and developed Fuzzy Slope mass rating (FSMR). Later, Tomas et al. (2012) introduced Graphical Slope mass rating (GSMR) based on an equiangular stereographical projection of discontinuities and slope. The angular relationship is being determined by these projections to determine orientation factors. Singh et al. (2013) conducted geotechnical and geophysical surveys on slopes of western Lesser Himalayas and proposed New Slope mass rating (NSMR) by adding some parameters to traditional SMR system. They incorporated the overburden thickness profile and slope angle in the existing SMR system. Aydan et al. (2014) published a new classification system Rock Mass Quality Rating (RMQR) by considering degradation degree, discontinuity set number, discontinuity spacing, discontinuity condition, groundwater seepage condition, groundwater absorption condition. Later, Fereidooni et al. (2015) developed Slope Quality Rating (SQR) method using three popular classification schemes RMR, Q, and SMR. Pinheiro et al. (2015) introduced a quality assessment index for rock slopes named as Slope Quality Index (SQI) by considering

parameters pertaining to slope stability. According to Rad et al. (2015), Bieniawski's RMR system contains uncertainties of input parameters in determining the definite boundary between the classes and assigning a specific value to a particular class is difficult. To overcome such problem they proposed Continuous Rock mass rating (CRMR) by introducing hybrid non-linear chaotic Neuro-Fuzzy system modeling for the basic RMR system. According to the authors, applying continuous functions in the RMR system, the maximum difference from judgments between experience and less experienced engineers can be reduced by 10%. According to Cai and Kaiser (2006), a large number of controlling factors and dimensions in different rock mass classification in different rock mass classification schemes made it often difficult for inexperienced users to understand the importance of each factor and its influence on classification.

2.4.1. Rock Mass Rating (RMR): Bieniawski (1973) was the first who proposed Rock mass rating (RMR), a comprehensive rating based approach for assessment of the behavior of the rock mass. RMR was developed at South African Council of Scientific and Industrial Research (CSIR) and also known as CSIR Geomechanics classification. With the passage of time, by a much comprehensive understanding of failure mechanism, factors influencing the quality of rock mass and available case histories, the RMR system was modified and rectified multitudinous times to attain and confirm the international standards and procedure to assess the quality of rock mass. Modifications were made in parameters and their ratings but the basic principle of the system had persisted. The progression and advancements in the RMR system are summarized in table 2.2.

Table 2.2: Evolution and progression of the RMR system (after Milne et al. 1998 and Rehman et al. 2018)

Parameters	RMR versions							
	1973	1974	1975	1979	1989	2011	2013	2014
Intact rock strength (MPa)	0-10	0-10	0-15	0-15	0-15	0-15	0-15	0-15
Rock quality designation (%)	3-16	3-20	3-20	3-20	3-20	–	–	–
Discontinuity spacing (m)	5-30	5-30	5-30	5-20	5-20	0-20	–	–
Discontinuity density (Joint/m)	–	–	–	–	–	–	0-40	0-40
Separation of joints (mm)	1-5	–	–	–	–	–	–	–
Continuity of joints (m)	0-5	–	–	–	–	–	–	–
Weathering	1-9	–	–	–	–	–	–	–
Groundwater conditions	2-10	2-10	0-10	0-15	0-15	0-15	0-15	0-15
Conditions of joints	–	0-15	0-25	0-30	0-30	0-30	0-30	0-20
Alterability (%)	–	–	–	–	–	–	–	0-10

For distinct geotechnical applications, many extensions of the RMR system were proposed by incorporating certain parameters in existing Bieniawski's RMR (table 2.3). In slope stability assessment, RMR_{1989} version is much exhaustive and widely used. It involves six fundamental geotechnical parameters (table 2.4):

1. Strength of intact rock material
2. Drill core quality by RQD%
3. Spacing of discontinuities
4. Conditions of discontinuities (persistence, aperture, roughness, infilling and weathering)
5. Groundwater conditions
6. Adjustment for the orientation of discontinuities

Each parameter in the RMR system is having a range of rating that symbolizes the quality of rock mass. The algebraic sum of ratings of the first five parameters tells about the basic quality of rock mass which is to be adjusted with the parameter discontinuity orientation to calculate total or adjusted RMR value. The adjusted RMR values have been grouped or categorized into five vulnerability classes (table 2.4).

Table 2.3: Major extensions of the RMR system with their authors, year of publication, applications, and country in which they were originated

System	Authors	Applications	Country
Rippability classification	Weaver (1975)	Rippability	South Africa
Mining Rock Mass Rating (MRMR)	Laubscher (1977)	Mining	South Africa
Rock Durability classification	Olivier (1979)	Weatherability	South Africa
Coal Mine Research Station (CMRS Geomechanics Classification)	Ghose and Raju (1981)	Coal Mining	India
Surface Rock Classification (SRC)	Vallejo (1983)	Tunnels	Spain and Italy
Slope Mass Rating (SMR)	Romana (1985)	Slopes	Spain
	Smith (1986)	Dredgeability	USA
	Venkateshwarlu (1986)	Coal mining	India
Slope Rock Mass Rating (SMR)	Robertson (1988)	Slopes	Canada
	Orr (1992)	Slopes	
	Unal (1996)	Weak rocks in the coal mine	Turkey
Dam Mass Rating (DMR)	Romana (2003)	Dams	Spain
Span Design Curve	Pakalnis et al. (2007)	Mines	Canada

Table 2.4: Rock Mass Rating (after Bieniawski, 1989)

A. Classification Parameters and their Ratings								
Parameters	**Range of values**							
1. Strength of intact rock material								
Point load strength index (MPa)	> 10	4 - 10	2 - 4	1 - 2	For this low range - uniaxial compressive test is preferred			
Uniaxial compressive strength (MPa)	> 250	100 - 250	50 - 100	25 - 50	5 - 25	1 - 5	< 1	
Ratings	*15*	*12*	*7*	*4*	*2*	*1*	*0*	
2. Drill core quality (RQD %)	90% - 100%	75% - 90%	50% - 75%	25% - 50%	< 25%			
Ratings	*20*	*17*	*13*	*8*	*3*			
3. Spacing of discontinuities	> 2 m	0.6 - 2m	200 - 600 mm	60 - 200mm	< 60 mm			
Ratings	*20*	*15*	*10*	*8*	*5*			
4. Condition of Discontinuities	Very rough surfaces Not continuous No separation Unweathered wall rock	Slightly rough surfaces Separation < 1 mm Slightly weathered walls	Slightly rough surfaces Separation < 1 mm Highly weathered walls	Slickensided surfaces or Gouge < 5 mm thick or Separation 1 – 5 mm Continuous	Soft gouge > 5 mm thick or Separation > 5 mm Continuous			
Ratings	*30*	*25*	*20*	*10*	*0*			
5. Groundwater								
Inflow per 10 m tunnel length (L/min)	None	< 10	10 - 25	25 - 125	> 125			
Joint water pressure/ Major principal σ	0	< 0.1	0.1 - 0.2	0.2 - 0.5	> 0.5			
General conditions	Completely dry	Damp	Wet	Dripping	Flowing			
Ratings	*15*	*10*	*7*	*4*	*0*			
B. Rating adjustment for discontinuity orientations								
Strike and dip orientations		**Very Favorable**	**Favorable**	**Fair**	**Unfavorable**	**Very Unfavorable**		
Ratings	*Tunnels and Mines*	*0*	*- 2*	*- 5*	*- 10*	*- 12*		
	Foundations	*0*	*- 2*	*- 7*	*- 15*	*- 25*		
	Slopes	*0*	*- 5*	*- 25*	*- 50*	*- 60*		
C. Rock mass classes determined from total ratings								
Rating		*100 - 81*	*80 - 61*	*60 - 41*	*40 - 21*	*< 21*		
Class No.		I	II	III	IV	V		
Description		Very good rock	Good rock	Fair rock	Poor rock	Very poor rock		
D. Meaning of rock classes								
Class No.		I	II	III	IV	V		
Average stand-up time		20 yr for 15 m span	1 yr for 10 m span	1 wk for 5 m span	10 h for 2.5 m span	30 min for 1 m span		
Cohesion of rock mass (kPa)		> 400	300 - 400	200 - 300	100 - 200	< 100		
Friction angle of rock mass (deg)		> 45	35 - 45	25 - 35	15 - 25	< 15		

Continued….

E. Guidelines for classification of discontinuity conditions					
Discontinuity length (persistence)	< 1 m	1 - 3 m	3 - 10 m	10 - 20 m	> 20 m
Rating	*6*	*4*	*2*	*1*	*0*
Separation (aperture)	None	< 0.1 mm	0.1 - 1.0 mm	1 - 5 mm	> 5 mm
Rating	*6*	*5*	*4*	*1*	*0*
Roughness	Very rough	Rough	Slightly rough	Smooth	Slickensided
Rating	*6*	*5*	*3*	*1*	*0*
Infilling (gouge)	None	Hard Filling < 5 mm	Hard Filling > 5 mm	Soft Filling < 5 mm	Soft Filling > 5 mm
Rating	*6*	*4*	*2*	*2*	*0*
Weathering	Unweathered	Slightly weathered	Moderately weathered	Highly weathered	Decomposed
Rating	*6*	*5*	*3*	*1*	*0*

F. Effect of discontinuity strike and dip orientation in tunneling			
Strike perpendicular to tunnel axis		Strike parallel to tunnel axis	
Drive with dip - Dip 45 - 90°	Drive with dip - Dip 20 - 45°	Dip 45 - 90°	Dip 20 - 45°
Very favourable	*Favourable*	*Very unfavorable*	*Fair*
Drive against dip - Dip 45 - 90°	Drive against dip - Dip 20 - 45°	Dip 0 - 20° - Irrespective of strike	
Fair	*Unfavorable*	*Fair*	

Applications of RMR system: RMR classification system is mainly used in tunnel drifting, driving and some other underground rock engineering projects. It provides a comprehensive assessment of rock mass quality, planning for pre-design excavation during the feasibility stage of the project. From a couple of decades, it has been employed to assess or determine unsupported span time of rock mass, support load, type of support to be used, modulus of elasticity, stand-up time, cohesion and angle of internal friction of rock mass. The revised version of RMR is widely used for foundation evaluation, mining and to evaluate the stability of slopes. However, while applying RMR in slopes, care should be taken as sometimes it may give meaningless or worthless results due to a certain lacuna in quantitative consideration of the parameter related to the orientation of discontinuities.

2.4.2. Slope Mass Rating (SMR): SMR Geomechanics classification was developed by Romana (1985) as a sequel to Bieniawski's RMR which sometimes give an unreliable estimate of stability classes particularly for slopes. SMR was developed on the basis of 28 natural and excavated slopes (Taheri, 2012). The RMR system lacks in the quantitative description in classes related to orientation factor and contemplation of their extreme range (up to 60 points in the maximum of 100). Slight misjudgment in the class related to orientation factor may mislead the results with great extent. To cope with these limitations, the SMR system is best suited. Furthermore, a remarkable modification in SMR was made by Anbalagan et al. (1992) by incorporating wedge mode of failure with its correction factors and proposed Modified Slope Mass Rating (MSMR). Many researchers from different parts of the globe applied SMR method to assess stability grade of engineered or excavated and natural slopes. However, there are certain limitations in SMR, as it does not consider non-structurally controlled failures and does not take an account of the geometry of slope. Despite this limitation, SMR is extensively employed for slope stability appraisal in jointed rock masses with appreciable success confidence in the feasibility stage of the project.

SMR is calculated as per equation 2.1 by adding RMR_{Basic} and some factorial adjustment factors related to the relative orientation of slope facet and discontinuities present within the rock mass and a factor depending upon the method of excavation (table 2.5).

$$SMR = RMR_{Basic} + (F_1 \times F_2 \times F_3) + F_4 \qquad \text{Equation 2.1}$$

where, F_1, F_2, F_3 are factorial adjustment factors depending upon the relative orientation of slope and discontinuity for the different mode of structurally controlled failures and F_4 is related to the method of excavation.

F_1 depends upon parallelism between the dip direction of discontinuity and slope facet which is calculated by using dip direction of slope and discontinuity causing planar or toppling mode of failure. While for wedge failure dip direction of slope and trend of line formed intersection of two potential discontinuities forming wedge failure is considered.

F_2 refers to dip amount of discontinuity for planar or wedge mode of failure while for toppling failure F_2 remains 1.

F_3 is related to the relationship between slope inclination and dip amount of discontinuity causing planar or toppling failure. While for wedge failure slope inclination and amount of plunge formed by the intersection of two potential discontinuities forming wedge is considered.

F_4 depends upon the method of excavation. Romana (1993) had published certain guidelines for the estimation F_4 parameter as follows:

Natural slopes (F_4 = +15)

Natural slopes are more stable due to long-time erosion and built-in protection mechanisms like vegetation crust desiccation etc.

Presplitting ($F_4 = +10$)

A row of holes is drilled along the final face.

Each hole is carefully marked in the field.

Holes must be parallel (± 2%).

The distance between boles is in the order of 50-80 cm.

Charges are decoupled from blast hole walls, leaving air space.

Charges are very light.

The row is fired before the main blast.

Smooth blasting($F_4 = +8$)

A row of boles is drilled along the final face.

Each hole is carefully marked in the field.

Holes must be parallel (± 2%).

The distance between holes is in the order of 60-100 cm.

Charges are light.

The row is fired after the main blast (sometimes using micro-delays).

Normal blasting ($F_4 = 0$)

Each blast is done according to a previously fixed scheme.

Each hole is marked in the field.

Charges are kept to the minimum possible.

Blast is fired sequentially, using delays or micro-delays.

Deficient blasting ($F_4 = –8$)

The blasting scheme is only a general one.

Charges are not the minimum possible.

Blast is not fired sequentially.

Table 2.5: Slope Mass Rating (after, Romana, 1985; Anbalagan et al. 1992; Romana, 1991; Romana, 1993; Romana et al. 2003; Romana et al. 2015; Tomas et al. 2007)

Type of Failure	*Parameters*	Auxiliary angles	Very Favorable	Favorable	Normal	Unfavorable	Very Unfavorable
P	A	$\lvert\alpha_j-\alpha_S\rvert$	>30°	30–20°	20–0°	10–5°	<5°
T		$\lvert\alpha_j-\alpha_S-180\rvert$					
W		$\lvert\alpha_i-\alpha_S\rvert$					
P/T/W	***F_1***		***0.15***	***0.40***	***0.70***	***0.85***	***1.00***
P/W	B	$\lvert\beta_j\rvert$ / $\lvert\beta_i\rvert$	<20°	20–30°	30–35°	35–45°	>45°
P/W	***F_2***		***0.15***	***0.40***	***0.70***	***0.85***	***1.00***
T	***F_2***		**1.00**				
P	C	$\beta_j-\beta_s$	>10°	10–0°	0°	0–(–10°)	<(–10°)
T		$\beta_j+\beta_s$	<110°	110–120°	>120°	–	–
W		$\beta_i-\beta_s$	>10°	10–0°	0°	0–(–10°)	<(–10°)
P/T/W	***F_3***		***0***	***–6***	***–25***	***–50***	***–60***
F_4 (Method of Excavation)			Natural Slope	Presplitting	Smooth Blasting	Blasting or Mechanical	Deficient Blasting
			+15	***+10***	***+8***	***0***	***–8***
Class number			Vb | Va	IVb | IVa	IIIb | IIIa	IIb | IIa	Ib | Ia
Description			Very Bad	Bad	Fair	Good	Very Good
Stability			Completely Unstable	Unstable	Partially Unstable	Stable	Completely Stable
Failures			Big Planar or Soil like	Planar or Big Wedges	Many Wedges	Some Blocks	None
Support			Reexcavation	Important/ Corrective	Systematic	Occasional	None

Note: P: Planar failure; T: Toppling failure; W: Wedge failure; A, B and C: Auxiliary angles; α: Dip Direction; β: Dip amount; s: Slope; j: Joint; i: Intersection of two joints; F_1, F_2 and F_2: Factorial adjustment factors related to orientation and F_4: Factor for method of excavation

2.4.3. Continuous Slope Mass Rating (CSMR): The SMR method is a discrete classification system which is calculated by assigning a particular rating to each parameter. The discrete nature may often cause major changes in the value due to the minor disparity in the value of the variable (Tomás et al. 2007). To cope with these constraints and to attain more realistic results, continuous functions were incorporated in Romana's SMR method and Continuous Slope Mass Rating was proposed by Tomás et al. (2007). Continuous functions had reduced the uncertainty that arises when values lie at the border of class intervals. Hence, close approximation and computation can be done by using continuous functions. The adjustment factors using continuous functions can be calculated by the following equations (2.2 to 2.5):

$$F_1 = \frac{16}{25} - \frac{3}{500}\arctan\left(\frac{1}{10}(|A| - 17)\right) \qquad \text{Equation 2.2}$$

where,

$A = |\alpha_j - \alpha_s|$ for planar failure

$A = |\alpha_j - \alpha_s - 180°|$ for toppling failure

$A = |\alpha_i - \alpha_s|$ for wedge failure

$$F_2 = \frac{9}{16} + \frac{1}{195}\arctan\left(\frac{17}{100}B - 5\right) \qquad \text{Equation 2.3}$$

where,

B = β_j for planar failure

B = β_i for wedge failure

F_2 remains 1 for toppling mode of failure

$F_3 = -30 + \frac{1}{3}\arctan C$ (For planar and wedge Failure) Equation 2.4

where,

C = βj-βs for planar failure

C = β_i-β_s for wedge failure

$F_3 = -13 - \frac{1}{7}\arctan(C - 120)$ (For Toppling Failure) Equation 2.5

where,

C = β_j+β_s for toppling failure

Note: For all the above equations, arctangent will be in degrees.

α_s is dip direction of slope, α_j is dip direction of joint, β_s is dip amount of slope, β_j is dip amount of joint, α_i is dip direction or trend of the line formed by the intersection of two discontinuities and β_i is the amount of plunge of the line formed by the intersection of two discontinuities.

2.4.5. Geological Strength Index (GSI): Geological Strength Index (GSI) classification system was proposed by Hoek et al. (1995). The characterization via GSI system is being done by a chart-based approach that relies upon blockiness of the rock mass or degree of fracturing and certain conditions related to discontinuity surfaces. It has been developed in engineering rock mechanics to meet the need for reliable input data related to rock mass properties that are required as input in various numerical modeling or closed form solutions for designing tunnels, slopes, foundations in rocks (Marinos et al. 2005). GSI system has been widely used to calculate the deformation and strength parameters of the rock mass in a large number of international tunneling projects. GSI classification tells about the quality of the rock mass and does not consider the effect of orientation of discontinuities. Nevertheless, it overcomes the limitations of expensive and time-consuming laboratory experiments of intact samples only. The geomechanical properties of intact rock i.e. devoid of any discontinuity always show higher values. As the rock mass is jointed, their effect come into play which is well accounted in the GSI system. Although GSI values can be estimated by various existing empirical relationships by distinct rock mass classifications like RMR and Q system, Hoek (2000) recommended that GSI chart should be used to acquire better results. Furthermore, Hoek (2000) also suggested that a single value of GSI should not be assigned to a particular rock

mass or site rather a range of GSI values should be determined in the field. As the GSI is directly correlated to several equations in GHB criterion and deformation modulus of rock mass the subjectivity of the system ought to be removed. To surmount these restrictions and constraints, Sonmez and Ulusay (1999 and 2002) proposed two parameters namely structure rating (SR) and surface condition rating (SCR). The former depends upon blockiness or degree of fracturing in the rock mass and it can be calculated by the empirical relationship among SR and volumetric joint count (Equation 2.6). The latter relies upon certain factors that are related to the conditions of discontinuities like roughness, weathering and infilling material (Equation 2.7). These parameters are calculated as follows and plotted in modified GSI chart Sonmez and Ulusay in 2002 (figure 2.1).

$SR = -17 \ln (J_v) + 79.8$ Equation 2.6

$SCR = Rr + Rw + Rf$ Equation 2.7

where, J_v: volumetric joint count; Rr: roughness rating, Rw: weathering rating; Rf :Infilling rating.

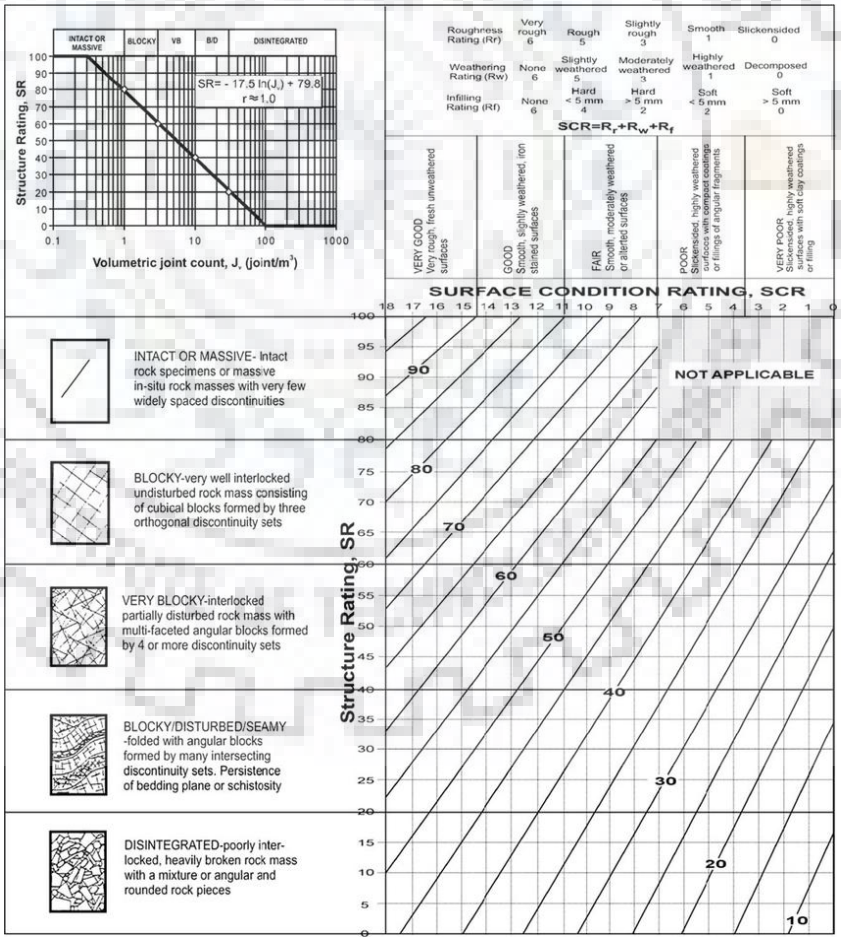

Figure 2.1: Quantitative Geological strength index chart (Sonmez and Ulusay, 2002)

2.5. Kinematic analysis: Kinematics also called as 'geometry of the motion'. It is the branch of classical mechanics that evaluate the motion of point/ object/ body irrespective to its cause of motion (Goodman, 1989). It is a purely geometric evaluation of slopes that determine the angular relationships among slope face and discontinuities in the rock mass. It identifies the potential for different modes of structurally controlled failures due to unfavorably oriented discontinuities. It widely conducted on Schmidt type stereonet. It does not consider external forces such as water pressure or reinforcement which can have a significant effect on stability (Wyllie and Mah, 2004). Only qualitative assessment of various structurally controlled failures like planar, toppling and wedge mode can be made by this method. The angle of internal friction plotted as friction cone on stereonet, the orientation of pertaining discontinuities and slopes represented by great circles or as their poles are some keys and essential inputs for the kinematic evaluation of slopes. According to Rocscience, Friction cone defines the limits of frictional stability on a stereonet while considering dip vectors. The angular relationship between structural discontinuities in rocks and the gradient along with the aspect of topography defines the probability for different modes of failures (Goodman and Bray, 1976; Hoek and Bray, 1981; Yoon et al. 2002; Wyllie and Mah, 2004). A sketch depicting structurally controlled failures has been shown in figure 2.2. According to Wyllie and Mah (2004) if the strike of discontinuity is nearly parallel (±20º) may to the trend of slope and dip of discontinuity is gentle than that of the slope, then planar failure is likely to occur. If the strike of discontinuity is nearly parallel (±20º) to the trend of the slope but discontinuity is dipping steeply in opposite to that of slope direction it will give rise to toppling failure mode conditions. In toppling mode of failure, the weight vector of rock blocks rests on an inclined plane falls outside the base of the block (Wyllie and Mah, 2004). Wedge failure is likely to occur when two discontinuity individually not forming any failure but they intersect in such a way that the line formed by their intersection daylight into slope face i.e. amount of plunge is smaller than the angle of slope provided the plunge of the intersection should also exceed the friction angle. However, Goodman (1989) suggested that parallelism direction may vary from ±20º to ±30º. The exact angle is not fixed, the vulnerability is most at zero degrees and decreases gradually as it approaches a higher degree.

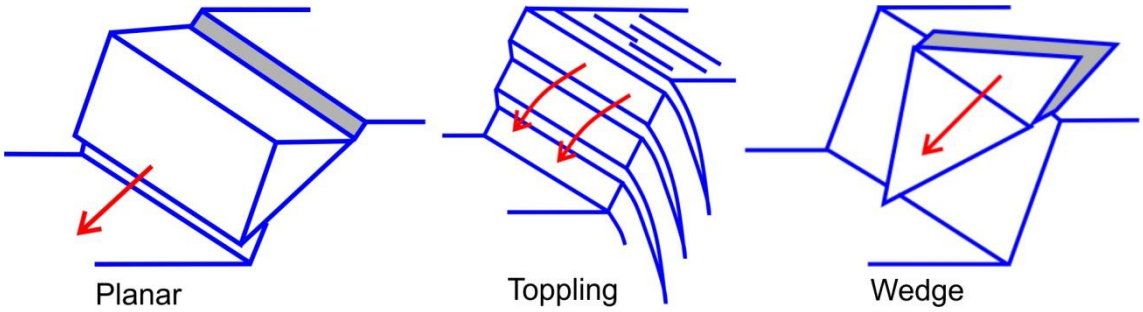

Figure 2.2: Sketch showing typical planar, toppling and wedge mode of failures

2.6. Numerical modeling: Due to the complexity of processes involved in driving slope failures and our inadequate knowledge of the underlying mechanism, researchers are still not capable to have excellent control over the prediction of slope failures. Numerical modeling is one of the most widely used techniques in different domains of geological engineering. This technique relies upon the computer-based approach that attempts to represent the mechanical response of the material subjected to a well-defined set of initial conditions such as geomechanical properties in situ stresses and water conditions, boundary conditions and induced changes like excavation, seismic shaking etc. (Wyllie and Mah, 2004). From a couple of decades, applications of numerical modeling had gained appreciable attentions and provided reasonable solutions to the complex geotechnical issues across the globe. The geomechanical behavior of the material under static and dynamic conditions is widely conducted by numerical modeling techniques (Singh and Monjezi, 2000; Monjezi et al. 2004; Singh et al. 2010; Verma and Singh, 2010; Sarkar et al. 2012). By virtue of rapid expansion and progression in computational potency, the use of such techniques had in slope stability assessment has been amplified to manifolds. Numerical modeling techniques are efficient in determining the prime cause of the problem. From a couple of decades, numerous researches have been undertaken to attain secure and functional design in various surface and underground geotechnical projects (Singh et al. 2010; Umrao et al. 2017). Computer-aided numerical modeling techniques are widely used to build conceptual models and theories by integrating the knowledge of geology, computer science, mathematics, physics and statistics (Jing and Hudson, 2002; Jing, 2003). In numerical modeling technique, the rock mass is divided into distinct zones and geomechanical properties of each zone are assigned. The robust advantage of such techniques enabled the users to identify the root cause and underlying concealed behavior of the mechanism of slope failures. Numerical methods can be categorized as continuum, discontinuum and hybrid methods. In Continuum method, the complete material is assumed as continuous mass and uniformly distributed while in discontinuum modeling the material is treated as heterogeneous

mass due to the presence of discontinuities (Jing and Hudson, 2002; Eberhardt, 2003; Jing, 2003). According to Jing and Hudson, 2002; Eberhardt, 2003; Jing, 2003; Nikolic et al. (2016) Continuum methods includes Finite Element Method (FEM), Finite Difference Method (FDM), Finite Volume Method (FVM), Boundary Element Method (BEM) and Meshless methods; Discontinuum methods includes Discrete Element Method (DEM) and Discrete Fracture Network Method (DFM) while Hybrid methods includes Discrete Finite Element method (DFEM) and Combined Finite-Discrete Element Method (FEM/DEM). The selection form aforementioned methods depend upon several site-specific factors, scale of the project and geometry of the fracture system (Eberhardt, 2003; Jing, 2003). In the present study, continuum modeling has been used because it is widely applicable and probably best suited for weak and jointed rock mass.

2.6.1. Limit Equilibrium Method (LEM): LEM is a conventional approach that has been extensively used in stability assessment of artificial dumps, debris, and soil slopes (Loukidis et al. 2003; Behera et al. 2016; Sarkar and Samanta, 2017). It is also known as the method of slices in which slip surfaces are supposed as perpendicular to the length of slope length and then equilibrium conditions are being assessed. In LEM the equilibrium for shear failure is assumed as independent of the stresses within the blocks that are bordered by shear surfaces (Morrison and Greenwood, 1989). In this method, material above assumed slip surface is divided into a large number or series of vertical slices. The iterative method is used to determine the factor of safety along each slip surface (Espinoza et al. 1992). The surface having least factor of safety is demarcated as critical slip surface and overall safety factor is determined. Although, the pre-assumption of locating slip surface is a major drawback of LEM by virtue of its simplicity, quick and cost-effective assessment it is widely employed during feasibility stage of the project where less capital is to be invested. Earlier, LEM involves a very tedious process in which the calculations were done by using a calculator, equations, and charts. But, rapid expansion in computer efficiency had reduced this issue and now it is being conducted by a computer package which is time and cost-effective means. From a couple of decades, Deterministic and sensitivity analyses by LEM were performed by using computer software packages which are being discussed here. In the deterministic analysis, a factor of safety (FoS) is determined. FoS it is the ratio of shear strength to stresses which give a quick estimate of stability condition of the slope. In other words, FoS may be defined as the ratio of ultimate shear strength to the mobilized shear stress at incipient failure (Cheng and Lau, 2014). If the FoS is less than 1, the slope is unstable and liable to fail. In sensitivity analysis, the effect

of an individual parameter on FoS is determined by changing one parameter at a time and keeping others constant (Siddique and Pradhan, 2018). However, multivariable sensitivity can also be performed in computer package SLIDE which enables the users to understand the influence of different parameters at a single time. There are several LE methods which are having minor differences from each other. Broadly LEM can be categorized into two as rigorous and non-rigorous. The former consider both force and moment equilibrium while later consider only i.e. one either force equilibrium or moment equilibrium. According to Cheng and Lau (2014), Moment equilibrium is applied for the rotational type of slides while force equilibrium is used in both translational and rotational type of landslides that are having a plane and polygonal slip surfaces. Some commonly limit equilibrium methods having disparities in consideration of inter-slices forces and shape of slip surfaces are summarized in table 2.6. Zhu et al. (2003) undertaken critical review over various limit equilibrium methods and suggested that while applying different method, the position of critical slip surface may differ and they also concluded that Morgenstern-Price and Spencer methods are the most useful among all especially in case of non-circular failure. Among various LE methods, the rigorous Morgenstern-Price (M-P) method is the most reliable that satisfies the complete equilibrium conditions (Zheng, 2012). Although FoS differ by using the distinct method but the differences are in decimals which is almost negligible while formulating any design. So, good engineering sense should be considered rather than too much relying on numbers.

Table 2.6: Some commonly used LEM and disparities among them (after Duncan and Wright; 1980; Fredlund, 1984; Duncan 1996)

Methods	Author(s) and year of publication	Type of method	Inter-slice forces		Shape of the slip surface
			Moment Equilibrium	Force Equilibrium	
Ordinary/Fellenius	Fellenius(1927)	Non-Rigorous	Yes	No	Circular
Bishop Simplified	Bishop (1955)	Non-Rigorous	Yes	No	Circular
Janbu Simplified	Janbu (1968)	Non-Rigorous	No	Yes	Any Shape
Janbu Corrected	Janbu (1973)	Rigorous	Yes	Yes	Any Shape
Spencer	Spencer(1967)	Rigorous	Yes	Yes	Any Shape
GLE/Morgenstern-Price method	Morgenstern & Price's, (1965)	Rigorous	Yes	Yes	Any Shape

2.6.2. Finite Element Method (FEM): FEM is well known advanced numerical simulator and able to assess the behavior of slope forming material (Pouya and Ghoreychi, 2001; Rocscience, 2001; Hammouri et al. 2008; Sitharam 2009; Singh et al. 2001). The most robust advantage of FE over LE method is that the factor of safety is calculated without prior assumption or commitment of failure mechanism (Griffiths and Lane, 1999). In recent times, FEM has been

successfully applied in slope stability assessment in precarious Himalayan slope conditions (Kanungo et al. 2013; Pain et al. 2014; Gupta et al. 2016; Jamir et al. 2017). Shear Strength Reduction (SSR) technique in FEM is one the most exhaustively used method in a variety of geotechnical practices (Matsui and San, 1992; Duncan, 1996; Dawson et al. 1999; Griffiths and Lane, 1999; Hammah et al. 2005). This technique was first employed in 1966 and gained tremendous popularity. Later, many researchers applied this technique successfully to deal with different geotechnical issues, some of the recent examples have been quoted here (Zheng et al. 2009; Gover and Hammah, 2013; Pain et al. 2014; Gupta et al. 2016; Krabbenhoft and Lyamin, 2015; Sharma et al. 2017; Acharya et al. 2017; Maji, 2017). In SSR method, shear strength parameters (cohesion and angle of internal friction) of slope forming material are reduced until failure occurs and critical Strength Reduction Factor (SRF) is calculated which is equivalent to Factor of Safety (Gover and Hammah, 2013; Sharma et al. 2017). FoS may be defined as the ratio of resistive to driving forces (Singh et al. 2008; Pradhan et al. 2014), thereby if FoS is less than 1, the slope is unstable and liable to fail. If FoS slightly higher than 1 (may be up to 1.2), the slope is marginally stable and extreme triggering events like heavy rainfall or seismicity may disrupt the slope equilibrium and can cause failure. However, if FoS is sufficiently greater than 1 (approximately greater than 1.2), then the slope is fairly stable. By thumb rule, higher the FoS more will be the stability.

Several attempts have been made to compare traditional LE and FEM in geotechnical engineering practices and most of them have suggested that FEM gives slightly lower safety factor than obtained by LEM (Dawson et al. 1999; Baba et al. 2012; Matthews et al. 2014; Singh et al. 2014; Alemdag et al. 2015; Liu et al. 2015; Tschuchnigg et al. 2015). Griffiths and Lane (1999) highlighted some key differences between traditional LEM and FEM and elaborated the advantage of FEM over LEM. Although LE approach is significantly quick and consume less time and also capable with low computational efficiency but the major drawback with LEM is the assumption of failure surface. It is quite obvious that due to more rigorous computations and simulation process in FEM enables it to provide much better insight into the problem and accurate outcomes. However, the choice of method largely depends upon the stage of investigation and some ground issues like allocated time for the project, budget sanctioned for the project etc. In this study, Phase2D was used which is an elasto-plastic finite element computer package.

FEM is an elasto-plastic based approach that has been widely accepted in research arena of geotechnical engineering domain because it does not require any prior assumption of locating slip surface (Gupte et al. 2013; Monjezi et al. 2004) and furthermore, the outcomes by

FEM are non-linear and iterative in nature (Griffiths and Lane, 1999; Rocscience, 2001). Earlier, assessment of slope stability analyses was conducted by hand-handled and time consuming traditional approaches that need lots of calculations by using tables, charts, and calculators which may have low accuracy and tedious task to execute in every circumstance. With time and rapid advancement in the efficiencies of computers facilitated the researchers to deal and solve complex geotechnical issues within a short span of time (Duncan, 1996). It is a cost and time effective approach with iterative potential makes it much trustworthy in designing the best efficient solutions to the various problems in slope engineering practices. In contrast to conventional LEM where pre-assumption of slip surface is mandatory, in FEM failure occurs naturally through the zone along which shear stresses overcome shear strength of the material without any such pre-assumption related to the location of slip surface (Griffiths and Lane, 1999; Eberhardt, 2003; Maji, 2017). This capability of FEM suppresses the LEM significantly. Ample case studies by FEM were conducted across the globe, particularly in assessment of landslides (Vishal et al. 2010; Baba et al. 2012; Pain et al. 2014; Sarkar et al. 2015; Mahanta et al. 2016; Verma et al. 2016; Jamir et al. 2017; Maji, 2017; Singh et al. 2017; Kumar et al. 2018). Majority of them had computed FoS and also determined the root cause of the instability along with their potential failure mechanism.

2.6.3. Shear Strength Reduction (SSR) technique: In numerical modeling methods, computation of FoS is the most convenient way to have a brief insight of existing stability of slopes at a glance. The quantification of FoS is probably the quickest and easiest way to determine the probability of risk posed due to slope failure. FoS may be defined as the ratio of actual shear strength to the minimum shear strength required to resist the failure (Zheng et al. 2009; Kundu et al. 2016; Siddique and Pradhan, 2018). In SSR technique enormous simulations are performed for a series of trial of FoS (Matsui and San, 1992). During successive iterations, shear strength is reduced until the failure occurs. In each trial, shear strength parameters i.e. cohesion (c) and angle of friction (φ) are reduced according to the equations below (2.8 & 2.9):

$$C_{trial} = \left(\frac{1}{f}\right) C \qquad \text{Equation 2.8}$$

$$\varphi_{trial} = \arctan\left(\frac{1}{f}\right) \tan\varphi \qquad \text{Equation 2.9}$$

Thus, critical strength reduction factor (SRF) is computed which is equivalent to FoS. SSR technique reduces the shear strength envelope of the material by a factor of safety and computes until the deformations are unacceptably large or solutions do not converge (Hammah

et al. 2005). Under variable site conditions, the SSR technique in FEM has been widely employed across the globe and provided appreciably fair outcomes which helped in suggesting best efficient and functional design (Matsui and San, 1992; Dawson et al. 1999; Hammah et al. 2005; Krabbenhoft and Laymin, 2015; Tschuchnigg et al. 2015).

2.7. Failure criteria for rock mass and debris slopes: The relationship among peak stress (σ_1) at failure with varying confining stresses ($\sigma_2 = \sigma_3$) determines the failure criterion (Singh et al. 2005). Some commonly used failure criteria in numerical modeling are: Mohr-Coulomb criterion (Coulomb, 1776 and Mohr, 1900); Hoek-Brown criterion (Hoek and Brown, 1980); Ramamurthy criterion (Ramamurthy et al. 1993); Ramamurthy and Arora criterion (Ramamurthy and Arora, 1994); Generalized Hoek-Brown criterion (Hoek et al. 1995); Modified Mohr-Coulomb criterion (Singh and Singh, 2012). Coulomb assumed that shear strength of rock is the function of cohesion and angle of internal friction and failure envelope is linear. The linear failure envelope is quite applicable to homogeneous material like artificial dumps, debris or debris slopes. Similarly, intact rock pieces are devoid of any discontinuities and treated as homogeneous, the failure in such circumstances is appreciably simple as compare to jointed rock. Due to the presence of multiple sets of discontinuities in the jointed rock mass, the failure mechanism changes continuously as a response of coupled effect of several factors due to which the shear strength envelope is curvilinear particularly at lower normal stresses. Therefore, it is an inadequate practice to use geomechanical strength properties of intact rock for any rock slope design involving heterogeneous mass. The degree and extent of joints along with their characteristics pertaining to shear strength must be considered. In discontinuous rock mass, the failure occurs primarily along existing discontinuities within the rock mass and partially through the intact rock. Furthermore, the failure in jointed rock mass largely depends upon the magnitude of stresses experienced. At low normal stresses, the individual block may move or rotate due to less cohesion but at high normal stress levels, friction is reduced and diminished due to the crushing of joint walls. Shear failure in such jointed rock mass occurs by coupling several mechanisms such as shearing of the rock mass, sliding of blocks along discontinuities and/or rotational and translational movement of individual intact rock blocks (Singh et al. 2019). The extensive experimental data of shear failure in jointed rock mass also suggest that the failure envelope is curvilinear which shows concavity towards the axis of normal stress (Singh et al. 2005; Hoek et al. 2013). According to Wyllie and Mah (2004) in case of large slopes, it is nearly unattainable to model each and every structural discontinuity and material characteristics varying at a small scale. Therefore under

such circumstances, the rock mass can be replicated by an equivalent continuum in which the impact of discontinuities can be included by using Hoek and Brown (H-B) failure criterion (Wyllie and Mah, 2004). H-B failure criterion for jointed rock mass is based upon several empirical equations that characterize the stress conditions related to a failure of intact rock and rock mass. It has been derived from the crack theory of Griffith (1920 and 1924) in brittle rocks (Hoek, 1968) and later modified several times according to the field observations and laboratory experiments (Marsal, 1967 and Jaeger, 1969). Unlike linear MC criterion, H-B is an empirically derived criterion which relies upon a non-linear increase in peak shear stress with confining stresses (Eberhardt, 2012). According to Barton (2013), while performing various numerical modeling, the non-linear failure envelope in jointed rock mass has been ignored from a long time. The original H-B failure criterion was introduced by Hoek and Brown (1980) in which empirical relationships were scaled with respect to the geological characteristics of the rock mass (Hoek and Marinos, 2007). The H-B (1968) criterion is expressed as equation 2.10:

$$\sigma_1' = \sigma_3' + \sigma_{ci}\sqrt{\frac{m\sigma_3'}{\sigma_{ci}} + s} \qquad \text{Equation 2.10}$$

where, σ_1' and σ_3' are major and minor effective principal stresses at failure respectively.
σ_{ci} is the uniaxial compressive strength of the intact rock; 'm' and 's' are material constants.

In the above equation, the parameter 'm' is equivalent to the friction of the rock mass. while, 's' is related to the degree of fracturing that relates to the cohesion of the rock mass (Eberhardt, 2012). Since, the development of the H-B criterion, several modifications and updates were incorporated in the original criterion. Some key modifications have been briefly illustrated and meticulous journey of the criterion was published by Hoek and Marinos (2007). During the early phases of the criterion, the authors want a simple and quick means for evaluating geological observations. For this purpose, they used Bieniawski's RMR system. Later, it was soon perceived by the authors that the RMR system is not sufficient to deal with very poor quality rock mass and it also relies on numbers too (Hoek and Marinos, 2007). Furthermore, to reduce the double count of certain factors like groundwater conditions and adjustment for orientation of discontinuities Hoek et al. (1988) recommended that the ratings of groundwater conditions and an adjustment factor for discontinuity orientation in RMR must set to be ten and zero respectively. Furthermore, separate empirical equations were proposed for disturbed and undisturbed rock mass. To surmount such drawbacks, a chart based approach i.e. Geological Strength Index (GSI) system was developed by Hoek et al. (1995). An attempt was made to characterize the rock mass on the basis of geological observations by visual inspection in the field. Moreover, a new parameter 'a' was incorporated by Hoek et al. (1992) which

provided logical means for changing the curvature of the failure envelope and forced it to produce zero tensile strength, this was published as Modified H-B criterion. Afterward, the most notable and key update in the original H-B criterion was incorporated by Hoek et al. (1995). The concept of Generalized Hoek-Brown (GHB) criterion was introduced in which RMR was substituted by the GSI system. Furthermore, the concept of disturbed and undisturbed rock mass was omitted and users were suggested to reduce the GSI values by the cautious judgment of existing conditions at the site. Along with these, several parameters like 'm_b, s and a' were incorporated for both good and poor quality rock mass that are having GSI values >25 and <25 respectively. The GHB (1995) criterion is written as equation 2.11:

$$\sigma_1' = \sigma_3' + \sigma_{ci}(m_b \frac{\sigma_3'}{\sigma_{ci}} + s)^a \qquad \text{Equation 2.11}$$

Where, σ_1' and σ_3' are major and minor effective principal stresses at failure respectively.

σ_{ci} is the uniaxial compressive strength of the intact rock.

For GSI>25 (Good Quality): $m_b = m_i \exp\left[\frac{(GSI-100)}{28}\right]$; $s = \exp\left[\frac{(GSI-100)}{9}\right]$; $a = 0.5$

For GSI<25 (Poor Quality): $s = 0$; $a = 0.65 - \frac{GSI}{200}$

Later, the importance of disturbances due to excavation and unloading was perceived and the concept of disturbance factor (D) was introduced by Hoek et al. (2002) to consider the damage posed due to blasting. The disturbance factor for undisturbed in-situ rock mass can be assigned as D=0 while for highly disturbed rock mass D=1. Hoek et al. (2002) suggested that disturbances in the rock masses are provoked due to vibrations during heavy blasting and stress reduction due to the removal of overburden. Furthermore, Sonmez and Ulusay (1999) illustrated various factors that can influence the disturbance within a rock mass. Besides this, it was realized by the developers and researchers that there exists a hiatus among poor and good quality rock mass. By taking this into consideration, an effort was made for a much smoother transition between poor and good quality rock mass and the equations of GHB (1995) were revised accordingly by Hoek et al. (2002). GHB (2002) is the most updated and restructured version of H-B criterion that was derived after considering all aforementioned amendments. The GHB (2002) failure criterion for slopes is expressed as equation 2.12:

$$\sigma_1' = \sigma_3' + \sigma_{ci}(m_b \frac{\sigma_3'}{\sigma_{ci}} + s)^a \qquad \text{Equation 2.12}$$

where, σ_1' and σ_3' are major and minor effective principal stresses at failure respectively.

σ_{ci} is the uniaxial compressive strength of the intact rock

$m_b = m_i \exp\left[\frac{(GSI-100)}{28-14D}\right]$; $s = \exp\left[\frac{(GSI-100)}{9-3D}\right]$; $a = \frac{1}{2} + \frac{1}{6}(e^{\frac{-GSI}{15}} + e^{\frac{-20}{3}})$

m_i is material constant that depends upon the lithology; m_b is the reduced value of m_i which accounts the strength by reducing the effects of jointed rock mass that relies upon GSI values and disturbance factor; 's' and 'a' are curve fitting parameters which are being determined by using GSI and D values.

$\sigma_3' = 0.72\sigma_{cm}' \left(\frac{\sigma_{cm}'}{\gamma H}\right)^{-0.91}$ (For slopes)

where, σ_{cm}' is the compressive strength of rock mass; γ is the unit weight; H is the height of the slope.

It is not adequate to consider deformation modulus of intact rock for numerical models because it is significantly controlled by certain factors related to the degree of fracturing and strength characteristics of the rock mass. To overcome this, Hoek and Diederichs (2006) proposed an empirical relationship to determine the deformation modulus of the rock mass. Generalized Hoek and Diederichs can be expressed as follows (Equation 2.13):

$E_{rm}(MPa) = 100000 \left(\frac{1-D/2}{1+e^{((60+15D-GSI)/11)}}\right)$ Equation 2.13

where, E_{rm} is deformation modulus of rock mass; D is disturbance factor; GSI is geological strength index value

Furthermore, it has been apprehended by the researchers that certain numerical modeling tools do not include H-B criterion, rather they consider linear MC criterion. To surmount this obstacle, a window based program known as 'Roclab' was developed to determine equivalent shear strength parameters (Hoek et al. 2002). It has been often noted that despite rigorous modifications in the original H-B criterion, the researchers still denote it by H-B criterion which is inadequate rather it should be designated as GHB criterion.

2.8. Failure criterion for joints: The term rock mass is used for in-situ rock that encompasses rigid blocks which are separated by discontinuities (Goodman et al. 1989; Hoek, 2006). In the case of jointed rock mass, stability is significantly influenced by existing discontinuities particularly at shallow depth or low-stress levels. Such stress regime conditions prevail significantly in road cut slopes. In such slopes, shear failures are liable to occur along the plane or zone of least resistance such as a jointed surface. The shear strength of jointed surface primarily depends upon certain factors like shape and roughness of asperities, degree of alteration, matching of either side walls and if present type and thickness of infilling material (Hoek, 2006). The shear strength behavior of jointed rock mass particularly those rock mass that are having unfilled joints is strongly governed by roughness and friction of joint surface (Singh et al. 2001). The earliest and well-recognized model for determining shear strength

along discontinuities is Mohr-Coulomb (MC) criterion. Shear strength along jointed can be determined by the in-situ test in the field itself and test may be performed in the laboratory also. It is based on the principle that, under differential normal loading conditions shear stresses are increased and displacement is recorded. Then, for different normal loads (at least three), points are obtained among shear stress and shear displacement that are plotted on a bivariate plot. The line formed by joining the points of normal load and ultimate shear stress is the failure envelope. The MC failure envelope is represented by the equation 2.14:

$$\tau_f = c_j + \sigma_n \tan \varphi_j \qquad \text{Equation 2.14}$$

where, τ_f is shear strength at failure; c_j is cohesion of joint; σ_n is effective normal stress; φ_f is friction of joint.

However, there are certain limitations in MC criterion. The failure envelope is linear and the in-situ tests are too expensive. Furthermore, from a practical standpoint, it is almost impossible to allow failure along joints for in-situ shear testing. However, such tests are performed on small scale in the laboratory. But they need lots of manpower and money to conduct such test in the laboratory and need certain correction of scale. Later, Patton (1966) perceived the significance of roughness and conducted a series of laboratory experiments by direct shear testing on saw-tooth triangular shaped joints. Consequently, Patton proposed a bilinear failure criterion. In this criterion, the shears strength behavior varies according to the loading or stress regime. At shallow depth, the normal stresses are low due to which shear displacement along the jointed surface is the function of the dip amount of joint and roughness of the jointed wall. While at high-stress levels asperities or roughness diminish as a response of crushing and shear strength of joints is nearly equal to that of intact rock (Goodman et al. 1989; Hoek, 2006). The effective normal stress acting on a particular jointed surface relies upon certain factors like orientation of joint, depth, weight of overburden, density of the material and hydrological characteristics (Hoek, 2006). Patton's saw-tooth model was failed to attract the researchers because in the real scenario such the joints are not ideally saw-tooth in shape. To overcome this drawback, Ladanyi and Archambault (1969) made an attempt by considering sliding and shearing along the jointed surface. But, the model was denounced by the scientific society. Patton (1966) also suggested that in shear strength assessment of jointed surface, consideration of only cohesion and friction is not adequate, rather scale and stress regime must be taken into consideration. In case of clean, smooth and unfilled joints, cohesion along potential jointed surface tends to zero and shear strength is mainly governed by the angle of friction which is principally the function of shape, size, and orientation of constituent minerals. By this time, the researchers conceived that the shear behavior along joints is non-linear. Later,

Barton (1973) suggested that the roughness of jointed wall or surface appreciably contribute to the non-linear shear behavior. Roughness may be classified as first and second order asperities. First order asperities are the major undulations which are being measured at large scale while second-order asperities are small bumps and ripples at a smaller scale. However, Barton (1973) studied the significance of first and second order asperities and suggested that the scale of asperities in shear strength behavior is directly related to the amount of normal load. At low normal stress, second order asperities are important while first-order asperities play a major role only at high normal stresses. The shear strength of discontinuity surfaces is the coupled effect of asperities or surface irregularities, normal stress, strength of the material, shear displacement along the potential sliding surface (Wyllie and Mah, 2004). A remarkable model was proposed by Barton (1973) by considering shearing of asperities and sliding along jointed wall simultaneously. The friction angle was replaced by a combined effect or function of basic friction angle, roughness, strength of the material and normal stress acting on the potential sliding surface. The Barton's (1973) shear strength criterion can be expressed as equation 2.15:

$$\tau_f = \sigma_n \tan\left[\varphi_b + \text{JRC} \log_{10}\left(\frac{\text{JCS}}{\sigma_n}\right)\right] \qquad \text{Equation 2.15}$$

where, τ_f is shear strength; σ_n is effective normal stress; φ_b is basic friction angle on unweathered surface; JRC is joint roughness coefficient which can be determined by comparing roughness profile of the joint surface with standard profiles proposed by Barton and Choubey (1977) or it can also be estimated by measuring the amplitude of roughness by straight edge method suggested by Barton (1982); JCS is joint wall compressive strength that can be estimated by Schmidt hammer rebound test or by the standards suggested by International Society of Rock Mechanics (ISRM, 1981). It has been often noticed that certain researchers conduct point load test suggested by Broch and Franklin (1972), but it may mislead the outcomes because the strength along the joint surface is slightly lesser especially in case of chemically altered or weathered joints. So, to attain much better and realistic outcomes, it is being suggested to employ the Schmidt hammer test in the field. However, while taking Schmidt rebound values, the attention ought to be given to the orientation of the hammer and if need proper corrections suggested by Barton and Choubey (1977) should be applied. Furthermore, Barton and Choubey (1977) considered φ_{peak} (peak friction angle) of saturated and weathered rock surface and replaced the basic friction angle with residual friction angle and made a slight modification in shear strength criterion for weathered and unweathered joints as follows (equation 2.16):

$$\tau_f = \sigma_n' \tan\left[\varphi_r + \text{JRC} \log_{10}\left(\frac{\text{JCS}}{\sigma_n}\right)\right] \qquad \text{Equation 2.16}$$

where, φ_r is residual friction angle

Barton and Choubey (1977) suggested that residual friction angle can be calculated by the following equation:

$$\varphi_r = (\varphi_b - 20) + 20\,(\frac{r}{R})$$

where, φ_r is residual friction angle; φ_b is basic friction angle; r and R are Schmidt hammer rebound values weathered and unweathered surface respectively.

The joint stiffness defines the deformation under both normal as well as in tangential loading. According to Barton (1972), normal stiffness is the normal stress per unit closure of the joint while shear stiffness is the ratio of peak shear stress to the shear displacement.

The normal stiffness of joint is as follows (equation 2.17): (Barton 1972)

$$K_n = \frac{E_i - E_m}{L\,(E_i - E_m)} \qquad \text{Equation 2.17}$$

where, k_n is normal stiffness of joints; E_m is modulus of rock mass; E_i is modulus of intact rock and L is mean spacing of joint.

The shear stiffness of joint is as follows (equation 2.18): (Barton, 1972)

$$K_s = \frac{G_i - G_m}{L\,(G_i - G_m)} \qquad \text{Equation 2.18}$$

where, k_s is shear stiffness of joints; G_m is shear modulus of rock mass; G_i is shear modulus of intact rock and L is mean spacing of joint.

Chapter 3

Field and laboratory investigations

3.1. Introduction: Field inspections serve as arteries for any geotechnical engineering project. Regardless or Irrespective of type of the geoengineering project, the geological and geotechnical field data is a foremost and utmost inspection. During preliminary stages of the work, initial field surveys have been conducted to demarcate landslide prone zones. Many large and small scale landslides scarps have been observed along the highway cut slopes. Moreover, occasional block failures were found to be much prominent in the region. Such failures had caused damage to the road and nearby structures. By considering geological and geotechnical constraints of the region, the target areas or sections were demarcated which are prone to instability. Variety meta-sedimentary rock formations and debris material have been encountered along road cut slopes from Rishikesh to Devprayag. A total number of 28 road cut slopes (20 rock and 8 debris slopes) were identified as prone to failure and selected for detailed geotechnical assessment. The 2D geometry of road cut rock and debris slopes were recorded using laser inclinometer, Brunton compass and measuring tape. Coordinates of investigated location were recorded by Global positioning system (GPS).

3.2. Field investigations of rock slopes: From rock slopes, discontinuity data related to slope stability have been carefully examined as per the standard procedures during detailed field investigations. Due to active tectonics and multiple phases of deformation, the road cut rock slopes are heavily fractured and posses 3 to 4 set of joints. The orientation of cut slope facet and prevailing discontinuities at a particular site were recorded by employing Brunton compass. Geotechnical survey sheets were prepared and the parameters pertinent to slope stability have been recorded from discrete locations (table 3.1 to 3.20). Discontinuity spacing, conditions of discontinuities like persistence, aperture, roughness, infilling and weathering; groundwater conditions and orientation of discontinuities were determined as per BIS, 1987. Schmidt hammer rebound values for each joint set were measured during field survey as per the guidelines suggested by International Society of Rock Mechanics (ISRM, 1981). A variety of failures were evidenced during the field survey. In rock slopes, structurally controlled failures are significantly distributed throughout the stretch. Many investigated slopes are having multiple sets of adversely oriented discontinuities. The identified rock slopes were designated as S1 to S20 while debris slopes were named as L1 to L8.

Recurrent nature of structurally controlled failure in the form of a wedge and planar failure was observed at slope S13 (figure 3). Pre and post-failure conditions at slope S13 have been depicted in figures 3.1(a), 3.1(b) and 3.1(d) in the year 2016, 2017 and 2018 respectively. A massive failed block of 5-6 feet is shown in the inset view (figure 3c) and even much larger block (~15 feet) has been witnessed in successive failure (figure 3d). Interestingly, S13 lies near to the township Kaudiyala, the zone which is proximal to thrust fault and slope S13 was evaluated as unstable by numerical simulation. Such correlation among existing field conditions and predicted stability dictate the soundness of the outcomes obtained by numerical simulation.

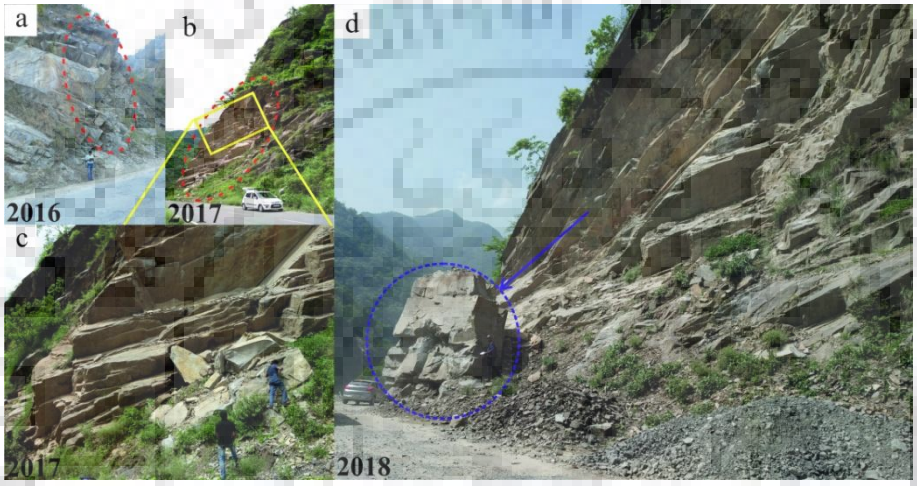

Figure 3.1: Field photographs depicting recurrent failure at slope S13 near Kaudiyala (a) Pre-failure condition of slope with encircled probable zone observed in during initial field surveys and measurement in the year 2016 (b) Structurally controlled mass failure observed during successive field survey in 2017 (c) Inset view showing the massive failed blocks (d) Much larger failure occurred in 2018

Furthermore, it was noted that large numbers of slopes are critical in the section which may experience similar type mass failures in near future. In contrast to massive mass failures, there are certain sections in the stretch that are prone to occasional and small scale block failures. Such failures are induced due to the intersection of discontinuities which may show overall stability as fair, but occasional wedges as rockfalls is a sustained threat to the ongoing traffic and people along the highway and many often damage roads and nearby structures. An issue with these grounds was manifested at slope S15, the slope is stable in terms of overall stability but block failure often destroyed the pavement of the road, roadside guarders and wall on either side of the road (figure 3.2). The spot of commencement of wedges have been marked (figure 3.2a) and the impacts have been depicted in figure 3.2 b&c.

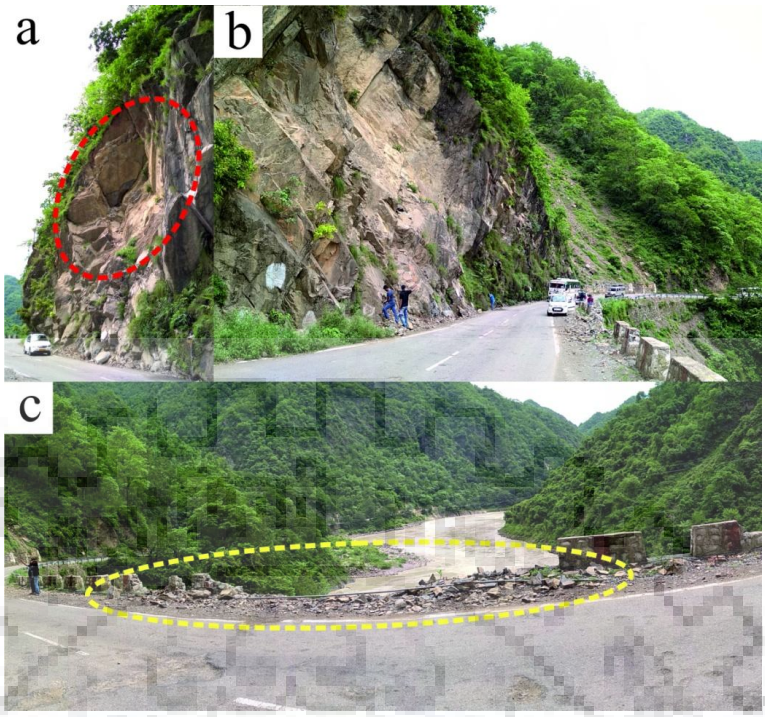

Figure 3.2: Rockfall on road at slope S15 near Kaudiyala (a) Encircled portion highlighting the zone of wedge initiation (b) Damaged road pavement roadside guarders and walls (c) Inset view showing the damage to the road and associated structures

Geotechnical field survey data:

Table 3.1: Geotechnical field survey data of slope S1

Location	S1	Coordinates	N30° 7' 11.1" E78° 22' 4.6"
Slope Height (m)	30		
Lithology	Quartzarenite		
Groundwater condition	Dry		
Infilling along joints	None		
Weathering along joints	Moderately weathered		
Orientation of slope	70°-75°/172°		

Discontinuity	Dip/Direction (°)	Persistence (m)	Aperture (mm)	Spacing (m)
J1	65/213	10-11	0.5-1	0.1-0.25
J2	69/335	8-9	0.9-1.5	0.20.25
J3	33/218	8-10	1.5	0.1-0.2

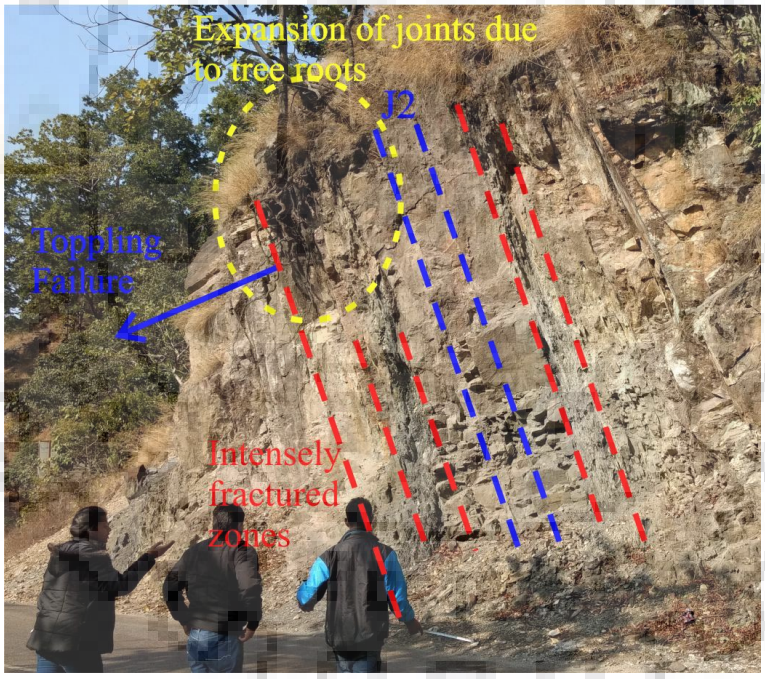

Figure 3.3: Steeply dipping joints (J2) forming toppling failure and the adverse impact of tree roots at Slope S1

Table 3.2: Geotechnical field survey data of slope S2

Location	S2	Coordinates	N30° 7' 22.13.6" E 78° 22' 36.3"
Slope Height (m)	60		
Lithology	Quartzarenite		
Groundwater condition	Dry		
Infilling along joints	None		
Weathering along joints	Slightly weathered		
Orientation of slope	75°-80°/175°		

Discontinuity	Dip/Direction (°)	Persistence (m)	Aperture (mm)	Spacing (m)
J1	48/200	16-17	1-2	0.15-0.35
J2	74/115	15-19	1.5-2	0.25-0.3
J3	42/013	10-12	1-2	0.1-0.2
J4	63/070	8-9	2-3.5	0.1-0.25

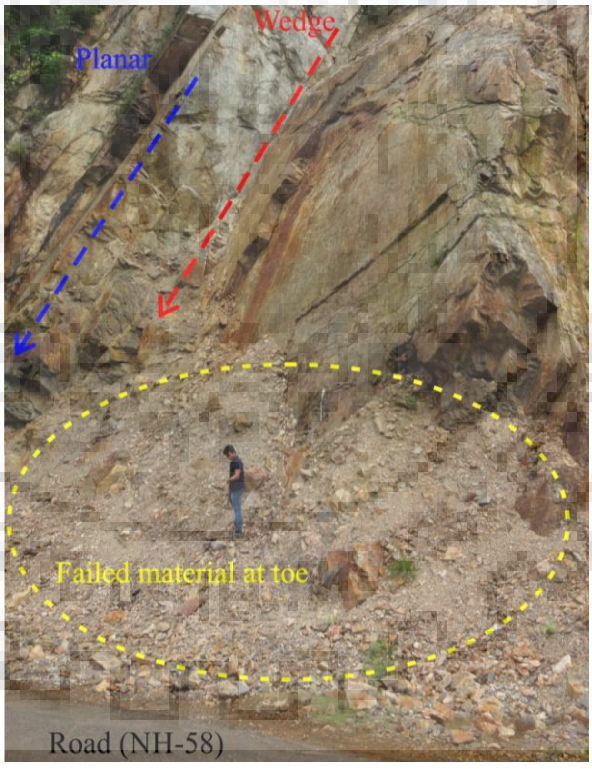

Figure 3.4: Extremely persistent discontinuities forming a wedge and planar failure, failed material (encircled) at the toe region of the slope at S2

Table 3.3: Geotechnical field survey data of slope S3

Location	S3	Coordinates	N 30° 7' 24.6" E78° 23' 13.7"
Slope Height (m)	42		
Lithology	Dolomitic Limestone		
Groundwater condition	Dry		
Infilling along joints	Hard infilling by quartz (>5mm)		
Weathering along joints	Slightly to moderately weathered		
Orientation of slope	75°-80°/160°		

Discontinuity	Dip/Direction (°)	Persistence (m)	Aperture (mm)	Spacing (m)
J1	36/080	22-25	2-3	0.15-0.2
J2	52/210	10-12	1.5-2	0.2-0.4
J3	43/340	13-14	3-4	0.3-0.4

Figure 3.5: Wedge failure due to the intersection of joints (J1-J2) at slope S3

Table 3.4: Geotechnical field survey data of slope S4

Location	S4	Coordinates	N 30° 8' 15.66" E78° 24' 29.64"
Slope Height (m)	42		
Lithology	Ferruginous Quartzarenite and Slate		
Groundwater condition	Dry		
Infilling along joints	None		
Weathering along joints	Slightly weathered		
Orientation of slope	75°-80°/192°		

Discontinuity	Dip/Direction (°)	Persistence (m)	Aperture (mm)	Spacing (m)
J1	43/195	15-16	1-2	0.2-0.3
J2	53/110	16-17	2-2.5	0.15-0.25
J3	49/230	10-12	1.5-2	0.2-0.4

Figure 3.6: Field photograph depicting the condition of rock mass at slope S4 (a) Showing the joints forming a wedge and planar sliding (b) Lithological contact between Slate and Sandstone (c) Inset image showing clast at lithological contact

Table 3.5: Geotechnical field survey data of slope S5

Location	S5	Coordinates	N30° 7' 47.94" E78° 25' 16.74"
Slope Height (m)	33		
Lithology	Sandstone		
Groundwater condition	Dry		
Infilling along joints	None		
Weathering along joints	Highly weathered		
Orientation of slope	80°-85°/210°		

Discontinuity	Dip/Direction (°)	Persistence (m)	Aperture (mm)	Spacing (m)
J1	81/163	20-21	2-3	0.17-0.25
J2	76/250	16-17	1-2	0.15-0.3
J3	28/160	10-12	1.5-2	0.3-0.4

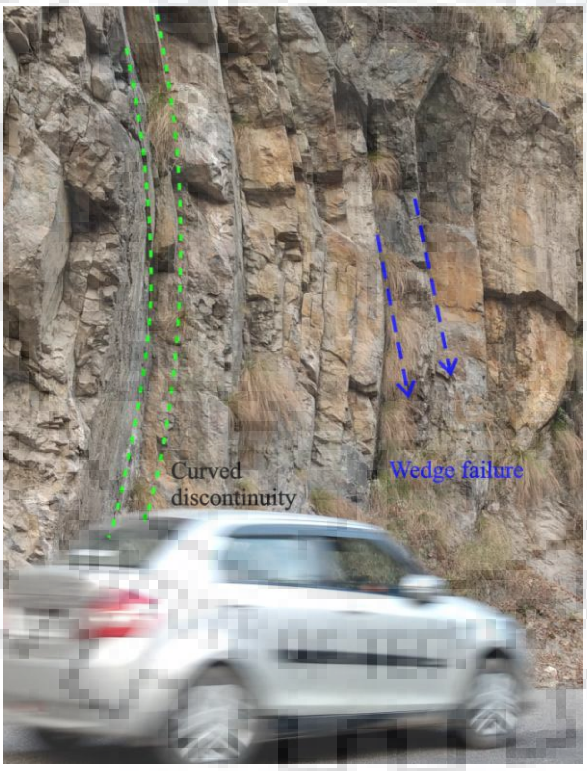

Figure 3.7: Persistent and curved discontinuities and the intersection of discontinuities offering favorable condition for wedge failure at slope S5

Table 3.6: Geotechnical field survey data of slope S6

Location	S6	Coordinates	N30° 7' 7.45" E78° 25' 24.15"
Slope Height (m)	19		
Lithology	Slate		
Groundwater condition	Dry		
Infilling along joints	Hard infilling by quartz (>5mm)		
Weathering along joints	Slightly weathered		
Orientation of slope	75°-80°/260°		

Discontinuity	Dip/Direction (°)	Persistence (m)	Aperture (mm)	Spacing (m)
F (Foliation)	61/200	21-22	0.5-1	0.05-0.1
J1	79/105	15-16	2-3	0.2-0.3
J2	15/015	8-9	1-2	0.3-0.5
J3	55/110	10-12	1-2.5	0.2-0.4

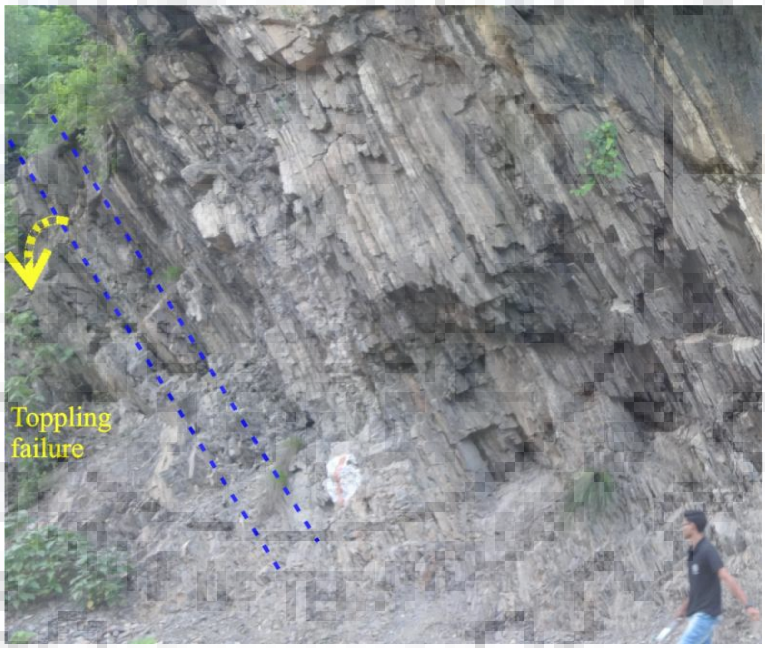

Figure 3.8: Steeply dipping discontinuities in Slate forming toppling failure at slope S6

Table 3.7: Geotechnical field survey data of slope S7

Location	S7	Coordinates	N30° 6' 52.5" E78° 26' 5.64"
Slope Height (m)	18		
Lithology	Phyllite		
Groundwater condition	Dry		
Infilling along joints	None		
Weathering along joints	Slightly weathered		
Orientation of slope	70°-75°/220°		

Discontinuity	Dip/Direction (°)	Persistence (m)	Aperture (mm)	Spacing (m)
F(Foliation)	65/213	10-15	1-1.5	0.05-0.08
J1	72/320	10-12	1-2	0.1-0.2
J2	52/028	6-9	1.5-2	0.1-0.25

Figure 3.9: Weathered and soft rock causing failure of small chunks and tilted trees indicating deformation within rock mass at slope S7

Table 3.8: Geotechnical field survey data of slope S8

Location	S8	Coordinates	N30° 5' 45.36" E78° 26' 5.70"
Slope Height (m)	18		
Lithology	Sub-Arkosic Sandstone		
Groundwater condition	Dry		
Infilling along joints	None		
Weathering along joints	Slightly weathered		
Orientation of slope	65°-70°/220°		

Discontinuity	Dip/Direction (°)	Persistence (m)	Aperture (mm)	Spacing (m)
J1	51/220	12-14	2-3	0.17-0.3
J2	64/108	8-9	1-2	0.4-0.5
J3	60/340	6-8	1.5-2.5	0.19-0.3

Figure 3.10: Daylighting conditions offering a planar mode of failure due to joint set J1 at slope S8 and failed blocks at the toe portion of the slope

Table 3.9: Geotechnical field survey data of slope S9

Location	S9	Coordinates	N30° 5' 32.52" E78° 26' 5.58"
Slope Height (m)	17		
Lithology	Quartzite		
Groundwater condition	Dry		
Infilling along joints	None		
Weathering along joints	Slightly weathered		
Orientation of slope	70°-75°/260°		

Discontinuity	Dip/Direction (°)	Persistence (m)	Aperture (mm)	Spacing (m)
J1	59/225	13-15	1-2	0.15-0.3
J2	73/322	10-12	1.5-2	0.4-0.5
J3	30/082	6-7	1-2	0.15-0.2

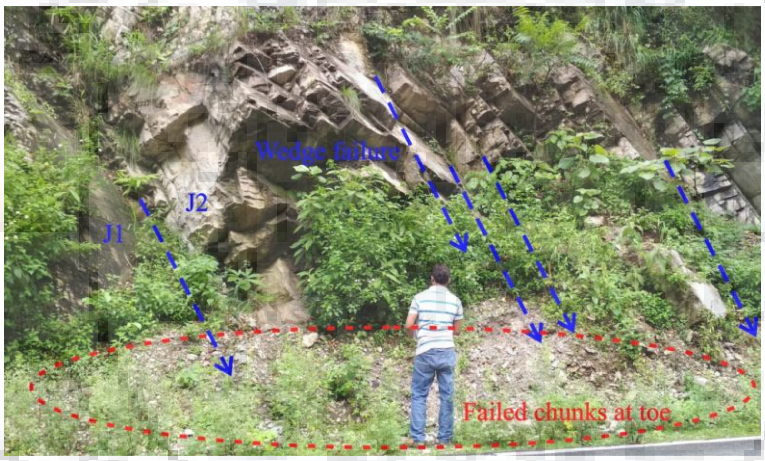

Figure 3.11: Unfavourably oriented jointed induced wedge sliding at slope S9 and failed chunks at bottom of the slope

Table 3.10: Geotechnical field survey data of slope S10

Location	S10	Coordinates	N30° 5' 24.5" E78° 26' 5.3"
Slope Height (m)	45		
Lithology	Quartzite		
Groundwater condition	Dry		
Infilling along joints	None		
Weathering along joints	Slightly to moderately weathered		
Orientation of slope	80°-85°/250°		

Discontinuity	Dip/Direction (°)	Persistence (m)	Aperture (mm)	Spacing (m)
J1	58/215	25-30	1-1.5	0.1-0.2
J2	80/115	10-12	0.2-0.6	0.07-0.1
J3	23/025	13-16	1-2	0.10-0.25

Figure 3.12: Rock mass having persistent joints offering planar failure followed by rockfall at slope S10

Table 3.11: Geotechnical field survey data of slope S11

Location	S11	Coordinates	N30° 3' 57.02" E78° 28' 49.65"
Slope Height (m)	30		
Lithology	Sub-Arkosic Sandstone		
Groundwater condition	Dry		
Infilling along joints	Hard infilling by quartz (<5mm)		
Weathering along joints	Slightly weathered		
Orientation of slope	70°-78°/230°		

Discontinuity	Dip/Direction (°)	Persistence (m)	Aperture (mm)	Spacing (m)
J1	76/208	11-14	1.5-2.2	0.1-0.15
J2	83/135	16-21	1-2	0.02-0.3
J3	31/295	10-12	2.9-1.7	0.6-0.7

Figure 3.13: Adversely oriented joints favoring planar and wedge sliding at slope S11

Table 3.12: Geotechnical field survey data of slope S12

Location	S12	Coordinates	N30° 3' 32.88" E78° 29' 5.43"
Slope Height (m)	40		
Lithology	Sub-Arkosic Sandstone		
Groundwater condition	Dry		
Infilling along joints	Hard infilling by quartz (~5mm)		
Weathering along joints	Moderately weathered		
Orientation of slope	65°-70°/130°		

Discontinuity	Dip/Direction (°)	Persistence (m)	Aperture (mm)	Spacing (m)
J1	64/125	20-23	1-2	0.1-0.2
J2	82/215	10-13	0.3-1	0.2-0.3
J3	35/340	16-17	0.5-1.5	0.15-0.2
J4	52/070	15-17	0.1-2	0.08-0.1

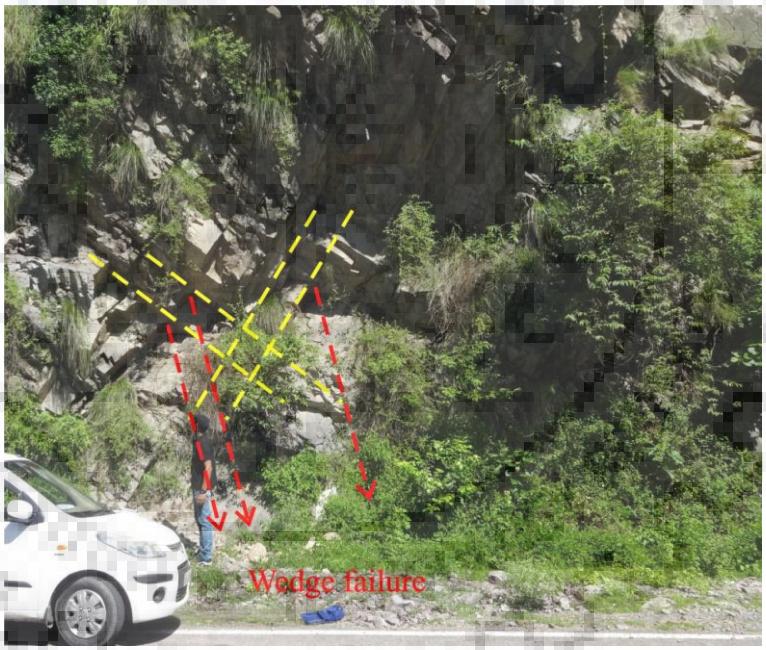

Figure 3.14: Discontinuities forming wedge failure at slope S12

Table 3.13: Geotechnical field survey data of slope S13

Location	S13	Coordinates	N30° 4' 16.05" E78° 29' 27.42"
Slope Height (m)	34		
Lithology	Sub-Arkosic Micaceous Sandstone		
Groundwater condition	Water dripping from joints		
Infilling along joints	None		
Weathering along joints	Weathered		
Orientation of slope	72°-75°/080°		

Discontinuity	Dip/Direction (°)	Persistence (m)	Aperture (mm)	Spacing (m)
J1	42/060	10-12	0.7-1	0.1-0.2
J2	55/230	20-22	1-1.5	0.2-0.25
J3	70/125	19-23	2-2.5	0.8-1.2

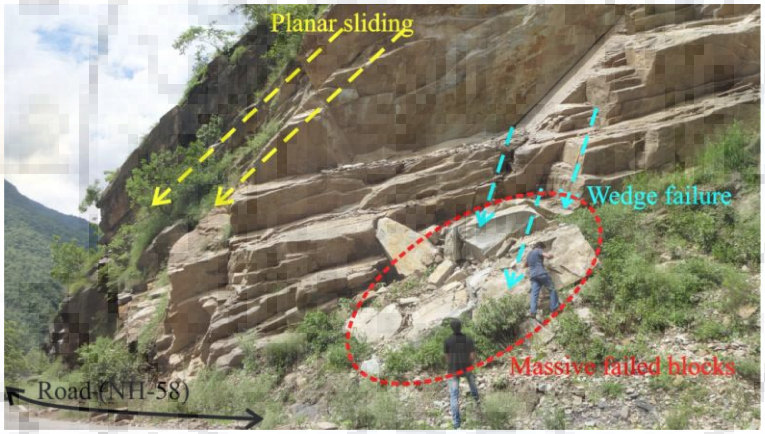

Figure 3.15: Field photograph depicting massive failed blocks and a potential site for planar and wedge sliding at slope S13

Table 3.14: Geotechnical field survey data of slope S14

Location	S14	Coordinates	N30° 4' 22.51" E78° 29' 30.74"
Slope Height (m)	42		
Lithology	Sub-Arkosic Micaceous Sandstone		
Groundwater condition	Dry		
Infilling along joints	None		
Weathering along joints	Slightly weathered		
Orientation of slope	75°-80°/074°		

Discontinuity	Dip/Direction (°)	Persistence (m)	Aperture (mm)	Spacing (m)
J1	53/313	20-22	0.1-1	0.2-0.6
J2	46/212	21-25	1-1.5	0.05-0.15
J3	58/080	16-17	0.6-2	0.15-0.2

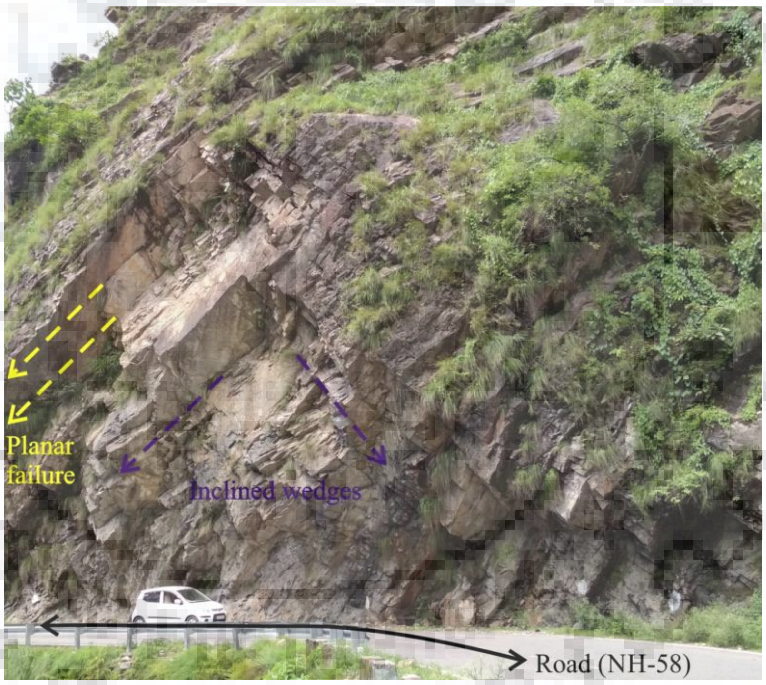

Figure 3.16: Wedge and planar failure conditions at slope S14

Table 3.15: Geotechnical field survey data of slope S15

Location	S15	Coordinates	N30° 4' 27.21" E78° 29' 32.28"
Slope Height (m)	33		
Lithology	Clay and Mica bearing Sandstone		
Groundwater condition	Water flowing from joints (12-15 liters/minute from 1 m^2)		
Infilling along joints	None		
Weathering along joints	Slightly weathered		
Orientation of slope	70°-75°/050°		

Discontinuity	Dip/Direction (°)	Persistence (m)	Aperture (mm)	Spacing (m)
J1	39/015	20-22	0.8-1.5	0.1-0.4
J2	63/205	25-27	0.5-1.5	0.2-0.3
J3	68/075	18-20	1.5-2.5	0.13-0.4

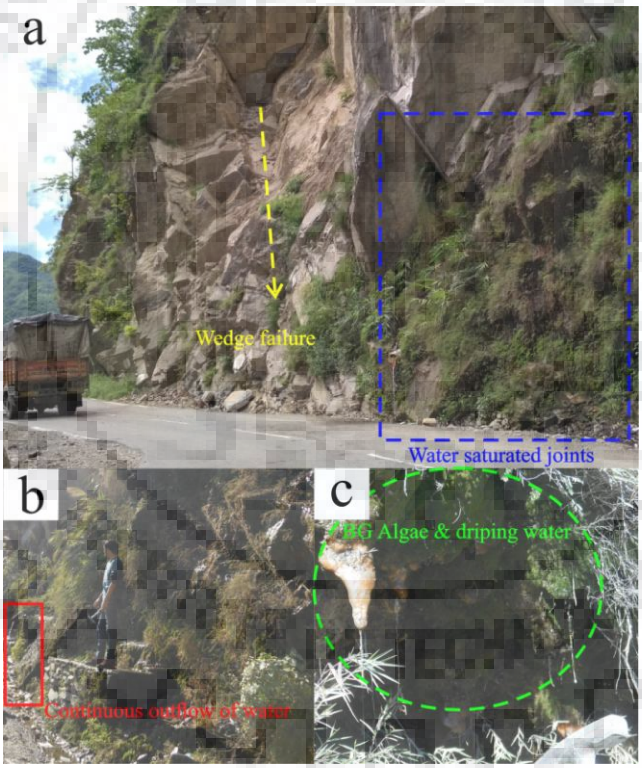

Figure 3.17: Condition of rock mass at slope S15 (a) Wedge failure and water saturation along joints (b) Continuous outflow of water along joints throughout the year (c) Formation of algae along joints and leaching out of mineralogical content

Table 3.16: Geotechnical field survey data of slope S16

Location	S16	Coordinates	N30° 3' 58.26" E78° 29' 59.70"
Slope Height (m)	33		
Lithology	Sub-Arkosic Sandstone		
Groundwater condition	Dry		
Infilling along joints	None		
Weathering along joints	Weathered		
Orientation of slope	65°-70°/255°		

Discontinuity	Dip/Direction (°)	Persistence (m)	Aperture (mm)	Spacing (m)
J1	59/207	21-23	1-2.5	0.08-0.3
J2	66/330	16-19	2-3	0.1-0.3
J3	78/100	25-27	2-2.5	02-0.3

Figure 3.18: Failed blocks and potential rockslide for different modes of structurally controlled failures at slope S16

Table 3.17: Geotechnical field survey data of slope S17

Location	S17	Coordinates	N30° 3' 56.96" E78° 30' 36.84"
Slope Height (m)	35		
Lithology	Micaceous Sandstone		
Groundwater condition	Dry		
Infilling along joints	None		
Weathering along joints	Weathered		
Orientation of slope	70°-75°/085°		

Discontinuity	Dip/Direction (°)	Persistence (m)	Aperture (mm)	Spacing (m)
J1	63/008	15-17	3-4	0.08-0.23
J2	71/110	20-22	2-2.5	0.14-0.25
J3	46/235	11-14	1.5-2	0.2-0.3

Figure 3.19: Blocky rock mass having significant potential for wedge failure at slope S17

Table 3.18: Geotechnical field survey data of slope S18

Location	S18	Coordinates	N30° 6' 35.5" E78° 35' 9.7"
Slope Height (m)	30		
Lithology	Micaceous Sandstone		
Groundwater condition	Dry		
Infilling along joints	None		
Weathering along joints	Slightly to moderately weathered		
Orientation of slope	55°-65°/100°		

Discontinuity	Dip/Direction (°)	Persistence (m)	Aperture (mm)	Spacing (m)
J1	48/112	10-12	1-2	0.2-0.3
J2	56/298	16-18	1.5-2	0.1-0.2
J3	67/020	13-15	2-3	0.15-0.3

Figure 3.20: Failed chunks and condition favorable for wedge failure at slope S18

Table 3.19: Geotechnical field survey data of slope S19

Location	S19	Coordinates	N30° 6' 43.78" E78° 34' 0.12"
Slope Height (m)	38		
Lithology	Micaceous Sandstone		
Groundwater condition	Dry		
Infilling along joints	None		
Weathering along joints	Slightly weathered		
Orientation of slope	75°-80°/350°		

Discontinuity	Dip/Direction (°)	Persistence (m)	Aperture (mm)	Spacing (m)
J1	69/040	15-16	1-2	0.3-0.4
J2	77/275	17-21	1.5-2	0.1-0.2
J3	48/328	20-23	1.5-2.5	0.1-0.25
J4	35/135	19-20	2-4	0.4-0.5

Figure 3.21: Adversely oriented discontinuities causing wedge and planar sliding at slope S19

Table 3.20: Geotechnical field survey data of slope S20

Location	S20	Coordinates	N30° 6' 42.01" E78° 34' 46.13"
Slope Height (m)	23		
Lithology	Micaceous Sandstone		
Groundwater condition	Dry		
Infilling along joints	None		
Weathering along joints	Slightly weathered		
Orientation of slope	75°-80°/350°		

Discontinuity	Dip/Direction (°)	Persistence (m)	Aperture (mm)	Spacing (m)
J1	46/290	20-21	1-2	0.1-0.3
J2	75/060	16-18	2-2.5	0.1-0.2
J3	56/170	22-25	2-4	0.07-1.5

Figure 3.22: Blocky rock mass favoring wedge failure at slope S20

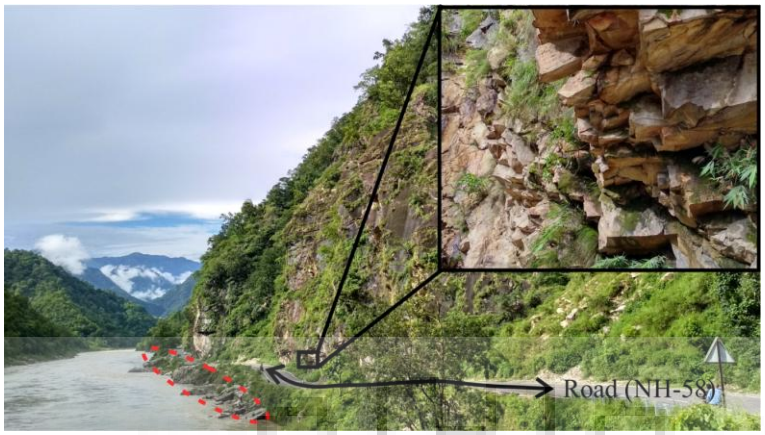

Figure 3.23: A panoramic view at slope S10 along NH-58 during monsoon season showing the level of water in the Ganga River, causing toe cutting and seepage through joints and Inset view is depicting jointed & blocky rock mass conditions at slope S10

Figure 3.24: Measurement of geotechnical parameters during field survey (a) Roughness profile of joint wall by using Barton comb (b) Schmidt hammer hardness of jointed surface

The Schmidt hammer rebound values of each joint wall surface were measured during field survey as per the specifications of ISRM (1981), JCS was determined by the empirical relationship proposed by Katz et al. (2000) and residual friction was determined by the tilt test (table 3.21).

Table 3.21: Residual friction, Schmidt hammer rebound values and JRC for each joint set from investigated locations

Slope	Joint	Residual Friction	Schmidt hardness values	JRC	Slope	Joint	Residual Friction	Schmidt hardness values	JRC
S1	J1	27	43	6	S11	J1	25	51	7
	J2	29	38	11		J2	26	56	11
	J3	28	46.5	8		J3	26	55	10
S2	J1	29	39.5	15	S12	J1	23	53.5	8
	J2	29	44	14		J2	22	54.5	5
	J3	27	43.5	9		J3	24	55.5	9
	J4	26	48	6		J4	22	53	6
S3	J1	29	43.5	7	S13	J1	23	55.5	7
	J2	31	42.5	12		J2	23	54	8
	J3	30	46	10		J3	22	55	3
S4	J1	27	54	10	S14	J1	24	54	10
	J2	26	53.5	7		J2	23	51.5	7
	J3	24	49.5	4		J3	24	53	9
S5	J1	24	47.5	11	S15	J1	22	53.5	4
	J2	26	49.5	13		J2	24	55.5	9
	J3	24	45.5	9		J3	23	55.5	7
S6	J1	21	25	3	S16	J1	26	54.5	8
	J2	25	21.5	9		J2	27	55	9
	J3	24	25.5	5		J3	29	54	12
	J4	23	25	6	S17	J1	27	52	6
S7	J1	22	18.5	4		J2	29	51	11
	J2	24	16.5	7		J3	28	53	8
	J3	24	18.5	8	S18	J1	28	53.5	6
S8	J1	26	48	7		J2	31	56	14
	J2	26	37.5	6		J3	29	54	8
	J3	28	45.5	12	S19	J1	27	54	9
S9	J1	23	60.5	9		J2	29	53.5	15
	J2	25	58.5	13		J3	28	53.5	12
	J3	26	54	15		J4	28	53	13
S10	J1	25	55.5	6	S20	J1	29	56	13
	J2	28	58.5	13		J2	26	55	7
	J3	26	59.5	9		J3	27	54.5	9

3.3. Field investigations of debris slopes: In addition to rock slopes, the stretch from Rishikesh to Devprayag comprises of several road cut debris and rock cum debris slopes. These slopes are prone to landslides. Debris slides are quite common and often road blockage is being reported especially during rainy season. Many often the failed debris reaches to river valleys and blocks the natural flow and degrade the quality of flowing water. Furthermore, such failures led to an aggravation of siltation in downstream reservoirs. Vulnerable zones were identified and eight critical slopes have been selected for detailed geotechnical inspection. The coordinates of the location were taken GPS are illustrated in table 3.22.

Table 3.22: Coordinates of investigated debris slopes along NH-58

Location	Latitude	Longitude
L1	30° 7' 43.2"	78° 23' 18.6"
L2	30° 6' 53.8"	78° 26' 13.1"
L3	30° 6' 09.8"	78° 26' 09.1"
L4	30° 5' 01.2"	78° 26' 08.5"
L5	30° 4' 10.1"	78° 27' 22.4"
L6	30° 3' 56.7"	78° 28' 49.8"
L7	30° 3' 58.8"	78° 29' 17.4"
L8	30° 5' 13.7"	78° 34' 34.9"

In contrast to rock slopes, the circular failures are encountered in debris slopes. Furthermore, certain talus failures were evidenced from those debris slopes which are having shallow bedrock. Temporal and seasonal monitoring was conducted and it was noted that slopes failures occur much frequently during and immediately after the monsoon. The investigated area witness heavy rainfall and often with cloud burst phenomena. Although it is a natural meteorological phenomenon which is impossible to control over, but appropriate drainage can reduce damage to a reasonable extent. The figures 3.25 (a&b) are pre-failure photographs of a debris slope (L1) near the village Shivpuri before monsoon of 2017 while figure 3.25(c) is showing the condition of the slope after failure. The failure was initiated primarily due to percolation of rainwater along the tension cracks at the crown portion of the slope (figure 3.25b). The formation of algae around tension cracks is indicating the moist condition. Furthermore, the removal of slope material from the toe portion by manual process decreased the loading at the toe that caused aggravated the disequilibrium (figure 3.25a). Apart from L1, there are many other slopes that are critical in terms of stability. It was often noted that preventive measure like retaining wall is rarely being taken along the road cut debris slope. If retaining wall was installed, proper and timely maintenance is rarely being done. As

witnessed from slopes at locations L5 & L7 (figure 3.29 & 3.31), immediate action is not been undertaken for the failed retaining wall. Among eight studied slopes, only two slopes were having retaining wall to prevent failure and slopes locations L1, L2, L3, L4, L6 & L8 are not being supported by retaining wall (figure 3.25, 3.26, 3.27, 3.28, 3.30, & 3.32). At critical slopes, retaining walls should be installed for prevention from slope failures and careful monitoring of drainage outlets ought to be done on a routine basis. Furthermore, there is not even a single section along the road that is having nets to retain occasional blocks. The panoramic view of debris slope (L4) is depicting failed debris at the toe (figure 3.28a) and a cross-sectional view is showing probable zones for failure in near future (figure 3.28b). The retaining wall at location L7 had failed (figure 3.31) which may further aggravate instability.

As mentioned in the earlier section, the geometry of slopes was recorded during field inspection by using laser inclinometer, Brunton compass and measuring tape. Most of the debris slopes lie at curved road sections. The old failure scarps and cross-sectional view of slopes were used to determine bedrock. The geomechanical characteristics of bedrock were determined at best efficient sections available during field inspection (table 3.23). The Geological Strength Index (GSI) determined by using the proposed by Marinos et al. (2005) and disturbance factor was estimated during the field study. The estimation of unconfined compressive strength (UCS) was being done by using Schmidt hardness values because it considers the variations in strength characteristics due to discontinuities and several geological factors within the rock mass. Various geotechnical issues highlighted and prevailing slope conditions have been depicted by field photographs from each slope (figure 3.25 to 3.32).

Table 3.23: Geotechnical characteristics of underlying bedrock at discrete debris slopes along NH-58

Location	Lithology of Bedrock	GSI value	Disturbance factor	Average Schmidt rebound value
L1	Crystalline Limestone	33	1	19.21
L2	Slate	40	0.9	21.13
L3	Crystalline Limestone	35	1	14.92
L4	–	–	–	–
L5	–	–	–	–
L6	Sandstone	43	1	51.71
L7	Sandstone	41	1	53.08
L8	–	–	–	–

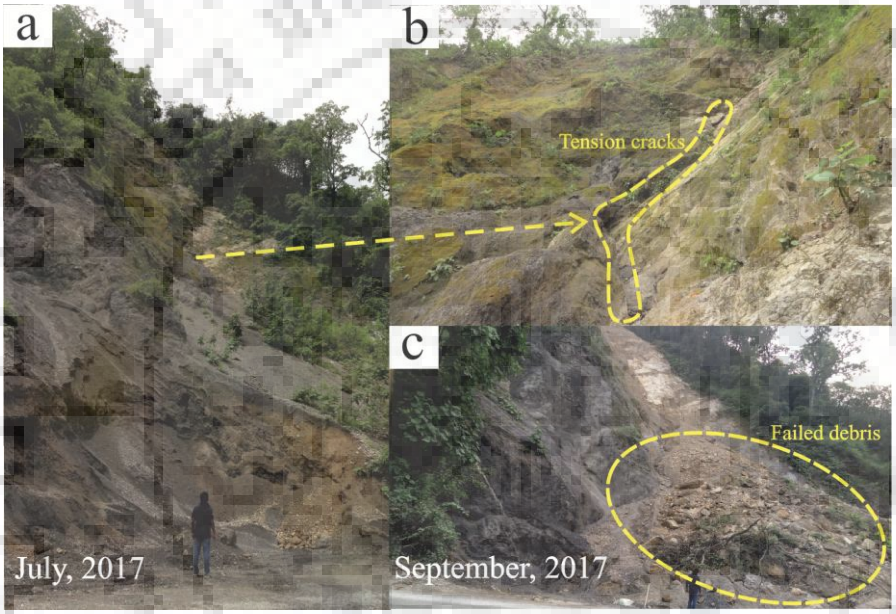

Figure 3.25: Road cut debris slope at location L1 near Shivpuri township along NH-58 (a) Without installing retaining wall, debris were excavated from toe portion of slope contributing towards disequilibrium in the stability of slope (b) Tension cracks at crown portion are indicating possible zone of initiation of failure and formation of algae is addressing moist condition which may also act as lubricant during failure (c) Post-failure photograph showing massive landslide along cut slope near Shivpuri township

Figure 3.26: Panoramic view of road cut debris slope at location L2 along NH-58

Figure 3.27: Photograph depicting river-borne debris slope at location L3

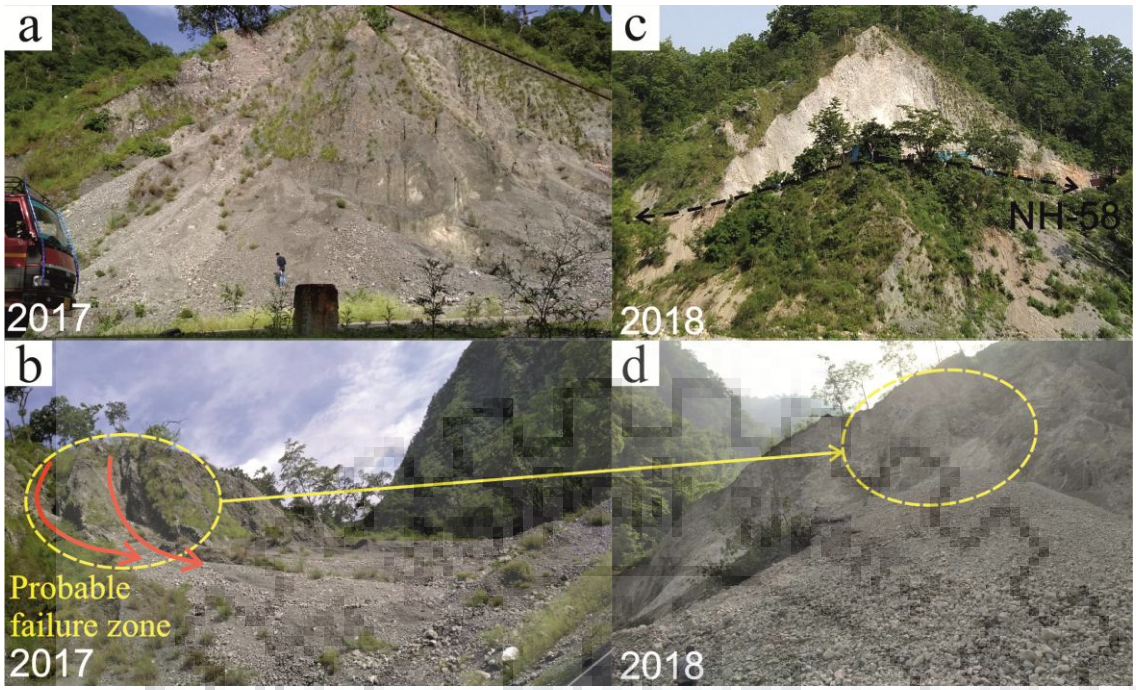

Figure 3.28: Extensive debris slope at location L4 along NH-58 (a) Front view showing massive failed debris at the toe portion of the slope (b) Cross-sectional view showing probable zones of failure in near future

Figure 3.29: Debris material with mixed clast size at location L5 and inset image showing damaged retaining wall

Figure 3.30: Failed debris at location L6 along NH-58

Figure 3.31: Debris slope at location L7 along NH-58 and inset image showing the failed retaining wall

Figure 3.32: Panoramic view of debris slope at location L8 along NH-58

3.4. Laboratory investigations of rock slopes: The determination strength is one of the major confronting issues in rock slope engineering practices. From each slope, undisturbed and representative chunks of rocks were collected to prepare at least three cores of NX size i.e. 54.7 mm in diameter from each location. To determine unconfined compressive strength (UCS), the compression test is being performed by employing universal testing machine and for weaker rocks like slate and phyllite point load index test has been performed as per the standards of BIS, 1998 (table 3.24). The test was conducted as per the guidelines recommended by International Society of Rock Mechanics (ISRM, 1978). The unit weight (table 3.24) of rock types has been determined according to the guidelines of the Bureau of Indian Standard codes (BIS, 1974). Furthermore, thin sections were prepared from rock exposed at each location and microscopic inspection was conducted by Polarising or transmitted light type microscope to identify lithology, mineralogical and textural attributes (figure 3.33). The rock constant value (mi) relies on lithology. There is certain range of mi values for distinct lithology. For much better approximation of rock constant value, mineralogical and chemical alteration was also considered along with lithology. Petrographic examination was conducted and depending upon modal percentage of resistant minerals and degree of chemical alteration was accounted by considering the lower bound. Depending upon modal percentage of micaceous and clay minerals, the mi values has been adjusted. For instance, sandstone at location S5 is of quartzarenite type having abundant resistant quartz, the assigned mi values is 17. While, sandstone at location S11 and S12 is sub-arkosic having some feldspar grains, the assigned mi value is 16. Similarly, the sandstone having significant mica content (S13, S14, S17, S18, S19

& S20), the assigned mi value is reduced to 15. The reduction in rock constant value has been done by considering lower bound values recommended in the GHB criterion.

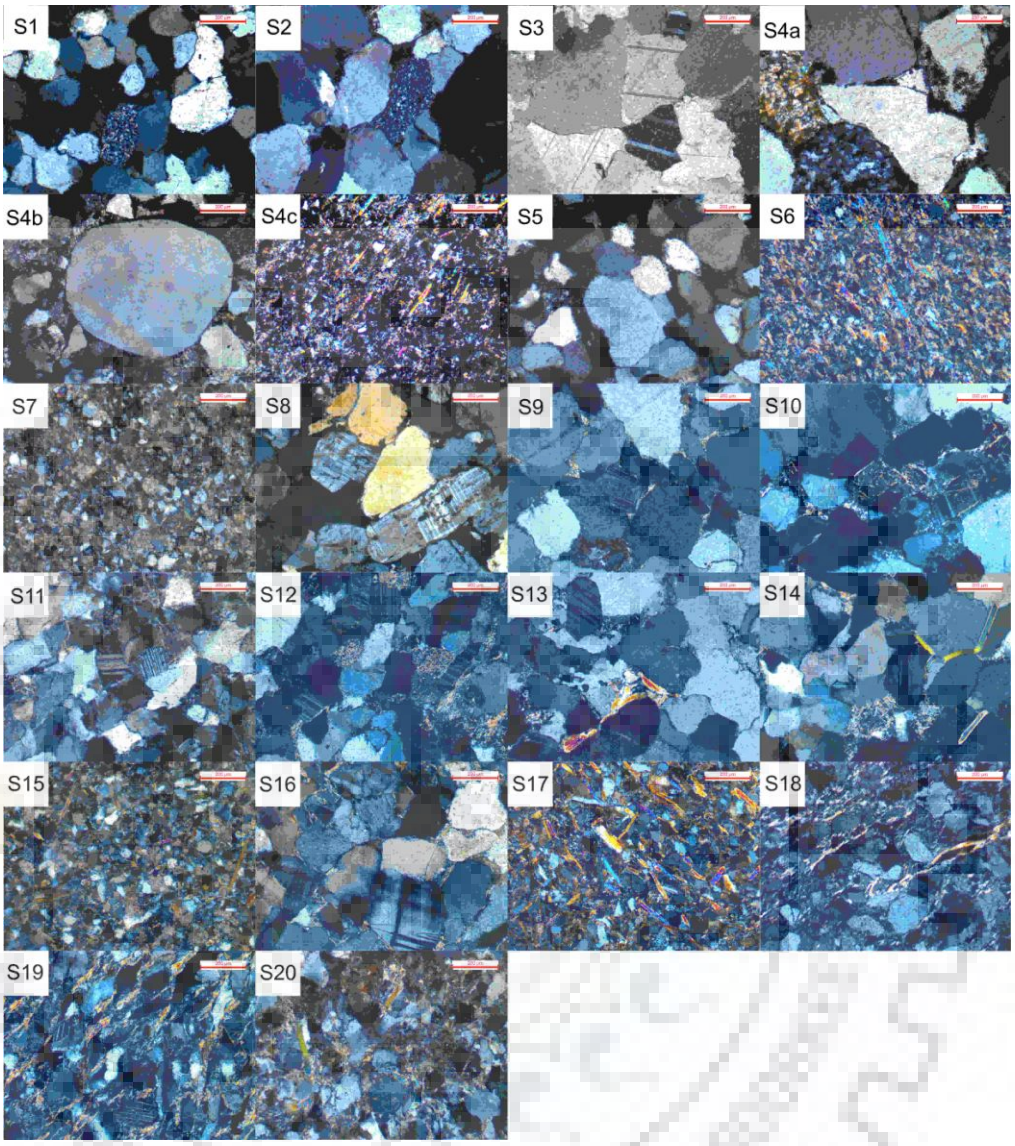

Figure 3.33: Photomicrographs of rock samples from all investigated slopes along NH-58

Table 3.24: Unconfined compressive strength of intact rock and unit weight samples from of investigated road cut rock slopes along NH-58 from Rishikesh to Devprayag

Slope	Lithology	UCS (MPa)			Average UCS (MPa)	Unit weight (MN/m^3)
S1	Quartzarenite	50	43	46	46.33	0.027
S2	Quartzarenite	47	44	49	46.67	0.027
S3	Dolomitic Limestone	37	45	43	41.67	0.0255
S4	Ferruginous Quartzarenite	40	43	48	43.67	0.027
	Slate	18	20	22	20	0.027
S5	Sandstone	49	47	41	45.67	0.027
S6	Slate	20	19	23	20.67	0.0265
S7	Phyllite	21	17	23	20.33	0.0265
S8	Sub-Arkosic Sandstone	43	48	46	45.67	0.027
S9	Quartzite	73	87	78	79.33	0.0275
S10	Quartzite	69	76	77	74.00	0.0275
S11	Sub-Arkosic Sandstone	46	51	44	47.00	0.027
S12	Sub-Arkosic Sandstone	43	47	46	45.33	0.027
S13	Sub-Arkosic Micaceous Sandstone	38	42	40	40.00	0.027
S14	Sub-Arkosic Micaceous Sandstone	37	43	41	40.33	0.027
S15	Clay and Mica bearing Sandstone	33	40	37	36.67	0.027
S16	Sub-Arkosic Sandstone	43	48	42	44.33	0.027
S17	Micaceous Sandstone	36	34	37	35.67	0.0265
S18	Micaceous Sandstone	44	42	47	44.33	0.027
S19	Micaceous Sandstone	45	40	46	43.67	0.027
S20	Micaceous Sandstone	38	42	40	40.00	0.027

3.5. Laboratory investigations of debris slopes: For slope stability analysis, the determination of geomechanical properties of debris material is an utmost part of landslide studies. The representative samples of debris were collected from eight slopes. The geotechnical characteristics pertaining to slope stability were determined in the laboratory as per the standard procedures (table 3.26). The type of soil was determined by conducting sieve analysis and Atterberg limit test. These tests were performed as per the standards of American Society of Testing Materials (ASTM, 1998 & 2005) and the characterization was done by using the Unified Soil Classification System (USCS). The outcomes of sieve analysis, Atterberg limits and type of soil by USCS are illustrated in table 3.25. The shear strength of any material is the resistance offered to sustain under shear stresses.

Table 3.25: Sieve analysis, grading parameters, Atterberg limits, plasticity index and type of soil as per USCS

Slope	d10	d30	d60	Cu	Cc	50% or more population	% of fines	LL	PL	PI	Type of Soil (USCS)
L1	1.3	4	9.5	7.31	1.30	Gravels	<5%	19.59	12.55	7.04	GW
L2	0.8	4.6	16.5	20.63	1.60	Gravels	<5%	19.55	10.79	8.76	GW
L3	0.15	0.35	4.4	29.33	0.19	Sand	5-12%	30.17	23.07	7.1	SP-SC
L4	0.48	2	7.38	15.38	1.13	Gravels	<5%	20.63	15.06	5.57	GW
L5	0.23	2.07	12.3	53.48	1.51	Gravels	5-12%	31.64	24.61	7.03	GW-GC
L6	0.32	1.85	6.5	20.31	1.65	Sand	>12%	20	15.33	4.67	SM-SC
L7	0.045	0.43	2.82	62.67	1.46	Sand	>12%	20.58	11.71	8.87	SC
L8	0.87	4	15	17.24	1.23	Gravels	5-12%	21.8	12.41	9.39	GW-GC

d10: 10% finer; d30: 30% finer; d60: 60% finer; Cu: Uniformity coefficient; Cc: Coefficient of curvature; LL: Liquid limit; PL: Plastic limit; PI: Plasticity index; USCS: Unified soil classification system; GW: Well graded gravels, gravel sand mixture with little or no fines; SP: Poorly graded sands, gravelly sands with little or no fines; SC: Clayey sands, poorly graded sand-clay mixture; GC: Clayey gravels, poorly graded gravel-sand mixture; SM: Silty sands, poorly graded sand-silt mixture

Shear strength of soil can also be defined as the internal resistance offered by the soil per unit area to sustain any failure or sliding or shearing through it. Furthermore, the peak and residual shear strength parameters i.e. cohesion (c) and angle of internal friction (φ) were determined by direct shear test. As Himalayan debris are often comprised of boulders, pebbles, and cobbles, so to consider the impact of larger clast, shear testing is being performed on large direct shear apparatus having a metallic shear box of size 30×30×20 cm as per specifications and guidelines suggested in Bureau of Indian standards (BIS, 1986). The stress controlled shear testing was performed by applying shear force until the sample fails at different normal load. For each debris slope, three shear tests were performed and bivariate curves were plotted among effective normal and shear stresses to calculate peak and residual shear strength parameters of debris (table 3.26).

Table 3.26: Geotechnical and strength characteristics of investigated debris slopes along NH-58

Location	Type of soil	Unit weight (γ in kN/m^3)	Peak Cohesion (kPa)	Peak Friction (°)	Residual Cohesion (kPa)	Residual Friction (°)
L1	GW	19.2	24.05	38.4	18.53	33.6
L2	GW	20.4	21.04	33.2	17.26	29
L3	SP-SC	24.3	26.42	34.8	21.86	30.5
L4	GW	19.7	24.3	38.8	22.05	30.5
L5	GW-GC	22.8	21.22	38.9	17.8	32.4
L6	SM-SC	24	26.25	37.9	20.89	29.3
L7	SC	21.3	28.97	38.1	23.32	34.1
L8	GW-GC	18.9	25.28	37	19.58	29.6

* Description as per Unified soil classification; GW: Well graded gravels, gravel sand mixture with little or no fines; SP: Poorly graded sands, gravelly sands with little or no fines; SC: Clayey sands, poorly graded sand-clay mixture; GC: Clayey gravels, poorly graded gravel-sand mixture; SM: Silty sands, poorly graded sand-silt mixture;

Chapter 4

Stability analyses of road cut rock slopes

4.1. Introduction: Stability appraisal of twenty vulnerable road cut rock slopes along NH-58 from Rishikesh to Devprayag in the precarious Lesser Himalayan terrain was conducted. The geological and geotechnical parameters related to slope stability were determined by extensive field survey and laboratory inspection. During the preliminary stage of the project, rock mass classification techniques often serve as a strong means to characterize slopes. There are certain classification systems those are widely employed for such purposes. In the present study, an attempt has been made to classify the rock mass by Rock mass rating (RMR), slope mass rating (SMR) and continuous slope mass rating (CSMR). The spatial variation in stability grades has been analyzed by employing geographic information system (GIS) tool. Furthermore, the kinematic analysis was also conducted to recognize the structurally controlled failures in the jointed rock mass. In addition to this conventional approach, the much advanced computer-aided numerical modeling based approach was also undertaken. The simulation results had provided much better insight into the problem. Different proxies employed to assess the stability of road cut rock slopes are fairly matching with each other and also showing good agreement with the existing field conditions. By considering all the outcomes of geotechnical assessment, some general preventive and remedial guidelines have been proposed to strengthen the safety along the highway.

4.2. Rock Mass Rating: The exposed rock mass along the highway was heavily jointed and comprises 3-4 sets of joints. Geotechnical parameters pertinent to slope stability was recorded during the field survey. Discontinuity data controlling stability was carefully recorded and examined during field survey and laboratory investigations. Most of the data has been reported in chapter 3 and the remaining ones are being discussed here. RMR is rating based classification system. There are six parameters in RMR method, the values and conditions of each parameter were determined accordingly rock masses have been rated as per RMR_{1989}. The measurement procedure of UCS has been discussed in chapter 3. The concept of Rock quality designation (RQD) was developed by Deere (1963). It provides a quantitative evaluation of the quality of the rock mass. It tells about the fracture frequency and softening in the rock mass and it is calculated from drill core logs. Fracture frequency and also influences permeability and groundwater seepage characteristics through the rock mass. But, it is very time consuming and expensive too. As the drilling cores are not available, RQD% was calculated by volumetric

joint count (Jv) using an empirical relationship (Equation 4.1) suggested by Palmstrom (1982). The volumetric joint count was calculated by the equation (Equation 4.2) suggested by Palmstrom (1974).

$RQD = 115 - 3.3\ Jv$ (Equation 4.1)

$Jv = 1/S1 + 1/S2 + 1/S3 + \ldots..1/Sn + Nr/5\sqrt{A}$ (Equation 4.2)

where, Jv is volumetric joint count; S1, S2, S3 is discontinuity spacing for set 1, set 2, set 3 respectively; A is area in m^2; Nr is the number of random set of discontinuities present in the rock mass.

Discontinuity spacing is the perpendicular distance between two discontinuities which also controls the size and shape of blocks in the jointed rock mass. From every location, discontinuity spacing of each set was measured with precision during field and accordingly ratings were assigned. Furthermore, conditions of discontinuities like persistence, aperture, roughness, infilling and weathering also affect the stability to a great extent. These parameters were determined as per Bureau of Indian Standards (BIS, 1987) during field survey and average values have been considered for rating. Seepage of water within jointed rock slopes usually takes place along discontinuities within it. It also affects water pressure and shear strength of the material. There are certain slopes in the studies section that were reported as moist during the field survey. Moreover, the flowing condition was also witnessed at slope S15 near Kaudiyala, where the groundwater discharges round the year. Continual discharge of groundwater is deteriorating the quality of rock mass to a great extent. Such adverse conditions increase pore pressure and reduce inherent shear strength of discontinuities and often cause softening of rock by forming slippery algae and clay material along joint walls which may act as lubricant or catalyst for failure. The distribution and orientation of discontinuities control the block size and structurally controlled failures. The relative orientations of slope and existing discontinuities were measured by Brunton compass. These planes were plotted in Schmidt type stereonet and qualitative assessment was made to identify planar, toppling and wedge failures. As per the site conditions and favourability to failure, ratings were assigned to a parameter related to the adjustment of the orientation of discontinuities. Total RMR rating is being calculated by the algebraic sum of ratings of all parameters viz. uniaxial compressive strength of intact rock material, RQD, spacing of discontinuities, conditions of discontinuities, groundwater conditions and adjustment for relative orientation of slope and discontinuities, (table 4.1). Accordingly, stability classes were also determined.

Table 4.1: Ratings of RMR parameters and results of investigated road cut rock slopes along NH-58

L	UCS	RQD	SD	CD					GW	RMR_B	AOF	Total RMR	Description of stability grade
				P	A	R	I	W					
S1	4	8	8	2	4	2	6	3	15	52	-25	27	Poor
S2	4	8	8	1	1	5	6	5	15	53	-25	28	Poor
S3	4	13	10	1	1	3	2	4	15	53	-5	48	Fair
S4	4	13	10	1	1	2	6	5	15	57	-25	32	Poor
S5	4	13	10	1	1	3	6	1	15	54	-25	29	Poor
S6	2	8	10	1	1	1	2	5	15	45	-25	20	Very Poor
S7	2	3	8	2	4	3	6	5	15	48	-25	23	Very Poor
S8	4	17	10	2	1	2	6	5	15	62	-25	37	Poor
S9	7	13	10	2	1	4	6	5	15	63	-25	38	Poor
S10	7	8	8	1	1	2	6	4	15	52	-25	27	Poor
S11	4	13	10	1	1	3	4	5	15	56	-5	51	Fair
S12	4	13	8	1	1	1	2	3	15	48	-25	23	Poor
S13	4	13	10	1	1	1	6	1	10	47	-25	22	Poor
S14	4	13	10	2	1	2	6	5	15	58	-25	33	Poor
S15	4	13	10	0	1	1	6	5	0	40	-25	15	Very Poor
S16	4	13	10	0	1	3	6	1	15	53	-25	28	Poor
S17	4	13	8	1	1	2	6	1	10	46	-25	21	Poor
S18	4	13	10	1	1	3	6	4	15	57	-25	32	Poor
S19	4	8	8	1	1	3	6	5	10	46	-25	21	Poor
S20	4	8	8	1	1	3	6	5	15	51	-25	26	Poor

L: Location number; UCS: Uniaxial compressive strength of intact rock material; RQD: Rock quality designation; SD: Spacing of discontinuities; CD: Conditions of discontinuities; P: Persistence; A: Aperture; R: Roughness; I: Infilling; W: Weathering; GW: Groundwater conditions; RMR_B: RMR_{basic}; AOF: Adjustment for discontinuity orientation factor

4.3. Slope Mass Rating: In RMR system, the adjustment parameter related to the orientation of discontinuities is a completely subjective assessment. In the case of slopes, there are no guidelines for quantitative assessment of the abovementioned parameter. SMR method reduces subjective interpretation and qualitative consideration of orientation factor. SMR system involves quantitative assessment of factors that are related to the orientation of discontinuities. It involves a detailed assessment angular relationship among the direction and amount of dip of discontinuities with respect to the slope facet. Due to these facts, it is the most reliable and robust classification systems for slope stability appraisal. SMR is the extension of Bieniawski's RMR which includes RMR_{basic}, and certain adjustment factors (F_1, $F_2$and F_3) that are being calculated by the relative orientation data of slope facets and the most vulnerable set of discontinuity. While F_4 is excavation related parameter that is to be determined by visual inspection during the field survey. For different modes of structurally controlled failures, the total SMR values were calculated for all investigated road cut slopes. Accordingly, class number and stability grades were determined (table 4.2).

Table 4.2: Slope Mass Rating results of studied road cut rock slopes along NH-58

Slope	RMR_{basic}	Type of Failure	F_1	F_2	F_3	F_4	SMR	Stability Class	Stability Grade
S1	52	P (J1)	0.15	1.00	-60.00	+10	53	III	PS
		T (J2)	0.70	1.00	-25.00	+10	44	III	PS
S2	53	W (J1-J2)	0.70	1.00	-60.00	+10	21	IV	UN
S3	53	W (J1-J2)	0.40	0.40	-60.00	+8	51	III	PS
S4	57	P (J1)	1.00	0.85	-60.00	+10	16	V	CU
		W (J1-J3)	1.00	0.85	-60.00	+10	16	V	CU
S5	54	W (J1-J2)	0.85	1.00	-60.00	+8	11	V	CU
S6	45	T (J1)	0.40	1.00	-25.00	+8	43	III	PS
S7	48	P (F)	0.85	1.00	-60.00	+10	7	V	CU
		W (F-J1)	0.15	1.00	-60.00	+10	44	III	PS
S8	62	P (J1)	1.00	1.00	-60.00	+10	12	V	CU
S9	63	W (J1-J2)	1.00	1.00	-60.00	+8	11	V	CU
S10	52	P (J1)	0.15	1.00	-60.00	+8	51	III	PS
		T (J2)	0.15	1.00	-25.00	+8	56	III	PS
S11	56	W (J1-J2)	0.15	1.00	-50.00	+10	58	III	PS
S12	48	P (J1)	0.85	1.00	-50.00	+10	15	V	CU
		W (J2-J4)	1.00	0.70	-60.00	+10	16	V	CU
S13	47	P (J1)	0.40	0.85	-60.00	+10	37	IV	UN
		W (J1-J3)	0.40	0.85	-60.00	+10	37	IV	UN
S14	53	P (J3)	0.70	1.00	-60.00	+10	26	IV	UN
S15	40	P (J3)	0.40	1.00	-50.00	+10	30	IV	UN
		W (J1-J3)	0.15	0.85	-60.00	+10	42	III	PS
S16	48	P (J1)	0.85	0.85	-60.00	+10	20	V	CU
S17	46	P (J2)	0.4	1.00	-50.00	+8	34	IV	UN
		W (J1-J2)	0.15	1.00	-60.00	+8	45	III	PS
S18	57	P (J1)	0.70	1.00	-60.00	+10	25	IV	UN
		W (J1-J3)	0.70	0.85	-60.00	+10	31	IV	UN
S19	57	P (J3)	0.40	1.00	-60.00	+10	43	III	PS
		W (J1-J2)	0.85	1.00	-60.00	+10	16	V	CU
S20	46	W (J1-J2)	0.7	0.85	-60.00	+8	18	V	CU

P: Planar failure; T: Toppling failure; W: Wedge failure; J: Joint; F: Foliation; CU: Completely unstable; UN: Unstable; PS: Partially stable; F_1, F_2, F_3 are adjustment factors related to relative orientation of discontinuities and slope; F_4: Adjustment factor for method of excavation

In conjunction with SMR, Continuous Slope Mass Rating (CSMR) method was employed (table 4.3). In contrast to SMR, the CSMR method involves continuous functions of adjustment factors. This reduces the ambiguity that arises when the values lie at the boundaries of class intervals of different parameters.

Table 4.3: Continuous Slope Mass Rating results of studied road cut rock slopes along NH-58

Slope	RMR_{basic}	Type of Failure	F_1	F_2	F_3	F_4	SMR	Stability Class	Stability Grade
S1	52	P (J1)	0.24	0.98	-58.10	+10	49	III	PS
		T (J2)	0.64	1.00	-25.52	+10	46	III	PS
S2	53	W (J1-J2)	0.80	0.93	-59.42	+10	19	V	CU
S3	53	W (J1-J2)	0.43	0.32	-59.66	+8	53	III	PS
S4	57	P (J1)	0.97	0.90	-59.48	+10	15	V	CU
		W (J1-J3)	0.99	0.90	-59.48	+10	14	V	CU
S5	54	W (J1-J2)	0.91	0.99	-58.27	+8	10	V	CU
S6	45	T (J1)	0.41	1.00	-25.65	+8	43	III	PS
S7	48	P (F)	0.91	0.98	-58.10	+10	6	V	CU
		W (F-J1)	0.25	0.96	-58.94	+10	39	IV	UN
S8	62	P (J1)	1.00	1.00	-59.00	+10	16	V	CU
S9	63	W (J1-J2)	0.97	0.96	-59.05	+8	16	V	CU
S10	52	P (J1)	0.27	0.96	-59.29	+8	44	III	PS
		T (J2)	0.13	1.00	-25.68	+8	57	III	PS
S11	56	W (J1-J2)	0.33	0.90	-51.14	+10	51	III	PS
S12	48	P (J1)	0.94	0.97	-56.8	+10	6	V	CU
		W (J2-J4)	1.00	0.76	-59.47	+10	13	V	CU
S13	47	P (J1)	0.54	0.90	-59.42	+10	28	IV	UN
		W (J1-J3)	0.35	0.90	-59.42	+10	38	IV	UN
S14	53	P (J3)	0.74	0.96	-59.13	+10	26	IV	UN
S15	40	P (J3)	0.41	0.98	-57.29	+10	27	IV	UN
		W (J1-J3)	0.21	0.86	-59.47	+10	39	IV	UN
S16	48	P (J1)	0.89	0.91	-59.27	+10	15	V	CU
S17	46	P (J2)	0.41	0.98	-55.32	+8	32	IV	UN
		W (J1-J2)	0.27	0.96	-59.00	+8	38	IV	UN
S18	57	P (J1)	0.80	0.93	-58.88	+10	23	IV	UN
		W (J1-J3)	0.74	0.92	-59.05	+10	27	IV	UN
S19	57	P (J3)	0.48	0.93	-59.40	+10	40	IV	UN
		W (J1-J2)	0.94	0.96	-59.27	+10	14	V	CU
S20	46	W (J1-J2)	0.83	0.81	-59.57	+8	14	V	CU

P: Planar failure; T: Toppling failure; W: Wedge failure; J: Joint; F: Foliation; CU: Completely unstable; UN: Unstable; PS: Partially stable; F_1, F_2, F_3 are adjustment factors related to relative orientation of discontinuities and slope; F_4: Adjustment factor for method of excavation

Among various rock mass classifications used here, CSMR is most appropriate and reliable method particularly for stability evaluation of slopes. It is due to much exhaustive and quantitative consideration of factors related to the orientation of discontinuities with respect to the slope facet. Moreover, in contrast to SMR, CSMR relies on continuous functions rather than discrete. Hence, the CSMR method provides much better approximation about the prevailing stability grades and the outcomes are much closer to the existing field conditions. As the rock mass in the investigated area comprises of multiple sets of discontinuities with steep slope angle, thereby CSMR method is best-suited rock mass classification in such conditions where structurally controlled failure are common.

The stability of slopes was evaluated by different methods like RMR, SMR, CSMR, critical SRF-GHB, and critical SRF-MC. The spatial variation in stability grades of the studied slopes is shown in on the geological map of the study area (figures 4.1, 4.2, 4.3, 4.7 and 4.8).

The outcomes of RMR, SMR, and CSMR were classified into five different classes as suggested while for critical SRF by GHB and MC, the outcomes were categorized into different classes of stability as <1 (unstable), 1-1.3 (marginally stable) and >1.3 (stable). The categorization is being done as per the guidelines suggested by Geotechnical Control Office, Hong Kong (GEO, 1984). Spatial variation by RMR is indicating that most of the studied slopes are falling under poor category (figure 4.1). The spatial variation by SMR and CSMR is nearly identical with a minor exception at slope S2. It is due to the fact that the value of SMR and CSMR is lying at the boundary of the adjacent class interval. It is quite notable that most of the unstable to completely unstable slopes lies near Kaudiyala where the rock mass is heavily jointed and also proximal to Duwadhar fault and Saknidhar thrust fault. Furthermore, spatial variation in critical SRF by GHB criterion is depicting that most of the slopes are marginally stable and liable to fail.

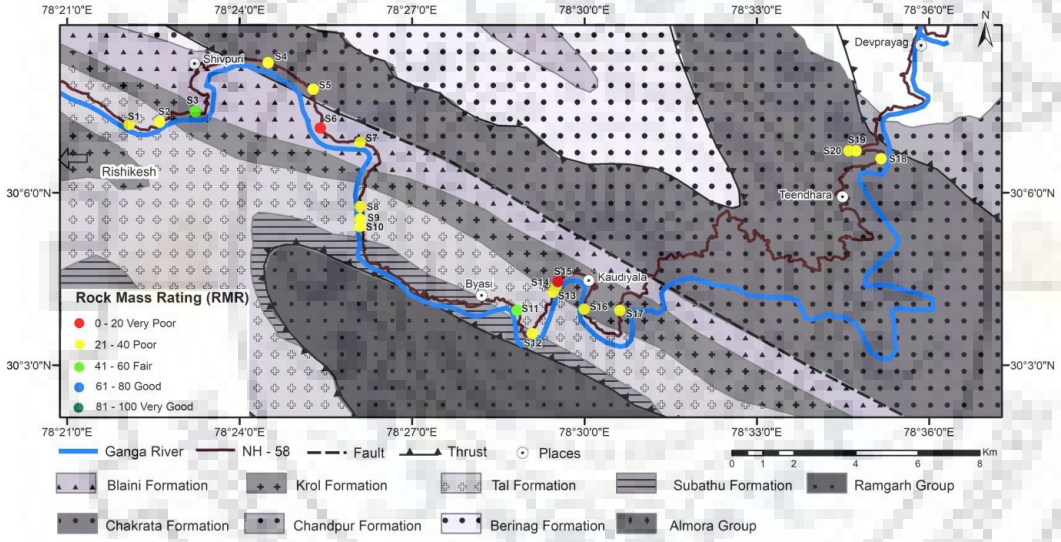

Figure 4.1: Spatial variation in RMR along NH-58

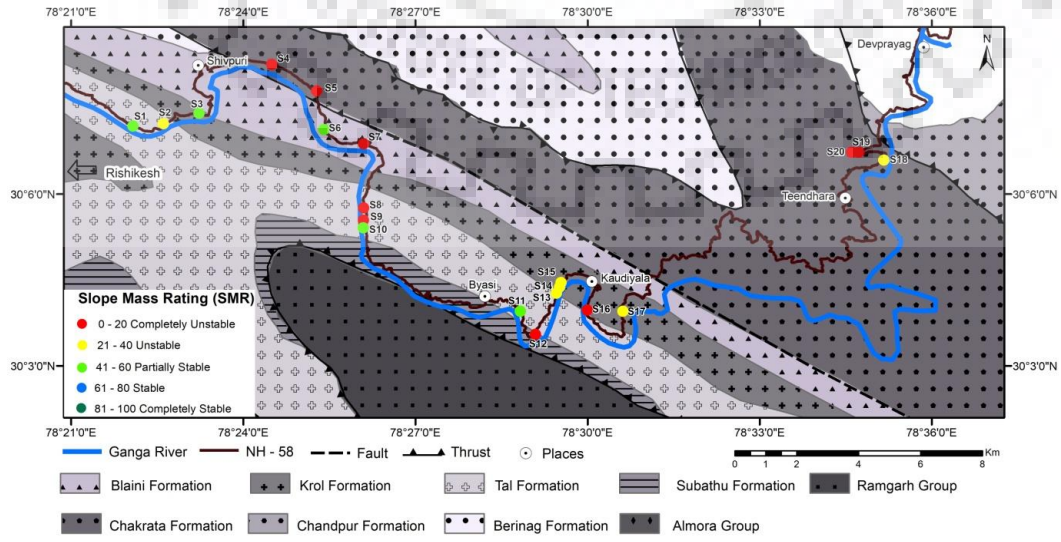

Figure 4.2: Spatial variation in SMR along NH-58

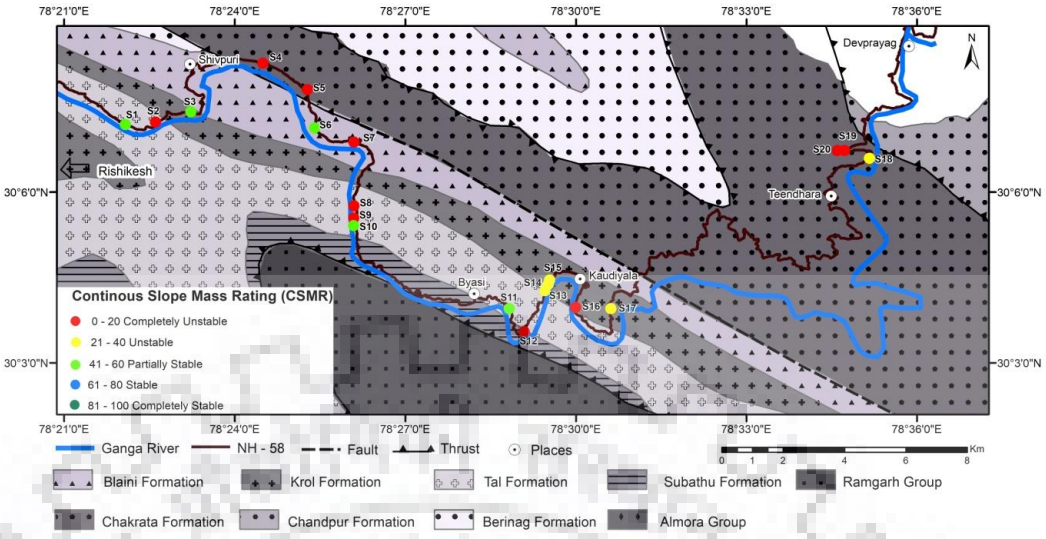

Figure 4.3: Spatial variation in CSMR along NH-58

4.4. Kinematic analysis: Structurally controlled failures are very prominent in the study area due to highly fragile conditions posed due to intensely jointed rock mass. Kinematic analysis revealed that most of the investigated slopes are under significant threat of structurally controlled failures. Planar and wedge failures are quite common at discrete locations and toppling failure was also evident in few slopes. The kinematic analysis of slope determines the possible mode of failures irrespective of its cause. The orientations of each slope face and the discontinuity sets present within the rock mass were measured on outcrop during field survey (table 4.4). The orientations of the planes were plotted on Schmidt net to determine angular relationships among those which enabled to identify the mode of structurally controlled failures like planar, toppling and wedge (figure 4.4). For instance in slope S5, the most probable mode of failure is of wedge type due to intersection of joint set J1 and J2 because the line formed by the intersection of these joint sets is plunging in the same direction as slope and amount of plunge is greater than friction angle but smaller than the amount of inclination of slope. In slope S8, the dip direction of joint set J1 is nearly parallel to the direction of slope inclination and the amount of dip amount of joint is in between slope inclination and friction. Hence, the slope face is under a critical condition to offer a planar mode of failure. However, at location S6, the joint set J1 is dipping steeply into the slope, thereby forming favorable conditions for toppling failure to occur. Similarly, all possible modes of failures at all locations are illustrated in table 4.4, along with the critical joint set(s) responsible for the failure.

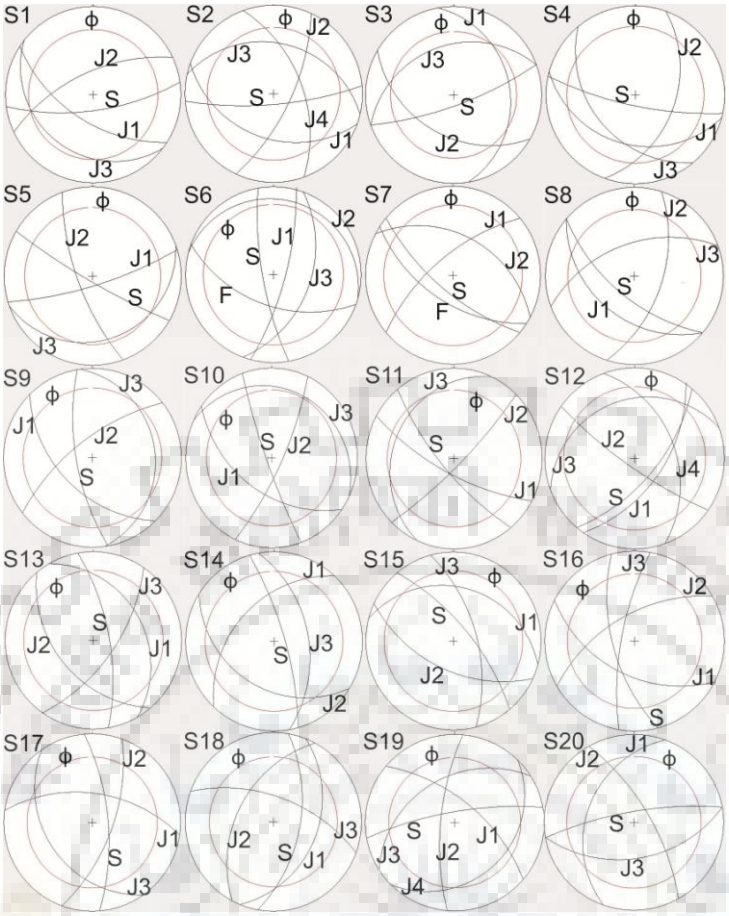

Figure 4.4: Kinematic analysis depicting angular relationship among slope and existing discontinuities at discrete investigated locations along NH-58

Table 4.4: The orientation of slope and existing discontinuities along with the probable mode of failure at discrete locations along NH-58

LN	Slope	J1	J2	J3	J4	Mode of failure
S1	75°/172°	65°/213°	69°/335°	33°/218°	-	P (J1) & T (J2)
S2	80°/175°	48°/200°	74°/115°	42°/013°	63°/070°	W (J1-J2)
S3	80°/160°	36°/080°	52°/210°	43°/340°	-	W (J1-J2)
S4	80°/192°	43°/195°	53°/110°	49°/230°	-	P (J1) & W (J1-J3)
S5	85°/210°	81°/163°	76°/250°	28°/160°	-	W (J1-J2)
S6	80°/260°	61°/200°	79°/105°	15°/015°	55°/110°	T (J1)
S7	75°/220°	65°/213°	72°/320°	52°/028°	-	P (F) & W (F-J1)
S8	70°/220°	51°/220°	64°/108°	60°/340°	-	P (J1)
S9	75°/260°	59°/225°	73°/322°	30°/082°	-	W (J1-J2)
S10	85°/250°	58°/215°	80°/115°	23°/025°	-	T (J2)
S11	78°/230°	76°/208°	83°/135°	31°/295°	-	W (J1-J2)
S12	70°/130°	64°/125°	82°/215°	35°/340°	52°/070°	P (J1) & W (J2-J4)
S13	75°/080°	42°/060°	55°/230°	70°/125°	-	P (J1) & W (J1-J3)
S14	80°/074°	53°/313°	46°/212°	58°/080°	-	P (J3)
S15	75°/050°	39°/015°	63°/205°	68°/075°	-	P (J3) & W (J1-J3)
S16	70°/255°	59°/207°	66°/330°	78°/100°	-	W (J1-J2)
S17	75°/085°	63°/008°	71°/110°	46/235°	-	P (J2) & W (J1-J2)
S18	65°/100°	48°/112°	56°/298°	67°/020°	-	P (J1) & W (J1-J3)
S19	80°/350°	69°/040°	77°/275°	48°/328°	35°/135°	P (J3) & W (J1-J2)
S20	80°/350°	46°/290°	75°/060°	56°/170°	-	W (J1-J2)
LN: Location; P: Planar failure; T: Toppling failure; W: Wedge failure; J: Joint; F: Foliation The orientation data is the format: Amount of dip/Dip direction						

4.5. Numerical simulation of rock slopes: Numerical modeling of demarcated vulnerable slopes is being conducted by employing Finite element method. Shear Strength Reduction (SSR) technique is one the most robust method to assess the factor of safety (FoS). In this method, the shear strength failure envelope is reduced steadily until the deformations are unacceptably large or it does not converge solutions. SSR technique is popular and widely applicable to a variety of rock engineering practices. A variety of geological and geotechnical data pertaining to slope stability was collected and amalgamated from rigorous field inspections, extensive calculations, and sophisticated laboratory experiments. The two-dimensional geometry of cut slope was generated by compiling data obtained by laser inclinometer, Brunton compass and measuring tape. A variety of geological formations comprises of distinct lithology and geological characteristics were reported from the stretch. The input geomechanical data of intact rock and rock mass are showing a wide range along

certain benchmark values. Due to widespread applicability under the diverse scenario, SSR method was adopted for the stability evaluation of road cut rock slopes and modeling was performed by two-dimensional plain-strain simulator Phase 2D. The plain-strain analysis was done in metric units and Gaussian elimination solver. Furthermore, the maximum 500 iterations with a tolerance of 0.001 were followed for stress analysis. The simulation was done under gravity loading conditions by discretization with a six-noded graded triangle. In the model of each cut slope, the base of the model has been fixed and slope face was made restrain free in both x & y directions whereas the displacements were restricted in x & y-axis of the model. For instance, the generated model has been illustrated in figure 4.5.

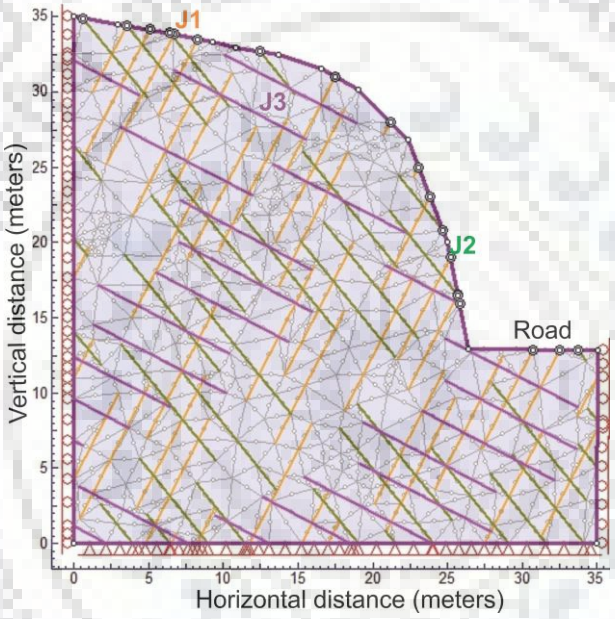

Figure 4.5: The input model of slope S17 along NH-58

The non-linear Generalized Hoek-Brown (GHB) criterion was employed for the stability analysis. For comparative analysis, Mohr-Coulomb (MC) criterion was also undertaken. The Geological Strength Index (GSI) values were calculated by careful assessment of discontinuities and their conditions). The structure ratings were determined by volumetric joint count and conditions of discontinuities were assessed by roughness, weathering and infilling data of every slope was determined as per the quantification method suggested by (Sonmez and Ulusay, 1999 and 2002). Accordingly, the GSI values were quantified (table 4.5) for all road cut slopes and the also demonstrated in GSI chart (figure 4.6).

Table 4.5: Geological strength index (GSI) of investigated road cut rock slopes along NH-58

Slope	Roughness (Rr)	Weathering (Rw)	Infilling (Rf)	Jv	SCR	SR	GSI
S1	2	3	6	19.7	11	27.58	40
S2	5	5	6	20.0	16	27.36	52
S3	3	4	2	12.5	9	35.59	39
S4	2	5	6	12.9	13	35.00	48
S5	3	1	6	12.6	10	35.37	41
S6	1	5	2	23.5	8	24.50	33
S7	1	5	6	28.1	12	21.38	40
S8	2	5	6	10.9	13	37.90	50
S9	4	5	6	12.7	15	35.21	53
S10	2	4	6	24.1	12	24.08	42
S11	3	5	4	16.3	12	30.86	44
S12	1	3	2	16.9	6	30.24	30
S13	1	1	6	12.5	8	35.58	37
S14	2	5	6	14.3	13	33.15	47
S15	1	5	6	12.3	12	35.78	46
S16	3	1	6	14.6	10	32.81	40
S17	2	1	6	16.1	9	31.08	37
S18	3	4	6	15.1	13	32.28	47
S19	4	3	6	17.4	13	29.75	46
S20	3	5	6	21.3	14	26.23	47

Rr = Roughness rating, Rw: weathering rating; Rf: Infilling rating; J_v: volumetric joint count; SCR: Surface condition rating; SR: Structure rating; GSI: Geological strength index

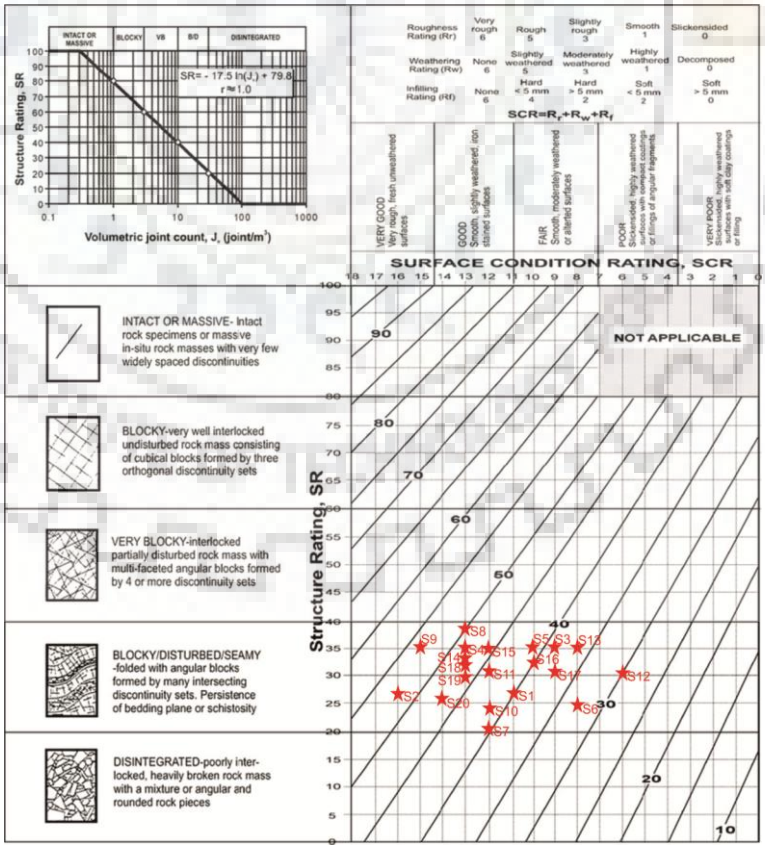

Figure 4.6: GSI values of investigated road cut rock slopes along NH-58

The fundamental geomechanical parameters used in the numerical simulation were determined during field inspection and laboratory experiments (table 4.6). The detailed illustrations of the procedure adopted for the determination of UCS and unit weight have been discussed in chapter 3 (Field and laboratory investigations). The rock constant (m_i value) for each slope was a macroscopic and microscopic examination. The macroscopic examination was done in the field while microscopic studies were conducted in the laboratory under a petrological microscope. The disturbances induced due to blasting and stress relaxation are considered in GHB by a parameter called Disturbance factor (D). It is the qualitative estimation of disturbances induced into the slopes. To estimate D, there are separate guidelines for underground excavations and slopes. As per the guidelines suggested in GHB criterion the disturbance factor was determined during field survey (table 4.6). Poisson's ratio controls elastic deformation in intact rocks and rock masses when subjected to static or dynamic stresses. In comparison to other geomechanical parameters, poisson's ratio has not been much appreciated because of the very narrow range of values (Grecek, 2007). The direct experiments on poisson's ratio of rocks are rarely being conducted (Vásárhelyi and Kovács, 2017). In literature, there are numerous graphical and empirical relationships to estimate the poisson's ratio of rocks. It is often in practice, to estimate poisson's ratio of rocks by indirect methods. In the present study, that chart proposed by Vásárhelyi (2009) was used to calculate poisson's ratio of the rock mass (ν_{rm}). This method is based on GSI values and rock material constant (m_i).

Table 4.6: Geomechanical properties of intact rock and rock mass used for numerical simulation of road cut rock slopes along NH-58

Slope	Height (m)	UCS (MPa)	GSI	m_i value	Disturbance factor	Unit weight (MN/m^3)	Poisson's ratio
S1	30	46.33	40	17	0.8	0.027	0.33
S2	60	46.67	52	17	0.8	0.027	0.295
S3	42	41.67	39	10	0.9	0.0255	0.375
S4	42	43.66 & 20	48	17 & 7	0.9	0.027 & 0.027	0.30 & 0.365
S5	33	45.67	41	17	0.9	0.027	0.32
S6	19	20.67	33	7	0.8	0.0265	0.365
S7	18	20.33	40	7	0.8	0.0265	0.37
S8	18	45.67	50	16	0.9	0.027	0.3
S9	17	79.33	53	20	0.9	0.0275	0.28
S10	45	74.00	42	20	0.8	0.0275	0.31
S11	30	47.00	44	16	0.8	0.027	0.315
S12	40	45.33	30	16	0.8	0.027	0.34
S13	34	40.00	37	15	0.8	0.027	0.33
S14	42	40.33	47	15	0.8	0.027	0.315
S15	33	36.67	46	14	0.8	0.027	0.32
S16	33	44.33	40	16	0.8	0.027	0.32
S17	35	35.67	37	15	0.9	0.0265	0.33
S18	30	44.33	47	15	0.8	0.027	0.315
S19	38	43.67	46	15	0.8	0.027	0.315
S20	23	40.00	47	15	0.9	0.027	0.315

Schmidt hammer rebound values for each joint set have been measured during field survey as per the guidelines suggested by International Society of Rock Mechanics (ISRM, 1981) and joint compressive strength (JCS) has been determined in light of equation proposed by Katz et al. (2000). The rebound (Hr) values were taken from each joint set. From each joint set at least 10 Hr values were taken during the field survey and the median value was calculated to determine joint wall compressive strength (JCS). As Schmidt hammer rebound test is a non-destructive in-situ and cost-effective test. By considering several geological and geotechnical constraints, there are enormous numbers of empirical co-relationships among Hr and compressive strength. The selection of the most appropriate one is an utmost component for reliable outcomes. While selecting any correlation, the rock type and range of Hr values considered for proposing equations should be taken into consideration. The relationship (equation 4.3) suggested by Katz et al. (2000) was used to calculate JCS (table 4.7) of each joint wall because of the correlation was suggested by considering similar rock type with

substantially fair regression (0.92). The Schmidt rebound values and joint compressive strength (JCS) range of suggested correlation (equation 4.3) is 24-73 and 11-259 respectively. So, the suits better to existing conditions in the area under investigation. The calculated JCS was used as an input in Barton-Bandis (BB) failure criterion. Furthermore, by considering similar grounds, Young's modulus (table 4.7) for each joint set was determined by an empirical relationship (equation 4.4) proposed by Yagiz (2009).

$$\text{UCS (MPa)} = 2.208e^{0.067\times H_r} \qquad \text{Equation 4.3}$$

$$\text{E (GPa)} = 0.0987 \times {H_r}^{1.5545} \qquad \text{Equation 4.4}$$

In jointed rock mass, the roughness or asperities of joint wall controls the shear strength of discontinuities. Smooth, planar and slickensided surfaces tend to offer least shear strength and often susceptible for sliding along the joints. The consideration of stress regimes at a particular site is an important aspect. In comparison to underground projects, joint roughness is very crucial in case of slopes because roughness plays a crucial role at low-stress levels whereas at higher stress regimes asperities are sheared and form a smooth surface. For each joint set, roughness profiles were recorded carefully by using Barton comb. The generated profiles were compared with standard profiles proposed by Barton and Choubey (1977) and joint roughness coefficient was determined for each joint set (table 4.8). Furthermore, friction along joints is also an important component that governs shear strength of joints. The tilt test was performed to determine the residual friction along rock joints (table 4.8) and used as an input in numerical simulation by adopting Barton-Bandis (BB) failure criterion for joints. The spacing of discontinuities controls fracture frequency and often directly related to a variety of strength characteristics of the rock mass. Joint spacing is the perpendicular distance between adjacent joints in a particular set. For each joint set, joint spacing (table 4.9) was measured cautiously during the field survey by using meter scale. Furthermore, rock mass modulus (table 4.9) was calculated by an empirical relationship (equation 4.5) suggested by Hoek and Diederichs (2006).

$$E_{rm}(\text{MPa}) = 100000\left(\frac{1-D/2}{1+e^{((60+15D-GSI)/11)}}\right) \qquad \text{Equation 4.5}$$

Table 4.7: Schmidt hammer hardness, Young's modulus and joint wall compressive strength of different joint sets at each investigated slopes

Slope	Joint	Schmidt hardness values	Young's Modulus (E in GPa)	JCS	Slope	Joint	Schmidt hardness values	Young's Modulus (E in GPa)	JCS
S1	J1	43	34.16	43.0	S11	J1	51	44.54	75.4
	J2	38	28.19	30.3		J2	56	51.51	106.9
	J3	46.5	38.58	55.0		J3	55	50.09	99.7
S2	J1	39.5	29.94	33.7	S12	J1	53.5	47.98	89.8
	J2	44	35.40	46.2		J2	54.5	49.38	96.3
	J3	43.5	34.78	44.6		J3	55.5	50.79	103.3
	J4	48	40.53	61.1		J4	53	47.28	86.7
S3	J1	43.5	34.78	44.6	S13	J1	55.5	50.79	103.3
	J2	42.5	33.55	41.6		J2	54	48.68	93.0
	J3	46	37.94	53.1		J3	55	50.09	99.7
S4	J1	54	48.68	93.0	S14	J1	54	48.68	93.0
	J2	53.5	47.98	89.8		J2	51.5	45.22	78.0
	J3	49.5	42.52	67.8		J3	53	47.28	86.7
S5	J1	47.5	39.88	59.0	S15	J1	53.5	47.98	89.8
	J2	49.5	42.52	67.8		J2	55.5	50.79	103.3
	J3	45.5	37.30	51.3		J3	55.5	50.79	103.3
S6	J1	25	14.70	12.2	S16	J1	54.5	49.38	96.3
	J2	21.5	11.63	9.6		J2	55	50.09	99.7
	J3	25.5	15.16	12.6		J3	54	48.68	93.0
	J4	25	14.70	12.2	S17	J1	52	45.90	80.8
S7	J1	18.5	9.21	7.7		J2	51	44.54	75.4
	J2	16.5	7.71	6.7		J3	53	47.28	86.7
	J3	18.5	9.21	7.7	S18	J1	53.5	47.98	89.8
S8	J1	48	40.53	61.1		J2	56	51.51	106.9
	J2	37.5	27.62	29.3		J3	54	48.68	93.0
	J3	45.5	37.30	51.3	S19	J1	54	48.68	93.0
S9	J1	60.5	58.08	146.5		J2	53.5	47.98	89.8
	J2	58.5	55.13	127.4		J3	53.5	47.98	89.8
	J3	54	48.68	93.0		J4	53	47.28	86.7
S10	J1	55.5	50.79	103.3	S20	J1	56	51.51	106.9
	J2	58.5	55.13	127.4		J2	55	50.09	99.7
	J3	59.5	56.60	136.6		J3	54.5	49.38	96.3

In numerical simulation of the jointed rock mass, joint stiffness is one of the fundamental geomechanical properties. It can be measured by expensive and time-consuming direct in-situ field test (Barton and Choubey, 1977 and Bandis et al. 1983). Joint stiffness relies upon certain parameters that are related to deformation of intact rock and rock mass. The normal stiffness of each joint set was calculated (table 4.9) by empirical relationship suggested by Barton (1972). The shear stiffness may range from $1/10^{th}$ to $1/30^{th}$ times of normal stiffness (Singh and Goel, 2002). In Himalayan terrain conditions, the shear stiffness was taken as $1/10^{th}$

of the normal stiffness (Pain et al. 2014). However, Barton (1972) also proposed an equation for the determination of shear stiffness of joints. The determination of shear modulus of intact rock and rock mass is tedious, time-consuming and costly technique. As shear modulus of intact rock and rock mass was not available, the shear stiffness of joints was estimated as $1/10^{th}$ of the normal stiffness (table 4.9).

Table 4.8: Residual friction angle and joint roughness coefficient at different joint sets in investigated road cut slopes along NH-58

Slope	Joint	Residual Friction (◦)	JRC	Slope	Joint	Residual Friction (◦)	JRC
S1	J1	27	6	S11	J1	25	7
	J2	29	11		J2	26	11
	J3	28	8		J3	26	10
S2	J1	29	15	S12	J1	23	8
	J2	29	14		J2	22	5
	J3	27	9		J3	24	9
	J4	26	6		J4	22	6
S3	J1	29	7	S13	J1	23	7
	J2	31	12		J2	23	8
	J3	30	10		J3	22	3
S4	J1	27	10	S14	J1	24	10
	J2	26	7		J2	23	7
	J3	24	4		J3	24	9
S5	J1	24	11	S15	J1	22	4
	J2	26	13		J2	24	9
	J3	24	9		J3	23	7
S6	J1	21	3	S16	J1	26	8
	J2	25	9		J2	27	9
	J3	24	5		J3	29	12
	J4	23	6	S17	J1	27	6
S7	J1	22	4		J2	29	11
	J2	24	7		J3	28	8
	J3	24	8	S18	J1	28	6
S8	J1	26	7		J2	31	14
	J2	26	6		J3	29	8
	J3	28	12	S19	J1	27	9
S9	J1	23	9		J2	29	15
	J2	25	13		J3	28	12
	J3	26	15		J4	28	13
S10	J1	25	6	S20	J1	29	13
	J2	28	13		J2	26	7
	J3	26	9		J3	27	9

Table 4.9: Intact and rock mass modulus along with spacing and normal and shear stiffness at different joint sets in the investigated road cut rock slopes

Slope	Joint	E_i (Intact rock Modulus) in MPa	E_{rm} (Rock Mass Modulus) in MPa	L (Joint spacing) in m	Kn (Normal Stiffness) in MPa/m	Ks (Shear Stiffness) in MPa/m
S1	J1	34162.05	650.20	0.15	4418.77	441.88
	J2	28189.72		0.25	2662.20	266.22
	J3	38580.94		0.12	5750.83	575.08
S2	J1	29938.31	1332.10	0.25	5576.53	557.65
	J2	35404.98		0.28	5033.38	503.34
	J3	34781.53		0.15	9234.33	923.43
	J4	40532.80		0.18	7870.67	787.07
S3	J1	34781.53	759.70	0.18	4438.08	443.81
	J2	33546.54		0.30	2591.01	259.10
	J3	37937.98		0.35	2214.92	221.49
S4	J1	48676.94	832.20	0.25	3386.70	338.67
	J2	47978.11		0.20	4234.45	423.44
	J3	42518.79		0.30	2829.38	282.94
S5	J1	39878.37	593.30	0.21	2867.91	286.79
	J2	42518.79		0.23	2674.20	267.42
	J3	37298.89		0.35	1722.54	172.25
S6	J1	14703.30	380.60	0.08	5209.52	520.95
	J2	11630.35		0.25	1573.91	157.39
	J3	15162.96		0.40	976.00	97.60
	J4	14703.30		0.30	1302.38	130.24
S7	J1	9207.37	570.50	0.07	9356.67	935.67
	J2	7707.19		0.15	4107.37	410.74
	J3	9207.37		0.18	3475.34	347.53
S8	J1	40532.80	980.70	0.24	4276.67	427.67
	J2	27615.24		0.45	2259.58	225.96
	J3	37298.89		0.25	4110.95	411.09
S9	J1	58083.92	1577.00	0.23	7204.49	720.45
	J2	55126.57		0.45	3607.65	360.76
	J3	48676.94		0.18	9313.15	931.31
S10	J1	50794.96	2792.00	0.15	19695.94	1969.59
	J2	55126.57		0.09	34599.42	3459.94
	J3	56598.35		0.18	16782.15	1678.22
S11	J1	44538.44	822.50	0.13	6703.80	670.38
	J2	51508.09		0.16	5224.04	522.40
	J3	50085.38		0.65	1286.51	128.65
S12	J1	47978.11	410.10	0.15	2757.57	275.76
	J2	49379.37		0.25	1654.14	165.41
	J3	50794.96		0.18	2362.50	236.25
	J4	47282.89		0.10	4136.88	413.69
S13	J1	50794.96	483.00	0.15	3250.91	325.09
	J2	48676.94		0.23	2168.18	216.82
	J3	50085.38		0.10	4877.03	487.70
S14	J1	48676.94	843.40	0.40	2145.68	214.57
	J2	45219.06		0.10	8594.30	859.43
	J3	47282.89		0.68	1272.17	127.22

Continued…

S15	J1	47978.11	722.00	0.25	2932.12	293.21
	J2	50794.96		0.25	2929.64	292.96
	J3	50794.96		0.27	2763.81	276.38
S16	J1	49379.37	622.00	0.19	3315.45	331.54
	J2	50085.38		0.20	3149.11	314.91
	J3	48676.94		0.25	2520.20	252.02
S17	J1	45903.35	384.80	0.16	2503.57	250.36
	J2	44538.44		0.20	1990.53	199.05
	J3	47282.89		0.25	1551.83	155.18
S18	J1	47978.11	927.00	0.25	3781.05	378.11
	J2	51508.09		0.15	6293.26	629.33
	J3	48676.94		0.23	4199.98	420.00
S19	J1	48676.94	859.80	0.35	2500.74	250.07
	J2	47978.11		0.15	5836.60	583.66
	J3	47978.11		0.18	5002.80	500.28
	J4	47282.89		0.45	1946.05	194.61
S20	J1	51508.09	719.00	0.20	3645.89	364.59
	J2	50085.38		0.15	4863.15	486.31
	J3	49379.37		0.11	6632.94	663.29

After collection and synthesizing all inputs, the model of each cut slope was generated in the simulator. To attain realistic results, the failure criterion must be selected as per the type of slope. As the rock mass in the investigated area is jointed, the non-linear GHB criterion was employed for rock mass and B-B criterion adopted for joints. Furthermore, an attempt was made to compare the outcomes of GHB and MC criterion. There are certain numerical simulators that do not involve GHB criterion. To overwhelm this limitation, Hoek et al. (2002) used hundreds of case histories related to rock slopes and underground projects across the globe and proposed and proposed a program known as Roclab. This window-based program is widely used to determine equivalent shear strength parameters such as cohesion and friction (Hoek and Marinos, 2007). By using Roclab, the equivalent cohesion and friction of rock mass were calculated (table 4.10).

Table 4.10: Equivalent Mohr-Coulomb shear strength parameters determined by GHB

Slope	Lithology	Cohesion (MPa)	Friction (°)
S1	Quartzarenite	0.215	43.22
S2	Quartzarenite	0.460	44.16
S3	Dolomitic Limestone	0.178	32.52
S4	Ferruginous Quartzarenite	0.293	42.07
	Slate	0.163	28.77
S5	Sandstone	0.208	40.28
S6	Slate	0.071	29.30
S7	Phyllite	0.088	33.42
S8	Sub-Arkosic Sandstone	0.201	49.05
S9	Quartzite	0.310	55.95
S10	Quartzite	0.371	45.95
S11	Sub-Arkosic Sandstone	0.241	44.89
S12	Sub-Arkosic Sandstone	0.182	34.66
S13	Sub-Arkosic Micaceous Sandstone	0.192	38.48
S14	Sub-Arkosic Micaceous Sandstone	0.295	42.22
S15	Clay and Mica bearing Sandstone	0.235	42.23
S16	Sub-Arkosic Sandstone	0.220	41.67
S17	Micaceous Sandstone	0.163	34.67
S18	Micaceous Sandstone	0.254	45.40
S19	Micaceous Sandstone	0.280	43.06
S20	Micaceous Sandstone	0.189	44.28

The model was computed and simulation results were obtained in terms of shear strain contours and safety factor or critical shear strength reduction factor (SRF). The numerical SRF value is the quantification of stability which provides an instant insight about the overall stability grade of slope. Furthermore, the two-dimensional shear strain contours of cut slopes enable to understand the failure pattern at a glance. The most prominent type of failure can be predicted or defined from distribution, dimensions, and pattern of maximum shear strain contours. In the majority of cut slopes, the zig-zag, sharp and planar distribution of shear strain contours is indicative of structurally controlled failures. It is also quite notable that the location of shear strain by GHB and MC are nearly matching with each other but the thickness of slip surfaces in MC is slightly lesser and thinner in contrast to the slip surfaces by GHB (Appendix-A & B). The critical SRF obtained by using GHB and MC criterion has been illustrated in (table 4.11) and a graphical representation of comparative analysis has been presented (figure 4.9). From the comparative analysis, it can be inferred that for cut slopes having SRF close to 1, the results and nearly identical. But, if SRF by GHB criterion is sufficiently greater than 1, then SRF by MC is 1.5 to 2 times to that of obtained by GHB. So, it can be derived that for fair and heterogeneous rock mass MC criterion gives higher stability. This infers that linear MC criterion is much applicable to extensively jointed or fractured rock mass which can be treated as a homogeneous mass. It is being proposed by the analyses, if non-linear GHB criterion is

available, MC criterion should be avoided in the jointed rock mass. A linear relationship among SRF by GHB and MC criteria is obtained (figure 4.10) and the empirical equation is $SRF_{MC}=1.3568SRF_{GHB}–0.1086$. The relation can be applied in slope mass having UCS > 30 MPa and volumetric joint count (Jv) < 20.

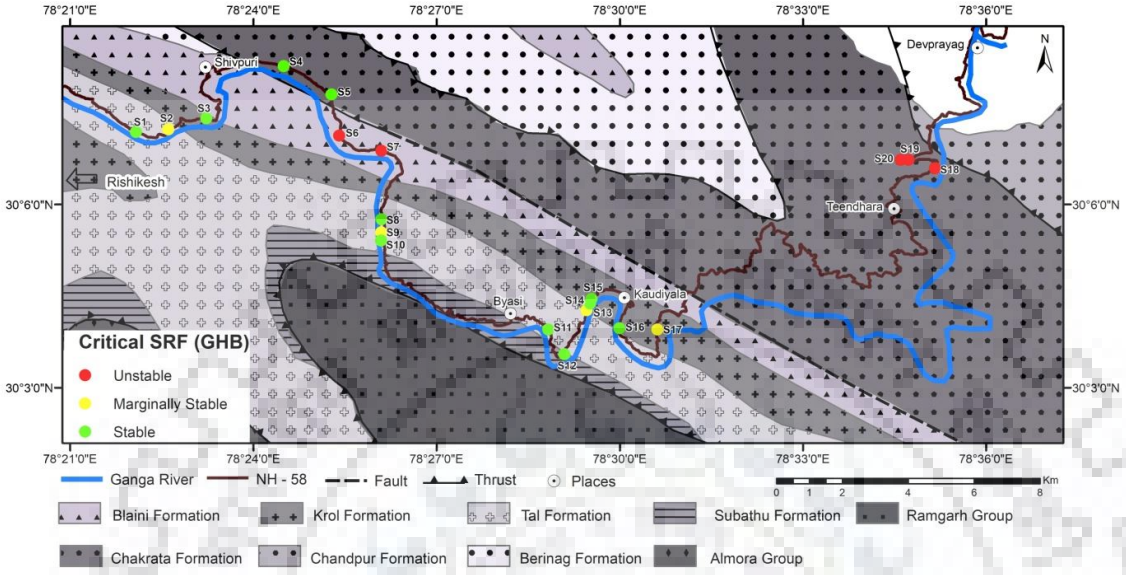

Figure 4.7: Spatial variation in critical SRF by GHB along NH-58

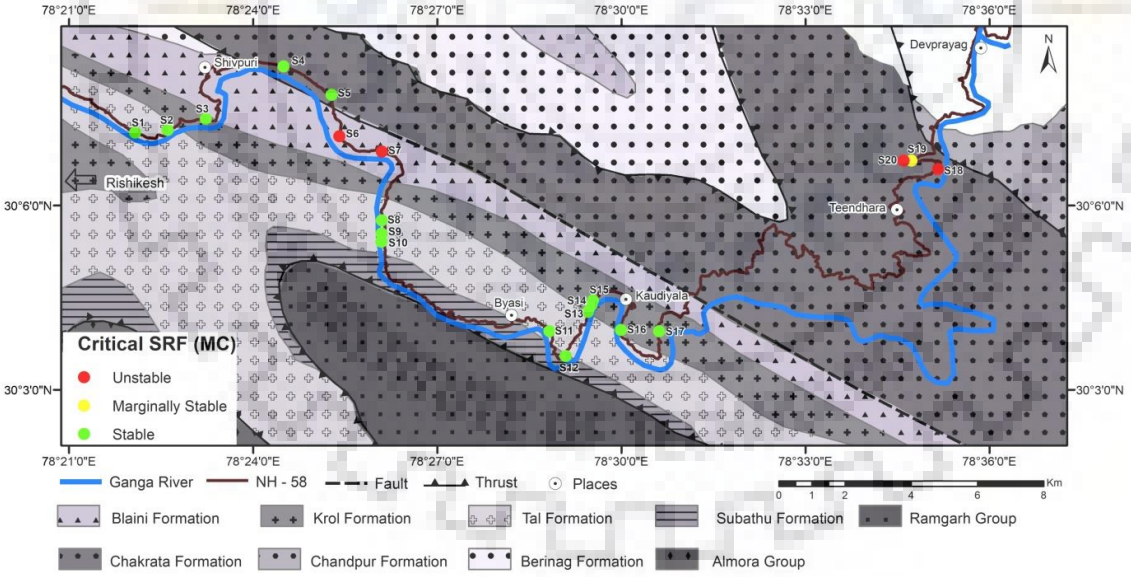

Figure 4.8: Spatial variation in critical SRF by MC along NH-58

Table 4.11: Stability grade and Critical SRF by GHB and MC criterion

Slope	SRF by GHB	Stability grade	SRF by MC	Stability grade
S1	1.39	Stable	2.09	Stable
S2	1.2	Marginally stable	1.49	Stable
S3	1.39	Stable	1.97	Stable
S4	2.37	Stable	3.13	Stable
S5	2.06	Stable	2.93	Stable
S6	0.67	Unstable	0.61	Unstable
S7	1	Unstable	1	Unstable
S8	3.42	Stable	4.16	Stable
S9	1.2	Marginally stable	1.32	Stable
S10	1.42	Stable	1.7	Stable
S11	2.22	Stable	3.09	Stable
S12	1.33	Stable	1.93	Stable
S13	1.22	Marginally stable	1.79	Stable
S14	2.02	Stable	2.73	Stable
S15	2.14	Stable	3	Stable
S16	1.95	Stable	2.19	Stable
S17	1.16	Marginally stable	1.96	Stable
S18	0.99	Unstable	0.99	Unstable
S19	1.01	Unstable	1.01	Unstable
S20	0.99	Unstable	0.99	Unstable

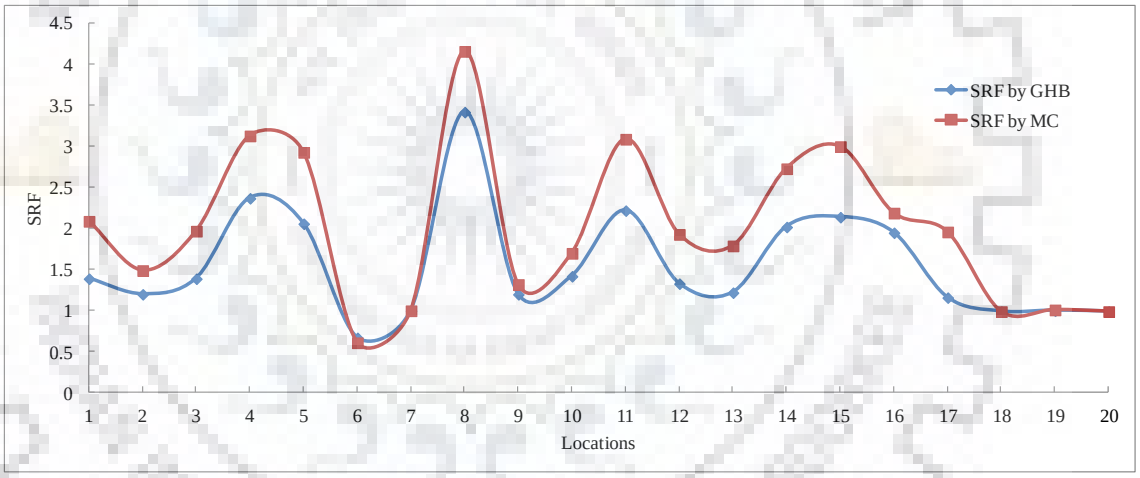

Figure 4.9: Graphical representation of outcomes by GHB and MC criterion

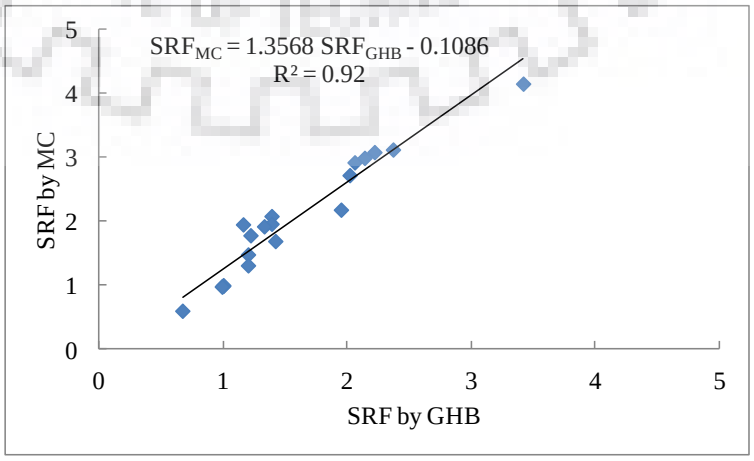

Figure 4.10: Linear relationship between SRF by GHB and MC criterion

Chapter 5

Stability analyses of road cut debris slopes

5.1. Introduction: Stability assessment of eight vulnerable road cut debris slopes along NH-58 from Rishikesh to Devprayag was conducted by limit equilibrium and finite element method based approach. Deterministic and sensitivity analysis was performed by Limit Equilibrium Method (LEM) and critical strength reduction factor which is equivalent to factor of safety has been calculated by the Finite Element Method (FEM) by using Phase 2D simulator. A significant variation in geomaterial ranging from meta-sedimentary rock to in-situ and ex-situ debris was evidenced during field inspection. In contrast to the Great Himalayas (Himadri Himalayas), the lesser Himalayan terrain encompasses a larger number of debris and rock-cum debris slopes. Such slopes are susceptible to the circular type of failures by forming circular or semi-circular failure scarp along the zone of least resistance. There are certain locations in the patch which are prone to talus mode of failure. Such failures occur when debris material ranging in size from soil to boulders is overlying shallow bedrock (less than 10-15 meters). Furthermore, the dip direction of underlying bedrock should be parallel to the dip direction of slope and gradient of bedrock should be lesser than the overall slope angle. One such large scale talus failure has been reported from location L1 and detailed discussion about pre and post failure and causative factors were discussed in chapter 3. Both talus and circular failures were evidenced in the patch along NH-58.

5.2. Numerical simulation of debris slopes: The stability appraisal is being conducted by coupling a variety of information obtained by desk study during preliminary stages and much extensive geotechnical field and laboratory inspection. The linear Mohr-Coulomb (MC) failure criterion is well applicable for numerical analysis of debris, dump and soil slopes (Kainthola et al. 2011). However, there are certain slopes that are having shallow bedrock below debris cover. In such slopes, GHB criterion was adopted for the bedrock portion. Chemical alteration at microscopic level affects overall strength characteristics of geomaterials. For instance, the alteration of certain minerals like plagioclase and microcline into clay minerals has been pondered while assigning rock constant in bedrock. Representative samples of debris were collected from each location. Geomechanical properties pertaining to slope stability analysis were determined by extensive field surveys and laboratory experiments (table 5.1). The standards and methods adopted for data generation have been discussed in detail in chapter 3. The grading of soil was determined by sieve analysis as per the standard procedure suggested

by ASTM (1998). The stiffness of soil fraction was determined by performing Atterberg limit tests and the test was conducted in light of guidelines suggested by ASTM (2005). By utilizing grading parameters obtained by sieve analysis and Atterberg limits, the characterization of soil was done according to the Unified soil classification system. The unit weight and shear strength parameters (cohesion and angle of friction) were determined as per the standards suggested by BIS (1986). However, Young's modulus and Poisson's ratio were taken from the literature on Himalayan debris. As mentioned earlier, debris slopes at certain studied locations (L1, L2, L3, L6, and L7) comprises of bedrock, for these slopes the geomechanical properties used as input in respective numerical models were determined during field investigations (table 5.1); and the detailed illustration of standards have been discussed in chapter 3 (Field and laboratory investigations). As the bedrock is jointed, the non-linear Generalized Hoek-Brown (GHB) failure criterion was adopted.

Table 5.1: Input parameters used for numerical simulation of road cut debris slopes

Type of Material	Properties	Locations							
		L1	L2	L3	L4	L5	L6	L7	L8
Debris	Type of soil	GW	GW	SP-SC	GW	GW-GC	SM-SC	SC	GW-GC
	Unit wt. (γ in kN/m3)	19.2	20.4	24.3	19.7	22.8	24	21.3	18.9
	Young Modulus (E in kPa)	119000	132000	93000	103000	108000	97000	98000	95000
	Poisson's ratio	0.3	0.3	0.3	0.3	0.3	0.3	0.3	0.3
	Peak cohesion (kPa)	24.05	21.04	26.42	24.3	21.22	26.25	28.97	25.28
	Peak friction (°)	38.4	33.2	34.8	38.8	38.9	37.9	38.1	37
	Residual cohesion (kPa)	18.53	17.26	21.86	22.05	17.8	20.89	23.32	19.58
	Residual friction (°)	33.6	29	30.5	30.5	32.4	29.3	34.1	29.6
Bedrock	Rock type	Crystalline Limestone	Slate	Crystalline Limestone	–	–	Sandstone	Sandstone	–
	Geological Strength Index (GSI)	33	40	35	–	–	43	41	–
	Disturbance factor	1	0.9	1	–	–	1	1	–
	Schmidt rebound value	19.21	21.13	14.92	–	–	51.71	53.08	–
	UCS (kPa)	29000	36000	28000	–	–	135000	130000	–
	Unit wt. (kN/m3)	24.75	25.80	25.41	–	–	24.99	24.47	–
	Young Modulus (Erm in kPa)	917519	899196	1014640	–	–	1590440	1415370	–
	Poisson's ratio (ν)	0.385	0.39	0.385	–	–	0.336	0.34	–

GW:Well graded gravels, gravel sand mixture with little or no fines; SP: Poorly graded sands, gravelly sands with little or no fines; SC: Clayey sands, poorly graded sand-clay mixture; GC: Clayey gravels, poorly graded gravel-sand mixture; SM: Silty sands, poorly graded sand-silt mixture; * Description of soil type is described as per Unified soil classification system

Deterministic analysis is being conducted and factor of safety (FoS) values were quantified for each slope (table 5.2). The various limit equilibrium methods (Ordinary/Fellenius, Bishop's, Janbu's simplified, Janbu's corrected, Spencer and GLE/Morgenstern-Price method). The critical SRF i.e. equivalent to factor of safety was also determined by shear strength reduction technique by two-dimensional plain strain simulator Phase 2D (table 5.2). The quantitative outcomes obtained by different LE methods and FEM were compared with each other by graphical means (figure 5.2). It can be evidenced from that FoS obtained by FEM method is slightly lower than calculated by LE methods. It is due to consideration of elastic parameters in computer-aided much advanced finite element method simulator tool. The spatial variation in critical SRF is being represented on the geological map of the study area (figure 5.1).

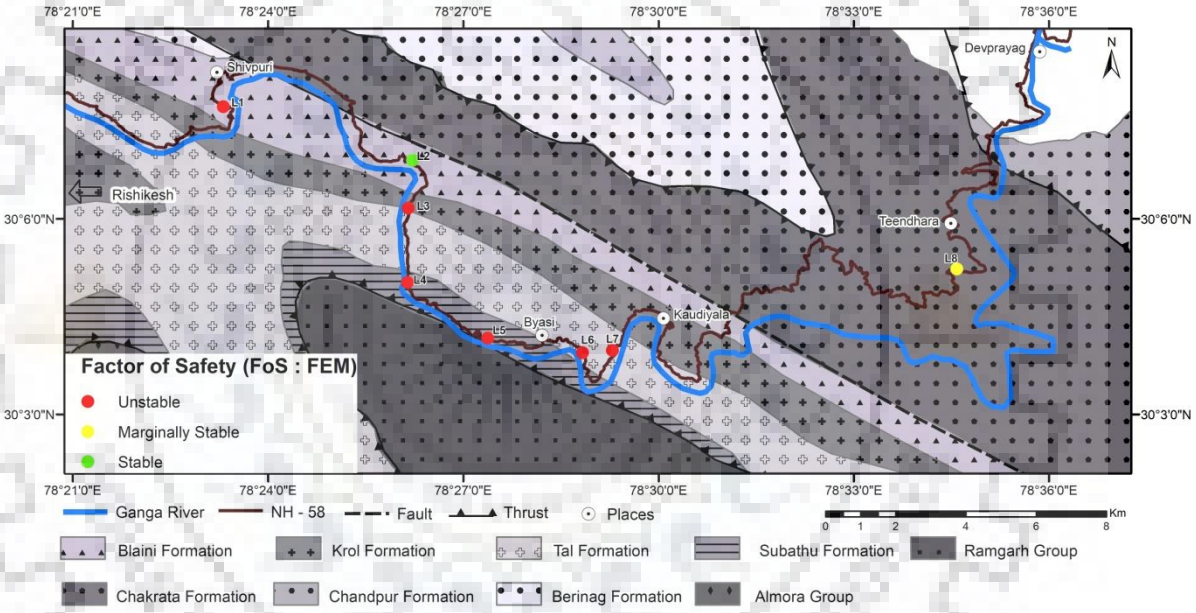

Figure 5.1: Spatial variation in critical SRF by FEM

The factor of safety and critical slip surfaces generated by simulation by LEM and shear strain contours of each slope has been compiled in Appendix C & D. In debris slope at location L1, the critical SRF is 0.99 and a higher concentration of shear strain (0.015) was found. The higher strain contours can be noted along the interface of bedrock and overlying debris. Such pattern is an indicator of talus mode of failure. This judgment is also matching with the existing field conditions. The slope L2 is relatively stable due to a relatively thin cover of debris which is overlying on moderately dipping bedrock. It is also evident from the value of critical SRF which is 1.34 and a lesser concentration of shear strain along the rock-debris interface. It is also noteworthy that the amount of shear strain at L2 is slightly lower as compared to L1. However,

due to weaker bedrock i.e. slate, very minor strain concentration is observed. The slope L2 is most stable among all investigated slopes which may be due to the fact that slope L2 experiences least gravitational loading because the height (19 m) is least as compared to other slopes with moderate slope angle (56°). Although bedrock was also encountered in slope L3, due to a considerable thickness of debris cover, circular failure is more prominent which is also confirmed by the distribution pattern of shear strain contours. Shear strain is concentrated in a thicker zone at the rear and crown portion of the slope, and toe portion of the slope is also experiencing a higher concentration of shear strain. Irrespective of the cause, if strain would be able to propagate from crown to the highly stresses toe region, the failure may be initiated. The critical SRF (0.98) is also indicating an alarming situation of the slope. However, slope L4 and L5 do not encompass bedrock at subsurface, they may experience massive failure by forming a circular slip surface along the least resistant surface. Out of the eight investigated slopes, slope L4 has the least FoS i.e. 0.84 which needs urgent consideration. Due to significant height of 40 m, the slope at location L4 experiences more gravitational loading as compared to slope L5, thereby posing significantly unstable conditions to the slope. Furthermore, shear strain contours are showing a sharp circular failure surface. In slope L5, the shear strain concentration band is wide and continuous seepage in subsequent rainy seasons may aggravate instability of the slope. Such slopes need immediate planning and proper execution to achieve a better and safe design along the highway. The slope at location 6 has SRF value 0.93 and shows higher strain concentration at the toe region in a definite plane which may trigger slope instability. The shear stress concentration is circular at the top part of the slope which may trigger talus mode of failure. Large talus failure is also quite evident in slope L7 (critical SRF 0.93) because maximum shear strain is concentrated within a thin band that lies at the interface of bedrock and debris. Among all investigated slopes, the height of the slope at location L7 is maximum i.e. 45 m. So the slope is experiencing the highest gravitational loading. In slope at location L8, the critical SRF is 1.27 which is an indication of the stable condition. It may be due to the fact that slope height is low (18 m) consequently the impact of gravitational loading is less. It can be concluded that critical understanding about failure mechanism, judgment from shear strain contours and critical SRF are vital in slope engineering practices. Such outcomes from numerical simulation methods facilitate in demarcating the zones having the maximum probability to fail. They serve as a guide to engineers and stakeholders to formulate the best efficient design as per the stability. The cut slopes designs would be an appreciably effective and safe design. The prevention and stabilization can be performed by keeping field conditions and simulation results parallel with each other.

Table 5.2: FoS by different LE and FEM for different debris slopes along NH-58

Methods	FoS							
	L1	L2	L3	L4	L5	L6	L7	L8
Ordinary / Fellenius	1.07	1.49	1.07	0.98	1.05	1.05	1.03	1.35
Bishop's Simplified	1.1	1.51	1.06	1.03	1.11	1.11	1.07	1.37
Janbu's Simplified	1.08	1.5	1.08	0.97	1.04	1.04	1.03	1.36
Janbu's Corrected	1.13	1.59	1.14	1.03	1.11	1.11	1.09	1.44
Spencer	1.11	1.51	1.08	1.02	1.1	1.11	1.07	1.37
GLE/Morgenstern-Price	1.1	1.51	1.09	1.02	1.1	1.1	1.06	1.38
Critical SRF by FEM	0.99	1.34	0.98	0.84	0.93	0.93	0.93	1.27

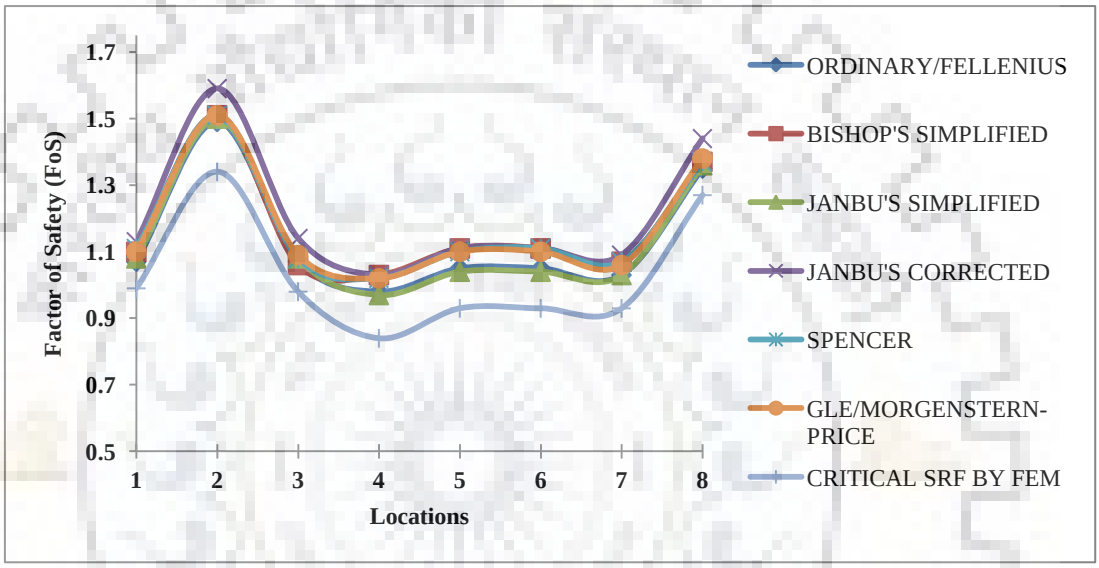

Figure 5.2: Graphical illustration of FoS by LE and FE methods

The geometrical parameters cut slopes (slope height and overall angle of slope) and some major outcomes of numerical simulation viz. maximum shear strain and critical SRF along with most prominent failure pattern at each debris slope has been summarized in table 5.3.

Table 5.3: Slope height, overall slope angle, critical SRF and maximum shear strain at different debris cut slopes along NH-58

Location	Slope Height (in meters)	Overall slope angle	Critical SRF by FEM	Maximum shear strain	Failure pattern
L1	42	58°	0.99	0.015	Talus failure
L2	19	56°	1.34	0.004	Talus failure and planar failure within the bedrock
L3	20	69°	0.98	0.004	Circular failure with thick zone of strain concentration
L4	40	65°	0.84	0.011	Circular failure
L5	20	68°	0.93	0.003	Nearly circular
L6	26	65°	0.93	0.013	Circular to talus failure
L7	45	61°	0.93	0.003	Talus failure
L8	18	67°	1.27	0.004	Circular failure

The factor of safety (FoS) depends upon the ratio of resistive and driving forces which are largely controlled by several geomechanical parameters. The multi-parameter sensitivity analysis for each road cut debris slope is being conducted to analyze the role of each parameter on FoS (figure 5.3). The most influential parameter was determined. Statistical attributes considered for sensitivity analyses are illustrated in table 5.4. In the present investigation, the role of shear strength parameters (cohesion and angle of friction) and unit weight of the material was assessed. It was evidenced that cohesion and angle of friction are directly proportional to FoS whereas unit weight of is inversely proportional. From the sensitivity plots of all cut slopes, it can also be noted that the gradient of unit weight is low as compared to the gradient of cohesion and angle of friction. This implies that shear strength parameters are influencing FoS to a greater extent and more sensitive than the unit weight of the slope forming material.

Table 5.4: Statistical parameters for sensitivity analysis of debris slopes along NH-58

Parameters	Distribution	Standard Deviation	Relative Minimum	Relative Maximum
Cohesion	Normal	2	6	6
Angle of friction	Normal	1	3	3
Unit Weight	Normal	0.5	1.5	1.5

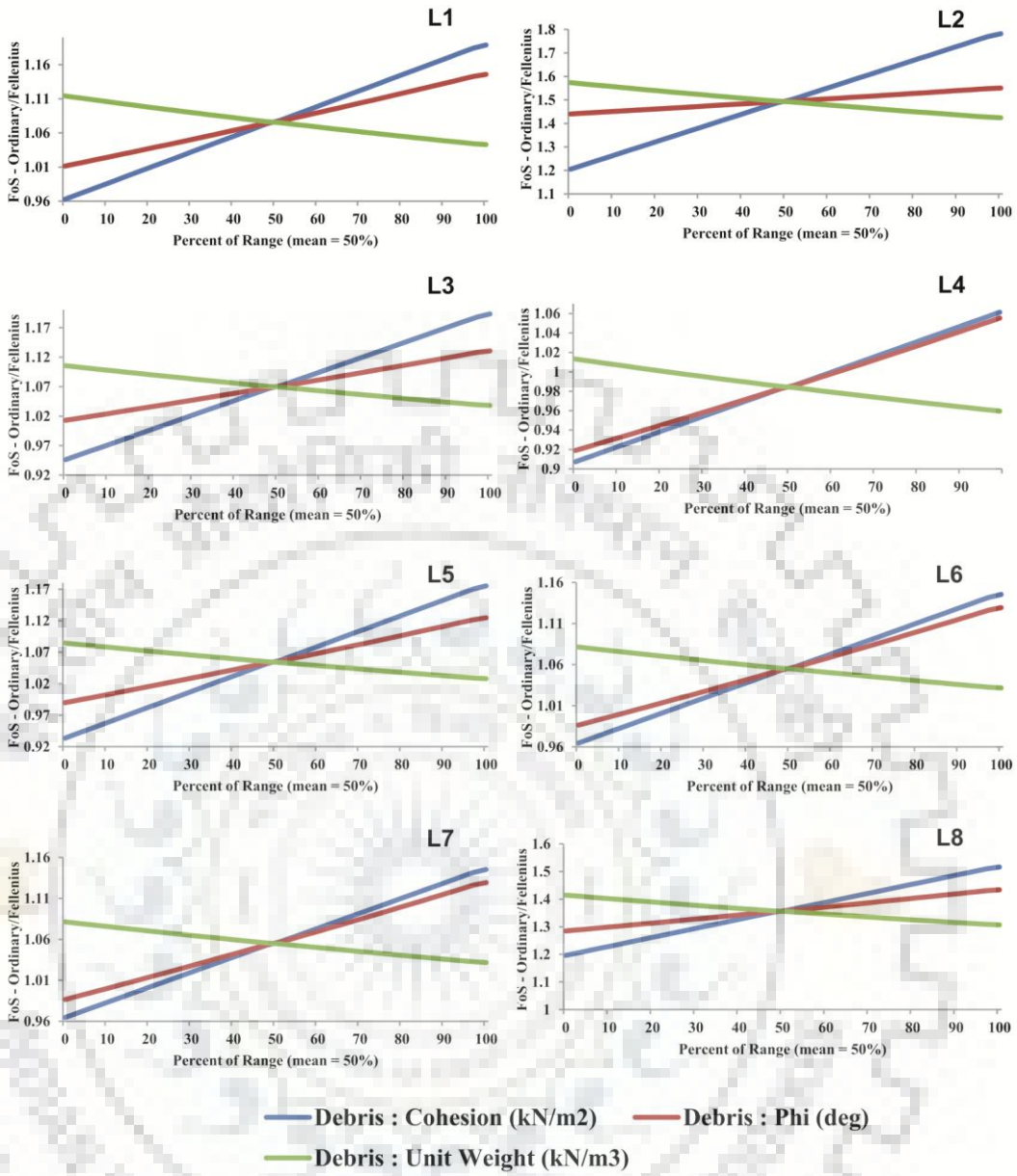

Figure 5.3: Multi-parameter sensitivity analysis of road cut debris slopes along NH-58

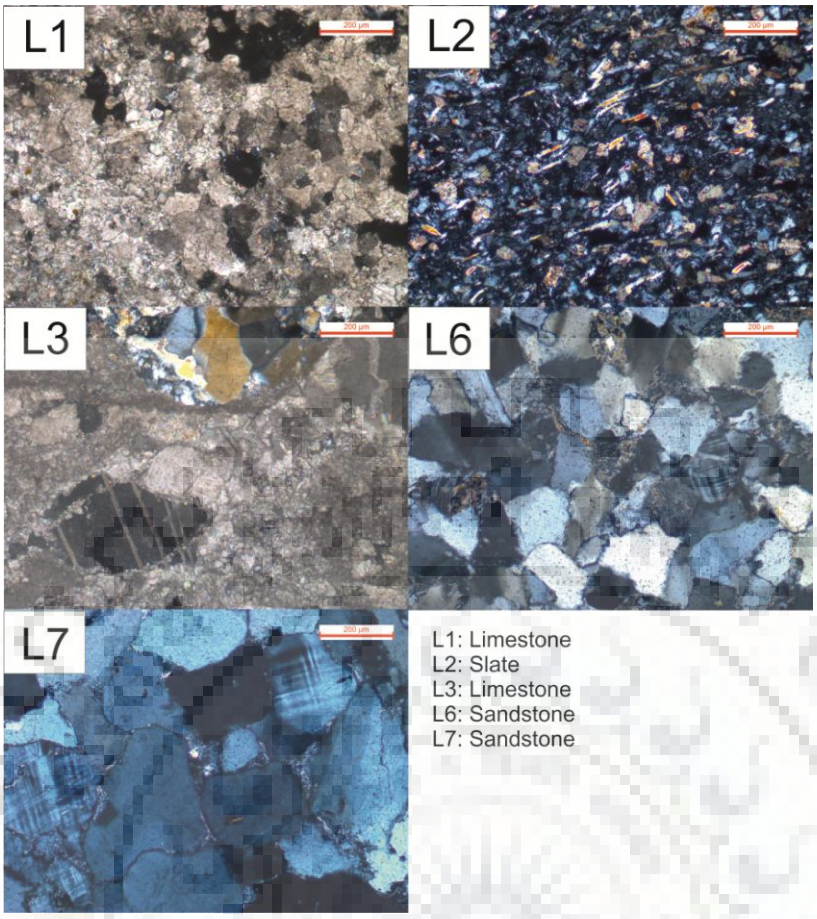

Figure 5.4: Photomicrographs of bedrock at distinct locations along NH-58; L1: Crystalline Limestone; L2: Slate with alternate bands foliated (mica and clay minerals) and non-foliated (quartz); L3: Coarsely crystalline Limestone with some quartz and dolomite; L6: Sub-Arkosic Sandstone with notable microcline surrounded by sericite as altered product; L7: Coarse-grained Sub-Arkosic Sandstone with microcline

One of the key reasons for the slope failure is the reduction of shear strength of slope forming material that is largely controlled by its interaction of geomaterial with water. Photomicrographs of bedrock at each location are depicting the chemical alteration at the microscopic level. The alteration of microcline into clay as sericite increase the clay content and reduce inherent shear strength characteristics of the rock (figure 5.4 L6 & L7). Mineralogical control over shear strain in the rock mass is quite notable. Bedrock at location 2 (figure 5.4 L2) comprises of micaceous minerals imparting foliation have low compressive strength. While photomicrographs of bedrock at L1 and L3 (figure 5.4 L1 & L3) comprises of carbonate minerals and resistant mineral quartz at L6 & L7 (figure 5.4 L6 & L7) indicating stable conditions and shear strain contours unable to pass through the corresponding bedrock rather running along bedrock-debris interface forming talus failure.

Chapter 6

Optimization of road cut rock slopes and Utility of the work

6.1. Optimization of rock slopes: Optimization is being conducted to evaluate the stability after altering the existing geometry of the slopes. The critical slopes identified by FEM have been categorized and optimization is being conducted on slopes having critical SRF less than 1.5. Reshaping of the cut slopes have been proposed by constructing benches of 10 m height and span of 5 m, and gradually reducing angle ranging from 75° to 50° (Simulation performed at every 5° reductions in angle). The SRF values have been computed to suggest the safer and functional design of the critical cut slopes (table 6.1). By reducing slope angle by 5°, the SRF values of optimized slopes increase from 11.5 to 32.5 %. The increase in SRF has some correlation with the height of slopes. In the case of higher slopes, the percentage of increase in SRF is lesser. Cross-sectional representation (figure 6.1, 6.2 and 6.3) and bivariate plots (figure 6.4, 6.5 and 6.6) of optimized geometry of the slopes are depicting the variation of SRF in response to benching and slope angle in critical slopes. The investigated route is one of the sections from Char Dham route. The road widening work is under progress and the results can be utilized for safer design along the highway.

Table 6.1: Optimization of critical road cut rock slopes along NH-58

SRF	Slope	Existing conditions			Optimization							
		Overall Slope angle	SRF	Height (m)	No. of Benches	SRF at angle 50°	55°	60°	65°	70°	75°	Increase in SRF by reducing angle by 5° (%)
≤1	S6	70°	0.67	18.9	2	1.92	1.72	1.58	1.47	N/A	N/A	22.4
	S7	75°	1	17.8	1	2.27	1.99	1.72	1.51	1.38	N/A	22.3
	S18	66°	0.99	29.6	2	1.97	1.66	1.44	1.14	N/A	N/A	27.9
	S19	72°	1.01	37.4	2	2.14	2.08	1.88	1.64	1.5	N/A	15.8
	S20	76°	0.99	22.3	2	2.66	2.32	2.1	1.47	1.14	1.05	32.5
1 to 1.3	S2	76°	1.2	60	3	2.75	2.51	2.37	2.17	2.04	1.74	16.8
	S9	73°	1.2	16.8	1	1.9	1.72	1.65	1.5	1.35	N/A	11.5
	S13	74°	1.22	34.2	2	2.92	2.66	2.38	1.91	1.83	N/A	22.3
	S17	76°	1.16	34.5	2	2.63	2.41	2.27	2.09	1.73	1.71	15.9
1.3 to 1.5	S1	80°	1.39	30	2	3.76	3.24	3.05	2.83	1.94	1.75	28.9
	S3	75°	1.39	42.3	3	2.68	2.46	2.28	2.13	2.04	N/A	11.5
	S10	77°	1.42	45	3	3.66	3.42	3.14	2.91	2.74	2.1	22.0
	S12	73°	1.33	40	3	2.65	2.55	2.29	2.17	1.65	N/A	18.8

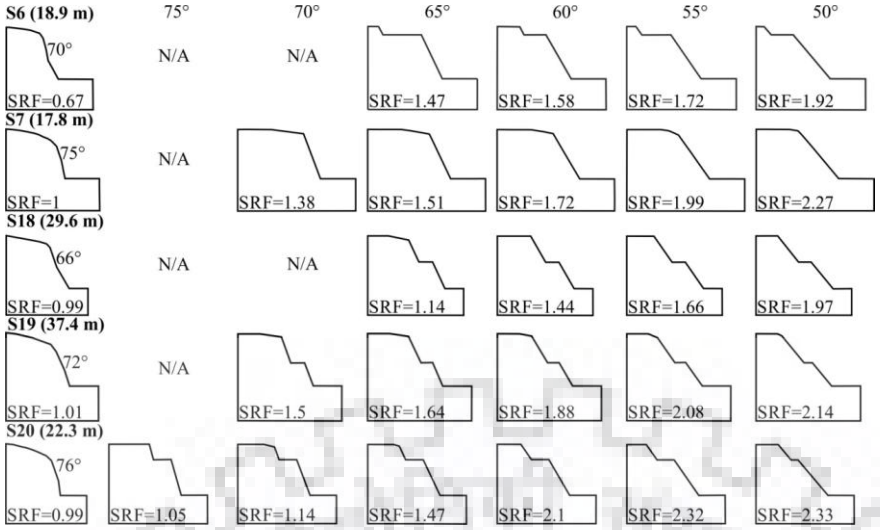

Figure 6.1: Cross-sectional view of existing and optimized cut slopes having SRF ≤1

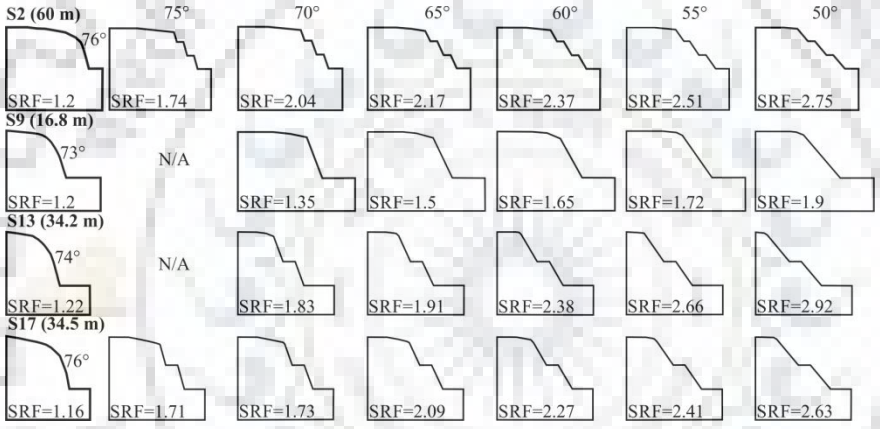

Figure 6.2: Cross-sectional view of existing and optimized cut slopes having SRF from 1 to 1.3

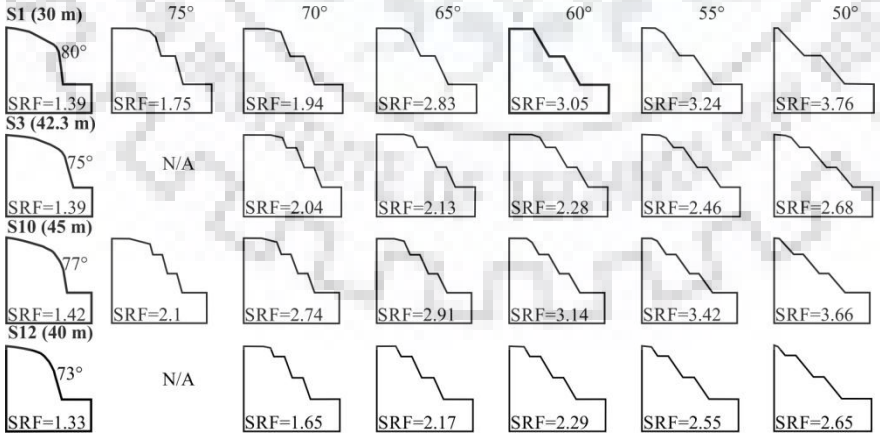

Figure 6.3: Cross-sectional view of existing and optimized cut slopes having SRF from 1.3 to 1.5

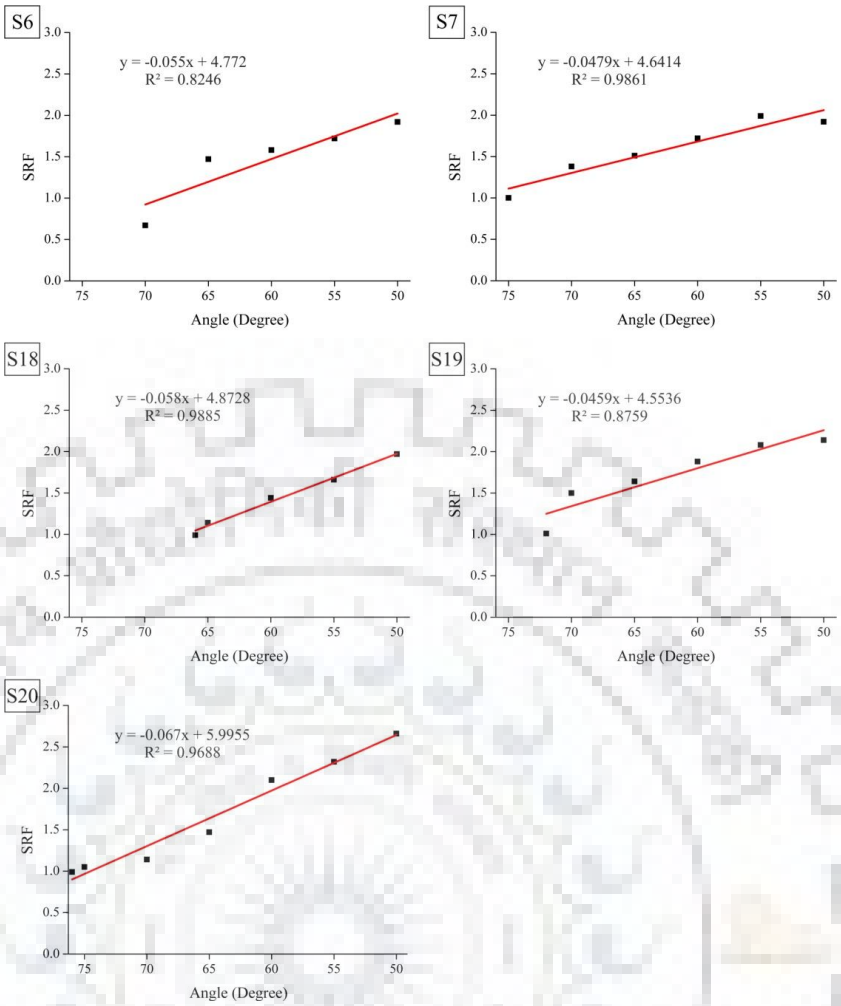

Figure 6.4: Bivariate plot showing the relationship of SRF in response to the overall slope angle of slopes having SRF less than 1

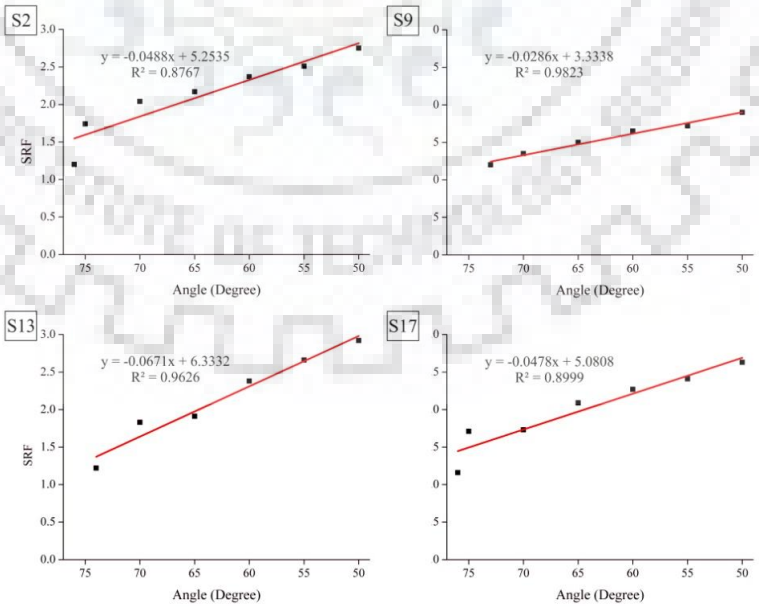

Figure 6.5: Bivariate plot showing the relationship of SRF in response to the overall slope angle of slopes having SRF from 1 to 1.3

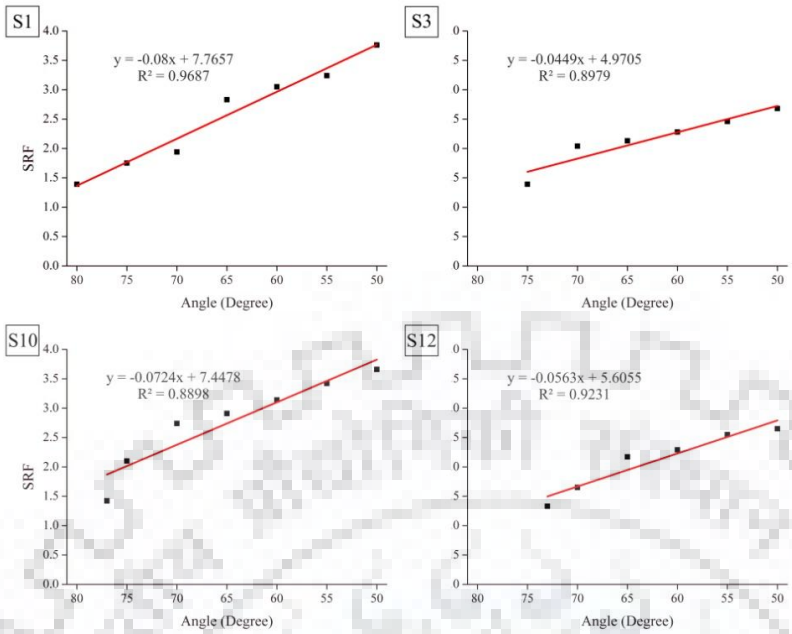

Figure 6.6: Bivariate plot showing the relationship of SRF in response to the overall slope angle of slopes having SRF from 1.3 to 1.5

6.2. Utility of the work: The road widening Char Dham Project has been started by the Central Government of India with a total budget of ~Rs. 11997 crores. In late 2017, the excavation work has been already started from different sections. The investigated patch in the study is a part of this project. The outcomes of slope stability analyses and optimization of road cut rock slopes may be utilized by various agencies involved in the project. During excavation for road widening and development, there are many faulty geo-engineering practices has been noticed along the investigated sections. The most frequently noticed issue is the location of dumping sites. The excavated mucks are being dumped along hairpin bends or along river banks. Thousands of trees were cut down for the sake of development. The excavation at a nearly vertical or steep angle may generate new avenues for sliding in near future.

Chapter 7
Summary and Conclusions

The investigated section witness large numbers of slope failures ranging from small occasional rock fall to massive mass failure from the road cut rock and debris slopes. The massive failures along distinct sections of the NH-58 often cause disruption and inconvenience to the ongoing traffic and sometimes even trigger injuries, fatalities with massive destruction to the economy. Critical slopes need immediate treatment and proper preventive and stabilization. While performing excavation for the alignment of road or widening of pre-existing roads such geotechnical investigations are advantageous and supportive during the planning and execution stages of the project. The various public and private agencies of the nation associated with the sector of transportation routes sector will be benefited by the outcomes. Successful execution of suggested preventive and remedial guidelines would reduce the continual threat landslides. The rock mass classification, kinematic analysis, and numerical simulation approaches were employed for stability assessment along precarious terrain conditions. The outcomes obtained from different proxies correlated were corroborated with each other and also possessing fair agreement with the existing site conditions.

The outcomes by RMR, SMR, and CSMR were classified into five different classes with an interval of 20 in each while for critical SRF by GHB and MC, the outcomes were categorized into three classes such as: <1 (unstable), 1-1.3 (marginally stable) and >1.3 (stable). It is quite notable that most of the critical slopes lie near township Kaudiyala which is proximal to Duwadhar and Singtali faults. Stability assessment by different rock mass classification schemes suggests that most of the road cut rock slopes are under sustained threat of failure. According to RMR, 16 slopes (S1, S2, S4, S5, S7, S8, S9, S10, S12, S13, S14, S16, S17, S18, S19, and S20) are poor, slopes (S6 & S15) are very poor and slopes (S3 & S11) are fair in quality. CSMR outcomes suggest that slopes (S2, S4, S5, S7, S8, S9, S12, S13, S14, S15, S16, S17, S18, S19, and S20) are completely unstable. Such slopes need immediate treatment and require modification in slope geometry, by creating benches and reducing slope angle. Slopes (S1, S3, S6, S10, and S11) are partially stable slopes. Some preventive measures should be taken by constructing ditches and steel mesh to retain potential free falling blocks and flexible barriers may be installed on the slope face to reduce the kinetic energy of falling blocks. The outcomes by SMR and CSMR are nearly identical except at slope S2. It is due to the fact that the value of SMR and CSMR is lying at the boundary of the adjacent class interval. Kinematic analysis indicate that the most prominent mode of failure is Wedge type that can be evidenced

at slopes (S2, S3, S4, S5, S7, S9, S11, S12, S13, S15, S16, S17, S18, S19, and S20), while planar mode is likely to occur at slopes (S1, S4, S7, S8, S12, S13, S14, S15, S17, and S18) and toppling may occur only at S1, S6, and S10. Furthermore, shear strain contours are indicative of large and small scale structurally controlled failures.

The $SRF_{(GHB)}$ values in the studied section suggest that out of twenty slopes, 5 slopes (S6, S7, S18, S19, and S20) are unstable. While, four slopes (S2, S9, S13, and S17) are marginally stable and dynamic factors like heavy rainfall and seismic shaking may trigger failure in such slopes. Due to heavy rainfall during the monsoon season of 2017 and 2018, recurrent failure occurred at slope S13 near township Kaudiyala. This suggests that marginally stable slopes can be triggered by such dynamic factors. Slopes (S1, S3, S4, S5, S8, S10, S11, S12, S14, S15, and S16) are stable. The overall stability of the slopes having SRF greater than 1.3 is acceptable in terms of mass failure (Geotechnical Control Office, 1984). But, in case of jointed rock mass, such slopes are under continual threat of generating occasional wedges as rockfall. Such adverse conditions were evidenced from slope S15, where free-falling wedges destroyed the roadside guarders and walls on either side of the road. To overcome such rockfall, nets of desired mesh should be installed. Among abovementioned slopes, there are few slopes (S4, S5, S12, S14, S15, and S16) which are unstable as per CSMR however results from FEM show the slopes are stable. In these slopes, the overall stability is good but they may experience small wedge failures due to less persistent discontinuities. Such disparities in outcomes may occur because CSMR relies much on the orientation factor.

Moreover, a comparative analysis was conducted among GHB and MC criterion for road cut rock slopes in the Himalayan terrain. It has been found that for weak or extensively jointed homogeneous rock mass both the criteria are giving similar SRF. But for moderately jointed heterogeneous rock mass, MC criterion shows higher stability. It has been noted from the field observations and pattern of failure that GHB suits better in the jointed rock mass. The empirical relationship has also been suggested by the study. While applying MC in the jointed rock mass, the correction in SRF values can be made for the higher range of SRF values accordingly to attain results much closer to real ground conditions.

Furthermore, stability appraisal of road cut debris slopes within the investigated patch is also under sustained threat of failure. The adverse impact due to percolation of rainwater through the tension cracks has been witnessed as slope L1 near Shivpuri township. The slope had failed immediately after the rainfall season. The implementation of proper surface and sub-surface drainage system is the foremost measure that is to be undertaken to cope with such landslides. In hilly terrains, debris slides are often associated with internal erosion caused by

water. To overcome from such landslides, horizontal drainage system with a proper outlet channel for excessive water and collection ditches needs to be constructed. To reduce damage or to restore inherent strength characteristics of the slope forming material, tension cracks at crown may be sealed by injecting concrete. Furthermore, horizontal drainage wells by using PVC perforated pipes with filter fabric should be installed. Filter fabric is vital in such practices as they hinder undesirable blockage due to vegetation or fine-grained soils. In the investigated patch, out of eight slopes, six are slopes (L1, L3, L4, L5, L6, and L7) having SRF less than 1 are unstable and are at the verge of failure. At slope L5 near township Byasi, damaged retaining wall should be repaired to support debris behind and loose boulders are also threat for rockfall initiation. The SRF of slope L7 is found to be 0.93. The retaining wall at this site was placed at the mid portion of the slope on weak debris material. The weight of the retaining wall adds instability to the slope. For marginally stable and smaller slope like L8, concrete or gabion walls are sufficient and would be cost-effective remedies for such slopes.

Sensitivity analysis shows that cohesion and angle of internal friction play a significant role in guiding the stability of slopes. Among shear strength parameters, cohesion is more sensitive than the angle of internal friction in controlling stability. However, unit weight of the slope-forming material is inversely proportional and has relatively least influence on the stability of slopes.

By considering existing field conditions at discrete sites an additional remark over vegetation is being made here. It is being perceived that vegetation increase stability but it is not true in every condition. In debris or soil slopes, vegetation cover enhances stability by holding slope forming material by via dense network of roots. As witnessed from different locations in the patch, the excessive vegetation or large trees may hamper the stability of rock slopes. The continual growth of tree roots causes widening of pre-existing joints in the rock mass thereby aggravating instability to the slopes. Excessive vegetation should be removed particularly from those sections that are experiencing joint widening issue due to roots.

From stability analyses, it is concluded that the investigated rock and debris slopes are prone to instability related issues. Weak and jointed rock mass with steep slope angle makes the slope more vulnerable to failure. The adverse orientation of discontinuities with respect to slope face is causing many structurally controlled failures. For cost-effective sustainable development, remedial measures must be executed by a critical understanding of the type of failure and its root cause. To ensure safer design along transportation routes, such studies should be performed by targeting hazard-prone areas in the Himalayas and likewise regions.

References

1. Acharya B, Kundu J, Sarkar K (2017) Stability Assessment of a Critical Slope near Nathpa Region, Himachal Pradesh, India. In Indian Geotechnical Conference GeoNEst, IIT Guwahati, India.
2. Aghdam IN, Pradhan B, Panahi M (2017) Landslide susceptibility assessment using a novel hybrid model of statistical bivariate methods (FR and WOE) and adaptive neuro-fuzzy inference system (ANFIS) at southern Zagros Mountains in Iran. 76: 237.
3. Agricola G (1556) De Re Metallica, California.
4. Ahmad M, Umrao RK, Ansari MK, Singh R, Singh TN (2013) Assessment of Rockfall Hazard along the Road Cut slopes of State Highway-72, Maharashtra, India. Geomaterials. 3(1): 15-23.
5. Ahmad T, Ramshoo SA, Singh B (2015) Map the Neighbourhood in Uttarakhand (MANU) Uttarakhand disaster 2013. Department of Science and Technology, Government of India, India. 145p.
6. Alemdag S, Kaya A, Karadag M, Gurocak Z, Bulut F (2015) Utilization of the limit equilibrium and finite element methods for the stability analysis of the slope debris: An example of the Kalebasi District (NE Turkey). Journal of African Earth Sciences. 106: 134-146.
7. Amanzio G, Tiwari AK, Lavy M, Maio MD (2019) Integration of terrestrial laser scanning and GIS analysis for Multi-temporal landslide monitoring: A case study of the Mont de La Saxe (Aosta Valley, NW Italy). In Landslides: Theory, Practice and Modelling, Pradhan et al. eds., Advances in Natural and Technological Hazards Research, Springer.
8. Anbalagan R, Sharma S, Raghuvanshi TK (1992) Rock Mass Stability Evaluation Using Modified SMR Approach. In Proceedings of 6th Natural Symposium on Rock Mechanics, Bangalore, India. 258-268.
9. ASTM (1998) Standard test method for particle-size analysis of soils. D- 422-63: 1-8.
10. ASTM (2005) Standard Test Methods for Liquid Limit, Plastic Limit, and Plasticity Index of Soils. D- 4318-05: 1-16.
11. Auden JB (1935) Traverses in the Himalaya. Records of the Geological Society of India. 69: 123-167.
12. Aydan Ö, Ulusay R, Tokashiki N (2014) A new rock mass quality rating system: rock mass quality rating (RMQR) and its application to the estimation of geomechanical characteristics of rock masses. Rock Mechanics and Rock Engineering. 47(4): 1255-1276.

13. Baba K, Bahi L, Ouadif L, Akhssas (2012) Slope stability evaluations by limit equilibrium and finite element methods applied to railway in the Moroccan Rif. Open Journal of Civil Engineering. 2(1): 27-32.
14. Bagati TN (1990) Lithostratigraphy and facies variation in the Spiti Basin (Tethys), Himachal Pradesh, India. Journal of Himalayan Geology. 1(1): 35-47.
15. Balaji P, Pavanaguru R, Reddy DV (2010) A note on the occurrence of landslides in Araku valley and its environs, Visakhapatnam district, Andra Pradesh, India. International Journal of Earth Sciences and Engineering. 3(1): 13-19.
16. Bandis SC, Lumsden AC, Barton NR (1983) Fundamentals of rock joint deformation. International Journal of Rock Mechanics and Mining Sciences Geomechanics Abstract. 20(6): 249-268.
17. Barbano MS, Pappalardo G, Pirrotta C, Mineo S (2014) Landslide triggers along volcanic rock slopes in eastern Sicily (Italy). Natural Hazards. 73: 1587-1607.
18. Barton NR (1972) A model study of rock-joint deformation. International Journal of Rock Mechanics and Mining Sciences. 9: 579-602.
19. Barton NR (1973) Review of a new shear-strength criterion for rock joints. Engineering Geology. 7(4): 287-332.
20. Barton NR (1982) Modeling rock joint behavior from in situ block tests: Implications for nuclear waste repository design. Prepared by Tera Tek, Inc. for Office of Nuclear Waste Isolation, Columbus, OH, United States. 114p.
21. Barton NR (2013) Shear strength criterion for rock, rock joints, rockfill and rock masses: Problems and some solutions. Journal of Rock Mechanics and Geotechnical Engineering. 5(4): 249-261.
22. Barton NR and Choubey V (1977) The shear strength of rock joints in theory and practice. Rock Mechanics. 10(1-2): 1–54.
23. Barton NR, Lien R, Lunde J (1974) Engineering classification of rock masses for the design of tunnel support. Rock Mechanics 6: 189-239.
24. Behera PK, Sarkar K, Singh AK, Verma AK, Singh TN (2016) Dump slope stability analysis – A case study. Journal Geological Society of India. 88(6): 725-735.
25. Bieniawski ZT (1973) Engineering classification of jointed rock masses. The civil engineer in South Africa 15: 335-344.
26. Bieniawski ZT (1974) Geomechanics classification in rock masses and its Application in tunnelling. In Proceedings of 3rd International Congress on Rock Mechanics, Denver, CO, USA: 27-32.

27. Bieniawski ZT (1975) Case studies: Prediction of rock mass behavior by geomechanics classification. In proceedings of 2nd Australia-New Zealand conference Geomechanics, Brisbane. 36-41.
28. Bieniawski ZT (1976) Rock mass classifications in Engineering; In Proceedings of the symposium on Exploration Rock Engineering, Johensberg: 97-106.
29. Bieniawski ZT (1989) Engineering rock mass classifications: A complete manual for Engineers and Geologists in Mining, Civil and Petroleum Engineering, Wiley-Interscience, New York. 251p.
30. Bieniawski ZT (1990) Tunnel Design by rock mass classifications. Technical report GL-79-19; Pennsylvania State University, Department of Mineral Engineering University Park, Pennsylvannia. 158 p.
31. Bieniawski ZT, Celada B, Fernandez GJM (2006) Rock Mass Excavability (RME): Specific applications to double shields. Civil Engineering, Mining Geology and Environment: 20-26.
32. Bhattacharya AR (2008) Basement rocks of the Kumaun-Garhwal Himalaya: Implications for Himalayan Tectonics. e-journal Earth Science India. 1(1):1-10.
33. BIS (1974) Method of test for determination of true specific gravity of natural building stones. New Delhi, India. 10p.
34. BIS (1986) Method of test for soils. Part 13- Direct shear test. New Delhi, India. 17p.
35. BIS (1987) Methods for quantitative description of discontinuities in rock mass. New Delhi, India. 12p.
36. BIS (1998) Method for determination of point load strength index of rocks. New Delhi, India. 17p.
37. BIS (2002) IS 1893–2002 (Part 1) Indian Standard Criteria for earthquake resistant design of structures, Part 1- General Provisions and Buildings. New Delhi, India. 38p.
38. Broch E and Franklin JA (1972) The point load strength test. International Journal of Rock Mechanics and Mining Sciences. 9(6): 669-697.
39. Brook N and Dharmaratne PGR (1985) Simplified rock mass rating system for mine tunnel support. Transactions, Institution of Mining and Metallurgy. 94: A148-A154.
40. Cai M and Kaiser P (2006) Visualization of rock mass classification systems. Geotechnical and Geological Engineering. 24: 1089-1102.
41. Célérier J, Harrison TM, Webb AAG, Yin A (2009) The Kumaun and Lesser Garhwal Himalaya, India: Part 1. Structure and Stratigraphy. GSA Bulletin. 121(9-10): 1262-1280.

42. Chakraborty I, Ghosh S, Bhattacharya D, Bora A (2011) Earthquake induced landslides in the Sikkim-Darjeeling Himalayas- An aftermath of the 18th September 2011 Sikkim earthquake. Kolkata. In report of Geological Survey of India, Eastern region, Kolkata, India. 8p.
43. Chen Z (1995) Recent developments in slope stability analysis. In Proceedings of the 8th International congress by International Society of Rock Mechanics and Rock Engineering, Tokyo. Japan. 8p.
44. Cheng YM, Lau CK (2014) Slope stability analysis and stabilization: New methods and insight. 2nd edition, Taylor and Francis, London. 438p.
45. Coulomb CA (1776) On an application of the maximis and minimis rules to some problems of static, relating to structure. Memoirs of Mathematics and Physics, Royal Academy of Science, France. 7: 343-382.
46. Crepaldi S, Zhao Ye, Amanzio G, Suozzi E, Maio MD (2015) Landslide analysis by multi-temporal terrestrial laser scanning (TLS) data: the Mont de la Saxe landslide. In Proceedings of Italian Geological Society, Roma. 35: 92-95.
47. Cruden D (1991) A simple definition of a landslide. Bulletin of the International Association of Engineering Geology. 43(1): 27-29.
48. Cruden DM and Varnes DJ (1996) Landslide Types and Processes. Special Report, Transportation Research Board. National Academy of Science. 247: 36-75.
49. Daftaribesheli A, Ataei M, Sereshki F (2011) Assessment of rock slope stability using the Fuzzy Slope Mass Rating (FSMR) system. Applied Soft Computing. 11(8): 4465-4473.
50. Dahal RK, Hasegawa S, Yamanaka M, Dhakal S, Bhandary NP, Yatabe R (2009) Comparative analysis of contributing parameters for rainfall-triggered landslides in the Lesser Himalaya of Nepal. Environmental Geology. 58(3): 567-586.
51. Dawson EM, Roth WH, Drescher A (1999) Slope stability analysis by strength reduction. Géotechnique. 49(6): 835-840.
52. Deere DU (1963) Technical description of rock cores for engineering purposes. In Rock Mechanics and Engineering Geology. 1(1): 16-22.
53. Deere DU and Deere DW (1988) The Rock Quality Designation (RQD) Index in practice. In Rock Classification for Engineering Purpose, ASTM STP 984, Philadelphia: 91-101.
54. Dev H and Sharma (2011) Rock mass classification system and applications. Central Soil and Materials Research station, New Delhi, India. 90p.
55. Devkota KC, Regmi A, Pourghasemi HR, Yoshida K, Pradhan B, Ryu IN, Dhital MR, Althuwaynee OF (2013) Landslide susceptibility mapping using certainty factor, index of

entropy and logistic regression models in GIS and their comparison at Mugling–Narayanghat road section in Nepal Himalaya. Natural Hazards. 65: 135-165.

56. Dewey JF and Bird JM (1970) Mountain belts and new global tectonics. Journal of Geophysical Research. 75: 2625-2685.
57. Dewey JF and Burke K (1973) Tibetan, Variscan and Precambrian basement reactivation: products of continental collision. Journal of Geology. 81: 683-692.
58. Dobhal DP, Gupta AK, Mehta M, Khandelwal DD (2013) Kedarnath disaster: Facts and plausible causes. Current Science. 105(2): 171-174.
59. Dubey AK (2014) Understanding an orogenic Belt: Structural evolution of the Himalaya. Springer International Publishing, Switzerland. 401p.
60. Dubey CS, Shukla DP, Ningreichon AS, Usham AL (2013) Orographic control of the Kedarnath disaster. Current Science. 105(11): 1474-1476.
61. Dudeja D, Bhatt SP, Biyani AK (2017) Stability assessment of slide zones in Lesser Himalayan part of Yamunotri pilgrimage route, Uttarakhand, India. Environmental Earth Sciences. 76(1): 2-18.
62. Duncan JM (1996) State of The Art: Limit Equilibrium and Finite-Element Analysis of Slopes. Journal of Geotechnical Engineering. 122(7): 557-596.
63. Duncan JM and Wright SG (1980) The accuracy of equilibrium methods of slope stability analysis. Engineering Geology. 16(1): 5-17.
64. Eberhardt E (2003) Rock slope stability analysis – utilization of advanced numerical techniques. Earth and Ocean Sciences at UBC Report. University of British Columbia, Vancouver, Canada, 41p.
65. Eberhardt E (2012) The Hoek-Brown Failure Criterion. Rock Mechanics and Rock Engineering. 45: 981-988.
66. Espinoza RD, Repetto PC, Muhunthan (1992) General framework for stability analysis of slopes. Géotechnique. 42(4): 603-615.
67. Fan X, Xu Q, Scaringi G, Dai L, Li W, Domg X, Zhu X, Pei X, Dai K, Havenith HB (2017) Failure mechanism and kinematics of the deadly June 24th 2017 Xinmo landslide, Maoxian, Sichuan, China. Landslides. 14(6): 2129-2146.
68. Fereidooni D, Khanlari GR, Heidari M (2015) Assessment of a Modified Rock Mass Classification System for Rock Slope Stability Analysis in the Q-system. Earth Sciences Research Journal. 19(2): 147-152.

69. Frank W, Grasemann B, Guntli P, Miller C (1995) Geological map of the Kishwar Chamba-Kulu region (NW Himalayas India). In yearbook of Federal Geological Survey. 138: 299-308.
70. Franklin JA (1975) Safety and Economy in Tunneling. In Proceedings of the 10th Canadian Rock Mechanics Symposium, Queens University, Kingston, Ontario. 1: 27-53.
71. Fredlund DG (1984) Analytical Methods for Slope Stability Analysis. In Proceeding of the 4th International Symposium on Landslides, State-of-the-Art, Toronto, Canada: 229-250.
72. Froude MJ and Petley DN (2018) Global fatal landslide occurrence from 2004 to 2016. Natural Hazards and Earth System Sciences. 18: 2161-2181.
73. Gabet EJ, Burbank DW, Putkonen JK, Pratt-Sitaula BA, Ojha T (2004) Rainfall thresholds for landsliding in the Himalayas of Nepal. Geomorphology. 63(3-4): 131-143.
74. Gansser A (1964) The Geology of the Himalayas. Wiley Interscience, New York, 289p.
75. Geotechnical Control Office (1984) Geotechnical Manual for Slopes. 2nd edition. Geotechnical Control Office, Hong Kong, 295p.
76. Gercek H (2007) Poisson's ratio values for rocks. International Journal of Rock Mechanics and Mining Sciences. 44: 1-13.
77. Gerrard J (1994) The landslide hazard in the Himalayas: geological control and human action. Geomorphology. 10(1-4): 221-230.
78. Ghosh S, Bora A, Nath S, Kumar A (2014) Analysing the Spatio-temporal Evolution of an Active Debris Slide in Eastern Himalaya, India. Journal of the Geological Society of India. 84(3): 292-302.
79. Ghose AK and Raju NM (1981) Characterization of rock mass vis a vis Application of Rock Bolting-Modeling of Indian coal mines. In Proceedings of the 2nd US Symposium in Rock Mechanics: 452-457.
80. Goel RK, Jethwa JL, Paithankar AG (1995) Indian experiences with Q and RMR systems. Tunnelling and Underground Space Technology. 10(1) 97-109.
81. Goodman RE and Bray JW (1976) Toppling of rock slopes. In proceedings of Speciality Conference on Rock Engineering for Foundations and Slopes, American Society of Civil Engineers, Boulder, Colorado. 2: 201-234.
82. Goodman RE (1989) Introduction to Rock Mechanics. John Wiley and Sons, New York. 562p.
83. Gover S and Hammah R (2013) A comparison of finite elements (SSR) & limit-equilibrium slope stability analysis by case study. Civil Engineering. 21(3): 31-34.

84. Griffith AA (1920) The phenomena of rupture and flow in solids. Philosophical Transactions of the Royal Society. A 221: 163-198.
85. Griffith AA (1924) The theory of rupture. In 1st International Congress of Applied Mechanics, Delft, Netherlands: 55-63.
86. Griffiths DV and Lane PA (1999) Slope stability analysis by finite element. Géotechnique. 49(3): 387-403.
87. Grimstand E and Barton NR (1993) Updating of the Q-System for NMT. In Proceedings of the International Symposium on Sprayed Concrete. Fagernes, Norway.
88. Grimstand E, Kankes K, Bhasin R, Magnussen A, Kaynia A (2002) Rock Mass Quality Q used in designing reinforced ribs of sprayed concrete and energy absorption. In Proceedings of International symposium on sprayed Concrete, Davos, Switzerland.
89. Gupta V, Bhasin RK, Kaynia AM, Kumar V, Saini AS, Tandon RS, Pabst T (2016) Finite element analysis of failed slope by shear strength reduction technique: a case study for Surabhi Resort Landslide, Mussoorie township, Garhwal Himalaya. Geomatics, Natural Hazards and Risk. 7(5): 1677-1690.
90. Gupte SS, Singh R, Singh TN (2013) In-pit Waste Dump Stability Analysis using two Dimensional Numerical Models. Mining Engineers' Journal. 14(7): 16-20.
91. Hack HRGK (1998) Slope stability probability classification, SSPC. In Ph.D. Thesis, International Institute for Aerospace Survey and Earth Sciences, ED Delft, Netherlands. ISBN 90 6164 154 3. 258p.
92. Haigh M and Rawat JS (2011) Landslide causes: Human impacts on a Himalayan landslide swarm. Belgeo. 3-4: 201-220.
93. Haines A and Terbrugge PJ (1991) Preliminary Estimate of Rock Slope Stability using Rockmass Classification. In Proceedings of the 7th Congress of International Society of Rock Mechanics and Rock Engineering, Aachea, Germany. 2: 887-892.
94. Hammah RE, Yacoub TE, Corkum B, Curran JH (2005) The Shear Strength Reduction Method for the Generalized Hoek-Brown Criterion. In Proceedings of the 40th US Symposium on Rock Mechanics, Alaska, United States.
95. Hammouri NA, Malkawi AIH, Yamin, MMA (2008) Stability analysis of slopes using the finite element method and limiting equilibrium approach. Bulletin of Engineering Geology and the Environment. 67(4): 471-478.
96. Harrison JP and Hudson JA (2000) Engineering Rock Mechanics, Part 2: Illustrative worked examples. Elsevier Science. 524p.

97. Heim AA and Gansser A (1939) Central Himalaya: Geological observations of the Swiss Expedition, 1936. Hindustan Publishing, New Delhi, India.
98. Highland LM and Bobrowsky P (2008) The landslide handbook-A guide to understanding landslides: US Geological Survey Circular, 1325, Reston, Virginia, United States. 129p.
99. Hoek E (1968) Brittle failure of rock. In Rock Mechanics in Engineering Practice, Stagg and Zienkiewicz eds., John Wiley, London: 99-124.
100. Hoek E (2000) Practical Rock Engineering. In Evert Hoek Consulting Engineer Inc., North Vancouver, British Columbia, Canada. 341p.
101. Hoek E and Bray JW (1981) Rock Slope Engineering. In 3rd edition, The Institution of Mining and Metallurgy, London. 368p.
102. Hoek E and Brown ET (1980) Underground Excavations in Rock. London: Institution of Mining and Metallurgy, London. ISBN 0 900488 55 7.
103. Hoek E and Brown ET (1988) The Hoek and Brown Failure Criterion-a 1988 update. In Proceedings of 15th Canadian Rock Mechanics Symposium, Toronto, Canada.
104. Hoek E and Diederichs MS (2006) Empirical estimation of rock mass modulus. International Journal of Rock Mechanics and Mining Sciences. 43(2): 203-215.
105. Hoek E and Marinos P (2007) A brief history of the development of the Hoek–Brown failure criterion. Journal of Soils and Rocks. 2: 1-8.
106. Hoek E, Carranza-Torres C, Corkum B (2002) Hoek-Brown criterion-2002 edition. In Proceedings of NARMS-TAC Conference, Toronto, Canada. 1: 267-273.
107. Hoek E, Carter TG, Diederichs MS (2013) Quantification of the Geological Strength Index Chart. In Proceedings of 47th US Rock Mechanics/Geomechanics Symposium, San Francisco, United States.
108. Hoek E, Kaiser PK, Bawden WF (1995) Support of underground excavations in hard rock. Mining Research Directorate and Universities Research incentives fund. 235p.
109. Hoek E, Wood, Shah S (1992) A modified Hoek-Brown criterion for jointed rock masses. In Rock characterization, Hudson ed., ISRM Symposium, Chester, United Kingdom: 209-213.
110. Hudson JA and Priest SD (1983) Discontinuity frequency in rock masses. International Journal of Rock Mechanics and Mining Sciences and Geomechanics. 20: 73-89.
111. Hungr O, Leroueil S, Picarelli L (2014) The Varnes classification of landslide types, an update. Landslides. 11(2): 167-194.

112. ISRM (1978) Suggested methods for determining the uniaxial compressive strength and deformability of rock materials. International Journal of Rock Mechanics, Mining Science and Geomechanical Abstracts 16: 135-140.

113. ISRM (1981) Suggested methods for determining hardness and abrasiveness of rocks. In Rock characterization, testing and monitoring: ISRM suggested Methods, Brown ed. Oxford, Pergamon: 95-103.

114. Jaegar JC (1969) The behavior of closely jointed rock. In Proceedinds of 11th Symposium in Rock Mechanics, Berkeley, California: 57-68.

115. Jain AK, Ahmad T, Singh S, Ghosh SK, Patel RC, Kumar R, Agarwal KK, Perumal J, R Islam, Bhargava ON (2012) Evolution of the Himalaya. In Proceedings of the Indian National Science Academy, India. 78(3): 259-275.

116. Jain AK, Dasgupta, Bhargava ON, Israil M, Perumal RJ, Patel RC, Mukul M, Parcha SK, Adlakha V, Agarwal KK, Singh P, Bhattacharyya K, Pant NC, Banerjee DM (2016) Tectonics and Evolution of the Himalaya. In Proceedings of the Indian National Science Academy, India. 82(3): 581-604.

117. Jamir I, Gupta V, Kumar V, Thong GT (2017) Evaluation of potential surface instability using finite element method in Kharsali Village, Yamuna Valley, Northwest Himalaya. Journal of Mountain Science. 14(8): 1666-1976.

118. Jeong U, Yoon WS, Park J, Han BH, Park HJ, Choi JW (2007) A new geomechanical evaluation system for slopes: SFi system. Rock Mechanics: Meeting Society's Challenges and Demands, Eberhardt, Stead and Morrison eds., Taylor and Francis Group, London. ISBN 978-0-415-44401-9.

119. Jiang G, Blick NC, Kaufman AJ, Banerjee DM, Rai V (2003) Carbonate platform growth and cyclicity at a terminal Proterozoic passive margin, Infra Krol Formation and Krol Group, Lesser Himalaya, India. Sedimentology. 50: 921-952.

120. Jing L (2003) A review of techniques, advances and outstanding issues in numerical modeling for rock mechanics and rock engineering. International Journal of Rock Mechanics and Mining Sciences. 40(3): 283-353.

121. Jing L and Hudson JA (2002) Numerical methods in rock mechanics. International Journal of Rock Mechanics and Mining Sciences. 39 (4): 409-427.

122. Kainthola A, Verma D, Gupte SS, Singh TN (2011) A coal mine dump slope stability analysis. Geomaterials. 1: 1-13.

123. Kanungo DP and Sharma S (2014) Rainfall thresholds for prediction of shallow landslides around Chamoli-Joshimath region, Garhwal Himalayas, India. Landslides. 11(4): 629-638.
124. Kanungo DP, Pain A, Sharma S (2013) Finite element modeling approach to assess the stability of debris and rock slopes: a case study from the Indian Himalayas. Natural Hazards. 69(1): 1-24.
125. Katz O, Reches Z, Roegiers JC (2000) Evaluation of mechanical rock properties using a Schmidt Hammer. International Journal of Rock Mechanics Mining Sciences. 37(4): 723-728.
126. Kavzoglu T, Sahin EK, Colkesen I (2014) Landslide susceptibility mapping using GIS-based multivariate criteria decision analysis, support vector machines, and logistic regression. Landslides. 11: 425-439.
127. Kavzoglu T, Sahin EK, Colkesen I (2015) An assessment of multivariate and bivariate approaches in landslide susceptibility mapping: a case study of Duzkoy district. Natural Hazards. 76: 471-496.
128. Kendorski F, Cummings R, Bieniawski ZT, Skinner E (1983) Rock mass classification for block caving mine drift support. In Proceedings of the 5th International Society of Rock Mechanics, Rotterdam, Balkema, Melbourne: B51-B63.
129. Krabbenhoft K and Lyamin AV (2015) Strength reduction finite-element limit analysis. Géotechnique. 5(4): 250-253.
130. Kristen HAD (1982) A classification system for excavation in natural materials. Civil Engineer in South Africa. 24(7): 293-308.
131. Kumar A and Pushplata (2015) Building regulations for hill towns of India. House and Building Research Centre Journal. 11: 275-284.
132. Kumar G and Dhaundiyal JN (1979) Stratigraphy and structure of "Garhwal Synform" Garhwal and Tehri Garhwal Districts, Uttar Pradesh. A reappraisal. Himalayan Geology. 9(1): 18-41.
133. Kumar G and Dhaundiyal JN (1980) On the stratigraphic position of the Tal formation, Garhwal Synform, Garhwal and Tehri Garhwal Districts, Uttar Pradesh. Journal of the Paleontological Society of India. 23-24: 58-66.
134. Kumar N, Verma AK, Sardana S, Sarkar K, Singh TN (2018) Comparative analysis of limit equilibrium and numerical methods for prediction of a landslide. Bulletin of Engineering Geology and the Environment. 7(2): 595-608.

135. Kundu J, Sarkar K, Singh AK (2016) Integrating structural and numerical solutions for road cut slope stability analysis – A case study, India. In Rock Dynamics: From Research to Engineering, Li et al. eds., Taylor and Francis Group, London. ISBN 978-1-138-02953-8.
136. Kundu J, Sarkar K, Tripathy A, Singh TN (2017) Qualitative stability assessment of cut slopes along the National Highway-05 around Jhakri area, Himachal Pradesh, India. Journal of Earth System and Science. 126: 112.
137. Ladanyi B and Archmbault G (1964) Simulation of shear behavior of a jointed rock mass. In Proceedings of 11th US Symposium of Rock Mechanics: 105-125.
138. Laubscher DH (1977) Geomechanics classification of jointed rock masses-mining applications. Transactions of the Institution of Mining and Metallurgy. 86: A1-A7.
139. Laubscher DH and Jakubec J (2000) The IRMR/MRMR rock mass classification for jointed rock masses, In Underground mining methods: Engineering Fundamentals and International case studies, Hustrulid and Bullock eds., Society of Mining, Metallurgy and Exploration, Inc.: 475-481.
140. Lauffer H (1958) Mountain Classification for the gallery construction. Geology and Construction. 24: 46-51.
141. LeFort P (1975) Himalayas: The collided range, present knowledge of continental arc. American Journal of Science. A275: 1-44.
142. Leroueil S (2001) Natural slopes and cuts: movement and failure mechanisms. Géotechnique. 51(3): 197-243.
143. Liu SY, Shao LT, Li HJ (2015) Slope stability analysis using the limit equilibrium method and two finite element methods. Computers and Geotechnics. 63: 291-298.
144. Loukidis D, Bandini P, Salgado R (2003) Stability of seismically loaded slopes using limit analysis. Géotechnique. 53(5): 463-479.
145. Mahanta B, Singh HO, Singh PK, Kainthola A, Singh TN (2016) Stability analysis of potential zones along NH-305, India. Natural Hazards. 83(3): 1341-1357.
146. Maji VB (2017) An Insight into Slope Stability Using Strength Reduction Technique. Journal Geological Society of India. 89(1): 77-81.
147. Malik JN and Mohanty C (2007) Active tectonic influence on the evolution of drainage and landscape: Geomorphic signatures from frontal and hinterland areas along Northwestern Himalaya, India. Journal of Asian Earth Sciences. 29(5-6): 604-618.
148. Marinos V, Marinos P, Hoek E (2005) The geological strength index: applications and limitations. Bulletin of Engineering Geology and the Environment. 64(1): 55-65.

149. Marsal RJ (1967) Large scale testing of rockfill materials. Journal of Soil Mechanics and Foundations Divison. 93(2): 27-44.
150. Matsui T and San KC (1992) Finite element slope stability analysis by shear strength reduction technique. Soils and Foundation. 32(1): 59-70.
151. Matthews C, Farook Z, Arup, Helm P (2014) Slope stability analysis – limit equilibrium or the finite element method?. Ground Engineering. May: 22-28.
152. Milne D (2007) Problems with rock mass classification for empirical and numerical design. In Proceedings of the International Workshop on Rock Mass Classification in Underground Mining, Atlanta, Georgia.
153. Milne D, Hadjigeorgiou J, Pakalnis R (1998) Rock mass characterization for underground hard rock mines. Tunnelling and Underground Space Technology. 13(4): 383-391.
154. Mithal RS (1988) Lithotectonic landslides and hazards in parts of Garhwal-Kumaon Himalayas. In Proceedings of the 2nd International Conference on Case Histories in Geotechnical Engineering. Missouri University of Science and Technology, Scholars' Mine, St. Louis, Missouri, United States.
155. Mohr O (1900) Which circumstances determine elastic limit and the fracture of a material?. Time to Ver Deut Ing. 44: 1524-1530.
156. Molinda G and Mark C (1994) Coal mine roof rating (CMRR): A practical rock mass classification for coal mines. Pittsburgh, PA: U.S. Department of the Interior, Bureau of Mines, IC 9387, United States.
157. Mondal MEA, Siddique T, Mondal B, Alam MM (2016) SMR Geomechanics and Kinematic Analysis near Rasulpur, Fatehpur Sikri, Uttar Pradesh. Journal Geological Society of India. 87(5): 623-627.
158. Monjezi M, Singh TN, Pandey A, Puri S (2004) Geomechanical modeling for optimization of rock slope in an opencast coal mine. In Proceedings of the 5th International Conference on case histories in Geotechnical Engineering, Missouri University of Science and Technology, Missouri, United States.
159. Morrison IM and Greenwood JR (1989) Assumptions in simplified slope stability analysis by the method of slices. Géotechnique. 39(3): 503-509.
160. Nair AS and Singh SK (2014) Understanding the causes of Uttarakhand disaster of June 2013: A scientific review. In Proceedings of the 2nd Disaster, Risk and Vulnerability conference, Trivandrum, India: 57-64.

161. Nicholson DT and Hencher SR (1997) Assessing the potential for deterioration of engineered rockslopes. In Proceedings of the International Association of Engineering Geology and the Environment Symposium, Athens, Greece: 911-917.
162. Nikolić M, Bonacci TR, Ibrahimbegović A (2016) Overview of the numerical methods for the modeling of rock mechanics problems. Technical Gazette. 23(2): 627-637.
163. Nirupama N (2015) A Understanding Risk from Floods and Landslides in the Himalayan Region: A Discussion to Enhance Resilience. GRF Davos Planet@Risk. 3(2): 231-235.
164. NSCGPRC (1994) GB 50218-94 Standard for engineering classification of rock masses. China Planning Press, Beijing: 1-22.
165. NRSC (2001) Landslide hazard zonation mapping along the pilgrim and tourist routes in the Himalayas of Uttarakhand and Himachal Pradesh States using Remote Sensing and GIS techniques. In LHZ project, National Remote Sensing Centre, Indian Space Organization, Hyderabad, India. 9p.
166. Olivier JH (1979) A new engineering-geological rock durability classification. Engineering Geology. 14(4): 255-279.
167. Orr CM (1993) Assessment of rock slope stability using the Rock Mass rating (RMR) system. Australian Institute of Mining and Metallurgy. 2:25-29.
168. Pacher F, Rabcewicz L, Golser J (1974) To the slide stand of the mountain classification in tunnels. In Proceedings of 22nd Geomechanics, Salzburg, Austria.
169. Pain A, Kanungo DP, Sarkar S (2014) Rock slope stability assessment using finite element based modeling-examples from the Indian Himalayas. Geomechanics and Geoengineering. 9(3): 2015-230.
170. Pakalnis R, Brady T, Hughes P, McLaughlin M (2007) Design guidelines for underground mining operations in weak rock masses. In Proceedings of 1st Canada U.S. Rock Mechanics Symposium. Atlanta, Georgia.
171. Pal R, Biswas SS, Mondal B, Pramanik MK (2016) Landslides and Floods in the Tista Basin (Darjeeling and Jalpaiguri Districts): Historical Evidence, Causes and Consequences. Journal of Indian Geophysical Union. 20(2): 209-215.
172. Palmstrom A (1974) Characterization of jointing density and the quality of rock masses. Internal report, Berdal, Norway. 26 p.
173. Palmstrom A (1982) The volumetric joint count - a useful and simple measure of the degree of jointing. In Proceedings of the 4th congress of International Association of Engineering Geology, New Delhi, India: V.221-V.228.

174. Palmström A (1995) RMi - A for rock mass characterization system for rock engineering purposes. Ph.D. Thesis, University of Oslo, Norway. 400 p.
175. Pantelidis L (2009) Rock slope stability assessment through rock mass classification systems; International Journal of Rock Mechanics and Mining Sciences. 46(2): 315-325.
176. Pantelidis L (2010) An alternative rock mass classification system for rock slopes. Bulletin Engineering Geology Environment. 69(1): 29-39.
177. Pappalardo G, Mineo S, Rapisarda F (2014) Rockfall hazard assessment along a road on the Peloritani Mountains (northeastern Sicily, Italy). Natural Hazards and Earth System Sciences. 14: 2735-2748.
178. Parkash S (2011) Historical Records of Socio-economically Significant Landslides in India. Journal of South Asia Disaster Studies. 4(2): 177-204.
179. Parkash S (2013) Brief Report on visit to Alaknanda Valley, Uttarakhand Himalaya during 22-24 June 2013. In brief report on Uttarakhand Disaster (16/17 June 2013) by National Institute of Disaster Management, Ministry of Home Affairs, Government of India, New Delhi. 12p.
180. Parkash Surya (2015) A Study on Flash Floods and Landslides Disaster on 3rd August 2012 along Bhagirathi Valley in Uttarkashi District, Uttarakhand. A report by National Institute of Disaster Management, Ministry of Home Affairs, Government of India, New Delhi, 230p.
181. Patching TH and Coates DF (1968) A recommended rock classification for rock mechanics purposes. Canadian Institute of Mining Bulletin: 1195-1197.
182. Patton FD (1966) Multiple modes of shear failure in rock. In Proceedings of the 1st congress of the International Society for Rock Mechanics, Lisbon, Portugal.
183. Pinheiro M, Sanches S, Miranda T, Neves A, Tinoco J, Ferreira A, Correia AG (2015) SQI–A quality assessment index for rock slopes. In Proceedings of the 16th Europena Conference on Soil Mechanics and Geotechnical Engineering, Edinburgh, Scotland.
184. Potvin Y, Dight PM, Wesseloo (2012) Some pitfalls and misuses of rock mass classification system for mine design. Journal of Southern African Institute of Mining and Metallurgy. 112(8): 697-702.
185. Pourghasemi HR, Yansari ZT, Panagos P, Pradhan B (2018) Analysis and evaluation of landslide susceptibility on articles published during 2005-2016 (periods of 2005-2012 and 2013-2016). Arabian Journal of Geosciences. 11:193.

186. Pouya A and Ghoreychi M (2001) Determination of rock mass strength properties by homogenization. International Journal for Numerical and Analytical Methods in Geomechanics. 25: 1285-1303.
187. Pradhan SP, Vishal V, Singh TN (2015) Study of slopes along river Teesta in Darjeeling Himalayan region. Engineering Geology for Society and Territory. 1: 517-520.
188. Pradhan SP, Vishal V, Singh TN, Singh VK (2014) Optimisation of dump slope geometry vis-à-vis fly ash utilisation using numerical simulation. American Journal of Mining and Metallurgy. 2(1): 1-7.
189. Rabcewicz L (1964) The New Austrian Tunnelling Method. Part one: Water Power, November 1964: 453-457 and Part two: Water Power, December 1964: 511-515.
190. Rad HN, Jalali Z, Jalalifar H (2015) Prediction of rock mass rating system based on continuous functions using Chaos-ANFIS model. International Journal of Rock Mechanics and Mining Sciences. 73: 1-9.
191. Rahim IA, Tahir S, Musta B (2009) Modified Slope Mass Rating (M-SMR) system: A classification scheme of interbedded Crocker Formation in Kota Kinabalu, Sabah, Malaysia. In Proceeding of the 8th Seminar on Science and Technology, Tuaran, Sabah.
192. Ramamurthy T and Arora VK (1993) A Classification for Intact and Jointed Rocks. In Geotechnical Engineering of Hard Soils-Soft Rocks, Anagnostopoulos et al. eds., Taylor and Francis, Rotterdam, ISBN: 10: 9054103442: 235-242.
193. Ramamurthy T and Arora VK (1994) Strength prediction for jointed rocks in confined and unconfined states. International Journal of Rock Mechanics Mining Sciences and Geomechanics Abstracts. 31(1): 9-22.
194. Ramamurthy T, Rao GV, Singh J (1993) Engineering behavior of phyllites. Engineering Geology. 33(3): 209-225.
195. Ramesh V, Mani S, Bhaskar M, Kavitha G, Anbazhagan S (2017) Landslide Hazard Zonation mapping and cut slope stability analyses along Yercaudghat road (Kuppanur-Yercaud) section, Tamil Nadu, India. International Journal of Geoengineering. 8(2): 1-22.
196. Reddy DV (2014) Landslides-Debris Flows Floods Earthquakes and Tsunamis of Indian Sub-Continent- Emergency Preparedness Plan – A Typical Analysis. In Proceedings of the 3rd World Conference on Applied Sciences, Engineering & Technology, Kathmandu, Nepal.
197. Rehman H, Nagi AM, Kim J, Yoo HK (2018) Empirical evaluation of Rock Mass Rating and Tunnelling Quality Index system for tunnel support design. Applied Sciences. 8: 782.
198. Ritter W (1879) Statics of the tunnel vaults. Berlin, Springer. 66p.

199. Robertson AM (1988) Estimating weak rock strength. In Proceedings of the annual meeting of American Institute of Mining, Metallurgical and Petroleum Engineers, Tucson, Arizona: 1-6.

200. Rocscience (2001) Phase^2 2D finite element program for calculating stresses and estimating support around underground excavations. Toronto, Ontario, Canada.

201. Romana M (1985) New adjustment ratings for application of Bieniawski classification to slopes. In Proceedings of the International Symposium on the role of rock mechanics, International Society of Rock Mechanics, Zacatecas, Mexico: 49-53.

202. Romana M (1991) SMR classification. In Proceedings of the 7th Congress on Rock Mechanics, International Society of Rock Mechanics and Rock Engineering, Aachen, Germany: 955-960.

203. Romana M (1993) A geomechanics classification for slopes: Slope Mass Rating. In Comprehensive Rock Engineering, Hudson ed., Pergamon. 3: 575-600.

204. Romana M (1995) The geomechanics classification SMR for slope correction. In Proceedings of the 8th Congress on Rock Mechanics, International Society of Rock Mechanics and Rock Engineering, Tokyo, Japan: 1085-1092.

205. Romana M (2003) DMR (Dam Mass Rating) An adaptation of RMR geomechanics classification for use in dams foundations. ISRM- Technology roadmap for rock mechanics, South African Institute of Mining and Metallurgy, Johannesburg, South Africa.

206. Romana M, Seron JB, Montalar E (2001) The Geomechanical classification SMR: Applications of experiences and validation. In National Symposium of unstable slopes. Madrid, Spain: 575-600.

207. Romana M, Seron JB, Montalar E (2003) SMR Geomechanics classification: Application, experience and validation. ISRM- Technology roadmap for rock mechanics, South African Institute of Mining and Metallurgy, Johannesburg, South Africa.

208. Romana M, Tomás R, Serón JB (2015) Slope Mass Rating (SMR) geomechanics classification: thirty years review. In Proceedings of the 13th Congress of International Symposium on Rock Mechanics, Quebec, Canada. 10 p.

209. Sajwan KS and Sushil K (2016) A Geological Appraisal of Slope Instability in Upper Alaknanda Valley, Uttarakhand Himalaya, India. Journal of Geology and Geophysics. 5(5): 258.

210. Sarkar K, Singh AK, Niyogi A, Behera K, Verma AK, Singh TN (2016) The assessment of Slope Stability along NH-22 in Rampur-Jhakri area, Himachal Pradesh. Journal Geological Society of India. 88(3): 387-393.

211. Sarkar K, Singh TN, Verma AK (2012) A numerical simulation of landslide-prone slope in Himalayan region-a case study. Arabian Journal of Geosciences. 5: 73-81.
212. Sarkar S and Samanta (2017) Stability Analysis and Remedial Measures of a Landslip at Keifang, Mizoram – A Case Study. Journal Geological Society of India. 89(6): 697-704.
213. Sarkar S, Kanungo DP, Patra AK (2006) Landslides in the Alaknanda valley of Garhwal Himalaya, India, Quarterly Journal of Engineering Geology and Hydrogeology. 39: 79-82.
214. Sarkar S, Kanungo DP, Sharma S (2015) Landslide hazard assessment in the upper Alaknanda valley of Indian Himalayas. Geomatics, Natural Hazards and Risk. 6(4): 308-325.
215. Sarkar S, Pandit K, Shamra M, Pippal A (2018) Risk assessment and stability analysis of a recent landslide at Vishnuprayag on the Rishikesh–Badrinath highway, Uttarakhand, India. Current Science. 114(7): 1527-1533.
216. Satendra, Gupta AK, Naik VK, Roy TKS, Sharma AK, Dwivedi M (2015) Uttarakhand Disaster 2013. National Institute of Disaster Management, Ministry of Home Affairs, Government of India, New Delhi, India. 184p.
217. Sati SP, Naithani A, Rawat GS (1998) Landslides in the Garhwal Lesser Himalaya, UP, India. The Environmentalist. 18(3): 149-155.
218. Sati SP, Naithani A, Rawat GS (1998) Landslides in the Garhwal Lesser Himalaya, UP,
219. Sati SP, Sunderiyal YP, Rana N, Dangwal S (2011) Recent landslides in Uttarakhand: nature's furry or human folly. Current Science. 100(11): 1617-1620.
220. Scaringi G, Fan X, Xu Q, Liu C, Ouyang C, Domenech G, Yang F, Dai L (2018) Some considerations on the use of numerical methods to simulate past landslides and possible new failures: the case of the recent Xinmo landslide (Sichuan, China). Landslides. 15(7): 1359-1375.
221. Schelling D and Arita K (1991) Thrust tectonics, crustal shortening, and the structure of the far-eastern Nepal, Himalaya. Tectonics. 10(5): 851-862.
222. Selby MJ (1980) A rock mass strength classification for geomorphic purposes: with tests from Antarctica and New Zealand. Geomorphology. 24: 31-51.
223. Şen Z and Sadagah BH (2003) Modified rock mass classification system by continuous rating. Engineering Geology. 67(3): 269-280.
224. Shang Y, Hyun CU, Park HD, Yang Z, Yuan G (2017) The 102 Landslide: human-slope interaction in SE Tibet over a 20-year period. Environmental Earth Sciences 76: 47.

225. Sharma LK, Umrao RK, Singh R, Ahmad M, Singh TN (2017) Stability Investigation of Hill Cut Soil Slopes along National Highway 222 at Malshej Ghat, Maharashtra. Journal Geological Society of India. 89(2): 165-174.
226. Shroder JF and Bishop MP (1998) Mass movement in the Himalaya: new insights and research directions. Geomorphology. 26(1-3): 13-35.
227. Shuk T (1994) Key elements and applications of the natural slope methodology (NSM) with some emphasis on slope stability aspects. In Proceedings of the 4th South American Congress on Rock Mechanics 2, International Society of Rock Mechanics, Balkema, Rotterdam: 955-960.
228. Siddique T and Pradhan SP (2018) Stability and sensitivity analysis of Himalayan road cut debris slopes: An investigation along NH-58, India. Natural Hazards. 93(2): 577-600.
229. Siddique T, Alam MM, Mondal MEA, Vishal V (2015) Slope Mass Rating and Kinematic analysis of slopes along National Highway-58, near Jonk, Rishikesh, India. Journal of Rock Mechanics and Geotechnical Engineering. 7(5): 600-606.
230. Siddique T, Pradhan SP, Vishal V (2016) Road Cut Slope Stability Investigation along NH-58, Near Shivpuri, Uttarakhand; In Proceedings of National Conference on Advances in Geotechnical Engineering, Aligarh Muslim University, Aligarh, India: 66-70.
231. Siddique T, Pradhan SP, Vishal V, Mondal MEA, Singh TN (2017) Stability assessment of Himalayan road cut slopes along National Highway 58, India. Environmental Earth Sciences. 76: 759.
232. Singh A and Connolly M (2003) VRFSR- An empirical method for determining volcanic rock excavations safety on construction sites. Journal of the Institution of Engineers India 84: 176-191.
233. Singh B and Goel RK (1999) Rock Mass Classification: A practical approach in civil engineering. Elsevier Science. 267p.
234. Singh B and Goel RK (2002) Software for engineering control of landslide and tunnelling hazards. Balkema, Netherlands. 344p.
235. Singh M (2019) Shear strength behavior of jointed rock mass. In Landslides: Theory, Practice and Modeling, Pradhan et al. eds., Advances in Natural and Technological Hazards Research, Springer, 50: 41-60.
236. Singh M and Singh B (2012) Modified Mohr-Coulomb criterion for non-linear triaxial and polyaxial strength of jointed rocks. International Journal of Rock Mechanics and Mining Sciences. 51: 43-52.

237. Singh M, Bhawani S, Shankar D (2005) Critical state in non-linear failure criterion for rocks. Journal of Rock Mechanics and Tunnelling Technology. 11(1): 13-24.
238. Singh R, Umrao RK, Singh TN (2014) Stability evaluation of road-cut slopes in the Lesser Himalaya of Uttarakhand, India: conventional and numerical approaches. Bulletin of Engineering Geology and the Environment. 73(3): 845-857.
239. Singh R, Umrao RK, Singh TN (2017) Hill slope stability analysis using two and three dimension analysis: A comparative study. Journal of Geological Society of India. 89(3): 229-356.
240. Singh RP, Dubey CS, Singh SK, Shukla DP, Mishra BK, Tajbakhsh M, Ningthoujam PS, Sharma M, Singh N (2013) A new slope mass rating in mountainous terrain, Jammu and Kashmir Himalayas: application of geophysical technique in slope stability studies. Landslides. 10(3): 255-265.
241. Singh TN, Monjezi M, Sawmliana C, Kumar S (2001) Shear behavior of jointed rockmass of sandstone quarry, Mizoram state, India. Indian Journal of Engineering and Materials Sciences. 8: 66-70.
242. Singh TN and Monjezi M (2000) Slope stability study in jointed rockmass- A numerical approach. Mining Engineering Journal. 1(10): 12-13.
243. Singh TN, Gulati A, Dontha L, Bhardwaj V (2008) Evaluating cut slope failure by numerical analysis-a case study. Natural Hazards. 47: 263-279.
244. Singh TN, Verma AK, Sarkar K (2010) Static and dynamic analysis of landslide. Geomatics, Natural Hazards and Risk. 1(4): 323-338.
245. Sitharam TG (2009) Equivalent continuum analyses of jointed rock mass: some case studies. International Journal of the Japanese Committee for Rock mechanics. 5(1): 39-51.
246. Smith HJ (1986) Estimating Rippability by Rock Mass Classification. In Proceedings of the 27th U.S. Symposium on Rock Mechanics, American Rock Mechanics Association, new York: 443-448.
247. Song WK, Jung YB, Sunwoo C, Lee Y (2008) Modification of SMR for simple users. In Proceedings of the 4th U.S. Rock Mechanics Symposium, San Francisco, California.
248. Sonmez H and Ulusay R (1999) Modifications to the geological strength index (GSI) and their applicability to the stability of slopes. International Journal of Rock Mechanics and Mining Sciences. 36(6): 743-760.
249. Sonmez H and Ulusay R (2002) A discussion on the Hoek–Brown failure criterion and suggested modification to the criterion verified by slope stability case studies. Geosciences. 26: 77-99.

250. Sorkhabi R (2010) Geologic formation of the Himalaya. Himalayan Journal. 66: 1-6.
251. Srivastava P and Mitra G (1994) Thrust geometries and deep structure of the outer and Lesser Himalaya, Kumaon and Garhwal (India): Implications for evolution of the Himalayan fold and thrust belt. Tectonics. 13: 89-109.
252. Stille H and Palmstrom A (2003) Classification as a tool in rock engineering. Tunnelling and Underground Space Technology. 18: 331-345.
253. Sundriyal YP, Shukla AD, Rana N, Jayangondaperumal R, Srivastava P, Chamyal LS, Sati SP, Juyal N (2015) Terrain response to the extreme rainfall event of June 2013: Evidence from Alaknanda and Mandakini valleys, Garhwal Himalaya, India. Episodes. 38(3): 179-188.
254. Taheri A (2012) Design of rock slopes using SSR classification system. In Proceedings of International Conference on Ground Improvement and Ground Control, Australia.
255. Taheri A and Tani K (2010) Assessment of the slope stability of Rock slopes by Slope Stability Rating classification system. Rock Mechanics and Rock Engineering 43(3): 321-333.
256. Tang SB, Huang RQ, Tang CA, Liang ZZ, Heap, MJ (2017) The failure processes analysis of rock slope using numerical modeling techniques. Engineering Failure Analysis. 79: 999-1016.
257. Tiwari M, Parcha SK, Shukla R, Joshi H (2013) Ichnology of the early Cambrian Tal group, Mussoorie syncline, Lesser Himalaya, India. Journal Earth System Sciences. 122(6): 1467-1475.
258. Terzaghi K (1946) Rock defects and loads on tunnel support. In Rock tunneling with steel supports, Commercial Shearing and Stamping Co., Youngstown, United States: 43-64.
259. Tomás R, Cuenca A, Cano M, García BJ (2012) A graphical approach for slope mass rating (SMR). Engineering Geology. 124: 67-76.
260. Tomás R, Delgado J, Serón JB (2007) Modification of slope mass rating (SMR) by continuous functions. International Journal of Rock Mechanics and Mining Sciences 44(7): 1062-1069.
261. Tripathi C (1986) Siwaliks of the Indian Subcontinent. Journal of the Palaeontological Society of India.
262. Tschuchnigg F, Schweiger HF, Sloan SW, Lyamin AV (2015) Comparison of finite-element limit analysis and strength reduction Techniques. Géotechnique. 65(4): 249-257.

263. Tzamos S and Sofianos AI (2007) A correlation of four rock mass classification systems through their fabric indices. International Journal of Rock Mechanics and Mining Sciences 44(4): 477-495.

264. Umrao RK, Singh R, Ahmad M, Singh TN (2011) Stability analysis of cut slopes using continuous slope mass rating and kinematic analysis in Rudraprayag district, Uttarakhand. Geomaterials. 1(3): 79-87.

265. Umrao RK, Singh R, Sharma LK, Singh TN (2017) Soil slope instability along a strategic road corridor in Meghalaya, north-eastern India. Arabian Journal of Geosciences. 10: 260.

266. Ünal E (1996) Modified rock mass classification: M-RMR system. In Bieniawski ZT Milestones in rock engineering, The Bieniawski Jubilee Collection, Balkema: 203-223.

267. Uniyal A (2004) Landslides at Karnaprayag: Another Uttarkashi in making?. Current Science. 87(8): 1031-1033.

268. Upreti BN (1999) An overview of the stratigraphy and tectonics of the Nepal Himalaya. Journal of Asian Earth Sciences. 17(5-6): 577-606.

269. Valdiya KS (1980) Geology of Kumaun Lesser Himalaya. Wadia Institute of Himalayan Geology, Dehradun, India. 291p.

270. Valdiya KS (1983) Lesser Himalayan Geology: Crucial problems and controversies. Current Science. 52(18): 839-857.

271. Valdiya KS (1992) Must we have high dams in geodynamically active Himalayan domain. Current Science. 63(4): 289-296.

272. Valdiya KS (1995) Proterozoic sedimentation and Pan- African geodynamic development in the Himalaya. Precambrian Research 74: 35-55.

273. Valdiya KS (2002) Emergence and evolution of Himalaya: reconstructing history in the light of recent studies. Progress in Physical Geography. 26(3): 360-399.

274. Valdiya KS (2014) Damming rivers in the tectonically resurgent Uttarakhand Himalaya. Current Science. 106(12): 1658-1668.

275. Valdiya KS and Bartarya SK (1991) Hydrogeological studies of springs in the catchment of Gaula river, Kumaun lesser Himalaya, India. Mountain Research and Development. 11(3): 239-258.

276. Vallejo LIGD (1983) SRC rock mass classification of tunnels under high tectonic stress excavated in weak rocks. Engineering Geology. 69: 273-285.

277. Varnes DJ (1954) Landslide types and processes. In Landslides and engineering practice, special report 28, Eckel ed., Highway Research Board. National Academy of Science, Washington DC: 20-47.

278. Varnes DJ (1978) Slope movement types and processes. In Landslides, analysis and control, special report 176, Schuster and Krizek eds., Transportation Research Board, National Academy of Science, Washington DC: 11-33.
279. Varnes DJ (1984) Landslide Hazard Zonation: A Review of Principles and Practice. Unesco, Paris.
280. Vásárhelyi B (2009) A possible for estimating the poisson's rate values of rock mass. Acta Geodaetica et Geophysica. 44(3): 313-322.
281. Vásárhelyi B and Kovács D (2017) Empirical methods of calculating the mechanical parameters of the rock mass. Periodica Polytechnica Civil Engineering. 61(1): 39-50.
282. Veerappan R, Negi A, Anbazhagan S (2017) Landslide susceptibility mapping and comparison using Frequency Ratio and Analytical Hierarchy Process in parts of NH-58, Uttarakhand Himalayas, India. In 4th World Landslide Forum, Mikos et al. eds. Ljubljana, Slovenia: 1081-1091.
283. Venkateshwarlu V (1986) Geomechanics classification of coal measure rocks vis-à-vis roof supports. Ph.D. Thesis, India School of Mines, Dhanbad, Jharkhand, India.
284. Verma AK and Singh TN (2010) Assessment of tunnel instability-a numerical approach. Arabian Journal of Geosciences. 3(2): 181-192.
285. Verma AK, Singh TN, Chauhan NK, Sarkar K (2016) A hybrid FEM-ANN approach for slope instability prediction. Journal of the Institution of Engineers (India) Series A 97(3): 171-180.
286. Vishal V, Pradhan SP, Singh TN (2010) Instability assessment of mine slope-a finite element approach. International Journal of Earth Sciences and Engineering. 3(6): 11-23.
287. Vishal V, Pradhan SP, Singh TN (2015) Analysis of slopes in Himalayan terrane along national highway: 109, India. Engineering geology for Society and Territory. 1: 511-515.
288. Vishal V, Siddique T, Purohit R, Phophliya MK, Pradhan SP (2017) Hazard assessment in rockfall-prone Himalayan slopes National Highway-58, India: rating and simulation. Natural Hazards. 85(1): 487-503.
289. Wadia DN (1953) Geology of India. 3rd edition. MacMillan and Co. Limited, London 553p.
290. Weaver DA (1975) Geological factors significant in the assessment of rippability. Journal South African Institute of Civil Engineering. 17(12): 313-316.
291. Wickham GE, Tiedemann HR, Skinner EH (1972) Support determination based on geologic predictions. In Proceedings of North American Rapid Excavation and Tunneling Conference, Chicago, New York: 43-64.

292. Williamson DA (1984) Unified rock classification system. Bulletin of Association of Engineering Geology. 21(3): 345-354.
293. Wyllie DC and Mah CW (2004) Rock Slope Engineering. 4th edition based on Hoek E and Bray JW, Rock Slope Engineering, Taylor and Francis Group, London and New York, 431p.
294. Yagiz S (2009) Predicting uniaxial compressive strength, modulus of elasticity and index properties of rocks using the Schmidt hammer. Bulletin of Engineering Geology and the Environment. 68(1): 55-63.
295. Yin A (2006) Cenozoic tectonic evolution of the Himalayan orogen as constrained by along-strike variation of structural geometry, exhumation history, and foreland sedimentation. Earth Science Reviews. 76(1-2): 1-131.
296. Yoon WS, Jeong UJ, Kim (2002) Kinematic analysis of sliding failure of multi-faced rock slopes. Engineering Geology. 67(1-2): 51-61.
297. Zheng H (2012) A three-dimensional rigorous method for stability analysis of landslides. Engineering Geology. 145-146: 30-40.
298. Zheng H, Sun G, Liu D (2009) A practical procedure for searching critical slip surfaces of slopes based on the strength reduction technique. Computers and Geotechnics. 36(1-2): 1-5.
299. Zhu DY, Lee CF, Jiang HD (2003) Generalised framework of limit equilibrium methods for slope stability analysis. Géotechnique. 53(4): 377-395.
300. Zihin Y, Guozhe MA, Binxiang Y, Fujun NIU (2012) The origin of the 2008 Wenchuan Earthquake determined by the Analysis on the Active Longmenshan Nappe in terms of Rockmass Mechanics. Journal of Mountain Science. 9(3): 395-402.

Appendix

Appendix A: Shear strain contours and SRF_{GHB} of all investigated rock slopes along NH-58

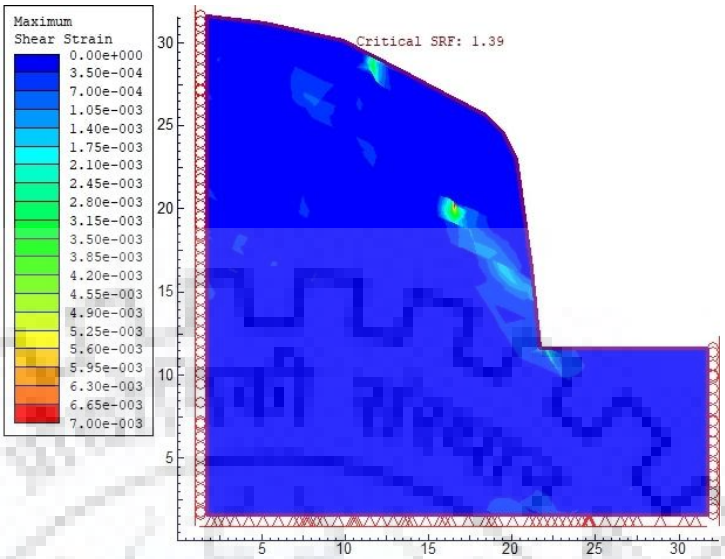

Shear strain contours and SRF_{GHB} of slope S1

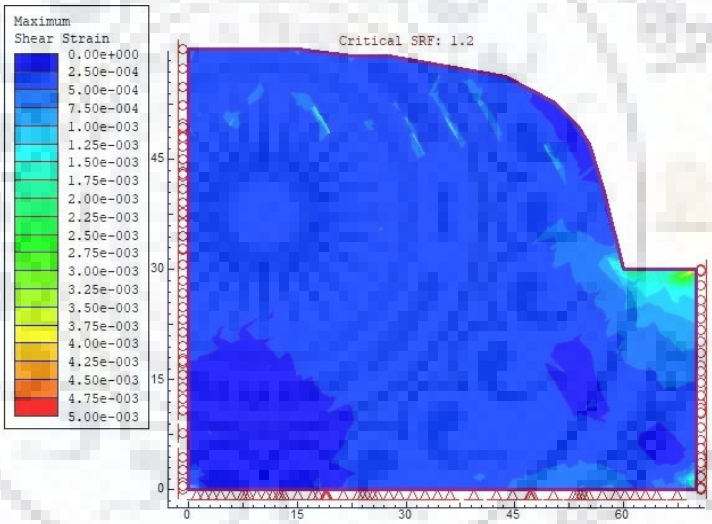

Shear strain contours and SRF_{GHB} of slope S2

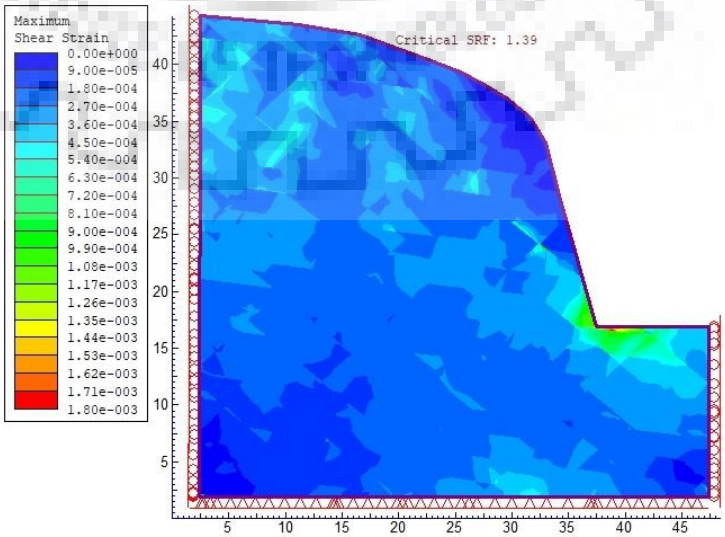

Shear strain contours and SRF_{GHB} of slope S3

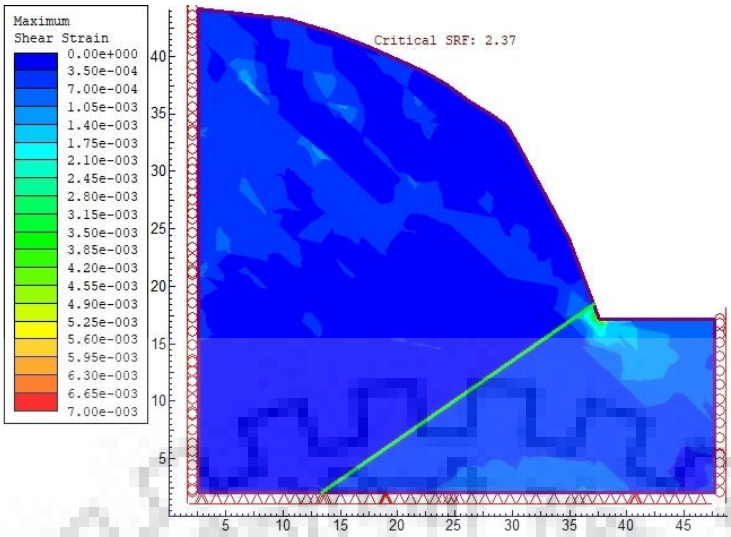

Shear strain contours and SRF_{GHB} of slope S4

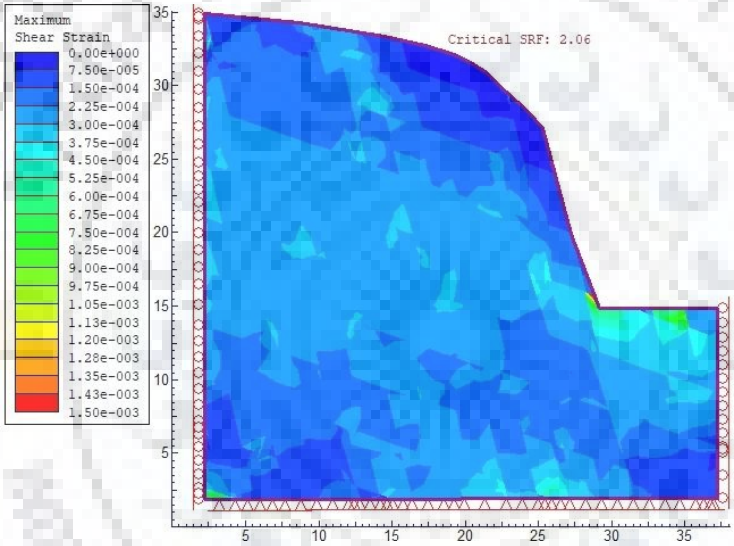

Shear strain contours and SRF_{GHB} of slope S5

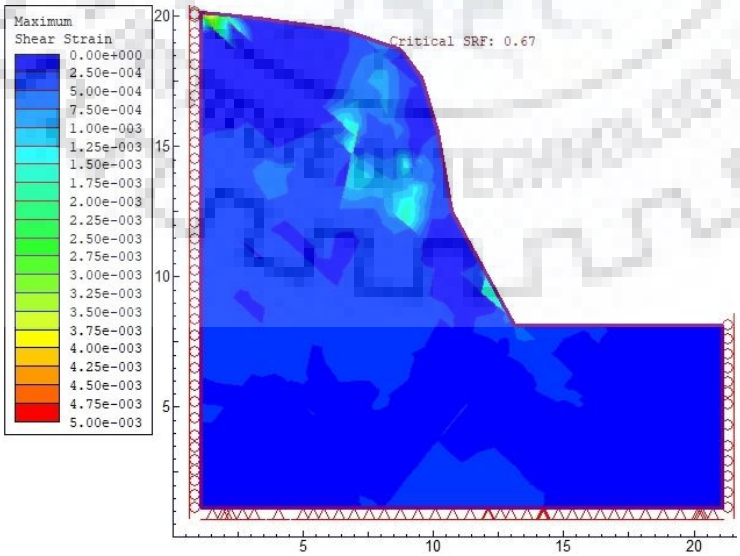

Shear strain contours and SRF_{GHB} of slope S6

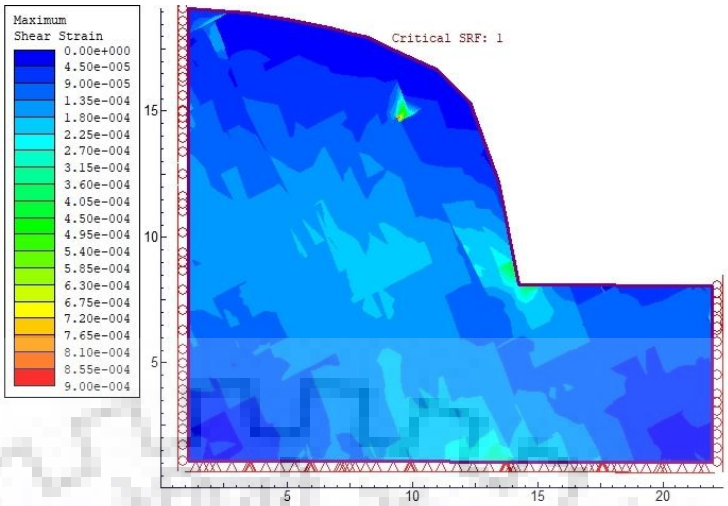

Shear strain contours and SRF_{GHB} of slope S7

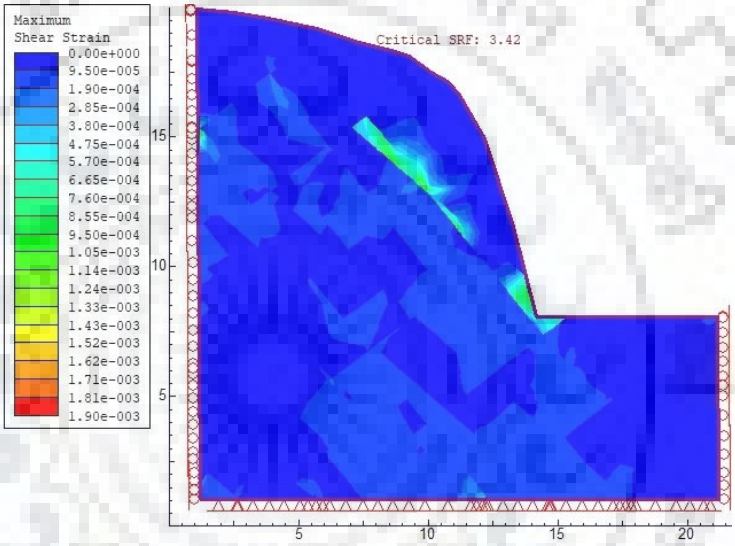

Shear strain contours and SRF_{GHB} of slope S8

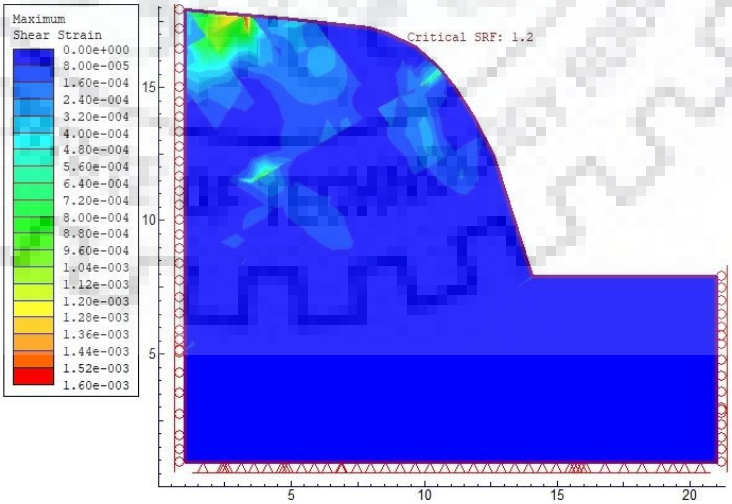

Shear strain contours and SRF_{GHB} of slope S9

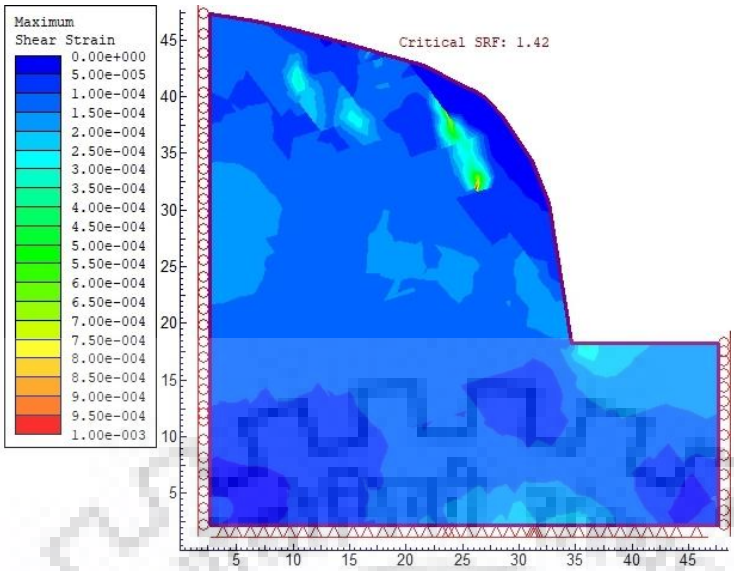

Shear strain contours and SRF_{GHB} of slope S10

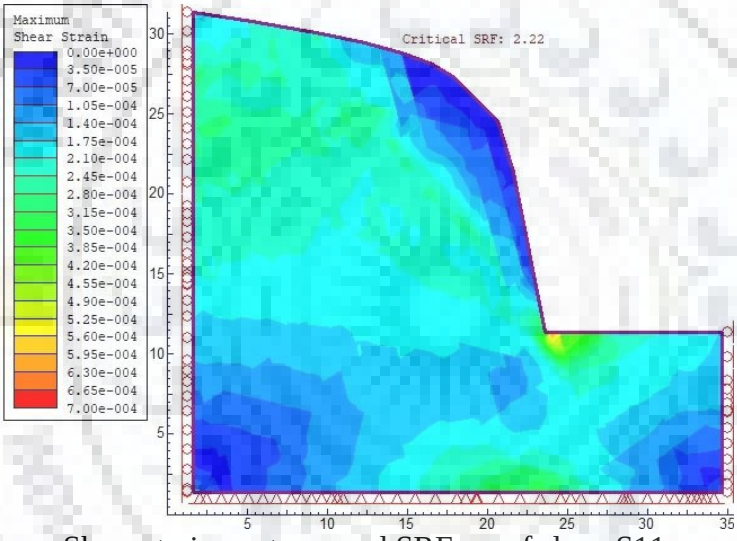

Shear strain contours and SRF_{GHB} of slope S11

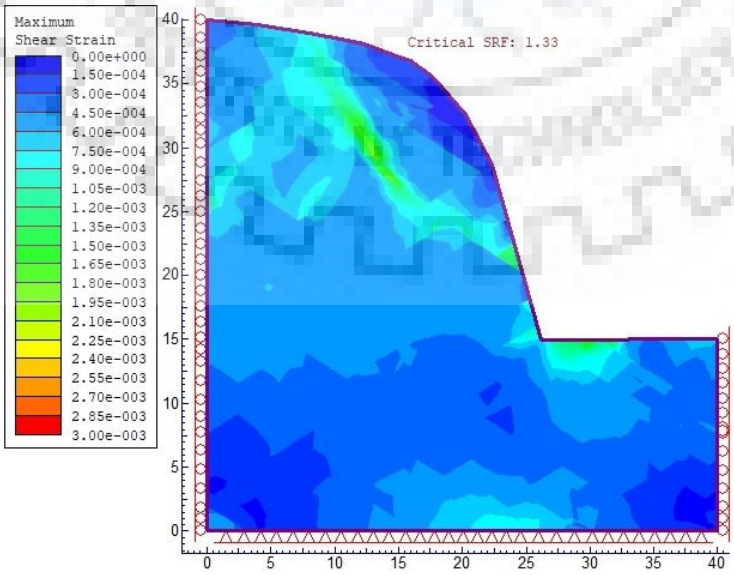

Shear strain contours and SRF_{GHB} of slope S12

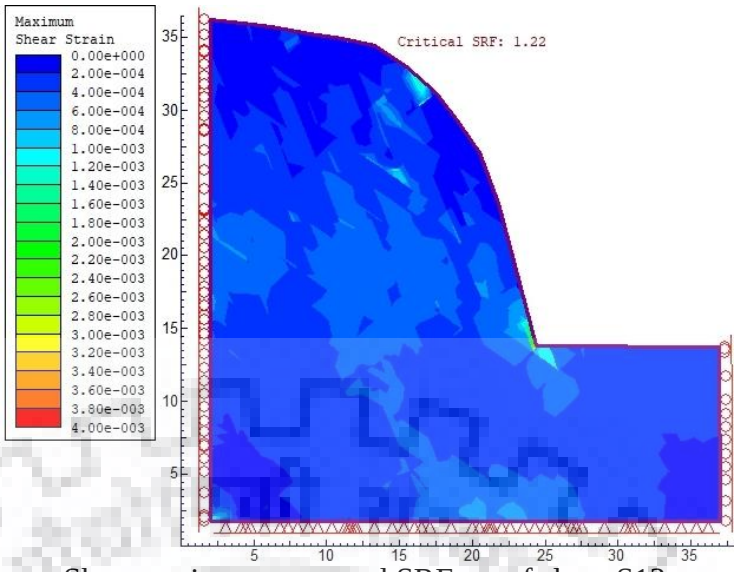

Shear strain contours and SRF_{GHB} of slope S13

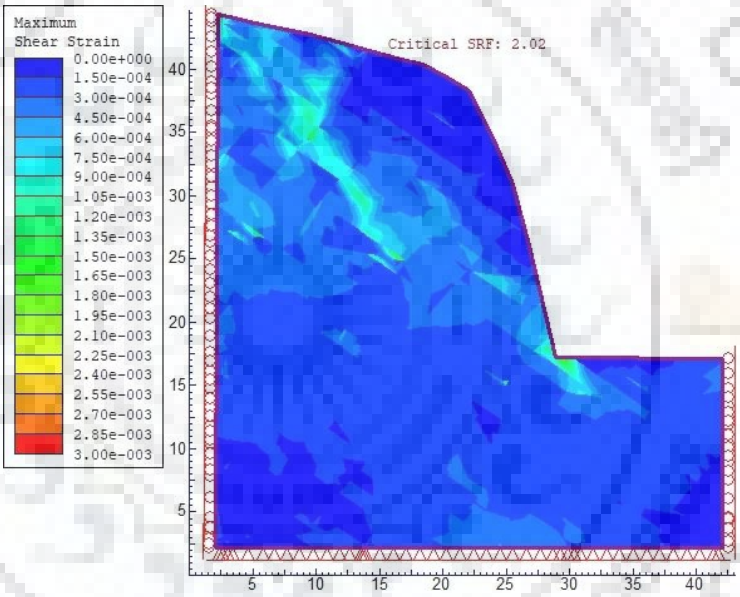

Shear strain contours and SRF_{GHB} of slope S14

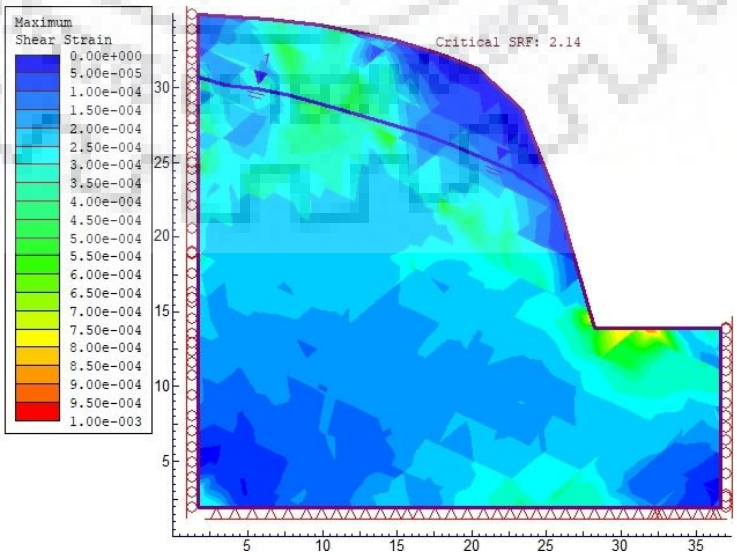

Shear strain contours and SRF_{GHB} of slope S15

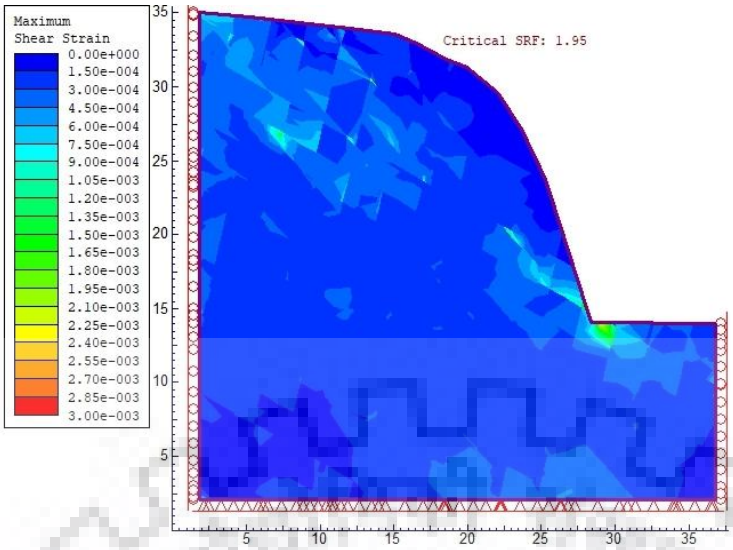

Shear strain contours and SRF_{GHB} of slope S16

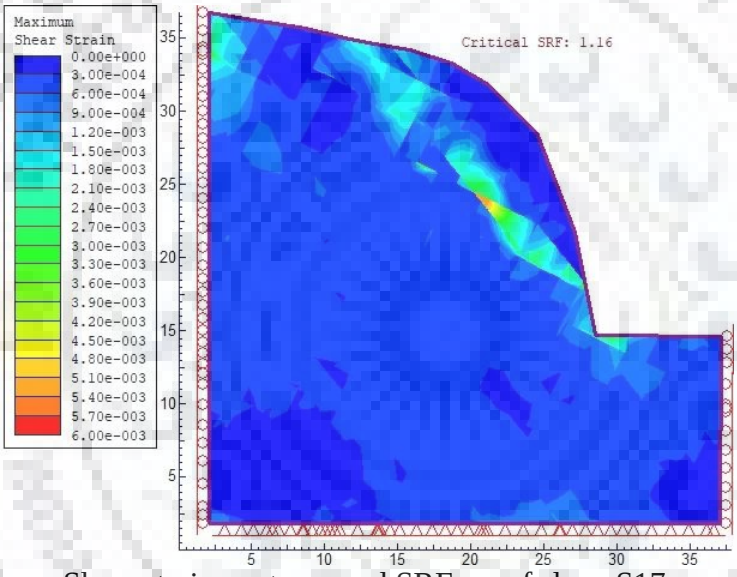

Shear strain contours and SRF_{GHB} of slope S17

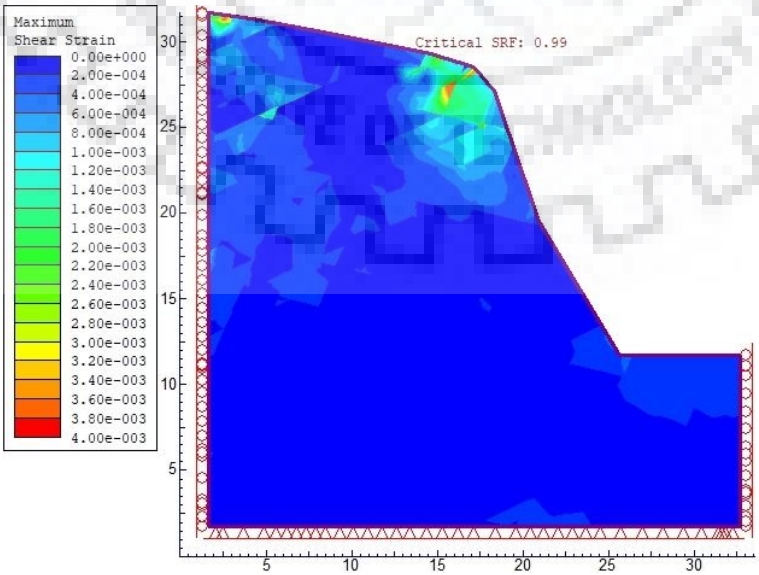

Shear strain contours and SRF_{GHB} of slope S18

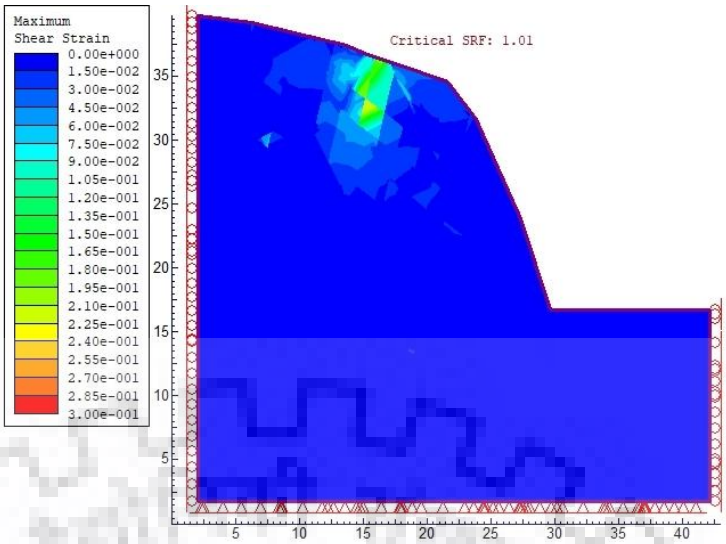

Shear strain contours and SRF_{GHB} of slope S19

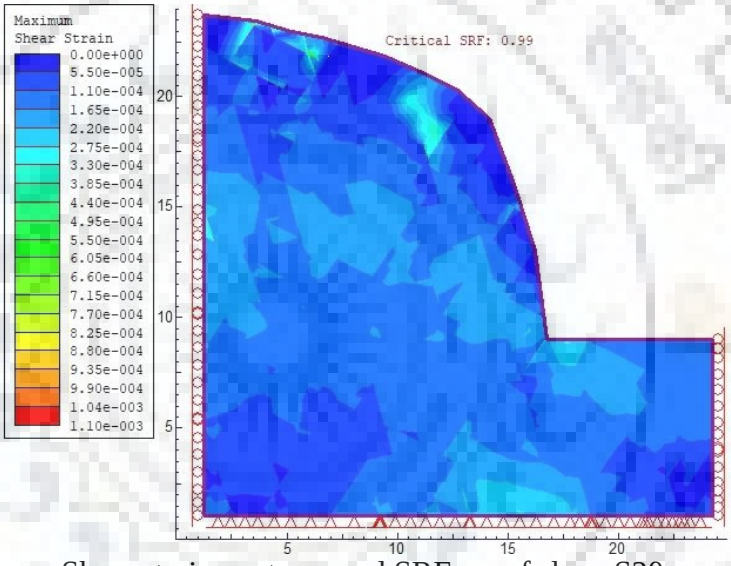

Shear strain contours and SRF_{GHB} of slope S20

Appendix B: Shear strain contours and SRF_{MC} of all investigated rock slopes along NH-58

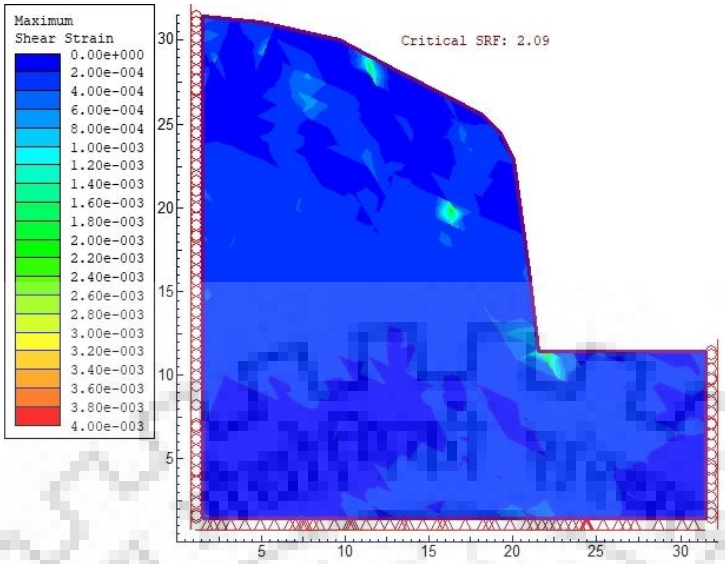

Shear strain contours and SRF_{MC} of slope S1

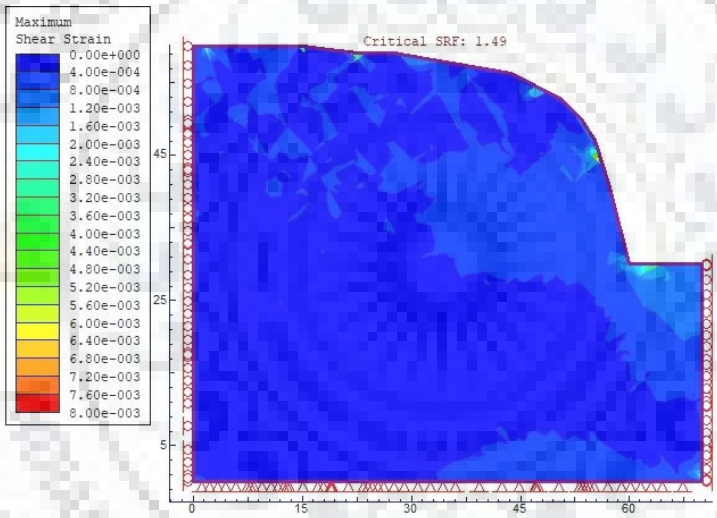

Shear strain contours and SRF_{MC} of slope S2

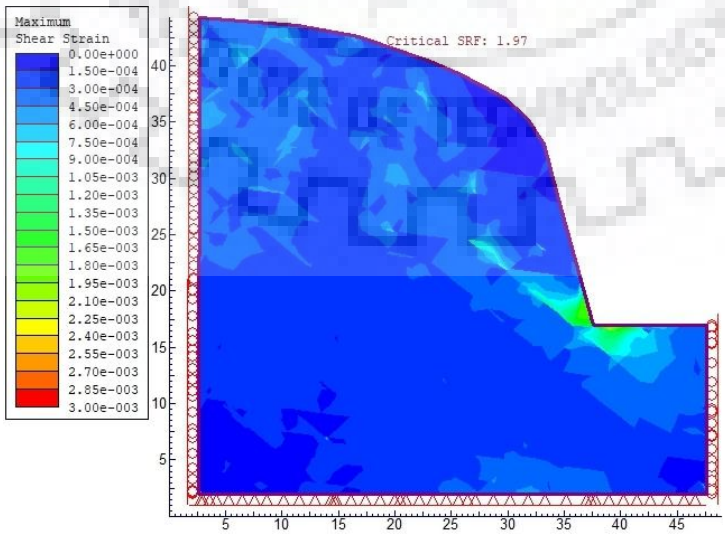

Shear strain contours and SRF_{MC} of slope S3

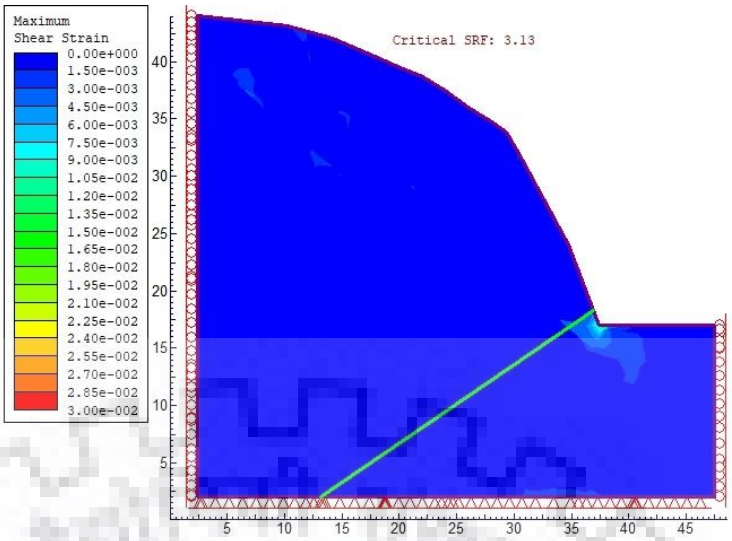

Shear strain contours and SRF_{MC} of slope S4

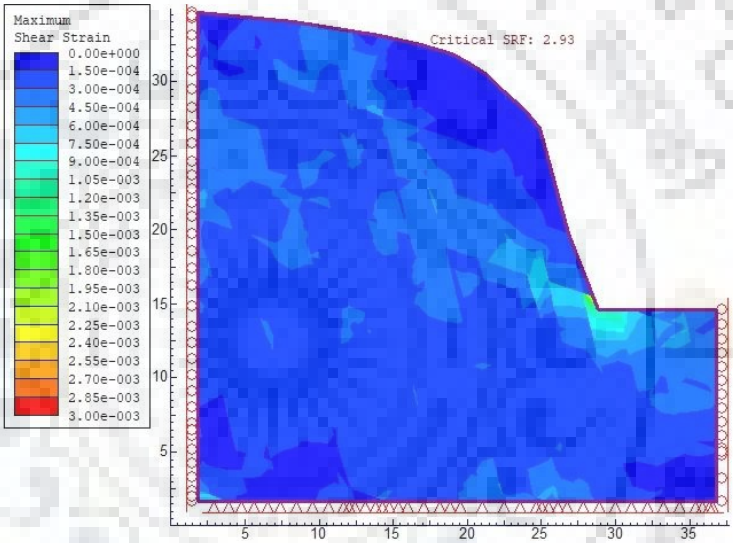

Shear strain contours and SRF_{MC} of slope S5

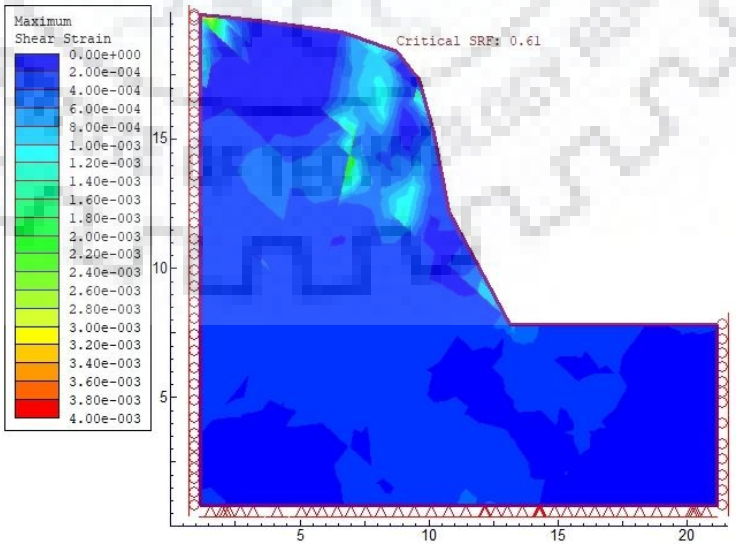

Shear strain contours and SRF_{MC} of slope S6

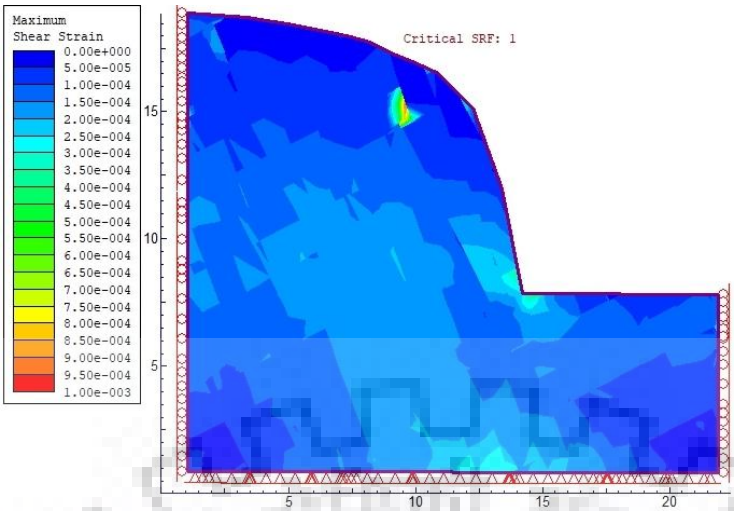

Shear strain contours and SRF_{MC} of slope S7

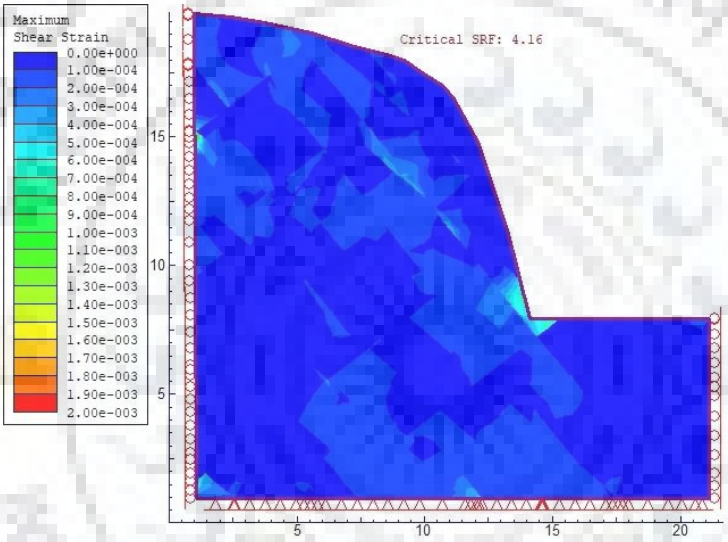

Shear strain contours and SRF_{MC} of slope S8

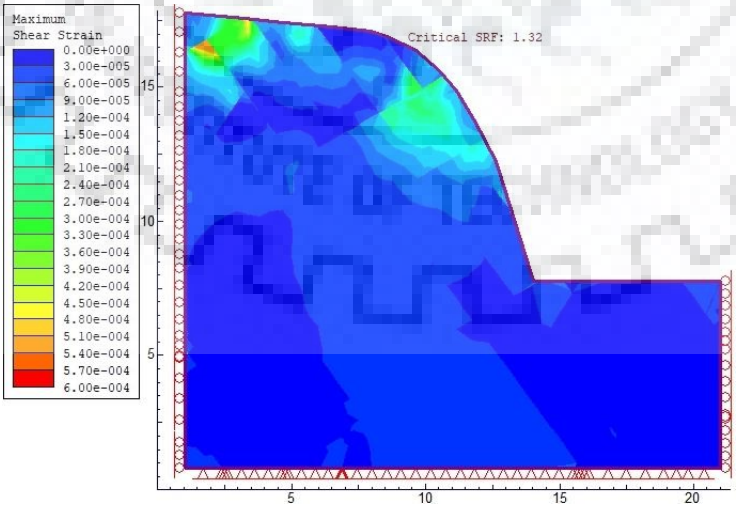

Shear strain contours and SRF_{MC} of slope S9

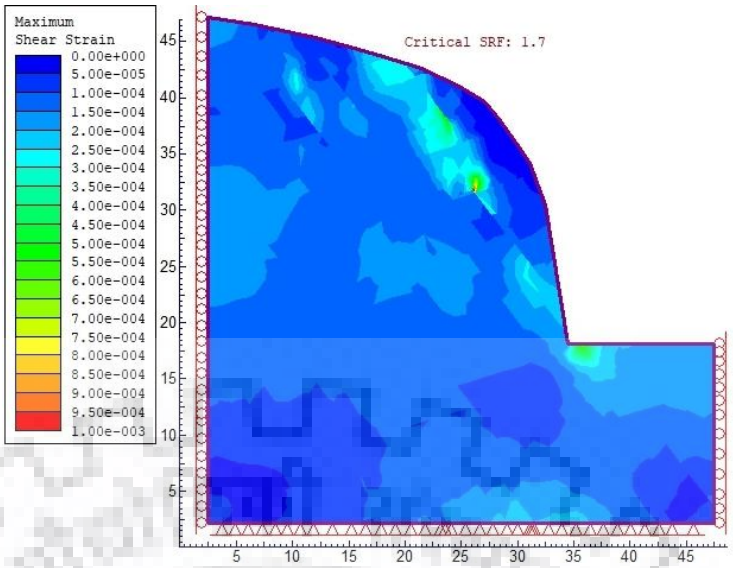

Shear strain contours and SRF_{MC} of slope S10

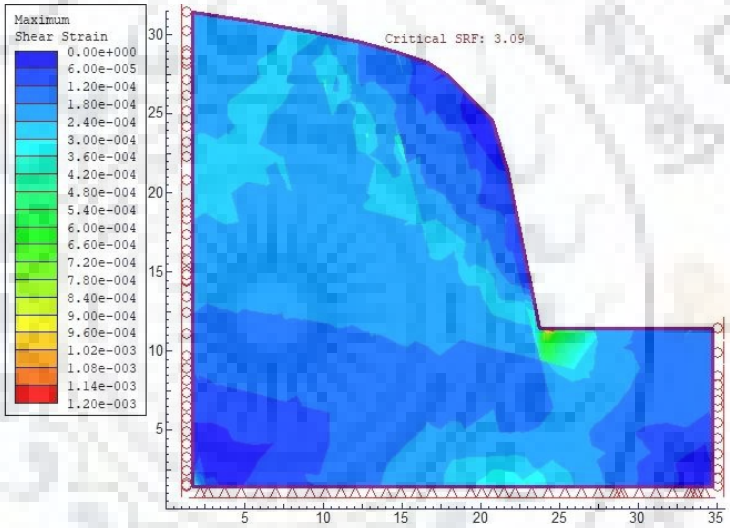

Shear strain contours and SRF_{MC} of slope S11

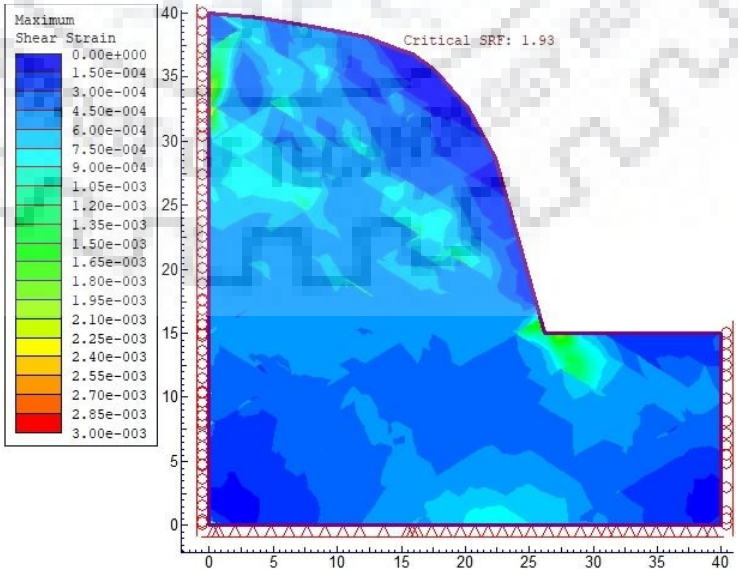

Shear strain contours and SRF_{MC} of slope S12

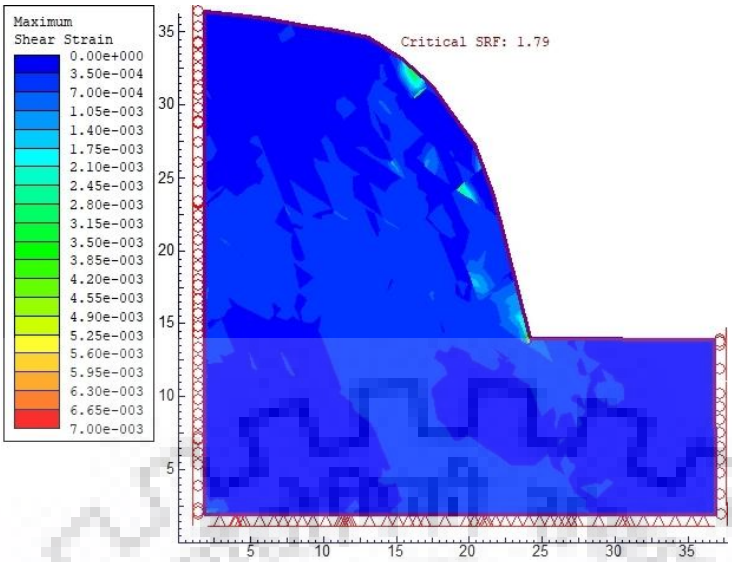

Shear strain contours and SRF_{MC} of slope S13

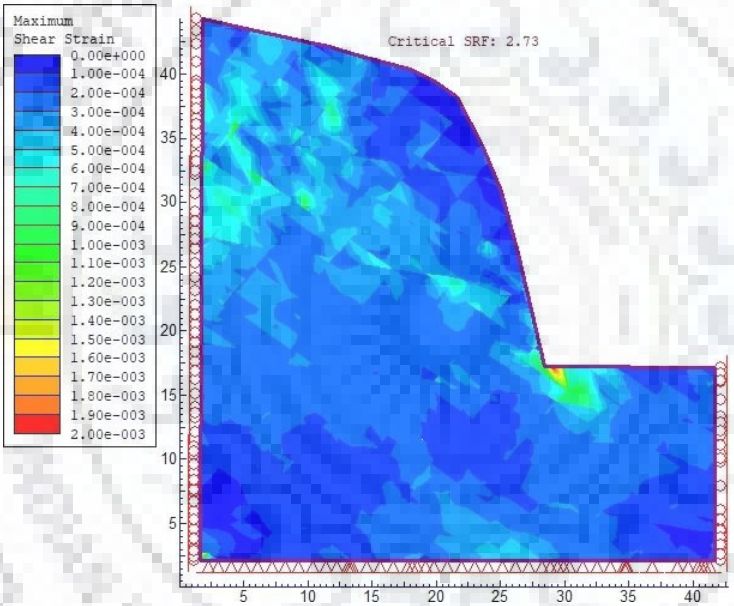

Shear strain contours and SRF_{MC} of slope S14

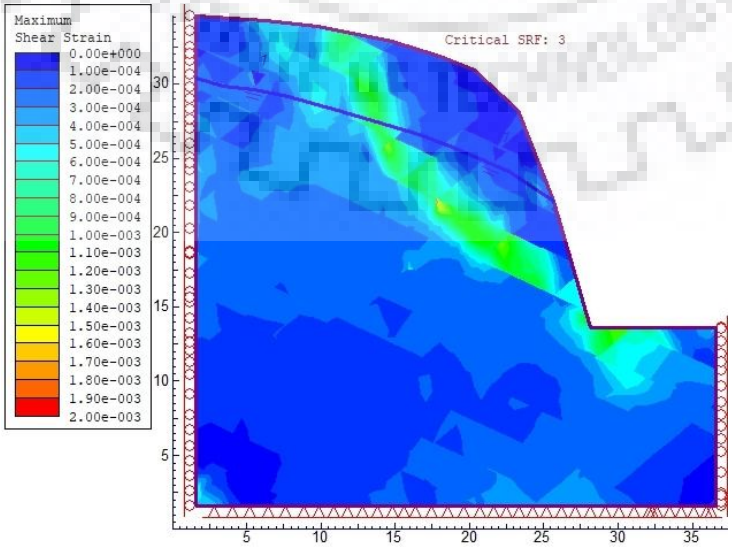

Shear strain contours and SRF_{MC} of slope S15

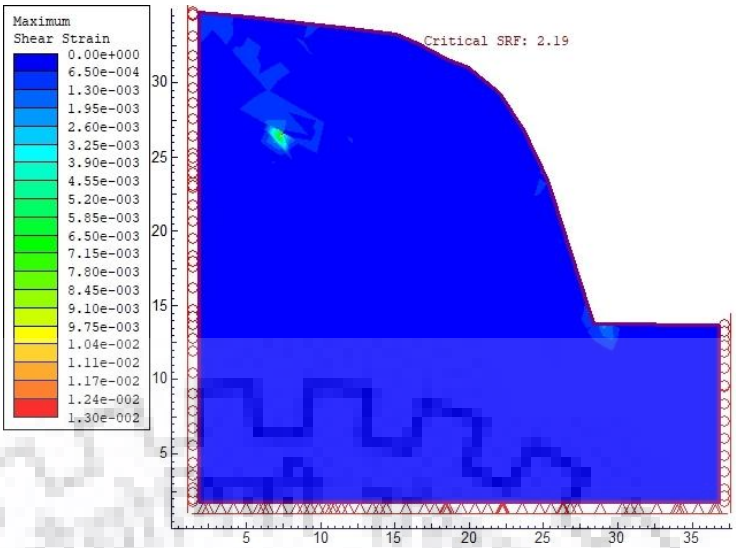

Shear strain contours and SRF_{MC} of slope S16

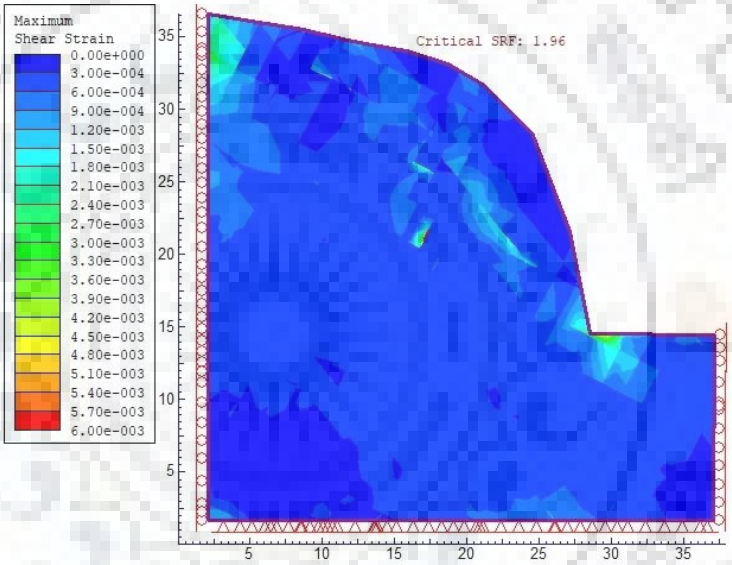

Shear strain contours and SRF_{MC} of slope S17

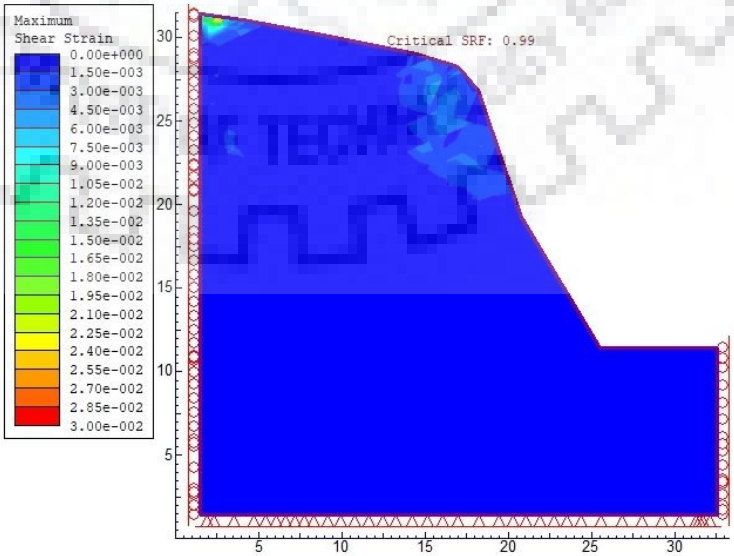

Shear strain contours and SRF_{MC} of slope S18

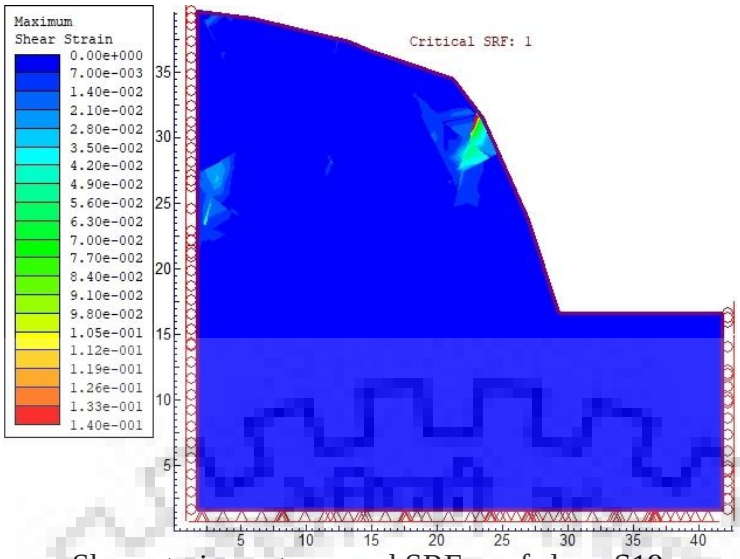

Shear strain contours and SRF_{MC} of slope S19

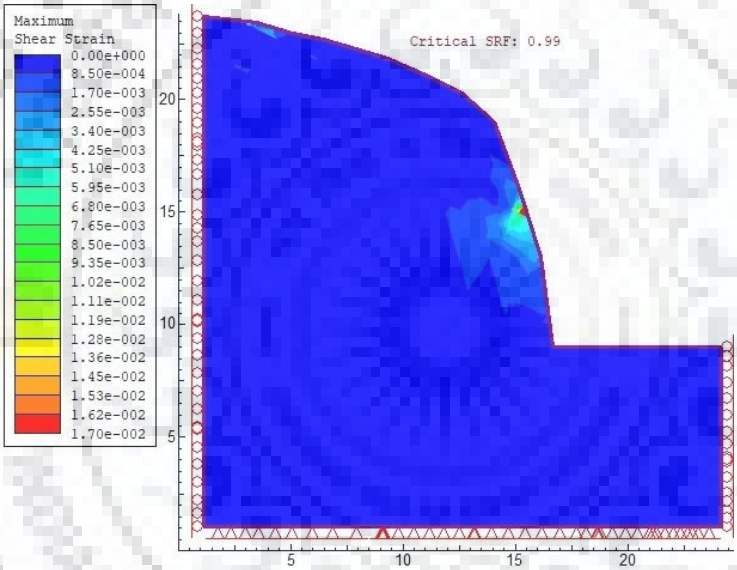

Shear strain contours and SRF_{MC} of slope S20

Appendix C: FoS and critical slip surface of all investigated debris slopes along NH-58

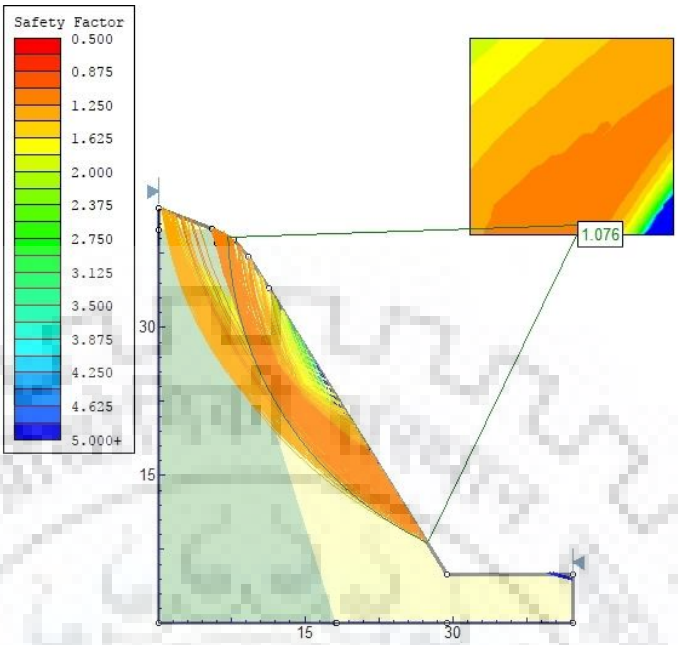

FoS and critical slip surface at slope L1

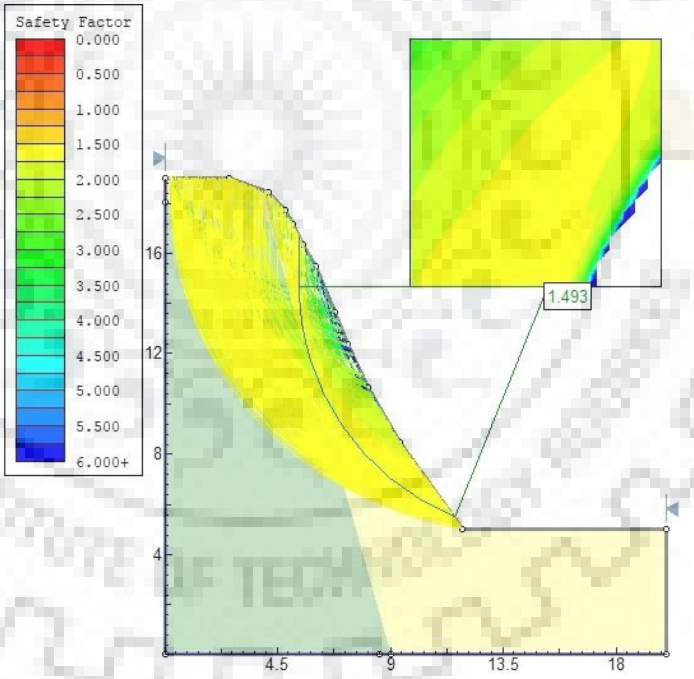

FoS and critical slip surface at slope L2

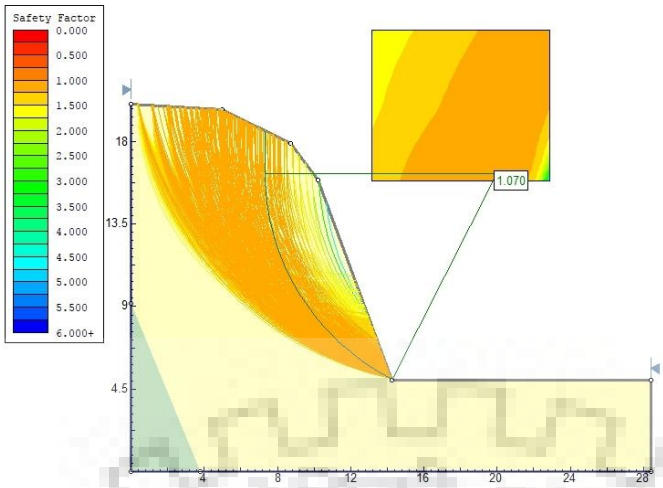

FoS and critical slip surface at slope L3

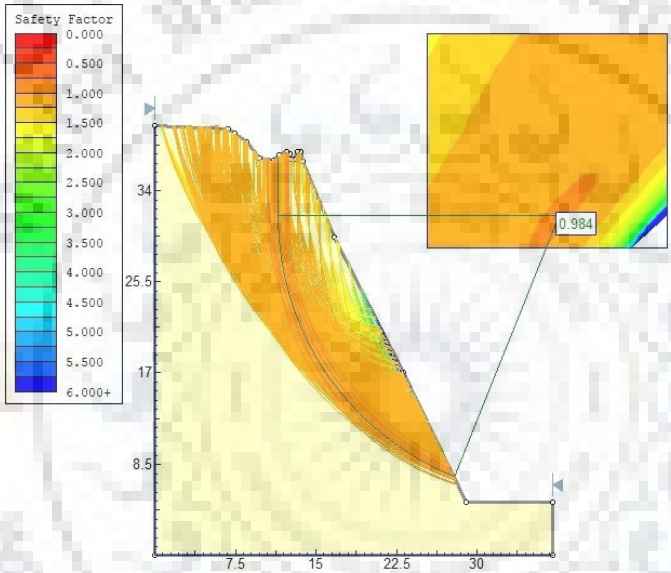

FoS and critical slip surface at slope L4

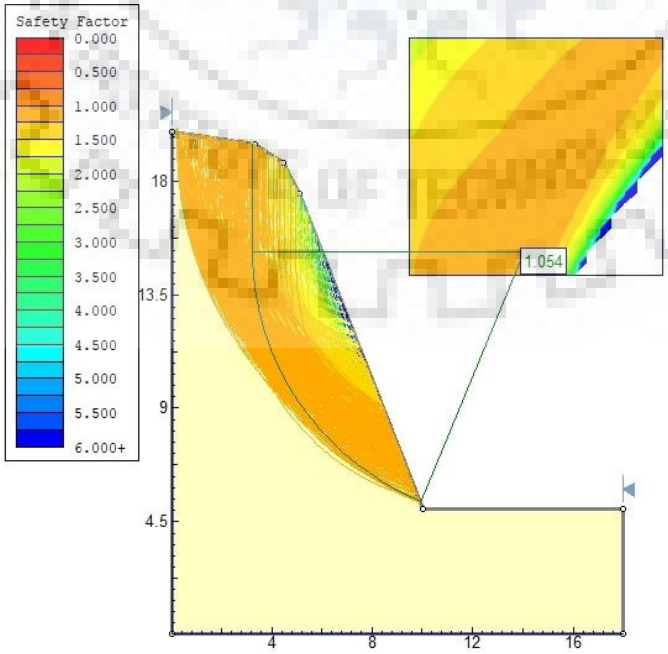

FoS and critical slip surface at slope L5

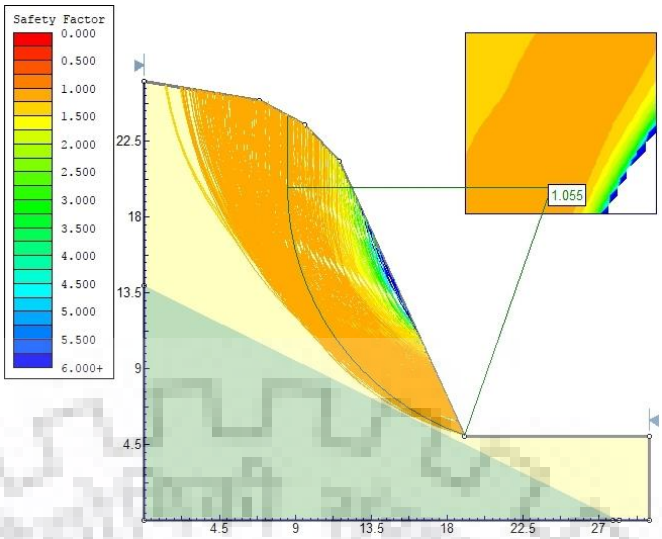

FoS and critical slip surface at slope L6

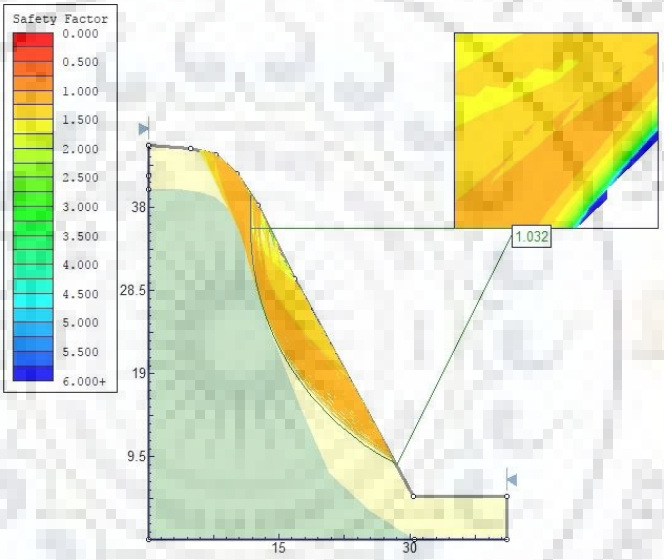

FoS and critical slip surface at slope L7

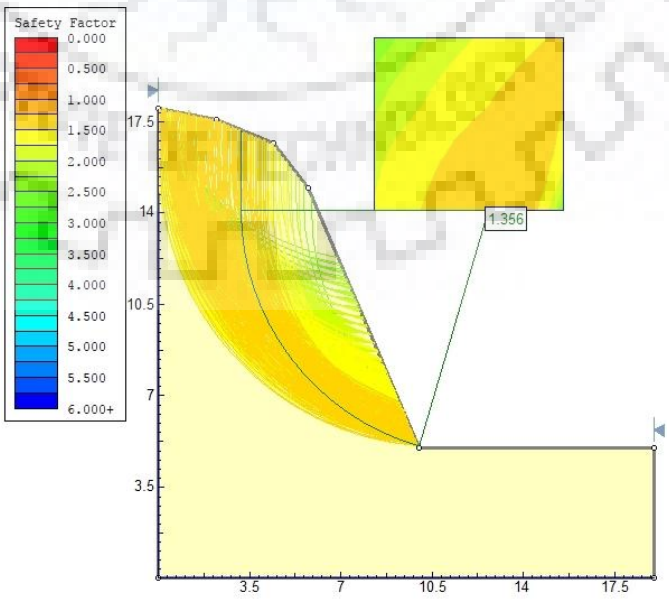

FoS and critical slip surface at slope L8

Appendix D: Shear strain contours and SRF of all investigated debris slopes along NH-58

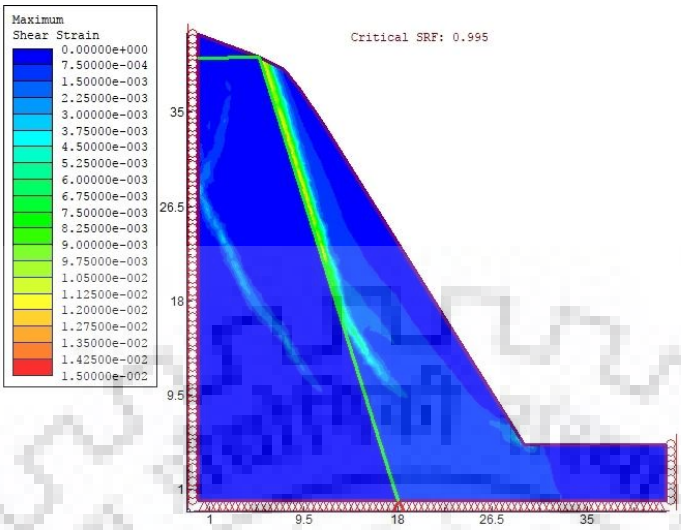

Shear strain contours and SRF at slope L1

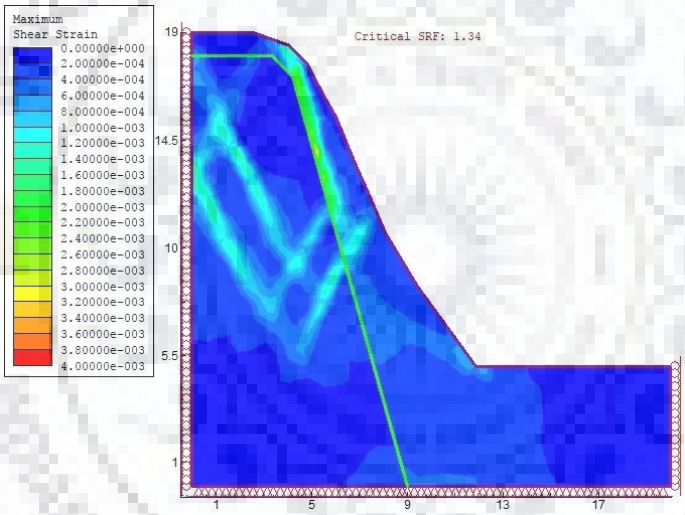

Shear strain contours and SRF at slope L2

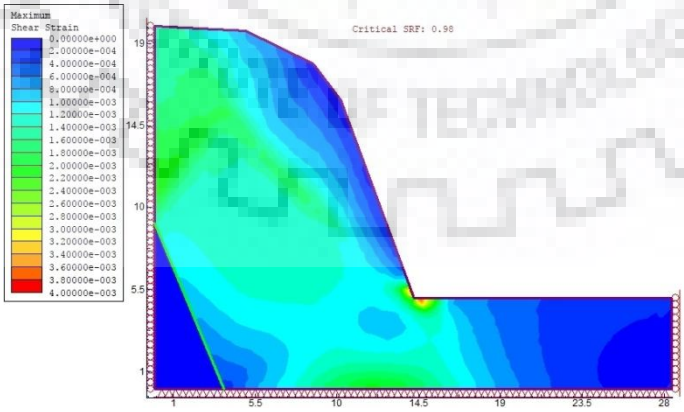

Shear strain contours and SRF at slope L3

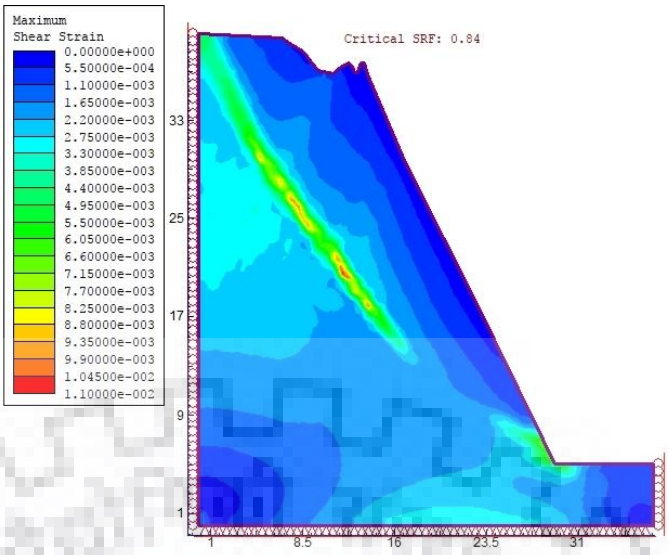

Shear strain contours and SRF at slope L4

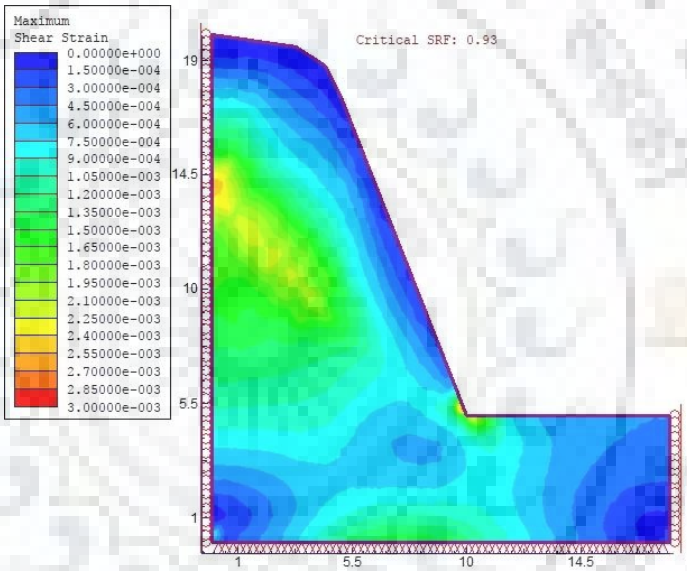

Shear strain contours and SRF at slope L5

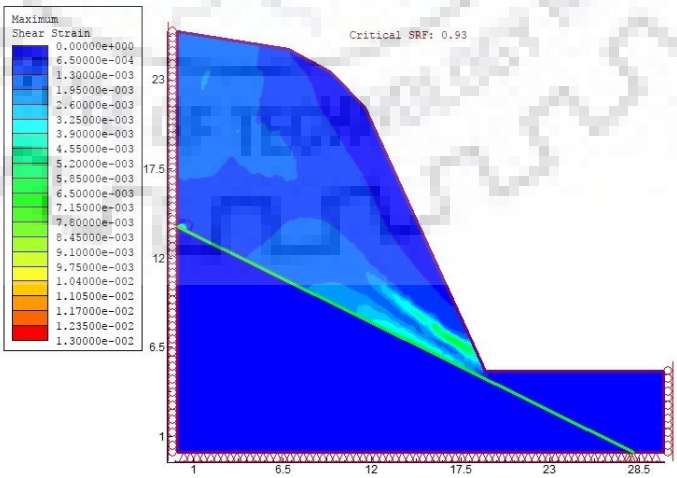

Shear strain contours and SRF at slope L6

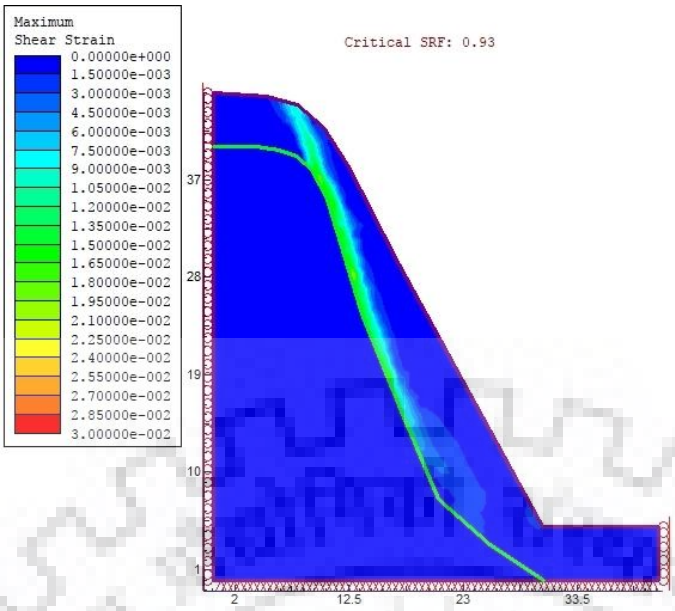

Shear strain contours and SRF at slope L7

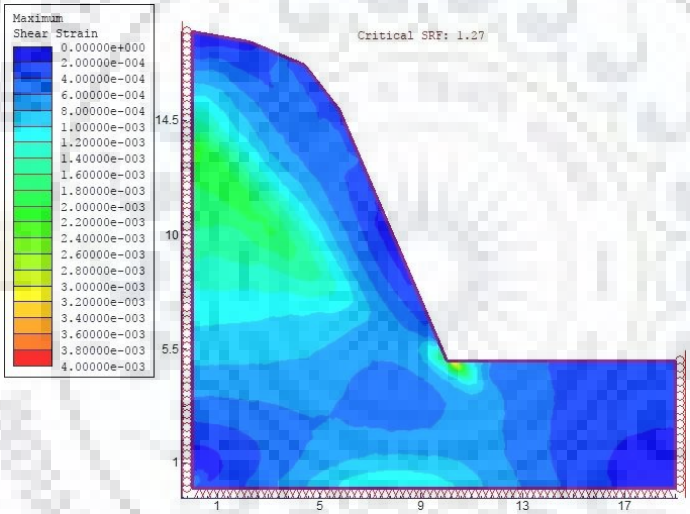

Shear strain contours and SRF at slope L8

Publications

In Journals

1. SP Pradhan and **T Siddique** (2019) Stability assessment of landslide-prone road cut rock slopes in Himalayan terrain: A finite element method based approach. *Journal of Rock mechanics and Geotechnical Engineering*. (Accepted).

2. **T Siddique** and SP Pradhan (2018) Stability and sensitivity analysis of Himalayan road cut debris slopes: an investigation along NH-58, India. *Natural Hazards*. 93: 577-600.

3. **T Siddique**, SP Pradhan, V Vishal, MEA Mondal, TN Singh (2017) Stability assessment of Himalayan road cut slopes along National Highway 58, India. *Environmental Earth Sciences*. 76: 759.

4. **T Siddique** and SP Pradhan (2018) Road widening along NH-58, Uttarakhand: Needs to seek attention. *Current Science. (Under review)*

In Book

1. SP Pradhan and **T Siddique** (2019) Mass Wasting: An Overview. In Pradhan SP, Vishal V, Singh TN (eds.) *Landslides: Theory, Practice and Modelling*. Advances in Natural and Technological Hazards Research, Springer: 3-20.

2. **T Siddique**, SP Pradhan, V Vishal (2019) Rockfall: A specific case of landslide. In Pradhan SP, Vishal V, Singh TN (eds.) *Landslides: Theory, Practice and Modelling*. Advances in Natural and Technological Hazards Research, Springer: 61-81.

In Seminars/Conferences

1. SP Pradhan and **T Siddique** (2018) Finite Element Method and Limit Equilibrium Method analysis of Shivpuri Landslide, Uttarakhand, *Nanital Workshop in Landslides*, Pithoragarh, India.

2. **T Siddique**, AP Yunus, SP Pradhan, MEA Mondal (2017) Landslide Hazard Zonation: A case study from Garhwal Himalaya. In International Conference "*Remote Sensing and GIS for Applications in Geosciences*" Department of Geology, Aligarh Muslim University, Aligarh, India.

3. **T Siddique**, SP Pradhan, AR Roul, MEA Mondal (2017) RMR, SMR, CSMR, Q-system and Kinematic analysis: Implications to slope stability. In National seminar on "*Recent Advances and Challenges in Geochemistry, Environmental and Sedimentary Geology*" Department of Geology, Aligarh Muslim University, Aligarh, India.

4. **T Siddique**, SP Pradhan, V Vishal (2016) Road Cut Slope Stability Investigation along NH-58, Near Shivpuri, Uttarakhand. In National Conference on "*Advances in Geotechnical Engineering*", Department of Civil Engineering, Aligarh Muslim University, Aligarh, India.